UNDERSTANDING ZEA MAYS GENETIC INFLUENCE ON THE STRUCTURE AND FUNCTION OF THE RHIZOSPHERE MICROBIOME

BY

ALONSO FAVELA

DISSERTATION

Submitted in partial fulfillment of the requirements
for the degree of Doctor of Philosophy in Ecology, Evolution, and Conservation Biology
in the Graduate College of the
University of Illinois Urbana-Champaign, 2021

Urbana, Illinois

Doctoral Committee:

Professor Angela D. Kent, Chair and Director of Research
Associate Professor Martin O. Bohn
Associate Professor Anthony C. Yannarell
Associate Professor Katy D. Heath
Professor Andrew D.B. Leakey

ABSTRACT

Assembly of the plant rhizosphere microbiome is driven by plant genetic and evolutionary history (Yeoh et al. 2017). Plant microbiomes play a major role in altering plant resilience, fitness, nutrition, and productivity (Busby et al. 2017). Plant hosts selectively filter microorganisms that colonize their rhizosphere (Bulgarelli et al. 2013; Philippot et al. 2013). This selective process is heritable across plant cultivars (Peiffer et al. 2013; Walters et al. 2018), yet the implication of heritability on rhizosphere microbiome *function* has been relatively unexplored. This dissertation attempts to characterize the N-cycling functions associated with heritable recruitment to the rhizosphere microbiome.

The following dissertation aims to address these specific objectives: examine whether the contemporary agricultural practices that maize has experienced over the past 50 years of breeding has altered the rhizosphere N-cycling microbiome assembly, determine how domestication altered modern maize rhizosphere microbiome assembly from its ancestral progenitor teosinte, assess whether these genotype driven microbiome assembly processes persist in the field setting and influence N-cycling ecosystem function and finally attempt to determine the underlying genetic regions and mechanisms contributing to differential microbial community assembly and function in the rhizosphere. The findings of these specific objectives suggest that the maize microbiome has been unintentionally altered through the process of contemporary breeding and domestication, resulting in the microbiome interaction to be less agriculturally sustainable. These anthropogenic driven changes to the maize microbiome can be characterized by changes in nitrifying and denitrifying microbiome recruitment that consequently alter the rates of nitrification and denitrification of a soil. Furthermore, wild genetic diversity appears to house more sustainable N-cycling microbiome interactions compared to modern maize. The

dissertation closes by showing how “rewilding” the plant microbiome interaction could be a potential solution to improve our agricultural system.

Modern agricultural practices have resulted in the unprecedented degradation of our global nitrogen cycle (Galloway et al. 2008). This N-cycle disruption by agriculture has been primarily driven by the over-application of synthetic N fertilizers. On average only about half of this applied synthetic N is taken up by our focal crop (Coskun et al. 2017), while the remainder is lost through microbiome activities such as nitrification and denitrification. Broadly, the work in this dissertation shows that genotype-driven rhizosphere microbiome assembly can have a considerable effect on N-cycling functional groups that carry out nitrification and denitrification. Additionally, this dissertation suggests that at least in maize, a global staple crop, it appears that breeding has disrupted N-cycling functional group control in the rhizosphere especially when compared to its wild progenitor teosinte. Finally, we show that modern maize can regain the ability to influence N-cycling microbes in the rhizosphere with genetic introgressions from teosinte. Overall, this dissertation uses a combination of microbial ecology and plant genetics to provide some explanations for why our contemporary agricultural system is so unsustainable (via N-pollution) and provides some potential solutions to improve it (via rewilding).

ACKNOWLEDGMENTS

Throughout the writing of this dissertation, I have received a great deal of support and assistance. I am extremely grateful to my supervisor, Dr. Angela Kent, whose expertise was invaluable in formulating the research questions and writing. Your insightful feedback pushed me to sharpen my questions and brought my science to a higher level. Furthermore, I would like to express my deepest appreciation to my committee Dr. Martin Bohn, Dr. Anthony C. Yannarell, Dr. Katy Heath, Dr. Andrew Leakey. The resources you provided, questions you asked, the ideas you discussed, and the feedback you have given me have been tremendously helpful to produce this work.

I thank the current and former members of the Kent-Yanarell lab group for feedback on ideas and writing: Dora Cohen, Ginny Li, Alyssa Beck, Maya Scott, Yanjun Ma, Sada Egenriether, Gabe Price, Sierra Raglin, Joe Edwards, Kevin Ricks, Isaac Klimasmith, Danyang Duan, Niuniu Ji, Di Liang, Sandy Simon, Monique Hazemi, Kathryn Solorzano Lowell, Daniel Cho, and Elle Lucadamo. Furthermore, I would like to show additional gratitude to Dora Cohen and Maya Scott who welcomed, trained, guided me when I joined the lab. Thank you to Martin Bohn and his research group for providing valuable seed resources that were an invaluable aspect of my field experiments. Formally, I would like to acknowledge and thank the Plant Care Facility staff, Heather Lash, Monte Flack, Clinton Shipley, Michael Maddock, and Nathan Deppe who helped me maintain healthy and happy plants. I especially thank undergraduate students Julia Antonson, Anjana Krishnan, Rachel Waltermire, Abbie Zastawny, Savanah Henderson, Nisarg Shah, Eduardo Tovar, and Katrina Cotten for help with fieldwork, lab work, and greenhouse work and for simply being there to help during the most chaotic and exhausting times of my research. I could not have done this without you.

Many, many thanks to my labmate Dora Cohen for all the training, and GC support. Thank you to the Genomic Ecology of Global Change lab for allowing me to use their equipment for my research and providing a welcoming environment to conduct lab work. I also thank Dr. Mark Band and members of the Roy J. Carver Biotechnology Center for providing excellent DNA sequencing services and for troubleshooting new technology that allowed much of the work in this dissertation. I also thank Dr. Heath, Dr. Marshall-Colon, Nick Morphew, and Dr. Kent for providing opportunities for me to teach students in a constructive environment. Furthermore, I would like to thank all of the people that helped me apply to grad school Ana Botello, Dr. Goggy Davidowitz, Dr. Chandreyee Mitra, and the Summer Research Institute at the University of Arizona. Also, I would like to thank the University of Illinois professors who acted as mentors and role models during my dissertation Dr. Andy Suarez, Dr. Carla Cáceres, and Dr. Brian Allan. Furthermore, I'd like to thank all of the administrative help from Kim Leigh, and Liz Barnabe without whom I wouldn't have been able to graduate.

Finally, I want to thank my family and friends who have supported me throughout my doctoral journey. My parents Ismael and Lourdes sacrificed a great deal of their life to make sure that their children had opportunities not available to them and for this, I want to thank them without the entity of my being. Their support and wisdom have guided me throughout this journey, and I would not be myself without them. I would like to thank Ingrid Holstrom for her love and support. I would like to acknowledge my amazing funding sources the National Science Foundation Integrated Graduate Research Traineeship Vertically Integrated Training with Genomics, and National Science Foundation Graduate Student Research Fellowship. Without this funding, I would not have been able to collect the same body of research and get to the same depth of understanding.

Dedicated to my amazing parents Ismael and Lourdes Favela who gave me the opportunity to investigate and understand science from a typically unexplored perspective.

TABLE OF CONTENTS

CHAPTER 1: INTRODUCTION

Over the 20th century, our industrial agricultural systems have had to meet and increased food demands by simplifying our agronomic management practices, increasing the number of external fertilizer inputs into the agricultural field, and increasing the density of plants (Hallauer 2009; Galloway et al. 2008). These changes consequently have resulted in large amounts of environmental degradation, increased greenhouse gas production, harm to human health, and have made agriculture a substantial contributor to climate change (Smith et al. 2008; Mora et al. 2018). In addition to this, recent reports show that 52% of all fertile, food-producing soils globally are now classified as degraded, and it has been projected that continued agricultural production on these degraded lands 12% decline in global food production over the next 25 years (United Nations Conventions to Combat Desertification 2015). As it stands, our current agricultural system is both sensitive and a major contributor to ecosystem-level changes caused by climate change. Rethinking our agricultural system to be sustainable and resilient will require the collaboration of scientists and industry to generate solutions that will balance our anthropogenic needs with our impacts on both local and global ecosystems.

A proposed solution to meet the challenge to improve resilience and sustainability is to harness capabilities of the plant-associated soil microbial communities and incorporate them into modern agriculture (Busby et al. 2017; Antwis et al. 2017). A recent renaissance in microbial ecology, spurred by technological advances in next-generation sequencing and culturing methods, has begun to reveal the pivotal role that soil microbes play in plant health and productivity. These advances in understanding have led to a paradigm shift in which microbial communities are seen as functional drivers of their plant host (Philippot et al. 2013; Bulgarelli et al. 2013; Cordovez et al. 2019). This is because microbial communities can expand the genomic

and metabolomic capabilities of their sessile plant hosts, providing them a mechanism by which to mitigate or evade stressors in their shared environment (Vandenkoornhuyse et al. 2015; Cordovez et al. 2019). Specifically, soil microbial assemblages have been implicated in the resistance of pathogens, amendments to plant nutrition, resistance against drought, and resistance against plant pests (Kwak et al. 2018; Philippot et al. 2013; Seabloom et al. 2019). The physiological and ecological link between soil microbial communities and plants should come as little surprise as these two systems have been interacting and coevolving since the inception of terrestrial land plants (Svistoonoff et al. 2008; Delaux and Schornack 2021). Incorporation and expansion of a plant-microbiome perspective with a fundamental view that the two systems are working in concert is necessary to improve the sustainability and resilience of our agroecosystems.

Currently, these advances in plant microbiome sciences have resulted in the emergence of agro-industrial ventures focused on the production of microbial bio-stimulants that improve plant performance (e.g., Novozymes, Pivot bio, Valagro, Aphea Bio, Azotic, etc.). These industries design, culture, and characterize microorganisms that are capable of have beneficial interactions with plants. Plant-growth-promoting microbes are then reintroduced back into the soil ecosystem or inoculated directly onto the plant (Kong, Hart, and Liu 2018; Sessitsch, Pfaffenbichler, and Mitter 2019). While this approach has been shown to have considerable success in improving plant performance in controlled and greenhouse settings, such findings rarely hold in the field (Backer et al. 2018). Typically, this lack of success is attributed to the complex and context-dependent nature of agricultural soils (Kong, Hart, and Liu 2018; Hart et al. 2018). Microorganisms and their functions are extremely sensitive to environmental conditions. Consequently, microbial biostimulants are developed under controlled laboratory conditions and

can fail to deliver the desired result when introduced to the highly variable environment of agroecosystems (Sessitsch, Pfaffenbichler, and Mitter 2019). Besides, to establish in the agricultural environment, microbial biostimulants must compete with native soil microbiota and be compatible with conditions in the soil environment (Hart et al. 2018; Woo and Pepe 2018; Kong, Hart, and Liu 2018). Furthermore, the biostimulant method of agricultural improvement is intractable at greater agronomic scales as the production and development of microbial inoculum is expensive, time-consuming, and not always rewarded. Significant advances in the usage of microbiome applicants are needed to bridge the gap between laboratory success and field in field settings.

As an alternative, we propose leveraging plant genetics and breeding to harness the plant-microbe interactions. Plant breeding is the genetic improvement of plants for human benefit. Plant breeders play a unique evolutionary role in the agricultural system as they test, cross, and select traits of specific germplasm for improvement. Traits that have been successfully incorporated into crop plants range in complexity. Easily characterized phenotypic traits (i.e., crop beauty, flavor, crop storage, and yield) have been the primary focus of breeders over human history (Diamond 2002), but work has shown that complex traits can be successful targets of selection (Anderson et al. 2014). Some examples of context-dependent traits that breeders have improved include abiotic stress tolerance (Trethowan and Mujeeb-Kazi 2008), resistance against pathogens (Wille et al. 2019), increased tolerance to insect pests (Foyer, Noctor, and van Emden 2007), herbicide resistance and plant-soil allelopathy (Fragasso, Iannucci, and Papa 2013). Complex traits started playing a prominent role in the agricultural system over the past 30 years. Here, we want to examine if plant-associated microbial communities behave like the previously mentioned complex traits and if they can be used to improve the sustainability of the

agroecosystem. Understanding the potential for a genetic basis for the plant to influence recruitment and function of the plant microbiome would allow researchers and breeders to work toward controlling complex soil microbial communities and plant symbioses across a variety of environments and soil types.

The purpose of this mini-review is to explore the present knowledge of the connection between plant genetics and the structure and function of the microbiome and to illustrate the viability of incorporating plant microbiome selection traits into breeding programs. We aim to cover: 1) how and when do plant genetic factors play a role in shaping the soil microbiome; 2) the mechanistic underpinnings by which plant genotype can influence microbiome interaction and selection; 3) the link between microbiome selection and ecosystem function. After reviewing these topic areas, I will present an overview of how this dissertation contributes to our understanding of how plant genetics influence the microbiome.

Plant genotypes influence the soil microbiome:

i. Evidence for plant species impacts of the rhizosphere microbiome

A large body of research dating back to the early 19th century has focused on understanding how plants alter the physicochemical properties of soil in the zone surrounding the root zone, known as the rhizosphere effect (Waksman 1927). These plant rhizosphere effects have been shown to influence the establishment of individual soil microorganisms from the environment (Bashan 1986; J. L. Neal, Larson, and Atkinson 1973) thereby altering the composition of the soil microbial community as a whole (Bulgarelli et al. 2013; Philippot et al. 2013). Plants species from agroecosystems (Matthews et al. 2019) to natural systems (Saad et al. 2020) have been shown to have the ability to alter soil microbial communities. Furthermore, a variety of plants

ranging from citrus (Xu et al. 2018), rice (Edwards et al. 2014; Kim and Lee 2019; Ding et al. 2019), maize (Peiffer et al. 2013; Walters et al. 2018; (Favela, Bohn, and Kent 2021), wheat (Mahoney, Yin, and Hulbert 2017), barley (Bulgarelli et al. 2015), *Arabidopsis* (Lundberg et al. 2012; Schlaeppi et al. 2014), beet (Zachow et al. 2014), lettuce (Cardinale et al. 2015), agave (Coleman-Derr et al. 2015), lotus (Zgadzaj et al. 2016), and dessert grasses (Eida et al. 2018; Marasco et al. 2018) have to host different microbiome assemblages in the rhizosphere compared to bulk soil. Furthermore, evidence suggests that the strength of microbial recruitment across plant species varies immensely (Fitzpatrick et al. 2018, 2019). A large amount of literature, across several plant species, shows that plants broadly have a selective effect in the rhizosphere, yet a functional understanding of why plants do this is still not understood.

Studies across many of the aforementioned plant species have reported results with varying levels if support for a predictive relationship between host genotype and rhizosphere microbiome assembly. Within *Poaceae* for example, plant phylogenetic differences are correlated with differential recruitment of the microbial community (Bouffaud et al. 2012; Bouffaud et al. 2014). These studies suggest that more highly related grasses recruit more similar microbial communities. Additionally, an in-depth analysis of plant microbiome assembly across 30 angiosperm species, which span 140 million years of evolution, show that while plant species still had a rhizosphere microbiome effect, not all bacterial phyla respond to plant-rhizosphere selection, or have a phylogenetic signal in the rhizosphere microbiome recruitment (Fitzpatrick et al. 2018). Fitzpatrick et al. also determined that specific plant traits (physiology, productivity, root, architecture) that are expected to shape the rhizosphere compartment, are themselves uncorrelated with host-plant phylogeny. Interestingly, this work shows that plants that recruit similar microbial communities have more robust negative soil feedbacks on each other, thereby

providing a potential selective pressure against closely related species with similar root microbiomes.

ii. Genes underlying genotypic differences in microbiomes

Gene-level allelic differences cause substantial variation in microbiome assembly across germplasm. For example, knockout mutations in genes related to ATP-binding transporters (Badri et al. 2008), secondary metabolite production (Huang et al. 2019), phytohormone production (Lebeis 2014), immune system (Castrillo et al. 2017), symbiotic association (Zgadzaj et al. 2016), and host circadian clock homeostasis (Hubbard et al. 2017) have all been drivers of the rhizosphere microbiome. As the rhizosphere microbiome is an extremely complex quantitative trait this is not surprising. Many genes likely play a role in the assembly of the rhizosphere microbiome as the roots and their systemic interactions are critical to plant productivity. Further work needs to be done to understand the extend of these genes on the microbiome in plant.

iii. Rules of genotype-driven microbial assembly

Unlike other phenotypic traits, microbiome assembly is highly dependent on ecological processes (Agler et al. 2016; Banerjee et al. 2018). Using gene-knockout experiments, Zgadzaj et al. (2016) showed that Lotus-diazotroph symbiotic nodule formation additionally reshaped the rhizosphere microbial community. In the lotus system, it appears as if symbiotic rhizobia populations act as an ecological ‘hub’ within the lotus microbiome for tens of species. Similarly, work done in oat has displayed that rhizosphere microbial establishment is sequential, structuring and promoting microbial interconnectedness (Zhalnina et al. 2018). Succession and founder effects have also been shown to play a substantial role in assembly across the plant (Gupta and Sharma 2021). Furthermore, the presence of an individual bacterial genus within the microbial

could suppress and alter typical microbiome assembly processes and alter plant growth (Finkel et al. 2020). These ecological factors will need to be understood and incorporated to predictively select for genetic variation that modifies root-associated microbial communities.

Importantly for breeders, it has also been shown that within-population genetic variation exists that results in the differential recruitment of taxa to the rhizosphere (Peiffer et al. 2013; Walters et al. 2018; Bulgarelli et al. 2015; Mahoney et al. 2017; Lundberg et al. 2012; Zgadzaj et al. 2016; Xu et al. 2018; Edwards et al. 2014), but this is not always the case. There are numerous examples where the genetic variation within and across plant species and populations does not appear to impact the recruitment of microbial taxa to the rhizosphere. Understanding when and where plant genotype plays a role in the recruitment of taxa, and which taxa are actively recruited will allow us to start defining the rules for breeding microbial assembly and interaction in the plant rhizosphere. (Inspired by the work of Thomas Whitman's Genetic Community (Whitham et al. 2006, 2012) Specifically, we propose a set of rules governing plant microbiome genotype effects. To observe a heritable microbiome, three conditions need to be present (Fig. 1.1): (1) There must be plant population genetic variation in the set of phenotypes that are driving the microbiome (i.e., no genetic erosion: limitation of the gene pool of a population). (2) There must be sufficient microbial species diversity to be shaped by the plant phenotype. (i.e., no microbiome erosion: limited number of microbial species diversity). (3) The plant and the microbiome must have a common dimension of interaction/limitation (i.e., endosymbiosis or ectosymbiosis, share space, nutrient, etc.) Additionally, we want to make the point that selective events can decrease genetic variation in the plants and microbiome and can lead to genetic and microbiome erosion, which would lead to the absence of a plant genotype-driven microbiome.

Studies that have reported the greatest genotype-driven rhizosphere effects have a few common design elements, including 1) observations across a large range of environments (Xu et al. 2018; Walters et al. 2018) thereby maximizing the microbial diversity that the genotype may select from; 2) a genetically diverse crop (maize, *Arabidopsis*) (Peiffer et al. 2013; Lundberg et al. 2012); or 3) extensive genetic differences exist between the two cultivars (e.g. wild vs domesticated) (Bulgarelli et al. 2015; Pérez-Jaramillo et al. 2018). These three factors maximize different components of microbial recruitment. Extensive geographical analyses of rice, wheat, maize, and citrus microbiomes suggest certain microbes are consistently recruited, considering they are present in the starting community. While studies exist that find many plant species recruit unique sets of microorganisms, evidence exists showing that this is not always the case. For example, different species of speargrass from the climatically extreme Namib desert all recruit similar plant-associated microorganisms from the surrounding soil and lack a host-specific genotype effect. This is interesting as these grasses appear to vary in root traits (i.e., sheath-root system morphology), features that are typically associated with differential selection of the plant microbiome (Marasco et al. 2018). While other studies have shown that successive intense selection on the microbial community through time can reduce microbial diversity and supersede previously important plant genotype selection on the microbiome (Morella et al. 2019). Selection, abiotic or biotic, can erode the genetic diversity and traits of the microbial community, limiting the ability of plants to select on the community. Thereby if degradation of the microbiome has occurred, genetic variation in plants that typically alters microbiome assembly would not be observed as there is no microbial community variation to select upon (Fig. 1.1).

A mechanistic underpinning of plant microbiome interactions:

Within the rhizosphere, three genetically-controlled traits have been cited as playing a role in mechanistically shaping the microbial community: plant phytochemical allelopathy, immune response system, and genes governing symbiotic interactions. Here, I will cover our understanding of both the genetic and mechanistic underpinnings of microbial interaction, and the challenges in controlling these belowground plant traits. Understanding the relationship of these traits to the microbiome is crucial, as they will be important in selection by plant breeders. These characteristics are important as they determine the width/strength of microbiome filtering present (Fig. 1.1).

i. Plant phytochemistry

Plant allelopathy, commonly defined as biological phenomena by which a plant exudes one or more metabolites to influence the survival of a competing organism, has a long history in the agricultural and ecological sciences (Cheng and Cheng 2015; Pascale et al. 2020). These types of exudates are commonly cited as playing a role in driving the host-associated microbiota of plants (Dakora and Phillips 2002; van Dam and Bouwmeester 2016; Sasse, Martinoia, and Northen 2018; Canarini et al. 2019). A considerable amount of literature reveals that phytochemical alterations in a single plant species influence how the microbial community will assemble. For example, in *Arabidopsis thaliana,* the simple alteration of a regulatory gene MYB72 involved in coumarin production and exudation was shown to have sweeping effects on the composition of the microbial community they established (Stringlis et al. 2018). Additionally, the coumarin, scopoletin, had a differential effect on soil microbes, acting as an attractant for nutritional mutualists and an antimicrobial for fungi (Stringlis et al. 2018). Interestingly, studies focusing on maize and benzoxazinoid exudation have drawn similar

conclusions. Genetic modifications of the plant's phytochemical production alter rhizosphere microbial assembly (Neal et al. 2012; Hu et al. 2018; Cotton et al. 2019; Kudjordjie et al. 2019). In controlled settings, benzoxazinoids have also been shown to attract and repel different common microorganisms. A single benzoxazinoid molecule can have variable effects enriching mutualist bacteria (*Pseudomonas putida*) and the suppression of pathogens *(Ralstonia solanacearum)* (Neal et al. 2012). Conceptual Fig. 1.2, highlights how genetic variation in a single metabolic pathway contributed to altered microbial selection.

Furthermore, breeding for allopathic characteristics has already been proposed in previous research reviews (Cheng and Cheng 2015; Mikic and Ahmad 2018). These reviews outline approaches for breeding for these biochemical characteristics. These articles found that a significant amount of phenotypic variation exists within the biochemical characteristics of numerous crop cultivars and across wild species (Mikic and Ahmad 2018). This is important, as without extant genetic variation in metabolite traits, our ability to select the microbiome would be severely limited.

ii. Plant immune system

The plant immune system plays a critical role in shaping the microbiome – as it allows for the compartmentalized and specialized responses to microbes (Jones and Dangl 2006; Chuberre et al. 2018). Several reviews on the plant immune system have shown that roots can activate specific defense mechanisms in response to various elicitors including molecular/pathogen associated molecular patterns (MAMPS/PAMPS), and signal metabolites (Jones and Dangl 2006; Chuberre et al. 2018). Further, research has shown that the exposure of specific effectors can trigger plant metabolic pathways related to changes in exudate profiles (Stringlis et al. 2018; Sasse, Martinoia, and Northen 2018). In many cases, the immune system-

mediated responses to the microbial are typically thought to be systemic, thereby if a plant senses a specific effector is sensed by the plant entire plant exudation patterns are altered (Korenblum et al. 2020). In summary, genetic variation in the plant's immune system should strongly be considered as it informs how a plant will respond to the microorganisms.

iii. Plant symbioses

Many agricultural plant species can form a tight symbiosis with fungal and bacterial partners (O'Brien et al. 2021; Porter and Sachs 2020). The genetic elements that underlie these phenotypes have been shown to have considerable influence on the formation and interaction with the entire microbiome (Zgadzaj et al. 2016). This is because microbial symbiosis is a process that requires multiple steps of interactions, from microbial attraction via phytochemical production, plant immune responses that recognize the symbiotic partner, and genes involved in controlling colonization and establishment (Sandal et al. 2006). Research has shown that a genetic alteration to any of these elements will result in the alteration of the rhizobacteria to the microbiome (Zgadzaj et al. 2016). While covering all of the interactions included under the umbrella of plant-microbiome symbioses is out of the scope of this review, here we want to highlight how genetic variation in symbiotic partnerships can alter the entity of the rhizosphere microbiome.

Microbial genomes under plant selection:

A functional understanding of microbial assembly should not be limited to only understanding plant characteristics. Microorganisms present in soil are immensely speciose and highly diverse with complex genomes that encode a huge array of functions, metabolites, and metabolic strategies (Vigdis Torsvik 2002; Banerjee et al. 2018; Levy et al. 2018). A large

survey of 3,847 bacterial genomes revealed that thousands of gene clusters are involved in plant-association (Levy et al. 2018). Functionally, genomes of bacteria that associate with plants encode for more carbohydrate metabolism pathways and have a lower abundance of genetic mobile elements compared to non-plant-associated bacteria. Besides, Levy et al. 2018 found that across different bacterial genomes, genes clustered into functional units of common interest (i.e. genetic linkage), and those bacterial genes that are enriched in bacterial genomes from the plant environment are also likely to be involved in adaptation to the many other organisms that share the same niche.

Under the rhizosphere ecological filter model previously presented (Fig. 1.1), functional genes within microorganisms will determine whether a microbe is competent under plant rhizosphere selection conditions. Connecting our understanding of bacterial genomics and plant genomics is central to providing a useful model for controlling rhizosphere microbial communities and simplifying complex ecology to a lock-and-key model. In this metaphor, the lock is plant mechanisms of selection (e.g., phytochemistry, immune system, symbiosis) and the key is the microbial genome and functional genes. Plant mechanisms underlying microbial interaction provide a selection pressure on microbial populations in the microbiome. Well-adapted microbes will have genes to evade or benefit from plant mechanisms of selection while maintaining their primary metabolism for growth. Maladapted microbes will lack the essential genes necessary to survive the rhizosphere selection pressure and will be unable to maintain their primary metabolism. Clearly defining the interactions between plant mechanisms of selection and the microbiome will provide a codex to driving the rhizosphere and ecosystem function.

Furthermore, we attempt to highlight how to plant mechanisms of selection (both direct and indirect) may be interacting with the microbial ecosystem (Fig. 1.3). As mentioned above

plant inputs into the microbial ecosystem can differentially select taxa – what is critical about this plant selection is that the genetic element in the bacterial genome under selection by the plant's selective pressure for are, in many cases physically linked to other genes. These linked genes can carry out functional processes that can be mutualistic, antagonistic, or commensal with respect to the plant host and have the potential to alter ecosystem fluxes. In the direct selection example (Fig. 1.3A), I use a common metabolite, DIMBOA-Glu, to show how microbial interactions (i.e., degradation, detoxification, consumption, derivation) with a plant metabolite can alter their proceeding interactions within the soil environment. I further highlight differential effects on contrasting functional groups such as nitrifiers (*Nitrosomonas)* and diazotroph (*Rhizobium*) taxa could take place. In this scenario, the exudate would inhibit the nitrifier thereby limiting nitrification, while alternatively, this same metabolite would act as a signal for *Rhizobium* and ultimately lead to N-fixation. Alternatively, in our hypothetical indirect selection example, plants would we release signals that would stimulate microbial predators – that would then allow the plant to have top-down control of the community (Fig. 1.3B).

Breeding for the rhizosphere microbiome:

We see two major approaches available to breed for plant-microbiome interactions: 1) identify genetic variation that alters the microbiome phenotype then modify the genomic region to alter microbial interaction, or 2) approach microbiome function as a plant phenotype to characterize across a genetically diverse panel of lines and perform directional selection. The first scenario is ideal for well-characterized phenotypes like plant secondary metabolites where the genes involved in phytochemical production and the antibiotic capacities of the phytochemical are well understood. Breeding for these characteristics is relatively

straightforward as marker-assisted selection and genetic manipulation can be carried out on existing genetic variation for these traits. As an example, MYB72 gene-dependent coumarin production has been shown to recruit plant growth-promoting microorganisms (Stringlis et al. 2018). This gene can therefore be targeted for selection in breeding programs or be introduced into elite lines to gain plant growth-promoting microbial interactions. The major drawback of this approach is the limitations of our understanding of the mechanistic traits shaping plant-microbe interactions. Only a few secondary plant metabolites (of the thousands) have been characterized for their effects on soil microbial communities. A secondary approach to breeding for plant microbiome interactions is to treat the desired function of the rhizosphere microbiome as a phenotype for selection and approach the plant-microbe mechanisms as a "black box". For example, if we were interested in developing lines that stimulated microbial mineralization of soil nutrients for organic agriculture, we would grow a breeding population under organic conditions and survey rhizosphere microbial communities for their ability to mineralize organic nitrogen as the phenotype of interest and select lines with the highest nitrogen mineralization rates. After selection on these lines is done, plant traits could then be further characterized to identify the causative agents involved in driving changes in microbiome function. The major downside of this approach is that it is time-consuming and large enough genetic variation needs to be present in the founding population to select for microbiome differences. Several potential approaches could be taken to breed plant-microbiome interactions into our modern agricultural system. The most straightforward method would be to select a plant trait with a known microbial/microbiome phenotype.

Overview of dissertation:

In this dissertation, I attempted to understand how genetic variation in maize altered rhizosphere microbiome assembly and related ecosystem processes. The following dissertation chapters aim to address these specific objectives: (Ch. 2) examine whether the contemporary agricultural practices that maize has experienced over the past 50 years of breeding have altered assembly of the rhizosphere N-cycling microbiome assembly, (Ch. 3) determine how modern maize rhizosphere microbiome assembly differs from its ancestral progenitor teosinte, (Ch. 4) assess whether these genotype driven microbiome assembly processes persist in the field setting and influence ecosystem function and finally (Ch. 5) attempt to determine the underlying genetic variation and mechanisms contributing to differential microbial community assembly and function. Ch. 2 and 3 examined *Zea* genetic effects on the microbiome under tightly controlled greenhouse conditions where the starting soil microbiome inoculum, and nutrients were standardized across maize genotypes. Ch. 4 and 5 were both large, randomized-block field experiments that tested a genetically diverse panel of maize lines and their influence on stochastic soil communities.

In Ch. 2: *Maize germplasm chronosequence shows crop breeding history impacts recruitment of the rhizosphere microbiome,* I performed a common garden study to characterize recruitment of rhizosphere microbiome, functional groups, for 20 expired Plant Variety Protection Act maize lines spanning a chronosequence of development from 1949 to 1986. This time frame brackets a series of agronomic innovations, namely improvements in inbreeding and the application of synthetic nitrogenous fertilizers, technologies that define modern industrial agriculture. I found that both genetic relatedness of host plant and decade of germplasm development were significant factors in the recruitment of the rhizosphere microbiome. More

recently developed germplasm recruited fewer microbial taxa with the genetic capability for sustainable nitrogen provisioning and larger populations of microorganisms that contribute to N losses. This study indicates that the development of high-yielding varieties and agronomic management approaches of industrial agriculture inadvertently modified interactions between maize and its microbiome.

In Ch. 3: *Differences in N-cycling microbiome recruitment between inbred and wild Zea mays*, using a greenhouse experiment I characterized how modern inbred maize differed in microbial recruitment to wild teosinte to assess whether potentially beneficial wild plant-microbiome traits were lost during domestication. Using a combination of high-throughput sequencing and quantitative PCR, I found that modern inbred and wild teosinte rhizosphere microbiomes differed substantially in taxonomic composition, species richness, and abundance of microbial N-cycling genes. Furthermore, the modern vs wild designation explained 27% of the variation in the prokaryotic microbiome, 62% of the variation in N-cycling gene richness, and 66% of N-cycling gene abundance. Surprisingly, we found that modern inbred genotypes had higher taxonomic and functional N-cycling gene diversity within their microbiomes when compared to ancestral genotypes. These results imply that inbred maize and wild maize seem to differ in their interaction with N-cycling microorganisms in the rhizosphere and that genetic variation exists to potentially 'rewild' these microbiome-associated traits.

In Ch. 4: *Genetic variation within Zea mays alters microbiome assembly and nitrogen cycling function in the agroecosystem,* I wanted to determine whether the genetic effects driving by microbial community differences within modern maize in Ch. 2 and across maize and teosinte Ch. 3 were still present in the field. Specifically, we wanted to characterize whether plants' influence on soil nitrogen cycling activities was heritable (in a field setting) and thereby able to

be selected for plant breeding. To capture an extensive amount of genetic diversity within maize we sampled ex-PVP inbred lines, hybrids, and wild teosinte (*Z. mays* ssp. *mexicana* and *Z. mays* ssp. *parviglumis*). Within this germplasm panel, we found that plant genetics explained a significant amount of variation in the microbiome and across different nitrification and denitrification functional genes. We found that potential nitrification, potential incomplete denitrification, and overall denitrification rates were influenced by time of sampling (season) and plant genetics (genotype and group). Teosinte genotypes suppressed N-cycling activity while more modern inbred genotypes stimulated N-cycling activity. Taken together these results suggest that modern maize lines may have lost some of their capacity to modulate microbial nitrogen cycling activities and that reintroducing teosinte traits into our modern germplasm may be a way soil microbiome at both a composition and functional level to improve sustainability.

Up to this point, results suggested that modern maize lines may have lost some of their capacity to modulate microbial nitrogen cycling activities (Ch. 2) and that reintroducing teosinte extended phenotypes into modern germplasm may be a way to restore sustainable soil microbiome functions (i.e., rewilding) (Ch. 3, 4). In Ch. 5: *Mapping the genetic regions underlying plant extended phenotype microbiome recruitment and function,* to assess the viability of "rewilding" and further dissect the genetic basis of these ancestral microbiome traits, I used newly developed teosinte-maize near-isogenic lines (NILs). Using NIL populations allows the fine mapping of traits to specific genetic loci in the plant genome. From this teosinte-maize NIL population, I identified several candidate genetic regions that drove major alterations to the root zone microbiome composition and N-cycling function. This study concludes that genetic elements originating from maize's wild progenitor teosinte can be used to "rewild" the modern maize microbiome interaction towards agricultural improvement. Approaching the microbiome

and its functions as an extended phenotype of the plant genome will be a necessary step towards optimizing agricultural systems for sustainability.

Significance:

Modern agricultural practices have resulted in the unprecedented degradation of our global nitrogen cycle (Galloway et al. 2008). This N-cycle disruption by agriculture has been primarily driven by the over-application of synthetic N fertilizers. On average only about half of this applied synthetic N is taken up by our focal crop (Coskun et al. 2017), while the remainder is lost through microbiome activities such as nitrification and denitrification. Broadly, the work in this dissertation shows that genotype-driven influence on rhizosphere microbiome assembly can have a considerable effect on the N-cycling functional groups that carry out nitrification and denitrification. Additionally, this dissertation suggests that at least in maize, a global staple crop, it appears that breeding has disrupted N-cycling functional group control in the rhizosphere, especially when compared to its wild progenitor teosinte. Finally, we show that modern maize can regain the ability to influence N-cycling microbes in the rhizosphere with genetic introgressions from teosinte. Overall, this dissertation uses a combination of microbial ecology and plant genetics to provide some explanations for why our contemporary agricultural system is so unsustainable (via N-pollution) and provides some potential solutions to improve it (via. rewilding).

Figures:

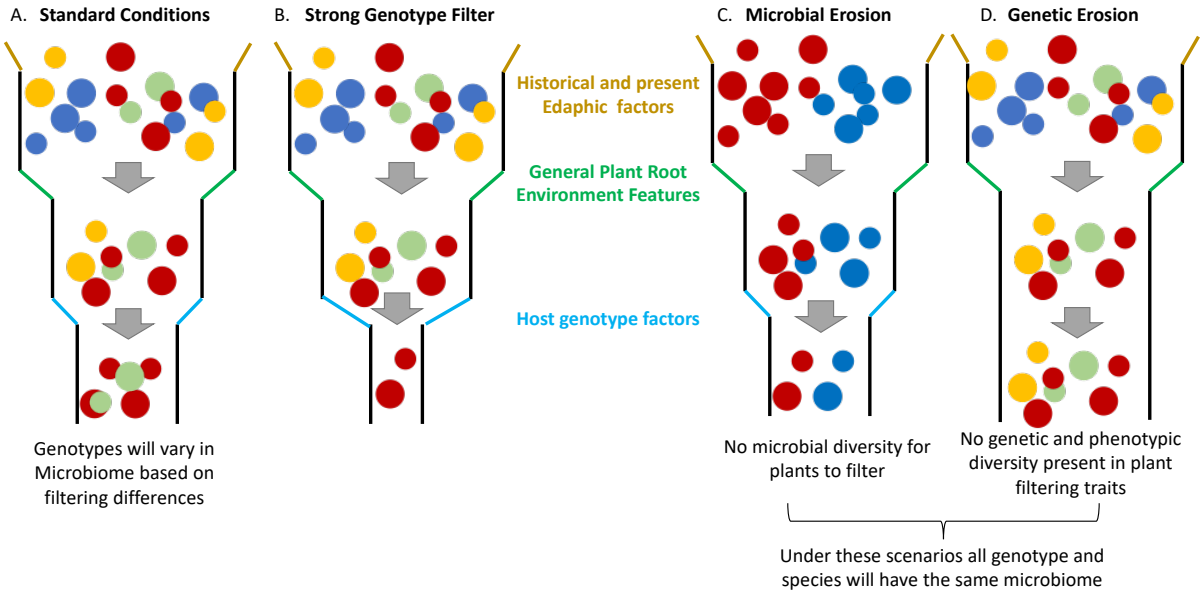

Figure 1.1 Visualization of three major factors playing a role in plant genotype recruitment of root microbiome from edaphic soil microbial community. **A.** The standard model of plant microbiome recruitment originally proposed in Bulgarelli et al. 2013. This original two-step selection model has been modified by the addition of an edaphic filtering effect which alters the microbial diversity present for a plant to select upon. Under the standard conditions, microorganisms from the soil environment that interact with the rhizospheres/plant root conditions, and then finally are selected upon via individual host genotype differences. **B, C, D** Proposed modifications on the previous model, hypothesized from the literature. **B.** In this minor modification of the model, plant genotype selection plays a strong role in rhizosphere microbiome selection. This type of selection strongly narrows the microorganisms that are present in the rhizosphere. **C.** This is an example where edaphic factors have already reduced the diversity of the surrounding soil microbial community. While plant root and genetic filters are still present, these factors have no microbial diversity to select upon because of microbiome erosion. **D.** An additional scenario where plants lack meaningful genetic variation that would enable differential filtering of microorganisms in the rhizosphere. In scenarios **C-D** no plant-genotype-specific microbiomes will be present.

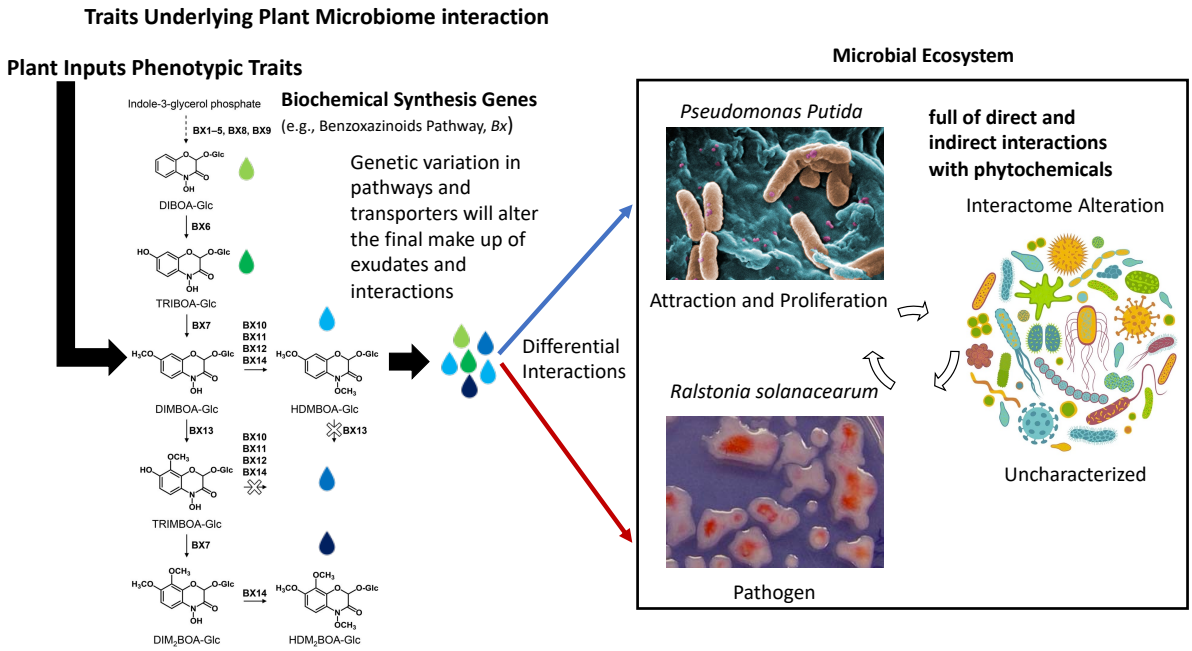

Figure 1.2 Overview illustrating how genetic variation within a single maize benzoxazinoid pathway can contribute to microbiome selection. Several benzoxazinoid synthesis genes exist in maize that alter the chemical characteristics of the compound. Modulating these compounds has the potential to vary their influence on the microbiome. The pathway is adapted from Dutartre et al. 2012

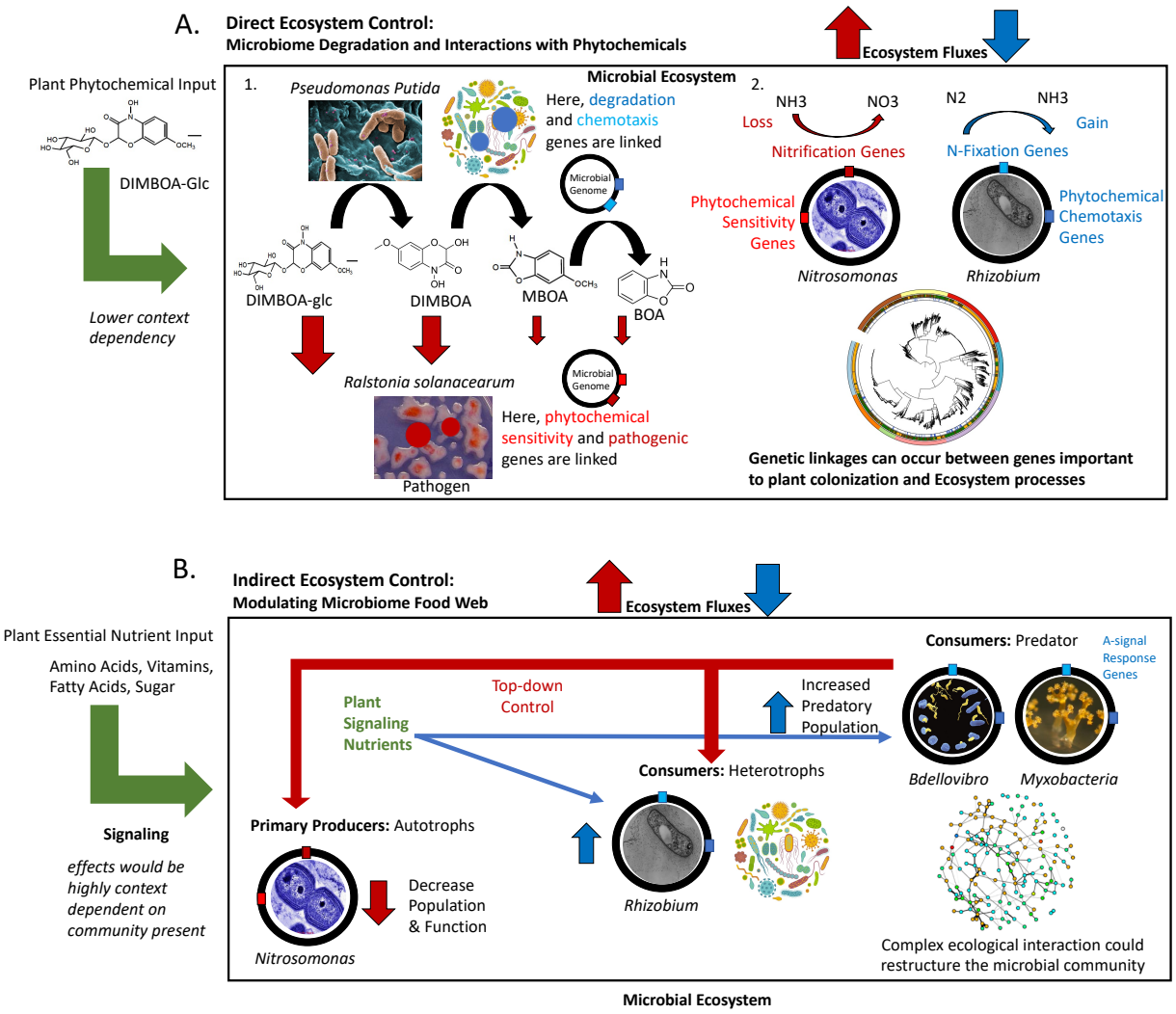

Figure 1.3 A. Microbial breakdown of phytochemical products is of interest for shaping microbiomes as research has shown that microbial bioproducts can sometimes enhance resistance against pathogens and act as a future signal to plants grown in the same soil (Kwak et al. 2018). **A1.** Microorganisms potentially may be breaking down metabolites, thus altering the metabolite's interactions with other microbes (specific *Pseudomonas*, and *Ralstonia*). **A2.** Genetic elements in the bacterial genome are sensitive to phytochemicals and additionally linked to other functional genes. Here N-cycling taxa are used to highlight how phytochemical selection can alter ecosystem fluxes from the rhizosphere microbiome. Red arrows show negative interactions and blue arrows show positive interactions. Metabolites are from (Neal et al. 2012) and the genetic linkage figure comes from Levy et al. 2018. **B.** An alternative model where a plant phytochemical attracts a predator to the microbial community. This is an example of top-down control by the plant host.

References:

Agler, Matthew T., Jonas Ruhe, Samuel Kroll, Constanze Morhenn, Sang Tae Kim, Detlef Weigel, and Eric M. Kemen. 2016. "Microbial Hub Taxa Link Host and Abiotic Factors to Plant Microbiome Variation." *PLoS Biology* 14 (1): 1–31. https://doi.org/10.1371/journal.pbio.1002352.

Anderson, J. T., M. R. Wagner, C. A. Rushworth, K. V.S.K. Prasad, and T. Mitchell-Olds. 2014. "The Evolution of Quantitative Traits in Complex Environments." *Heredity* 112 (1): 4–12. https://doi.org/10.1038/hdy.2013.33.

Antwis, Rachael E., Sarah M. Griffiths, Xavier A. Harrison, Paz Aranega-Bou, Andres Arce, Aimee S. Bettridge, Francesca L. Brailsford, et al. 2017. "Fifty Important Research Questions in Microbial Ecology." *FEMS Microbiology Ecology* 93 (5): 1–10. https://doi.org/10.1093/femsec/fix044.

Backer, Rachel, J. Stefan Rokem, Gayathri Ilangumaran, John Lamont, Dana Praslickova, Emily Ricci, Sowmyalakshmi Subramanian, and Donald L. Smith. 2018. "Plant Growth-Promoting Rhizobacteria: Context, Mechanisms of Action, and Roadmap to Commercialization of Biostimulants for Sustainable Agriculture." *Frontiers in Plant Science* 871 (October): 1–17. https://doi.org/10.3389/fpls.2018.01473.

Badri, Dayakar V., Victor M. Loyola-Vargas, Corey D. Broeckling, Clelia De-la-Peña, Michal Jasinski, Diana Santelia, Enrico Martinoia, et al. 2008. "Altered Profile of Secondary Metabolites in the Root Exudates of Arabidopsis ATP-Binding Cassette Transporter Mutants." *Plant Physiology* 146 (2): 762–71. https://doi.org/10.1104/pp.107.109587.

Banerjee, Samiran, Klaus Schlaeppi, and Marcel G A Heijden. 2018. "Keystone Taxa as Drivers of Microbiome Structure and Functioning." https://doi.org/10.1038/s41579-018-0024-1.

Banerjee, Samiran, Klaus Schlaeppi, and Marcel G.A. van der Heijden. 2018. "Keystone Taxa as Drivers of Microbiome Structure and Functioning." *Nature Reviews Microbiology*, 2018. https://doi.org/10.1038/s41579-018-0024-1.

Bashan, Y. 1986. "Significance of Timing and Level of Inoculation with Rhizosphere Bacteria on Wheat Plants." *Soil Biology and Biochemistry* 18 (3): 297–301. https://doi.org/10.1016/0038-0717(86)90064-7.

Bouffaud, Marie-lara, Marie-andrée Poirier, Daniel Muller, and Yvan Moënne-loccoz. 2014. "Root Microbiome Relates to Plant Host Evolution in Maize and Other Poaceae" 16: 2804–14. https://doi.org/10.1111/1462-2920.12442.

Bouffaud, Marie Lara, Martina Kyselkov, Brigitte Gouesnard, Genevieve Grundmann, Daniel Muller, and Yvan Mo??nne-Loccoz. 2012. "Is Diversification History of Maize Influencing Selection of Soil Bacteria by Roots?" *Molecular Ecology*. https://doi.org/10.1111/j.1365-294X.2011.05359.x.

Bulgarelli, Davide, Ruben Garrido-Oter, Philipp C. Münch, Aaron Weiman, Johannes Dröge, Yao Pan, Alice C McHardy, and Paul Schulze-Lefert. 2015. "Structure and Function of the Bacterial Root Microbiota in Wild and Domesticated Barley." *Cell Host and Microbe* 17 (3): 392–403. https://doi.org/10.1016/j.chom.2015.01.011.

Bulgarelli, Davide, Klaus Schlaeppi, Stijn Spaepen, Emiel Ver Loren Van Themaat, and Paul Schulze-Lefert. 2013. "Structure and Functions of the Bacterial Microbiota of Plants." *Annual Review of Plant Biology*. https://doi.org/10.1146/annurev-arplant-050312-120106.

Busby, Posy E., Chinmay Soman, Maggie R. Wagner, Maren L. Friesen, James Kremer, Alison Bennett, Mustafa Morsy, Jonathan A. Eisen, Jan E. Leach, and Jeffery L. Dangl. 2017. "Research Priorities for Harnessing Plant Microbiomes in Sustainable Agriculture." *PLoS Biology* 15 (3): 1–14. https://doi.org/10.1371/journal.pbio.2001793.

Canarini, Alberto, Christina Kaiser, Andrew Merchant, Andreas Richter, and Wolfgang Wanek. 2019. "Root Exudation of Primary Metabolites: Mechanisms and Their Roles in Plant Responses to Environmental Stimuli." *Frontiers in Plant Science*. Frontiers Media S.A. https://doi.org/10.3389/fpls.2019.00157.

Cardinale, Massimiliano, Martin Grube, Armin Erlacher, Julian Quehenberger, and Gabriele Berg. 2015. "Bacterial Networks and Co-Occurrence Relationships in the Lettuce Root Microbiota." *Environmental Microbiology* 17 (1): 239–52. https://doi.org/10.1111/1462-2920.12686.

Castrillo, Gabriel, Paulo José Pereira Lima Teixeira, Sur Herrera Paredes, Theresa F. Law, Laura De Lorenzo, Meghan E. Feltcher, Omri M. Finkel, et al. 2017. "Root Microbiota Drive Direct Integration of Phosphate Stress and Immunity." *Nature* 543 (7646): 513–18. https://doi.org/10.1038/nature21417.

Cheng, F, and Z Cheng. 2015. "Research Progress on the Use of Plant Allelopathy in Agriculture and the Physiological and Ecological Mechanisms of Allelopathy." *Front. Plant Sci* 6: 1020. https://doi.org/10.3389/fpls.2015.01020.

Chuberre, Coralie, Barbara Plancot, Azeddine Driouich, John P. Moore, Muriel Bardor, Bruno Gügi, and Maïté Vicré. 2018. "Plant Immunity Is Compartmentalized and Specialized in Roots." *Frontiers in Plant Science* 871 (November): 1–13. https://doi.org/10.3389/fpls.2018.01692.

Coleman-Derr, Devin, Damaris Desgarennes, Citlali Fonseca-Garcia, Stephen Gross, Scott Clingenpeel, Tanja Woyke, Gretchen North, Axel Visel, Laila P. Partida-Martinez, and Susannah Tringe. 2015. "Biogeography and Cultivation Affect Microbiome Composition in the Drought-Adapted Plant Subgenus Agave." *In Review*, 798–811. https://doi.org/10.1111/nph.13697.

Cordovez, Viviane, Francisco Dini-Andreote, Víctor J Carrión, and Jos M Raaijmakers. 2019. "Ecology and Evolution of Plant Microbiomes." https://doi.org/10.1146/annurev-micro-090817.

Coskun, Devrim, Dev T Britto, Weiming Shi, and Herbert J Kronzucker. 2017. "Nitrogen Transformations in Modern Agriculture and the Role of Biological Nitrification Inhibition." *Nature Plants*. https://doi.org/10.1038/nplants.2017.74.

Cotton, T E Anne, Pierre Pétriacq, Duncan D Cameron, Moaed Al Meselmani, Roland Schwarzenbacher, Stephen A Rolfe, and Jurriaan Ton. 2019. "Metabolic Regulation of the Maize Rhizobiome by Benzoxazinoids." *The ISME Journal* 13: 1647–58. https://doi.org/10.1038/s41396-019-0375-2.

Dakora, Felix D, and Donald A Phillips. 2002. "Root Exudates as Mediators of Mineral Acquisition in Low-Nutrient Environments," 35–47.

Dam, Nicole M. van, and Harro J. Bouwmeester. 2016. "Metabolomics in the Rhizosphere: Tapping into Belowground Chemical Communication." *Trends in Plant Science* 21 (3): 256–65. https://doi.org/10.1016/j.tplants.2016.01.008.

Delaux, Pierre-Marc, and Sebastian Schornack. 2021. “Plant Evolution Driven by Interactions with Symbiotic and Pathogenic Microbes.” *Science* 371 (6531): eaba6605-undefined. https://doi.org/10.1126/science.aba6605.

Diamond, Jared. 2002. “Evolution, Consequences and Future of Plant and Animal Domestication.” *Nature* 418 (6898): 700–707. https://doi.org/10.1038/nature01019.

Ding, Long Jun, Hui Ling Cui, San An Nie, Xi En Long, Gui Lan Duan, and Yong Guan Zhu. 2019. “Microbiomes Inhabiting Rice Roots and Rhizosphere.” *FEMS Microbiology Ecology* 95 (5): 1–13. https://doi.org/10.1093/femsec/fiz040.

Edwards, Joseph, Cameron Johnson, Christian Santos-Medellín, Eugene Lurie, Natraj Kumar Podishetty, Srijak Bhatnagar, Jonathan A Eisen, and Venkatesan Sundaresan. 2014. “Structure, Variation, and Assembly of the Root-Associated Microbiomes of Rice.” *Proc Natl Acad Sci USA*. https://doi.org/10.1073/pnas.1414592112.

Eida, Abdul Aziz, Maren Ziegler, Feras F. Lafi, Craig T. Michell, Christian R. Voolstra, Heribert Hirt, and Maged M. Saad. 2018. “Desert Plant Bacteria Reveal Host Influence and Beneficial Plant Growth Properties.” Edited by Graziella Berta. *PLOS ONE* 13 (12): e0208223. https://doi.org/10.1371/journal.pone.0208223.

Favela, Alonso, Martin O. Bohn, and Angela D. Kent. 2021. “Maize Germplasm Chronosequence Shows Crop Breeding History Impacts Recruitment of the Rhizosphere Microbiome.” *ISME Journal*. https://doi.org/10.1038/s41396-021-00923-z.

Finkel, Omri M., Isai Salas-González, Gabriel Castrillo, Jonathan M. Conway, Theresa F. Law, Paulo José Pereira Lima Teixeira, Ellie D. Wilson, Connor R. Fitzpatrick, Corbin D. Jones, and Jeffery L. Dangl. 2020. “A Single Bacterial Genus Maintains Root Growth in a Complex Microbiome.” *Nature* 587 (7832): 103–8. https://doi.org/10.1038/s41586-020-2778-7.

Fitzpatrick, Connor R., Julia Copeland, Pauline W. Wang, David S. Guttman, Peter M. Kotanen, and Marc T.J. Johnson. 2018. “Assembly and Ecological Function of the Root Microbiome across Angiosperm Plant Species.” *Proceedings of the National Academy of Sciences of the United States of America* 115 (6): E1157–65. https://doi.org/10.1073/pnas.1717617115.

Fitzpatrick, Connor R, Anurag A Agrawal, Nathan Basiliko, Amy P Hastings, Marney E Isaac, Michael Preston, Marc T J Johnson, et al. 2019. “The Importance of Plant Genotype and Contemporary Evolution for Terrestrial Ecosystem Processes” 96 (10): 2632–42.

Foyer, Christine H., Graham Noctor, and Helmut F. van Emden. 2007. “An Evaluation of the Costs of Making Specific Secondary Metabolites: Does the Yield Penalty Incurred by Host Plant Resistance to Insects Result from Competition for Resources?” *International Journal of Pest Management* 53 (3): 175–82. https://doi.org/10.1080/09670870701469146.

Fragasso, Mariagiovanna, Anna Iannucci, and Roberto Papa. 2013. “Durum Wheat and Allelopathy: Toward Wheat Breeding for Natural Weed Management.” *Frontiers in Plant Science* 4 (SEP): 1–8. https://doi.org/10.3389/fpls.2013.00375.

Galloway, James N, Alan R Townsend, Jan Willem Erisman, Mateete Bekunda, Zucong Cai, John R Freney, Luiz A Martinelli, Sybil P Seitzinger, and Mark A Sutton. 2008. “Transformattion of the Nitrogen Cycle: Recent Trends, Questions, and Potential Solutions.” *Science* 320: 889–92. http://science.sciencemag.org/content/sci/320/5878/889.full.pdf.

Hallauer, Arnel R. 2009. “Corn Breeding.” *Iowa State Research Farm Progress Reports*. http://lib.dr.iastate.edu/farms_reports/475.

Hart, Miranda M., Pedro M. Antunes, Veer Bala Chaudhary, and Lynette K. Abbott. 2018. "Fungal Inoculants in the Field: Is the Reward Greater than the Risk?" *Functional Ecology* 32 (1): 126–35. https://doi.org/10.1111/1365-2435.12976.

Hu, Lingfei, Christelle A.M. Robert, Selma Cadot, Xi Zhang, Meng Ye, Beibei Li, Daniele Manzo, et al. 2018. "Root Exudate Metabolites Drive Plant-Soil Feedbacks on Growth and Defense by Shaping the Rhizosphere Microbiota." *Nature Communications* 9 (1). https://doi.org/10.1038/s41467-018-05122-7.

Huang, Ancheng C, Ting Jiang, Yong Xin Liu, Yue Chen Bai, James Reed, Baoyuan Qu, Alain Goossens, Hans Wilhelm Nützmann, Yang Bai, and Anne Osbourn. 2019. "A Specialized Metabolic Network Selectively Modulates Arabidopsis Root Microbiota." *Science* 364 (6440). https://doi.org/10.1126/science.aau6389.

Hubbard, Charley J, Marcus T Brock, Linda Ta Van Diepen, Loïs Maignien, Brent E Ewers, and Cynthia Weinig. 2017. "The Plant Circadian Clock Influences Rhizosphere Community Structure and Function." *Nature Publishing Group* 12 (10). https://doi.org/10.1038/ismej.2017.172.

Jones, Jonathan D G, and Jeffery L. Dangl. 2006. "The Plant Immune System." *Nature* 444 (7117): 323–29. https://doi.org/10.1038/nature05286.

Kim, Hyun, and Yong-Hwan Lee. 2019. "Phytobiomes Journal • XXXX • XX:X-X The Rice Microbiome: A Model Platform for Crop Holobiome." https://doi.org/10.1094/PBIOMES-07-19-0035-RVW.

Kong, Zhaoyu, Miranda Hart, and Hongguang Liu. 2018. "Paving the Way from the Lab to the Field: Using Synthetic Microbial Consortia to Produce High-Quality Crops." *Frontiers in Plant Science* 9 (October): 1–5. https://doi.org/10.3389/fpls.2018.01467.

Korenblum, Elisa, Yonghui Dong, Jedrzej Szymanski, Sayantan Panda, Adam Jozwiak, Hassan Massalha, Sagit Meir, Ilana Rogachev, and Asaph Aharoni. 2020. "Rhizosphere Microbiome Mediates Systemic Root Metabolite Exudation by Root - to - Root Signaling." *PNAS*, 1–10. https://doi.org/10.1073/pnas.1912130117.

Kudjordjie, Enoch Narh, Rumakanta Sapkota, Stine K Steffensen, Inge S Fomsgaard, and Mogens Nicolaisen. 2019. "Maize Synthesized Benzoxazinoids Affect the Host Associated Microbiome." *Microbiome* 7 (1). https://doi.org/10.1186/s40168-019-0677-7.

Kwak, Min Jung, Hyun Gi Kong, Kihyuck Choi, Soon Kyeong Kwon, Ju Yeon Song, Jidam Lee, Pyeong An Lee, et al. 2018. "Rhizosphere Microbiome Structure Alters to Enable Wilt Resistance in Tomato." *Nature Biotechnology* 36 (11): 1100–1116. https://doi.org/10.1038/nbt.4232.

Lebeis, Sarah L. 2014. "The Potential for Give and Take in Plant-Microbiome Relationships." *Frontiers in Plant Science* 5 (June): 1–6. https://doi.org/10.3389/fpls.2014.00287.

Levy, Asaf, Isai Salas Gonzalez, Maximilian Mittelviefhaus, Scott Clingenpeel, Sur Herrera Paredes, Jiamin Miao, Kunru Wang, et al. 2018. "Genomic Features of Bacterial Adaptation to Plants." *Nature Genetics* 50 (1): 138–50. https://doi.org/10.1038/s41588-017-0012-9.

Lundberg, Derek S., Sarah L. Lebeis, Sur Herrera Paredes, Scott Yourstone, Jase Gehring, Stephanie Malfatti, Julien Tremblay, et al. 2012. "Defining the Core Arabidopsis Thaliana Root Microbiome." *Nature* 488 (7409): 86–90. https://doi.org/10.1038/nature11237.

Mahoney, Aaron K., Chuntao Yin, and Scot H. Hulbert. 2017. "Community Structure, Species Variation, and Potential Functions of Rhizosphere-Associated Bacteria of Different Winter Wheat (Triticum Aestivum) Cultivars." *Frontiers in Plant Science* 8 (February): 1–14. https://doi.org/10.3389/fpls.2017.00132.

Marasco, Ramona, María J Mosqueira, Marco Fusi, Jean Baptiste Ramond, Giuseppe Merlino, Jenny M Booth, Gillian Maggs-Kölling, Don A Cowan, and Daniele Daffonchio. 2018. "Rhizosheath Microbial Community Assembly of Sympatric Desert Speargrasses Is Independent of the Plant Host." *Microbiome* 6 (1). https://doi.org/10.1186/s40168-018-0597-y.

Matthews, Andrew, Sarah Pierce, Helen Hipperson, and Ben Raymond. 2019. "Rhizobacterial Community Assembly Patterns Vary between Crop Species." *Frontiers in Microbiology* 10 (APR): 1–13. https://doi.org/10.3389/fmicb.2019.00581.

Mikic, Sanja, and Shakoor Ahmad. 2018. "Benzoxazinoids - Protective Secondary Metabolites in Cereals: The Role and Application." *Ratar. Povrt.* 55 (1): 49–57. http://ridum.umanizales.edu.co:8080/jspui/bitstream/6789/377/4/Muñoz_Zapata_Adriana_Patricia_Artículo_2011.pdf.

Mora, Camilo, Daniele Spirandelli, Erik C. Franklin, John Lynham, Michael B. Kantar, Wendy Miles, Charlotte Z. Smith, et al. 2018. "Broad Threat to Humanity from Cumulative Climate Hazards Intensified by Greenhouse Gas Emissions." *Nature Climate Change* 8 (12): 1062–71. https://doi.org/10.1038/s41558-018-0315-6.

Morella, Norma M., Francis Cheng Hsuan Weng, Pierre M. Joubert, C. Jessica E. Metcalf, Steven Lindow, and Britt Koskella. 2019. "Successive Passaging of a Plant-Associated Microbiome Reveals Robust Habitat and Host Genotype-Dependent Selection." *BioRxiv*. https://doi.org/10.1101/627794.

Neal, Andrew L., Shakoor Ahmad, Ruth Gordon-Weeks, and Jurriaan Ton. 2012. "Benzoxazinoids in Root Exudates of Maize Attract Pseudomonas Putida to the Rhizosphere." *PLoS ONE* 7 (4). https://doi.org/10.1371/journal.pone.0035498.

Neal, J. L., Ruby I. Larson, and T. G. Atkinson. 1973. "Changes in Rhizosphere Populations of Selected Physiological Groups of Bacteria Related to Substitution of Specific Pairs of Chromosomes in Spring Wheat." *Plant and Soil* 39 (1): 209–12. https://doi.org/10.1007/BF00018061.

O'Brien, Anna M., Chandra N. Jack, Maren L. Friesen, and Megan E. Frederickson. 2021. "Whose Trait Is It Anyways? Coevolution of Joint Phenotypes and Genetic Architecture in Mutualisms." *Proceedings. Biological Sciences* 288 (1942): 20202483. https://doi.org/10.1098/rspb.2020.2483.

Oxtoby, Elli, and Monica A. Hughes. 1989. "Breeding for Herbicide Resistance Using Molecular and Cellular Techniques." *Euphytica* 40 (1–2): 173–80. https://doi.org/10.1007/BF00023313.

Pascale, Alberto, Silvia Proietti, Iakovos S Pantelides, and Ioannis A Stringlis. 2020. "Modulation of the Root Microbiome by Plant Molecules: The Basis for Targeted Disease Suppression and Plant Growth Promotion." *Frontiers in Plant Science*. https://doi.org/10.3389/fpls.2019.01741.

Peiffer, J. A., A. Spor, O. Koren, Z. Jin, S. G. Tringe, J. L. Dangl, E. S. Buckler, and R. E. Ley. 2013. "Diversity and Heritability of the Maize Rhizosphere Microbiome under Field Conditions." *Proceedings of the National Academy of Sciences* 110 (16): 6548–53. https://doi.org/10.1073/pnas.1302837110.

Pérez-Jaramillo, Juan E, Víctor J Carrión, Mattias de Hollander, and Jos M Raaijmakers. 2018. "The Wild Side of Plant Microbiomes." *Microbiome* 6 (1). https://doi.org/10.1186/s40168-018-0519-z.

Philippot, Laurent, Jos M Raaijmakers, Philippe Lemanceau, and Wim H. Van Der Putten. 2013. "Going Back to the Roots: The Microbial Ecology of the Rhizosphere." *Nature Reviews Microbiology* 11 (11): 789–99. https://doi.org/10.1038/nrmicro3109.

Porter, Stephanie S, and Joel L Sachs. 2020. "Agriculture and the Disruption of Plant–Microbial Symbiosis." *Trends in Ecology and Evolution*. https://doi.org/10.1016/j.tree.2020.01.006.

S. R. Gupta, Vadakattu V., and Anil K. Sharma. 2021. *Rhizosphere Biology: Interactions Between Microbes and Plants*.

Saad, Maged M, Abdul Aziz Eida, Heribert Hirt, and Peter Doerner. 2020. "Tailoring Plant-Associated Microbial Inoculants in Agriculture: A Roadmap for Successful Application." *Journal of Experimental Botany*. https://doi.org/10.1093/jxb/eraa111.

Sandal, Niels, Thomas Rørby Petersen, Jeremy Murray, Yosuke Umehara, Bogumil Karas, Koji Yano, Hirotaka Kumagai, et al. 2006. "Genetics of Symbiosis in Lotus Japonicus: Recombinant Inbred Lines, Comparative Genetic Maps, and Map Position of 35 Symbiotic Loci." *Molecular Plant-Microbe Interactions* 19 (1): 80–91. https://doi.org/10.1094/MPMI-19-0080.

Sasse, Joelle, Jacob S Jordan, Markus Deraad, Katherine Whiting, Katherina Zhalnina, and Trent Northen. n.d. "Root Morphology and Exudate Availability Is Shaped by Particle Size and Chemistry in Brachypodium Distachyon Authors and Affiliations." Accessed September 9, 2019. https://doi.org/10.1101/651570.

Sasse, Joelle, Enrico Martinoia, and Trent Northen. 2018. "Feed Your Friends: Do Plant Exudates Shape the Root Microbiome?" *Trends in Plant Science* 23 (1): 25–41. https://doi.org/10.1016/j.tplants.2017.09.003.

Schlaeppi, Klaus, Nina Dombrowski, R. G. Oter, E. Ver Loren van Themaat, and Paul Schulze-Lefert. 2014. "Quantitative Divergence of the Bacterial Root Microbiota in Arabidopsis Thaliana Relatives." *Proceedings of the National Academy of Sciences* 111 (2): 585–92. https://doi.org/10.1073/pnas.1321597111.

Seabloom, Eric W., Elizabeth T. Borer, Bradford Condon, Linda Kinkel, Candice Lumibao, and Georgiana May. 2019. "Effects of Nutrient Supply, Herbivory, and Host Community on Fungal Endophyte Diversity." *Ecology* 0 (0): 1–13. https://doi.org/10.1002/ecy.2758.

Sessitsch, Angela, Nikolaus Pfaffenbichler, and Birgit Mitter. 2019. "Microbiome Applications from Lab to Field: Facing Complexity." *Trends in Plant Science*. https://doi.org/10.1016/j.tplants.2018.12.004.

Smith, Pete, Daniel Martino, Zucong Cai, Daniel Gwary, Henry Janzen, Pushpam Kumar, Bruce McCarl, et al. 2008. "Greenhouse Gas Mitigation in Agriculture." *Philosophical Transactions of the Royal Society B: Biological Sciences*. https://doi.org/10.1098/rstb.2007.2184.

Stringlis, Ioannis A, Ke Yu, Kirstin Feussner, Ronnie De Jonge, Sietske Van Bentum, Marcel C Van Verk, Roeland L Berendsen, Peter A.H.M. Bakker, Ivo Feussner, and Corné M.J. Pieterse. 2018. "MYB72-Dependent Coumarin Exudation Shapes Root Microbiome Assembly to Promote Plant Health." *Proceedings of the National Academy of Sciences of the United States of America* 115 (22): E5213–22. https://doi.org/10.1073/pnas.1722335115.

Svistoonoff, Sergio, Florence Auguy, Katharina Markmann, Gabor Giczey, Hassen Gherbi, Martin Parniske, Joan Estevan, et al. 2008. “SymRK Defines a Common Genetic Basis for Plant Root Endosymbioses with Arbuscular Mycorrhiza Fungi, Rhizobia, and Frankiabacteria.” *Proceedings of the National Academy of Sciences* 105 (12): 4928–32. https://doi.org/10.1073/pnas.0710618105.

Trethowan, Richard M., and A. Mujeeb-Kazi. 2008. “Novel Germplasm Resources for Improving Environmental Stress Tolerance of Hexaploid Wheat.” *Crop Science*. https://doi.org/10.2135/cropsci2007.08.0477.

Vandenkoornhuyse, Philippe, Achim Quaiser, Marie Duhamel, Amandine Le Van, and Alexis Dufresne. 2015. “The Importance of the Microbiome of the Plant Holobiont.” *New Phytologist* 206 (4): 1196–1206. https://doi.org/10.1111/nph.13312.

Vigdis Torsvik, Lise Øvreås. 2002. “Microbial Diversity and Function in Soil: From Genes to Ecosystems.” *Current Opinion in Microbiology* 5:240–245. https://ac.els-cdn.com/S1369527402003247/1-s2.0-S1369527402003247-main.pdf?_tid=cfe2f573-92db-4e97-a0c9-e1ec283ca71e&acdnat=1524029182_2920354489713a9dfdb6b9a15cfbccbf.

Waksman, Selman. 1927. *Principles of Soil Microbiology*.

Walters, William A, Zhao Jin, Nicholas Youngblut, Jason G Wallace, Jessica Sutter, Wei Zhang, Antonio González-Peña, et al. 2018. “Large-Scale Replicated Field Study of Maize Rhizosphere Identifies Heritable Microbes.” *Proceedings of the National Academy of Sciences of the United States of America* 115 (28): 7368–73. https://doi.org/10.1073/pnas.1800918115.

Whitham, Thomas G., Joseph K. Bailey, Jennifer A. Schweitzer, Stephen M. Shuster, Randy K. Bangert, Carri J. Leroy, Eric V. Lonsdorf, et al. 2006. “A Framework for Community and Ecosystem Genetics: From Genes to Ecosystems.” *Nature Reviews Genetics*. https://doi.org/10.1038/nrg1877.

Whitham, Thomas G., Catherine A. Gehring, Louis J. Lamit, Todd Wojtowicz, Luke M. Evans, Arthur R. Keith, and David Solance Smith. 2012. “Community Specificity: Life and Afterlife Effects of Genes.” *Trends in Plant Science*. https://doi.org/10.1016/j.tplants.2012.01.005.

Wille, Lukas, Monika M. Messmer, Bruno Studer, and Pierre Hohmann. 2019. “Insights to Plant–Microbe Interactions Provide Opportunities to Improve Resistance Breeding against Root Diseases in Grain Legumes.” *Plant Cell and Environment* 42 (1): 20–40. https://doi.org/10.1111/pce.13214.

Woo, Sheridan L., and Olimpia Pepe. 2018. “Microbial Consortia: Promising Probiotics as Plant Biostimulants for Sustainable Agriculture.” *Frontiers in Plant Science* 9 (2003): 7–12. https://doi.org/10.3389/fpls.2018.01801.

Xu, Jin, Yunzeng Zhang, Pengfan Zhang, Pankaj Trivedi, Nadia Riera, Yayu Wang, Xin Liu, et al. 2018. “The Structure and Function of the Global Citrus Rhizosphere Microbiome.” *Nature Communications* 9 (1): 4894. https://doi.org/10.1038/s41467-018-07343-2.

Zachow, Christin, Henry Müller, Ralf Tilcher, Gabriele Berg, and Yusuke Saijo. 2014. “Differences between the Rhizosphere Microbiome of Beta Vulgaris Ssp. Maritima-Ancestor of All Beet Crops-and Modern Sugar Beets.” https://doi.org/10.3389/fmicb.2014.00415.

Zgadzaj, Rafal, Ruben Garrido-Oter, Dorthe Bodker Jensen, Anna Koprivova, Paul Schulze-Lefert, and Simona Radutoiu. 2016. “Root Nodule Symbiosis in Lotus Japonicus Drives the Establishment of Distinctive Rhizosphere, Root, and Nodule Bacterial Communities.” *Proceedings of the National Academy of Sciences of the United States of America* 113 (49): E7996–8005. https://doi.org/10.1073/pnas.1616564113.

Zhalnina, Kateryna, Katherine B Louie, Zhao Hao, Nasim Mansoori, Ulisses Nunes Da Rocha, Shengjing Shi, Heejung Cho, et al. 2018. “Dynamic Root Exudate Chemistry and Microbial Substrate Preferences Drive Patterns in Rhizosphere Microbial Community Assembly.” *Nature Microbiology* 3 (4): 470–80. https://doi.org/10.1038/s41564-018-0129-3.

CHAPTER 2: MAIZE GERMPLASM CHRONOSEQUENCE SHOWS CROP BREEDING HISTORY IMPACTS RECRUITMENT OF THE RHIZOSPHERE MICROBIOME[1]

Abstract:

Recruitment of microorganisms to the rhizosphere varies among plant genotypes, yet an understanding of whether the microbiome can be altered by selection on the host is relatively unknown. Here, we performed a common garden study to characterize recruitment of rhizosphere microbiome functional groups for 20 expired Plant Variety Protection Act maize lines spanning a chronosequence of development from 1949 to 1986. This time frame brackets a series of agronomic innovations, namely improvements in breeding and the application of synthetic nitrogenous fertilizers, technologies that define modern industrial agriculture. We assessed the impact of chronological agronomic improvements on recruitment of the rhizosphere microbiome in maize, with emphasis on nitrogen cycling functional groups. Additionally, we quantified the microbial genes involved in nitrogen cycling and predicted functional pathways present in the microbiome of each genotype. Both genetic relatedness of host plant and decade of germplasm development were significant factors in the recruitment of the rhizosphere microbiome. More recently developed germplasm recruited fewer microbial taxa with the genetic capability for sustainable nitrogen provisioning and larger populations of microorganisms that contribute to N losses. This study indicates that the development of high-yielding varieties and agronomic management approaches of industrial agriculture inadvertently modified interactions between maize and its microbiome.

[1] **This is the peer reviewed version of the following article:** Favela, A., O. Bohn, M. & D. Kent, A. Maize germplasm chronosequence shows crop breeding history impacts recruitment of the rhizosphere microbiome. ISME J (2021). https://doi.org/10.1038/s41396-021-00923-z

Introduction:

For the past 70 years, modern industrial agriculture has been characterized by technological advances in crop breeding and high input application of nitrogenous fertilizers (Evenson and Gollin 2003). Adoption of these agricultural practices has led to increases in global food security, human population growth, and spurred industrialization (Evenson and Gollin 2003). While the benefits of these advances for humanity cannot be overstated, they also have far-reaching environmental consequences from the overuse of inorganic nitrogen fertilizers (Vitousek et al. 1997). Currently, more than five million tons of nitrogen fertilizer is applied annually to maize production in the United States (USDA (National Agricultural Statistics Service).). A large fraction of nitrogen fertilizer applied to arable lands is lost through microbial transformations that alter the mobility of nitrogen (Robertson and Vitousek 2009; Davidson et al. 2012). Understanding how the plant-associated microbiome has been altered by technological innovations in agriculture could assist in addressing these agronomic problems (Busby et al. 2017). Sustaining future agricultural demands will require controlling the detrimental outcomes of the industrial agricultural systems pioneered over the past century.

Assembly of the plant rhizosphere microbiome is driven by plant genetic and evolutionary history (Yeoh et al. 2017). Plant microbiomes play a major role in altering plant resilience, fitness, nutrition, and productivity (Busby et al. 2017). Plant hosts selectively filter microorganisms that colonize their rhizosphere (Bulgarelli et al. 2013; Philippot et al. 2013). This selective process is heritable across plant cultivars (Peiffer et al. 2013; Walters et al. 2018), yet the implication of heritability on rhizosphere microbiome *function* has been relatively unexplored. In modern agriculture, microbiome functions that contribute to crop growth and sustainability have been replaced with agronomic management practices, and the development of

modern crop germplasm has been carried out without consideration of the plant microbiome and its functions as an extended phenotype of the crop genome.

Throughout the 20th century, maize breeders have made concerted efforts to optimize yield under a range of agronomic management environments (Smith et al. 2004; FAO 2020). Since the 1930s, advances in breeding and agricultural management have resulted in steady increases in yield (Duvick, Smith, and Cooper 2003). The introduction of synthetic nitrogen fertilizers to maize began in the 1940s and reached modern levels around the 1980s (Cao, Lu, and Yu 2018). During this time, germplasm was selected to produce the greatest grain yield possible under increased nitrogen conditions and plant density (Duvick, Smith, and Cooper 2003). The selection of maize over this period resulted in alterations to plant nitrogen acquisition, root architecture, insect pest interactions, and grain quality (Khush 1999; Haegele et al. 2013; Hauck et al. 2014; York et al. 2015). Additionally, similar selection pressures in other major cereal crops, rice and wheat, have shown modulation of plant carbon and nitrogen metabolism, resulting in less efficient nitrogen usage (Li et al. 2018). Without selection for maintenance of microbiome functions that contribute to sustainable nutrient acquisition, crop breeding carried out under high nitrogen (N) conditions may have altered how maize interacts with its rhizosphere nitrogen cycling taxa.

Here, we used a germplasm chronosequence of expired Plant Variety Protection Act maize inbred lines ranging from 1949 to 1986 (Hauck et al. 2014). These lines act as a genotypic time capsule of the extended phenotype selected by the historic agronomic breeding environment. This time frame was selected as it covers the introduction and increased usage of synthetic N-fertilizers (Fig. 2.1, Table A.1). The lines used in the study come from two major

genetic families: Stiff Stalk (SS) and Non-Stiff Stalk (NSS). These heterotic groups represent the inbred genetic diversity underlying our modern agricultural elite hybrid varieties.

The goal of this study was to examine if breeding and selection of maize genotypes during the decades of increasing nitrogen application altered how maize germplasm recruits its rhizosphere microbiome, as well as microbiome function. First, we set out to determine if the bacterial and fungal rhizosphere microbiome changed across our chronosequence of maize germplasm. Second, we sought to determine if maize lines developed over the past 50 years differ in their ability to recruit microbial functional groups related to nitrification, denitrification, and nitrogen fixation. Finally, to understand how the metabolic genes of rhizosphere microorganisms change across the germplasm chronosequence, we predicted the metabolic pathways of microbes that responded to the germplasm chronosequence. These results will allow us to determine if crop breeding for yield combined with changing agricultural practices disrupted the interactions between plants and their microbiomes, with potential consequences for nutrient cycling in agroecosystems. If modern breeding has unintentionally transformed interaction of maize with key functional groups in its microbiome, it must be rewilded to improve agroecosystem sustainability.

Materials and Methods:

Plant genotype selection and greenhouse experiment

Maize seed stocks were obtained from the USDA North Central Regional Plant Introduction Station (Ames, Iowa) and Maize Genetics Cooperation Stock Center (Urbana, Illinois). Twenty inbred lines were selected for comparison: these 20 lines span a breeding period from 1949-1986, come from two heterotic genetic groups (SS, NSS), and are adapted for maize

production in the U.S. Corn Belt (Table A.1). The usage of heterotic groups as a treatment factor was validated using genetic information collected in (Romay et al. 2013) and available at www.panzea.org. Supplemental Figure A.7 shows that maize genomes cluster based on heterotic genetic grouping. Additional metadata on these lines was acquired from Maize GDB (www.maizegdb.org) and USDA GRIN (www.ars-grin.gov). More information about the history and development of these maize lines is presented in Table A.1. Seeds were surface sterilized by soaking for 5 mins in 8.25% NaClO, followed by one rinse with sterilized distilled water, a single rinse of 70% ethanol, and three rinses with sterile distilled water. Surface-sterilized seeds were dried on sterile filter paper in a sterile petri dish, then stored at 4°C overnight before sowing.

Maize lines were grown in greenhouse conditions to isolate the effects of inbred genotype on the microbiome. Planting medium was a combination of live and autoclaved soil mix. The live inoculum soil was collected from agricultural soil located on the Crop Sciences Research and Education Center - South Farms at the University of Illinois at Urbana-Champaign, Urbana, IL. (40°03'31.0"N 88°14'13.4"W). At the time, the soil was out of agricultural rotation (corn-soy) for at least 2 years. Inoculum soil was sieved (2mm) then added (10%) to a steam pasteurized mix of soil: calcined clay: torpedo sand (1:1:1). An inoculum sample was collected before plant growth to characterize the microbiome before plant treatment. For each genotype, 10 replicate classic 600 pots (2 gallon) were sown with three seeds in each. Pots were thinned a week after germination leaving only a single plant per pot for the remainder of growth. In total, 200 plants were grown. They were placed in a completely randomized design in the greenhouse with 16 hours of light and 8 hours of darkness. All plants were connected to an irrigation system that fertilized plants twice a week. Plants were fertilized with a liquid nutrient solution, specifically

Cal-Mag (N15-P5-K15), at a rate of 150 ppm. Nitrogen was applied as 11.8% nitrate nitrogen, 1.1% ammoniacal nitrogen, and 2.1% urea nitrogen. All plant treatments were maintained under the same fertilizer regime. While direct comparison of greenhouse fertilization regime to field rates is difficult, the nitrogen level used in this study would be comparable to modern high fertilization levels (Fig. 2.1).

Implementation of this study in the greenhouse allowed for reduced complexity of environmental factors and homogenization of diverse soil microbiomes typical for a field setting. By reducing random variation, we gained further precision and insight on how different genotypes alter a standardized microbiome.

The roots were harvested 36 days after emergence. Plants were approximately in V4-V5 growth stage with 4-6 fully collared leaves. Plant rhizospheres were harvested by extracting root systems from the soil and shaking vigorously to separate loosely adhering soil. Rhizosphere soil was extracted by placing the root system in a 1-liter bottle with 40 mL of sterile distilled water and shaking vigorously for 5 minutes. The resulting soil slurry was placed into 50 mL centrifuge tubes and lyophilized before DNA extraction using the FastDNA for Soil DNA extraction kit (MPBio, Solon, OH). Rhizosphere samples of all 10 replicates for each genotype were harvested for molecular analysis.

Microbial community amplicon sequencing

For this experiment, we characterized the microbiome and diagnostic functional genes related to transformations that occur in the nitrogen cycle: nitrogen fixation, nitrification, and denitrification. Amplicon sequencing was performed on prokaryotic 16S rRNA genes, fungal ITS2, *amoA, nirS, nirK, nosZ, norB,* and *nifH* genes. The Fluidigm Access Array IFC chip was used to prepare sequencing amplicons. This method allows for the simultaneous amplification of

target functional genes using multiple primer sets (Fluidigm, San Francisco, CA). DNA sequencing was performed for bacterial, archaeal, and fungal amplicons using an Illumina HiSeq 2500 Sequencing System (Illumina, San Diego, CA). Primer information is provided in supplemental Table A.2. Fluidigm amplification and Illumina sequencing were conducted at the Roy J. Carver Biotechnology Center, University of Illinois (Urbana, IL, USA). Fast Length Adjustment of Short reads (FLASH) (Mag and Salzberg 2011) software was used to merge paired-end sequences from 16S rRNA genes. For functional genes and fungal ITS, only forward read sequences were used. Once reads were merged, they were filtered by quality using the FASTX-Toolkit (Gordon, Hannon, and Gordon 2014). Reads that did not have a minimum quality score of 30 across 90% of the bases were removed. Using the FASTX-Toolkit, *nirK* reads were trimmed to its amplicon size of 165-bp.

Once quality preprocessing was performed, FASTQ reads were converted to FASTA format. Using USEARCH-UPARSE version 8.1 (Edgar 2010a), sequences were binned into discrete OTUs based on 97% similarity and singleton DNA sequences were removed. Quantitative Insights into Microbial Ecology (QIIME) was used to generate OTU tables for downstream statistical analysis and to assign taxonomic information, this is done with a combination of the UCLUST algorithm and SILVA database (Edgar 2010b; Quast et al. 2013). Once taxonomy was assigned, chloroplast and mitochondrial OTUs were removed from the dataset. Rarefaction was performed to correct for differential sequencing depth across samples. Functional gene sequences were also assigned using QIIME (Caporaso et al. 2010) with the BLAST (Altschul et al. 1997) algorithm and custom gene-specific databases generated from reference sequences obtained from the FunGene repository (http://fungene.cme.msu.edu/) (Fish

et al. 2013). All OTU tables used in statistical analyses were generated in QIIME. Singleton OTUs were filtered prior to statistical analysis.

The number of raw reads generated from sequencing run, reads present after quality filter, and the rarefaction level of reads per sample for 16S rRNA, ITS, and N-cycling genes are reported in supplemental Table A.3. Amplicon sequence data for 16S rRNA genes, fungal ITS2 region, and N-cycling functional genes is available for download on the NCBI SRA database at accession number: PRJNA635735 (https://www.ncbi.nlm.nih.gov/sra/PRJNA635735).

Quantifying nitrogen cycling functional groups

Quantitative PCR (qPCR) was used to determine the abundance of functional genes in each of the rhizosphere microbial communities. Specific target amplification (STA), explained in (Ishii et al. 2014), was carried out on samples and standards to increase template DNA for amplification. STA and qPCR master mix recipes from (Edwards et al. 2018) were used for all samples. STA product and qPCR master mix were loaded into the Dynamic Array™ Microfluidics Fluidigm Gene Expression chip where amplification and quantification of functional genes were carried out simultaneously (Fluidigm, San Francisco, CA). All samples and standards were analyzed in 12 technical replicates. Fluidigm Real-Time PCR Analysis software version 4.1.3 was used to calculate gene threshold cycles (C_T). C_T values were converted to gene copy number using gene length and standard curves. All Fluidigm qPCR was conducted at the Roy J. Carver Biotechnology Center (Urbana, IL, USA). The final copy number of each functional gene amplicon was standardized by the ng of template DNA in the qPCR reaction.

Statistical analysis

The microbial communities were evaluated as separate datasets for each amplicon (16S rRNA, fungal ITS, *nifH, nosZ, norB, nirK, nirS*, bacterial *amoA* and archaeal *amoA*). The relative effect of genotype, heterotic group, genetic relatedness, and decade of germplasm development on the rhizosphere microbiome composition was assessed using permutational analysis of variance (PERMANOVA) with the 'adonis' function, from the community ecology R package, 'vegan' (Oksanen et al. 2007). To visualize differences from these models, non-metric multidimensional scaling (NMDS) ordinations were created using R package 'phyloseq' and plotted with R package 'ggplot2' (McMurdie and Holmes 2013; Wickham 2007). Significant differences in functional gene abundance were evaluated using an ANOVA model, and the Tukey's HSD test from the 'stats' package in base R (R Core Team 2013). Correlation between year of germplasm development and gene abundance was evaluated using 'cor.test' and 'lm', packages in base R (R Core Team 2013). Using the 'asreml-r' package (Butler et al. 2017), additional restricted maximum-likelihood mixed effects models were used to examine the correlation between functional gene abundance and year of germplasm development while controlling for the genetic relatedness between maize inbred lines. TASSEL was used to calculate the pedigree tree, genetic relatedness matrix, and the haplotype diversity (Tajima's D) across the genome (Bradbury et al. 2007; Korneliussen et al. 2013).

To control for the variance within individual genotypes when performing our analysis for decade and heterotic group effects, we used the mean microbiome for each genotype (n=10) (referred to as the genotypic mean microbiome). These mean microbial communities were generated using the 'aggregate' function in base R; here this function was used to find the mean of the amplicon data matrix based on the replicates within each genotype.

Modules of microbial taxa responding to the germplasm chronosequence were determined using a weighted correlation network analysis (WGCNA) in R (Langfelder and Horvath 2008). Prior to WGCNA, amplicon data was transformed using a central log ratio transformation (Gloor et al. 2017). PICRUSt2 was used to predict functional pathways present in modules of microbial taxa that change over the germplasm chronosequence (Douglas et al. 2020). Additional meta-information on predicted PICRUSt2 output was obtained from MetaCyc Database (Caspi et al. 2016). Similarity percentages analysis (SIMPER) from the 'vegan' package was carried out to identify metabolic pathways that were significantly altered in representation across the germplasm chronosequence (Clarke 1993). Correlation between year of germplasm release and pathway abundance was evaluated using 'cor.test' and 'lm' packages in R.

Results:

In this common garden study, we identified 15,072 different 16S rRNA operational taxonomic units (OTUs, 97% similarity), and 1027 fungal OTUs were identified from the ITS2 region.

Rhizosphere microbiome response across the maize germplasm chronosequence

The decade of germplasm development, heterotic genetic group, and genotype all had a significant effect on rhizosphere microbiome composition. Plant genotype explained a significant amount of variance in the rhizosphere microbiome (PERMANOVA prokaryotic: R^2=0.17, $p<0.001$; fungal: R^2=0.13, $p<0.001$). When performing our analysis on the genotypic mean microbiome, we revealed that decade of germplasm development explained 16.79% of the variance in the prokaryotic microbiome. In comparison, heterotic group explained 8.1% of the variance (Fig. 2.2A, 2.2B, decade $p<0.01$, heterotic $p<0.008$, Table A.4.1). Fungal microbiomes

did not significantly respond to the germplasm chronosequence ($p = 0.37$) but differed among heterotic groups ($p = 0.028$) (Fig. 2.2C, 2.2D and Table A.4.2).

Response of nitrogen cycling functional groups to the germplasm chronosequence

From our analysis of nitrogen cycling functional genes, we observed 1498 *nifH* OTUs, 95 archaeal *amoA* OTUs, 200 bacterial *amoA* OTUs, 8632 *nirK* OTUs, 1186 *nirS* OTUs, 1068 *norB* OTUs, and 1864 *nosZ* OTUs. In response to the germplasm chronosequence, 3 of 7 nitrogen cycling genes showed changes in community membership, and 3 of 7 nitrogen cycling genes changed in copy number per ng of DNA (Table A.5).

Nitrogen fixation genes

There is a clear shift in the recruitment of nitrogen fixing taxa across the germplasm chronosequence (Fig 2.3A, Table A.5). The composition of diazotrophs, detected through the nitrogenase *nifH* gene, was significantly impacted by the decade of germplasm development (R^2=0.16, $p<0.001$) and heterotic group (R^2=0.13, $p<0.009$), Fig. 2.3A, Table A.6). The qPCR results also showed that the abundance of *nifH* in the microbiome significantly decreased across the germplasm chronosequence (r= -0.44, $p<0.05$, Fig. 2.3B, linear model statistics in Table A.9.3). These differences were detected even though the use of N fertilizer in our experiment abrogated any reliance on N fixation.

Nitrification genes

The recruitment of nitrifiers (indicated by gene sequences for bacterial and archaeal ammonia monooxygenase – *amoA*) was shown to be significantly impacted by the germplasm chronosequence and heterotic group. We found a significant change in the composition of bacterial *amoA* genes (R^2=0.13, $p<0.05$, Fig. 2.3C, Tables A.7.1), but did not see a significant change in the abundance of bacterial *amoA* detected in response to the chronosequence ($p=0.14$,

Table A.9.2). Archaeal nitrifiers showed no change in community composition over the chronosequence, but archaeal *amoA* genes did increase in abundance ($p<0.05$, Tables A.7.2, A.9.1). Total gene abundance of bacterial and archaeal *amoA* is significantly correlated with our chronosequence ($r=0.47$, $p<0.05$, Fig. 2.3D, Table A.9).

Denitrification genes

Several of the denitrification genes were significantly different among the chronosequence and heterotic groups (Figs. 2.3E-F, Tables A.5, A.8). Overall, changes in denitrifier communities had the weakest relationship to the chronosequence, but rather were consistently driven by heterotic genetic group (Table A.8). Denitrifiers possessing the cytochrome cd_1-type nitrite reductase, encoded by *nirS*, were the only denitrifier group showing altered composition in response to germplasm development ($p=0.07$, Fig. 2.3E, Table A.8.1). Only nitric oxide reductase, *norB,* gene abundance was correlated to time ($p=0.056$, Tables A.5, A.9.6). All other denitrification genes lacked a significant correlation to the chronosequence. To summarize the gene abundance results, we averaged all the denitrification genes and regressed the mean abundance against the chronosequence (Fig. 2.3F). While this regression was not significant ($p=0.35$, Table A.9), gene abundance and chronosequence still had a positive relationship ($r=0.22$).

Identification and potential function of taxa that respond to the germplasm chronosequence

Weighted gene correlation network analysis (WGCNA) (Langfelder and Horvath 2008) identified three unique sets of OTUs (modules) with a significant response to the germplasm chronosequence (Fig. 2.4A, Table A.9). Modules 1 and 2 contained OTUs that were positively correlated to the decade of germplasm release, while Module 3 OTUs were negatively correlated with time. Module 1 contained 98 OTUs and was dominated by *Proteobacteria*. Module 2

contained 140 OTUs and was dominated by *Actinobacteria*. Module 3 contained 178 OTUs and was dominated by *Proteobacteria*. Lists of dominant taxonomic classes from each module are presented in Table A.10. Metagenomic functional predictions using PICRUSt2 were performed to predict the function of the taxa identified by WGCNA. Metagenomic functional predictions for the taxa in each module are presented in Figs. A.5-6. PICRUSt2 predicted that the taxa in Module 1 had 304 pathways, Module 2 had 286 pathways, and Module 3 had 378 pathways. Among all modules, there was a high degree of shared predicted metabolic pathways (Fig. 2.4B). Module 1 and 2 (taxa increasing over the chronosequence) cumulatively contained only five unique pathways not present in Module 3. Module 3 (taxa decreasing in relative abundance across the chronosequence) had 62 unique pathways (Fig. 2.4B, Tables A.12-A.14). All modules revealed changes in predicted abundance of pathways across the germplasm chronosequence: 83% of pathways in Module 1, 85% of pathways in Module 2, and 78% of pathways in Module 3 significantly changed across the germplasm chronosequence (Table A.14). The rhizosphere microbiomes from germplasm developed during the 1940-50s were the most distinct in the predicted abundance of pathways compared to the lines released during the 1960s, 1970s, and 1980s. When comparing predicted microbial metabolic pathway differences among maize lines from the 1960-70s to the 1980s, little to no difference in abundance (0 - 0.002%) was found. This analysis allowed us to determine the pathways that showed the strongest response to our chronosequence (Table A.14). Module 3 showed the most complex patterns of enrichment and depletion across our three decadal classifications (Fig. A.5A). Module 1 and 2, while taxonomically distinct, appeared to be functionally redundant. Module 3 showed decreases across the chronosequence in pathways related to the degradation of organic nitrogen sources (Fig. A.5B, Table A.14). Across time all three modules were predicted to contain a greater

number of gene pathways related to aerobic respiration and amino acid synthesis (Fig. A.5C-D, Table A.14). PICRUSt2 analysis was performed on correlated taxa modules. Description and analysis are presented in appendix A.

Genomic changes across chronosequence

Supplementary analysis of the genomic variation within these maize lines was performed to assess whether we could gain mechanistic insight in the phenotypes causing our observed microbiome pattern. First, using TASSEL we scanned the haplotype diversity within the chronosequence population and found 87 large genetic regions ($p<0.05$) showing evidence of undergoing recent selection events according to Tajima's D statistic. Eighty-five of these regions were suggestive of a selective sweep and two of balancing selection (supplemental materials Fig. A.8). Next, we attempted to determine if changes in genomic variation corresponded to changes in our chronosequence timeline (Fig. A.9). Using the maize HapMap, we first determined the population G matrix in TASSEL and then found the non-metric multidimensional scaling (NMDS) axes that explained most of the genetic variation (Figs. A.7-9). These major NMDS axes were then regressed against our chronosequence timeline. Taken together this additional genetic analysis on the maize lines used in this study suggest that multiple alleles and a considerable amount of genetic variation was changed across this time period of maize development. Unfortunately, the design of this study lacks the power to determine the exact genes and traits driving this chronosequence microbiome pattern.

Discussion:

Plant rhizosphere microbiomes are, in part, shaped by plant genetics (Peiffer et al. 2013; Walters et al. 2018). Here we provide one of the few examples showing that selection (via

breeding) on the plant genotype across a changing agronomic environment (i.e., increased synthetic N, increased plant density) drives changes in recruitment of the plant microbiome. We show that altered rhizosphere microbiome recruitment was reflected in functional genes for nitrification and nitrogen fixation and predicted metabolic pathways. Ultimately, these results suggest that breeding has altered the recruitment of soil microbiome and specific N-cycling functional groups in the maize rhizosphere.

Our results show a shift in rhizosphere prokaryotic microbiomes across a chronosequence of inbred maize lines, independent of broad genetic relatedness (heterotic group) (Fig. 2.2). These conclusions are based entirely on inbred maize lines and do not include hybrids. We decided to focus solely on inbred lines as hybrid maize genotypes exhibit a high degree of heterosis (Hauck et al. 2014) and typically represent a highly genetically diverse combination of different heterotic pedigrees. This is important, as recent research has now established that this hybrid vigor can have considerable impacts on the assembly of the rhizosphere microbiome (Wagner, Roberts, et al. 2020; Wagner, Tang, et al. 2020). Consequently, previous studies that included hybrids in their attempts to examine the effects of selection on maize through time unknowingly confounded heterosis and selection effects (Emmett et al. 2018; Schmidt et al. 2020). Further research is needed to fully disentangle how hybridization shapes maize's interactions with microbiomes and microbial functions related to agricultural sustainability.

The consequences of these microbiome changes extended to the composition and abundance of microbial genes associated with nitrogen cycling observed in the rhizosphere. We saw decreases in the abundance and changes in composition of diazotrophs, indicated by *nifH*, in more recently developed germplasm (Fig. 2.2A, 2.2B). The increased usage of synthetic nitrogen fertilization through time has decreased maize's reliance on microbial N provisioning. It is well

established that the maintenance of belowground mutualistic N-fixation comes at a carbon cost (Vitousek et al. 2013), and alters aboveground carbon allocation across the plant (Morgan, Bending, and White 2005). Additionally, altering nutrient availability modifies how a plant host assembles the microbiome (Berg and Koskella 2018). In the breeding process, selection has been tuned to grain production (Diamond 2002) and weakened belowground carbon allocation (Schmidt, Bowles, and Gaudin 2016). Other findings in maize suggest that some landrace cultivars have a heightened ability to recruit associative diazotrophs (Van Deynze et al. 2018). Maize lines that host nitrogen-fixing bacteria produce specialized carbon-rich mucilage exudates to attract these microbes and gain substantial plant-available nitrogen from this interaction (Van Deynze et al. 2018; Vitousek et al. 2013). Allocating carbon resources to the production of exudates comes at a cost to yield, and reliance on fixed N from diazotrophs is unnecessary under high nitrogen conditions (Morgan, Bending, and White 2005), weakening any selection for maintenance of nutritional mutualisms that may have been present in ancestral maize lineages. Furthermore, under continuous high nitrogen fertilization, diazotrophs can evolve to become less efficient mutualistic nitrogen fixers (Weese et al. 2015). A combination of these factors explains why maize's recruitment of diazotrophs changes as a consequence of decades of crop selection.

Various functional genes related to denitrification and nitrification increased in abundance and changed in composition through the germplasm chronosequence (Fig. 2.2C-F, Table A.5). While not all functional genes related to these processes responded to the chronosequence, especially those genes related to denitrification, there is still a clear pattern across time and germplasm selection. Changes in the abundance of N-cycling genes could be important in predicting losses of nitrogen and the production of GHGs from agroecosystems (Bowles et al. 2018), as microorganisms that perform denitrification and nitrification can remove

or alter the chemical structure and mobility of plant-available N (Kuypers, Marchant, and Kartal 2018). Selective exudation of specialized metabolites from maize roots could be an explanation for shifts in the nitrifiers and denitrifiers across the germplasm represented in this study. For instance, different cereal grasses (sorghum, rice, wheat) have the ability to exude secondary phytochemical compounds that can suppress the metabolism of nitrifying organisms (Coskun et al. 2017). Here we hypothesize that a narrowing of germplasm diversity by inbreeding (Smith et al. 2004) could have eroded complex metabolic characteristics important for shaping interactions with nitrogen cycling microbial taxa (Zhou, Richter, and Jander 2018). Breeding of maize may have resulted in trait changes that influence how different cultivars recruit nitrogen cycling microbes. A growing body of research suggests that plants can drive the variability and activity of nitrifiers and denitrifers in the soil ecosystem (Woldendorp 1975; Skiba et al. 2011; Coskun et al. 2017; Guyonnet et al. 2017; Achouak et al. 2019). Demonstrating that agroecosystem management and crop breeding altered the plant microbiome and potentially its functions suggest that plant-microbiome interactions are mutable – theoretically mutable enough that we can intentionally select for rhizosphere microbiome traits that contribute to nutrient retention, reduced GHG production, and improved soil health.

Plant species regulate microbial enzyme production and metagenomic capacity in the rhizosphere (Reinhold-Hurek et al. 2015; Xu et al. 2018). Here we predicted changes in the microbial metagenome as a function of germplasm development. We found increases in the relative abundance of gene pathways related to amino acid biosynthesis and aerobic respiration. Gene pathways related to nitrogen substrate degradation decreased through the germplasm chronosequence (Fig. 2.3, 2.4). These results imply that plants from earlier decades in this chronosequence support microbiomes that mineralize soil organic nitrogen, while later lines do

the opposite. The rhizosphere microbiome of more recent germplasm is enriched for microbial taxa that have greater numbers of predicted metabolic pathways for respiration and amino acid synthesis. The predicted metagenome results suggest that the microbiome recruited by more modern germplasm is in a state of growth and biosynthesis. Coincidentally, these modern microbiomes are also predicted to have a lower capacity to mineralize free organic nitrogen sources; we hypothesize they are obtaining their nitrogen for biosynthesis from inorganic fertilizers, thereby potentially competing with the plant for nutrients instead of working mutualistically. The shift to aerobic respiration and simple sugar breakdown may indicate that the newer maize lines are recruiting copiotrophs (Trivedi, Anderson, and Singh 2013). These alterations to belowground predicted microbial metabolism could explain the observed yield gap between conventional and organic agroecosystems (Kravchenko, Snapp, and Robertson 2017). Maize lines that recruit fewer nutrient-mineralizing microbes may be compromised for acquisition of nitrogen through organic nitrogen sources, resulting in lower yields. Currently, it is not well-established what type of soil metabolism would be ideal to meet our sustainability goals (Busby et al. 2017; Leach et al. 2017). However, these results indicate that we could breed germplasm to recruit microorganisms with traits that are aligned with soil management practices.

In conclusion, industrial breeding practices and agronomic management approaches have transformed maize's interactions with its rhizosphere microbiome at a taxonomic and functional genomic level. These microbiome differences potentially alter nitrogen processing among plant cultivars and the movement of nitrogen in the agroecosystem as a whole. These changes likely occurred because of the combination of intense selection for aboveground traits and increased use of synthetic nitrogen fertilizers that reduced reliance on microbially-mediated nitrogen cycling processes. Modern agricultural practices have disrupted and accelerated the reactive

nitrogen cycle. Maize has been a major contributor to this global disruption as it is one of the most farmed and fertilized crops in the world (Ladha et al. 2016). Alteration of plant microbiome function is indicated by recruitment of distinct assemblages of nitrogen-cycling taxa and predicted metabolic pathways in the rhizosphere microbiome of maize germplasm developed in different decades. Modern agricultural practices have accomplished the alteration of maize's interaction with its root microbiome in the span of 50 years. Following these observations, the next steps would be to determine if the differences in microbiome recruitment are contributing to unsustainable outcomes in the agroecosystem and if unsustainable aspects of this microbiome recruitment are reversible. Approaching the microbiome and its functions as an extended phenotype of the plant genome will be a necessary step towards optimizing agricultural systems for sustainability.

Figures:

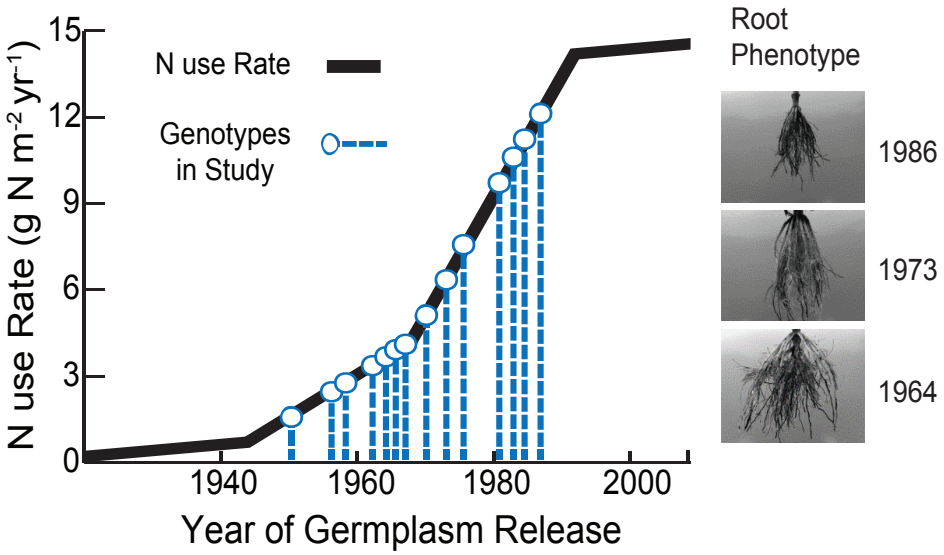

Figure 2.1 Germplasm chronosequence used in this study mapped on to nitrogen fertilizer use over time. Maize-specific nitrogen use rate was derived from Cao et al. 2018. Images highlight the changing root phenotype through time and are from Hauck et al. 2015.

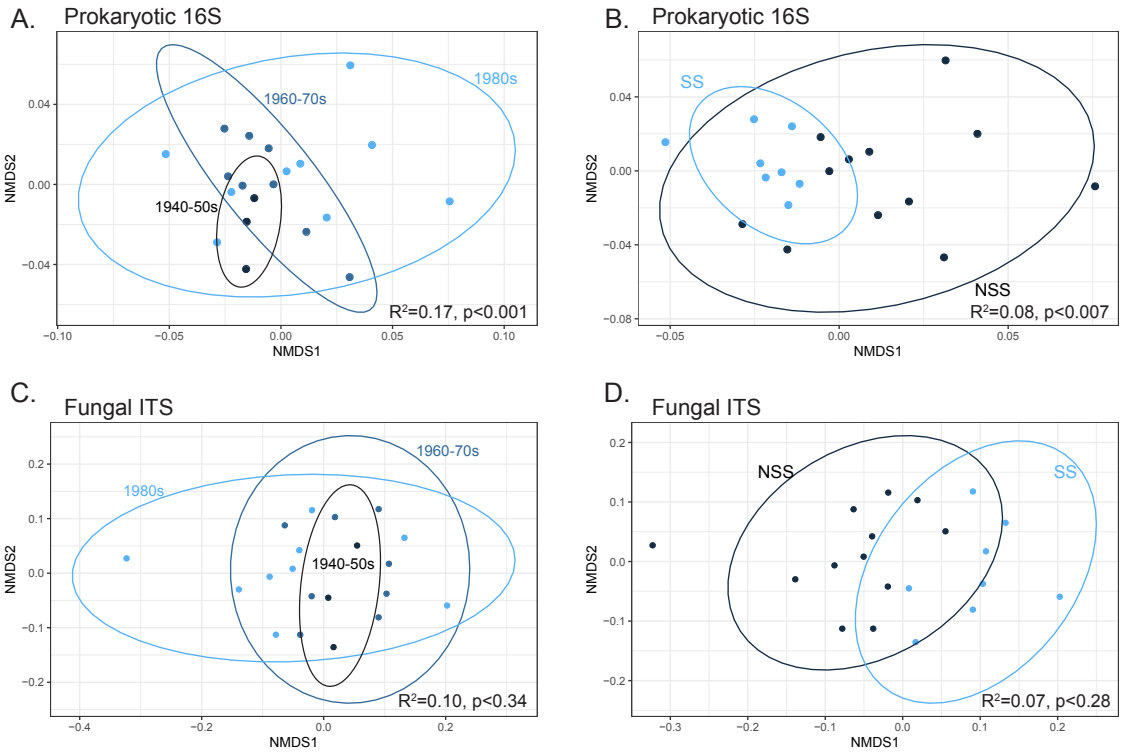

Figure 2.2 NMDS ordinations based on Bray-Curtis dissimilarity among prokaryotic 16S rRNA (**A-B**) and fungal ITS (**C-D**) rhizosphere microbiome samples compared among maize genotypes representing different decades of germplasm development (**A, C**) or heterotic group (**B, D**). The two heterotic groups are Non-Stiff Stalk (NSS) and Stiff Stalk (SS).

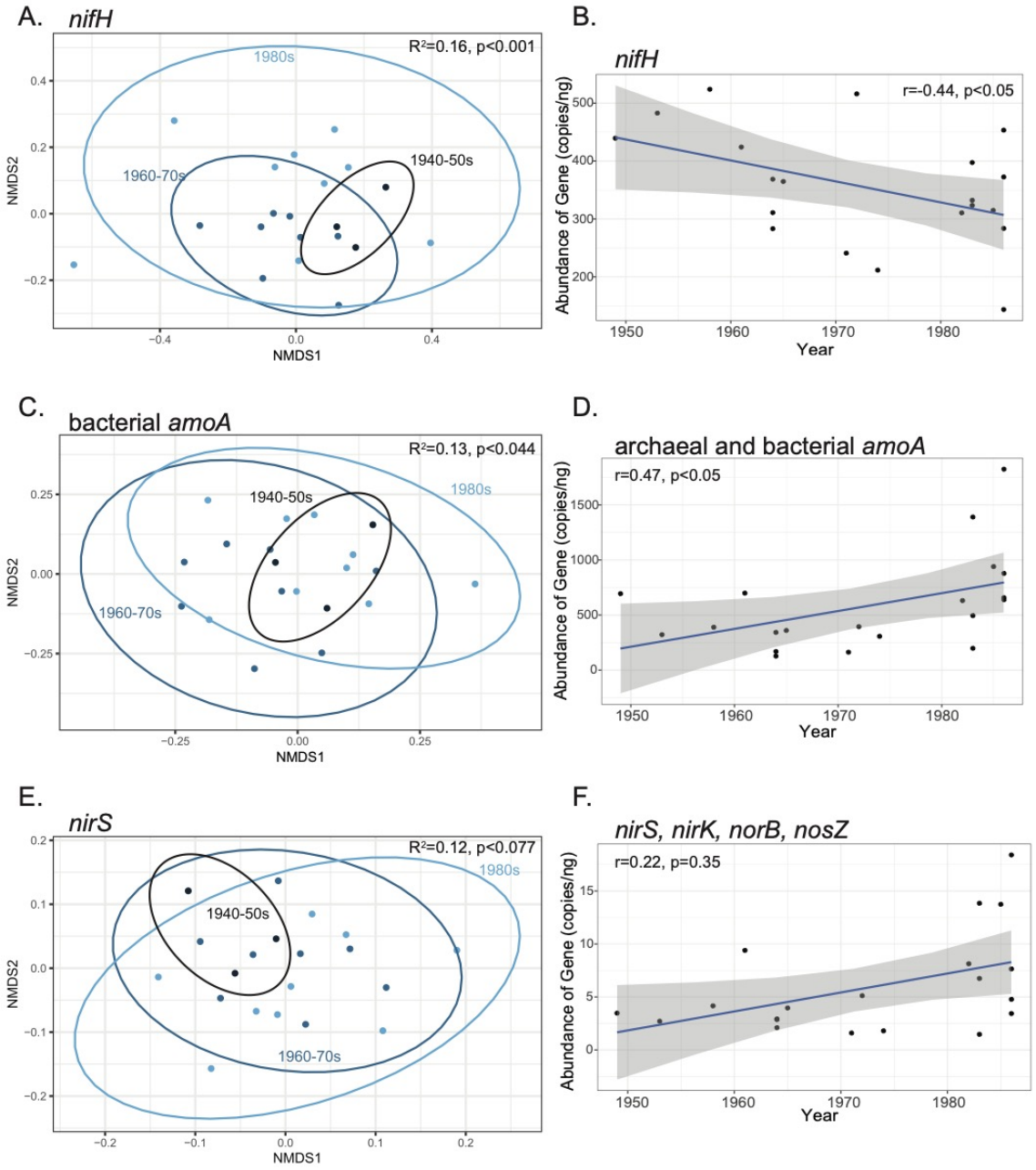

Figure 2.3 Changes in nitrogen cycling genes across chronosequence. A. NMDS ordination comparing maize rhizosphere *nifH* assemblages among decade of germplasm development. **B.** Linear regression of *nifH* gene copy number across the chronosequence. **C.** NMDS ordination comparing composition of bacterial ammonia oxidzer assemblages across decades of germplasm development. **D.** Linear regression of sum of archaeal *amoA* and bacterial *amoA* genes abundance across the chronosequence. **E**. NMDS ordination comparing assemblages of denitrifiers (based on *nirS* gene) across breeding decades. **F.** Linear regression of the average qPCR abundance of the denitrification genes across the chronosequence. A complete list of statistical analysis of nitrogen cycling genes present in the supporting information: Tables A.5-A.10, Fig. A.4.

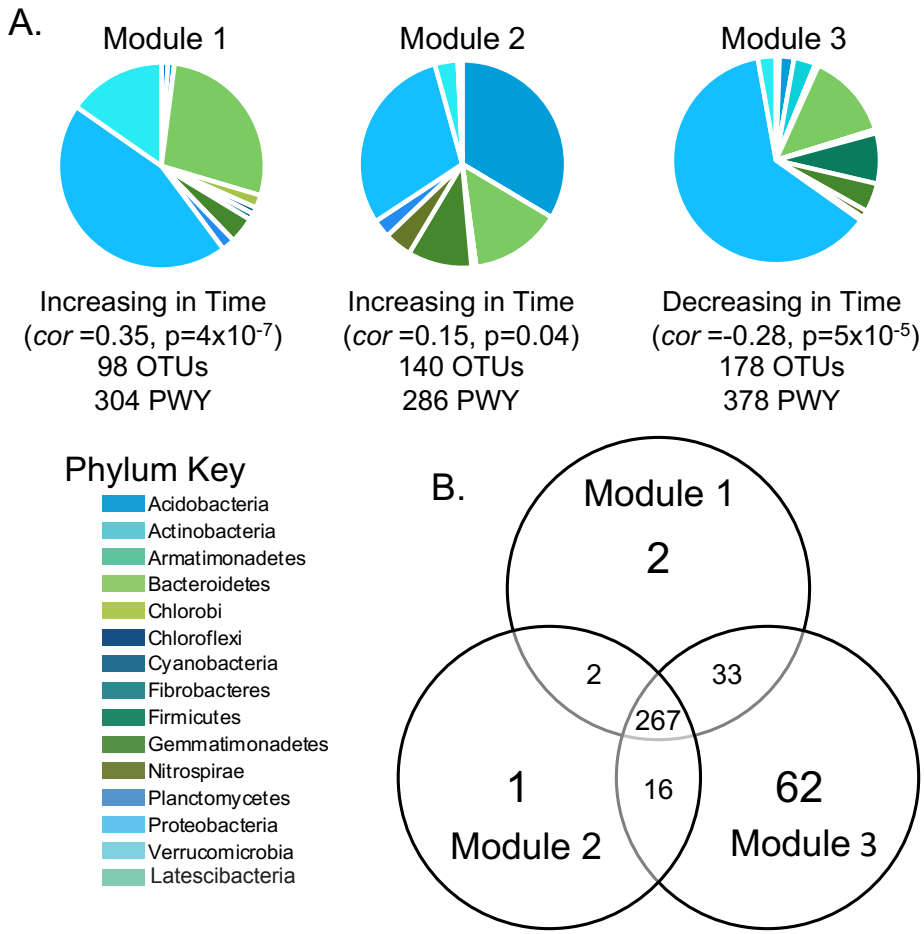

Figure 2.4 Taxa modules and predicted metabolic pathways for the maize rhizosphere microbiome based on WGCNA and PICRUSt2 metabolic pathway predictions. **A**. Modules (hierarchical clustered OTUs) that are significantly responding to the germplasm chronosequence. Module membership varies in size and taxonomic composition, grouped by phylum here. A list of dominant classes is presented in Table A.11. **B**. Venn diagram shows metabolic pathways shared across the three modules. Information on pathways present in Tables A.12-A.14.

References:

Achouak, Wafa, Danis Abrouk, Julien Guyonnet, Mohamed Barakat, Philippe Ortet, Laurent Simon, Catherine Lerondelle, Thierry Heulin, and Feth El Zahar Haichar. 2019. "Plant Hosts Control Microbial Denitrification Activity." *FEMS Microbiology Ecology* 95 (3): 21. https://doi.org/10.1093/femsec/fiz021.

Altschul, Stephen F, Thomas L Madden, Alejandro A Schäffer, Jinghui Zhang, Zheng Zhang, Webb Miller, and David J Lipman. 1997. "Gapped BLAST and PSI-BLAST: A New Generation of Protein Database Search Programs." *Nucleic Acids Research* 25 (17): 3389–3402.

Berg, Maureen, and Britt Koskella. 2018. "Nutrient- and Dose-Dependent Microbiome-Mediated Protection against a Plant Pathogen." *Current Biology* 28 (15): 2487-2492.e3. https://doi.org/10.1016/j.cub.2018.05.085.

Bowles, Timothy M, Shady S Atallah, Eleanor E Campbell, Amélie C.M. Gaudin, William R Wieder, and A Stuart Grandy. 2018. "Addressing Agricultural Nitrogen Losses in a Changing Climate." *Nature Sustainability* 1 (8): 399–408. https://doi.org/10.1038/s41893-018-0106-0.

Bradbury, Peter J., Zhiwu Zhang, Dallas E. Kroon, Terry M. Casstevens, Yogesh Ramdoss, and Edward S. Buckler. 2007. "TASSEL: Software for Association Mapping of Complex Traits in Diverse Samples." *Bioinformatics* 23 (19): 2633–35. https://doi.org/10.1093/bioinformatics/btm308.

Bulgarelli, Davide, Klaus Schlaeppi, Stijn Spaepen, Emiel Ver Loren Van Themaat, and Paul Schulze-Lefert. 2013. "Structure and Functions of the Bacterial Microbiota of Plants." *Annual Review of Plant Biology*. https://doi.org/10.1146/annurev-arplant-050312-120106.

Busby, Posy E., Chinmay Soman, Maggie R. Wagner, Maren L. Friesen, James Kremer, Alison Bennett, Mustafa Morsy, Jonathan A. Eisen, Jan E. Leach, and Jeffery L. Dangl. 2017. "Research Priorities for Harnessing Plant Microbiomes in Sustainable Agriculture." *PLoS Biology* 15 (3): 1–14. https://doi.org/10.1371/journal.pbio.2001793.

Butler, D G, B R Cullis, A R Gilmour, B J Gogel, and R Thompson. 2017. *ASReml-R Reference Manual Version 4*. *ASReml-R Reference Manual*.

Cao, Peiyu, Chaoqun Lu, and Zhen Yu. 2018. "Historical Nitrogen Fertilizer Use in Agricultural Ecosystems of the Contiguous United States during 1850-2015: Application Rate, Timing, and Fertilizer Types." *Earth System Science Data* 10 (2): 969–84. https://doi.org/10.5194/essd-10-969-2018.

Caporaso, J Gregory, Justin Kuczynski, Jesse Stombaugh, Kyle Bittinger, Frederic D Bushman, Elizabeth K Costello, Noah Fierer, et al. 2010. "QIIME Allows Analysis of High-Throughput Community Sequencing Data." *Nature Methods* 7 (5): 335–36. https://doi.org/10.1038/nmeth.f.303.

Caspi, Ron, Richard Billington, Luciana Ferrer, Hartmut Foerster, Carol A. Fulcher, Ingrid M. Keseler, Anamika Kothari, et al. 2016. "The MetaCyc Database of Metabolic Pathways and Enzymes and the BioCyc Collection of Pathway/Genome Databases." *Nucleic Acids Research* 44 (D1): D471–80. https://doi.org/10.1093/nar/gkv1164.

Clarke, K. R. 1993. "Non-Parametric Multivariate Analyses of Changes in Community Structure." *Australian Journal of Ecology* 18: 117–43. https://doi.org/10.1093/bioinformatics/bty844.

Coskun, Devrim, Dev T Britto, Weiming Shi, and Herbert J Kronzucker. 2017. "How Plant Root Exudates Shape the Nitrogen Cycle." *Trends in Plant Science* 22 (8): 661–73. https://doi.org/10.1016/j.tplants.2017.05.004.

Davidson, Eric A, Mark B David, James N Galloway, Christine L Goodale, Richard Haeuber, John A Harrison, Robert W Howarth, et al. 2012. "Excess Nitrogen in the U.S. Environment: Trends, Risks, and Solutions." *Issues in Ecology* 15: 1–16. https://www.esa.org/esa/wp-content/uploads/2013/03/issuesinecology15.pdf.

Deynze, Allen Van, Pablo Zamora, Pierre Marc Delaux, Cristobal Heitmann, Dhileepkumar Jayaraman, Shanmugam Rajasekar, Danielle Graham, et al. 2018. "Nitrogen Fixation in a Landrace of Maize Is Supported by a Mucilage-Associated Diazotrophic Microbiota." *PLoS Biology* 16 (8): e2006352. https://doi.org/10.1371/journal.pbio.2006352.

Diamond, Jared. 2002. "Impact of Plant Domestication on Rhizosphere Microbiome Assembly and Functions." *Nature*. https://doi.org/10.1038/nature01019.

Douglas, Gavin M., Vincent J. Maffei, Jesse R. Zaneveld, Svetlana N. Yurgel, James R. Brown, Christopher M. Taylor, Curtis Huttenhower, and, and Morgan G. I. Langille 1. 2020. "PICRUSt2 for Prediction of Metagenome Functions." *Nature Biotechnology* 38 (6): 669–73. https://doi.org/10.1038/s41587-020-0550-z.

Duvick, D N, J S C Smith, and M Cooper. 2003. "Long-Term Selection in a Commercial Hybrid Maize Breeding Program." *Plant Breeding Reviews: Part 2: Long-Term Selection: Crops, Animals, and Bacteria* 24: 109–51. https://doi.org/10.1002/9780470650288.ch4.

Edgar, Robert C. 2010a. "Search and Clustering Orders of Magnitude Faster than BLAST." *Bioinformatics* 26 (19): 2460–61. https://doi.org/10.1093/bioinformatics/btq461.

Edwards, Joseph D., Cameron M. Pittelkow, Angela D. Kent, and Wendy H. Yang. 2018. "Dynamic Biochar Effects on Soil Nitrous Oxide Emissions and Underlying Microbial Processes during the Maize Growing Season." *Soil Biology and Biochemistry* 122 (December 2017): 81–90. https://doi.org/10.1016/j.soilbio.2018.04.008.

Emmett, Bryan D, Daniel H Buckley, Margaret E Smith, and Laurie E Drinkwater. 2018. "Eighty Years of Maize Breeding Alters Plant Nitrogen Acquisition but Not Rhizosphere Bacterial Community Composition." *Plant and Soil* 431 (1–2): 53–69. https://doi.org/10.1007/s11104-018-3744-0.

Evenson, R. E., and D. Gollin. 2003. "Assessing the Impact of the Green Revolution, 1960 to 2000." *Science (New York, N.Y.)* 300 (5620): 758–62. https://doi.org/10.1126/science.1078710.

FAO. 2020. "World Food and Agriculture - Statistical Yearbook 2020." *World Food and Agriculture - Statistical Yearbook 2020*. https://doi.org/10.4060/cb1329en.

Fish, Jordan A., Benli Chai, Qiong Wang, Yanni Sun, C. Titus Brown, James M. Tiedje, and James R. Cole. 2013. "FunGene: The Functional Gene Pipeline and Repository." *Frontiers in Microbiology* 4 (OCT): 1–14. https://doi.org/10.3389/fmicb.2013.00291.

Gloor, Gregory B., Jean M. Macklaim, Vera Pawlowsky-Glahn, and Juan J. Egozcue. 2017. "Microbiome Datasets Are Compositional: And This Is Not Optional." *Frontiers in Microbiology* 8 (NOV): 1–6. https://doi.org/10.3389/fmicb.2017.02224.

Gordon, A, G J Hannon, and Gordon. 2014. "FASTX-Toolkit." *[Online] Http://Hannonlab. Cshl. Edu/Fastx_ Toolkit Http://Hannonlab. Cshl. Edu/Fastx_ Toolkit*.

Guyonnet, Julien P, Florian Vautrin, Guillaume Meiffren, Clément Labois, Amélie A.M. Cantarel, Serge Michalet, Gilles Comte, and Feth el Zahar Haichar. 2017. "The Effects of Plant Nutritional Strategy on Soil Microbial Denitrification Activity through Rhizosphere

Primary Metabolites." *FEMS Microbiology Ecology* 93 (4): 22. https://doi.org/10.1093/femsec/fix022.
Haegele, Jason W., Kevin A. Cook, Devin M. Nichols, and Frederick E. Below. 2013. "Changes in Nitrogen Use Traits Associated with Genetic Improvement for Grain Yield of Maize Hybrids Released in Different Decades." *Crop Science* 53 (4): 1256–68. https://doi.org/10.2135/cropsci2012.07.0429.
Hauck, Andrew L., G. Richard Johnson, Mark A. Mikel, Gregory S. Mahone, A. Jason Morales, Torbert R. Rocheford, and Martin O. Bohn. 2014. "Generation Means Analysis of Elite Ex-Plant Variety Protection Commercial Inbreds: A New Public Maize Genetics Resource." *Crop Science* 54 (1): 174–89. https://doi.org/10.2135/cropsci2013.03.0172.
Ishii, Satoshi, Gaku Kitamura, Takahiro Segawa, Ayano Kobayashi, Takayuki Miura, Daisuke Sano, and Satoshi Okabe. 2014. "Microfluidic Quantitative PCR for Simultaneous Quantification of Multiple Viruses in Environmental Water Samples." *Applied and Environmental Microbiology* 80 (24): 7505–11. https://doi.org/10.1128/AEM.02578-14.
Khush, Gurdev S. 1999. "Green Revolution: Preparing for the 21st Century." *Genome* 42 (4): 646–55. https://doi.org/10.1139/g99-044.
Korneliussen, Thorfinn Sand, Ida Moltke, Anders Albrechtsen, and Rasmus Nielsen. 2013. "Calculation of Tajima's D and Other Neutrality Test Statistics from Low Depth next-Generation Sequencing Data." *BMC Bioinformatics* 14 (1): 289. https://doi.org/10.1186/1471-2105-14-289.
Kravchenko, Alexandra N, Sieglinde S Snapp, and G Philip Robertson. 2017. "Field-Scale Experiments Reveal Persistent Yield Gaps in Low-Input and Organic Cropping Systems." *Proceedings of the National Academy of Sciences of the United States of America* 114 (5): 926–31. https://doi.org/10.1073/pnas.1612311114.
Kuypers, Marcel M.M., Hannah K. Marchant, and Boran Kartal. 2018. "The Microbial Nitrogen-Cycling Network." *Nature Reviews Microbiology* 16 (5): 263–76. https://doi.org/10.1038/nrmicro.2018.9.
Ladha, J K, A Tirol-Padre, C K Reddy, K G Cassman, Sudhir Verma, D S Powlson, C Van Kessel, Daniel B. De Richter, Debashis Chakraborty, and Himanshu Pathak. 2016. "Global Nitrogen Budgets in Cereals: A 50-Year Assessment for Maize, Rice, and Wheat Production Systems." *Scientific Reports* 6: 19355. https://doi.org/10.1038/srep19355.
Langfelder, Peter, and Steve Horvath. 2008. "WGCNA: An R Package for Weighted Correlation Network Analysis." *BMC Bioinformatics* 9 (559): 1–13. https://doi.org/10.1186/1471-2105-9-559.
Leach, Jan E., Lindsay R. Triplett, Cristiana T. Argueso, and Pankaj Trivedi. 2017. "Communication in the Phytobiome." *Cell* 169 (4): 587–96. https://doi.org/10.1016/j.cell.2017.04.025.
Li, Shan, Yonghang Tian, Kun Wu, Yafeng Ye, Jianping Yu, Jianqing Zhang, Qian Liu, et al. 2018. "Modulating Plant Growth–Metabolism Coordination for Sustainable Agriculture." *Nature* 560 (7720): 595–600. https://doi.org/10.1038/s41586-018-0415-5.
Mag, Tanja, and Steven L Salzberg. 2011. "FLASH: Fast Length Adjustment of Short Reads to Improve Genome Assemblies" 27 (21): 2957–63. https://doi.org/10.1093/bioinformatics/btr507.

McMurdie, Paul J., and Susan Holmes. 2013. “Phyloseq: An R Package for Reproducible Interactive Analysis and Graphics of Microbiome Census Data.” *PLoS ONE* 8 (4): e61217–e61217. https://doi.org/10.1371/journal.pone.0061217.

Morgan, J. A.W., G D Bending, and P J White. 2005. “Biological Costs and Benefits to Plant-Microbe Interactions in the Rhizosphere.” *Journal of Experimental Botany* 56 (417): 1729–39. https://doi.org/10.1093/jxb/eri205.

Oksanen, Jari, Roeland Kindt, Pierre Legendre, Bob O’hara, M Henry, and H Stevens Maintainer. 2007. “The Vegan Package Title Community Ecology Package.” Http://Cran.r-Project.Org/, Http://R-Forge.r-Project.Org/Projects/Vegan/. 2007. http://ftp.uni-bayreuth.de/math/statlib/R/CRAN/doc/packages/vegan.pdf.

Peiffer, Jason A, Aymé Spor, Omry Koren, Zhao Jin, Susannah Green Tringe, Jeffery L Dangl, Edward S. Buckler, and Ruth E. Ley. 2013. “Diversity and Heritability of the Maize Rhizosphere Microbiome under Field Conditions.” *Proceedings of the National Academy of Sciences of the United States of America* 110 (16): 6548–53. https://doi.org/10.1073/pnas.1302837110.

Philippot, Laurent, Jos M Raaijmakers, Philippe Lemanceau, and Wim H. Van Der Putten. 2013. “Going Back to the Roots: The Microbial Ecology of the Rhizosphere.” *Nature Reviews Microbiology* 11 (11): 789–99. https://doi.org/10.1038/nrmicro3109.

Quast, Christian, Elmar Pruesse, Pelin Yilmaz, Jan Gerken, Timmy Schweer, Pablo Yarza, Jörg Peplies, and Frank Oliver Glöckner. 2013. “The SILVA Ribosomal RNA Gene Database Project: Improved Data Processing and Web-Based Tools.” *Nucleic Acids Research* 41: D590–D596. https://doi.org/10.1093/nar/gks1219.

R Core Team. 2013. “R: A Language and Environment for Statistical Computing.” *R Foundation for Statistical Computing*. Vienna, Austria. URL http://www.R-project.org/. https://doi.org/10.1007/978-3-540-74686-7.

Reinhold-Hurek, Barbara, Wiebke Bünger, Claudia Sofía Burbano, Mugdha Sabale, and Thomas Hurek. 2015. “Roots Shaping Their Microbiome: Global Hotspots for Microbial Activity.” *Annual Review of Phytopathology* 53 (1): 403–24. https://doi.org/10.1146/annurev-phyto-082712-102342.

Robertson, G Philip, and Peter M Vitousek. 2009. “Nitrogen in Agriculture: Balancing the Cost of an Essential Resource.” *Annual Review of Environment and Resources* 34 (1): 97–125. https://doi.org/10.1146/annurev.environ.032108.105046.

Romay, Maria C, Mark J Millard, Jeffrey C Glaubitz, Jason A Peiffer, Kelly L Swarts, Terry M Casstevens, Robert J Elshire, et al. 2013. “Comprehensive Genotyping of the USA National Maize Inbred Seed Bank.” *Genome Biology* 14 (6): R55. https://doi.org/10.1186/gb-2013-14-6-r55.

Schmidt, Jennifer E., Timothy M. Bowles, and Amélie C.M. Gaudin. 2016. “Using Ancient Traits to Convert Soil Health into Crop Yield: Impact of Selection on Maize Root and Rhizosphere Function.” *Frontiers in Plant Science* 7 (MAR2016): 1–11. https://doi.org/10.3389/fpls.2016.00373.

Schmidt, Jennifer E, Jorge L. Mazza Rodrigues, Vanessa L Brisson, Angela Kent, and Amélie C.M. Gaudin. 2020. “Impacts of Directed Evolution and Soil Management Legacy on the Maize Rhizobiome.” *Soil Biology and Biochemistry* 145: 107794. https://doi.org/10.1016/j.soilbio.2020.107794.

Skiba, Marcin W., Timothy S. George, Elizabeth M. Baggs, and Tim J. Daniell. 2011. "Plant Influence on Nitrification." *Biochemical Society Transactions* 39 (1): 275–78. https://doi.org/10.1042/bst0390275.

Smith, J. Stephen C., Donald N Duvick, Oscar S Smith, Mark Cooper, and Lizhi Feng. 2004. "Changes in Pedigree Backgrounds of Pioneer Brand Maize Hybrids Widely Grown from 1930 to 1999." *Crop Science* 44 (6): 1935–46. https://doi.org/10.2135/cropsci2004.1935.

Trivedi, Pankaj, Ian C. Anderson, and Brajesh K. Singh. 2013. "Microbial Modulators of Soil Carbon Storage: Integrating Genomic and Metabolic Knowledge for Global Prediction." *Trends in Microbiology* 21 (12): 641–51. https://doi.org/10.1016/j.tim.2013.09.005.

USDA (National Agricultural Statistics Service). n.d. "National Statistics for Corn: Corn Grain—Yield, Measured in Bu/Acre. Statistics by Subject." *URL: Http://Www.Nass.Usda.Gov/Statistics_by_Subject/Index.Php*.

Vitousek, Peter M, John D Aber, Robert H Howarth, Gene E Likens, Pamela A Matson, David W Schindler, William H Schlesinger, and David G Tilman. 1997. "Human Alteration Of the Global Nitrogen Cycle: Source and Consequences." *Ecol Appl* 7 (3): 737–50. https://doi.org/10.1038/nn1891.

Vitousek, Peter M, Duncan N.L. Menge, Sasha C Reed, and Cory C Cleveland. 2013. "Biological Nitrogen Fixation: Rates, Patterns and Ecological Controls in Terrestrial Ecosystems." *Philosophical Transactions of the Royal Society B: Biological Sciences* 368 (1621): 20130119. https://doi.org/10.1098/rstb.2013.0119.

Wagner, Maggie R., Joe H. Roberts, Peter Balint-Kurti, and James B. Holland. 2020. "Microbiome Composition Differs in Hybrid and Inbred Maize." *BioRxiv*, 2020.01.13.904979. https://doi.org/10.1101/2020.01.13.904979.

Wagner, Maggie R, Clara Tang, Fernanda Salvato, Kayla M Clouse, Alexandria Bartlett, Shannon Sermons, Mark Hoffmann, Peter J Balint-kurti, and Manuel Kleiner. 2020. "Microbe-Dependent Heterosis in Maize." *BioRxiv*, 2020.05.05.078766. https://doi.org/10.1101/2020.05.05.078766.

Walters, William A, Zhao Jin, Nicholas Youngblut, Jason G Wallace, Jessica Sutter, Wei Zhang, Antonio González-Peña, et al. 2018. "Large-Scale Replicated Field Study of Maize Rhizosphere Identifies Heritable Microbes." *Proceedings of the National Academy of Sciences of the United States of America* 115 (28): 7368–73. https://doi.org/10.1073/pnas.1800918115.

Weese, Dylan J., Katy D. Heath, Bryn T.M. Dentinger, and Jennifer A. Lau. 2015. "Long-Term Nitrogen Addition Causes the Evolution of Less-Cooperative Mutualists." *Evolution; International Journal of Organic Evolution* 69 (3): 631–42. https://doi.org/10.1111/evo.12594.

Wickham, Hadley. 2007. "Ggplot2–Elegant Graphics for Data Analysis." *Journal of Statistical Software* 99 (2): 260. https://doi.org/10.18637/jss.v077.b02.

Woldendorp, J W. 1975. "Nitrification and Denitrification in the Rhizosphere." *Bulletin de La Societe Botanique de France* 122: 89–107. https://doi.org/10.1080/00378941.1975.10839356.

Xu, Jin, Yunzeng Zhang, Pengfan Zhang, Pankaj Trivedi, Nadia Riera, Yayu Wang, Xin Liu, et al. 2018. "The Structure and Function of the Global Citrus Rhizosphere Microbiome." *Nature Communications* 9 (1): 4894. https://doi.org/10.1038/s41467-018-07343-2.

Yeoh, Yun Kit, Paul G Dennis, Chanyarat Paungfoo-Lonhienne, Lui Weber, Richard Brackin, Mark A Ragan, Susanne Schmidt, and Philip Hugenholtz. 2017. "Evolutionary Conservation of a Core Root Microbiome across Plant Phyla along a Tropical Soil Chronosequence." *Nature Communications* 8 (1): 215. https://doi.org/10.1038/s41467-017-00262-8.

York, Larry M., Tania Galindo-Castañeda, Jeffrey R. Schussler, and Jonathan P. Lynch. 2015. "Evolution of US Maize (Zea Mays L.) Root Architectural and Anatomical Phenes over the Past 100 Years Corresponds to Increased Tolerance of Nitrogen Stress." *Journal of Experimental Botany* 66 (8): 2347–58. https://doi.org/10.1093/jxb/erv074.

Zhou, Shaoqun, Annett Richter, and Georg Jander. 2018. "Beyond Defense: Multiple Functions of Benzoxazinoids in Maize Metabolism." *Plant and Cell Physiology* 59 (8): 1528–33. https://doi.org/10.1093/pcp/pcy064.

CHAPTER 3: DIFFERENCES IN N-CYCLING MICROBIOME RECRUITMENT BETWEEN INBRED AND WILD *ZEA MAYS*

Abstract:

Rewilding our modern agricultural cultivars by reintroducing beneficial ancestral traits has been suggested as a means to improve sustainability of modern agricultural systems. In this study, we compared recruitment of the rhizosphere microbiome among modern inbred maize and wild teosinte to assess whether to assess whether potentially beneficial plant microbiome traits have been lost through maize domestication and modern breeding. To do this, we surveyed the bacterial, fungal, and nitrogen cycling rhizosphere microbial communities of 6 modern domesticated maize genotypes and ancestral wild teosinte genotypes while controlling for environmental conditions and starting soil inoculum. Using a combination of high-throughput sequencing and quantitative PCR, we found that modern inbred and wild teosinte rhizosphere microbiomes differed substantially in taxonomic composition, species richness, and abundance of N-cycling functional genes. Furthermore, the modern vs wild designation explained 27% of the variation in the prokaryotic microbiome, 62% of the variation in N-cycling gene richness, and 66% of N-cycling gene abundance. Surprisingly, we found that modern inbred genotypes hosted microbiomes with higher taxonomic and functional gene diversity within their microbiomes compared to ancestral genotypes. These results imply that modern maize and wild maize seem to differ in their interaction with N-cycling microorganisms in the rhizosphere and that genetic variation exists within *Zea* to potentially 'rewild' these microbiome-associated traits.

Introduction:

Domestication is a strong force shaping the ecological and physiological interactions of an organism (Diamond 2002b; Jensen et al. 2012). Ecologically complex interactions transformed by human domestication of plants range from above-ground chemical defenses (Whitehead, Turcotte, and Poveda 2016; Gaillard et al. 2018) to below-ground rhizosphere microbiome interactions (Bulgarelli et al. 2015; Shenton et al. 2016; Pérez-Jaramillo et al. 2018). While alterations to above-ground chemical defenses have clear consequences to plant productivity (Whitehead, Turcotte, and Poveda 2016; Gaillard et al. 2018), the full implications of domestication's effects on the rhizosphere microbiome are still unclear. To implement and re-wild our modern agricultural plant cultivars we need to comprehend the functional consequences of these alterations to the plant's microbiome interaction.

The rhizosphere microbiome plays a major role in altering plant fitness and productivity (Lau et al. 2012; Philippot, Raaijmakers, et al. 2013). Microbial taxa present in the rhizosphere have been implicated in providing disease resistance (Ryan et al. 1995), amending plant nutrition (Pandey et al. 2017), improving environmental stress tolerance (L. Xu et al. 2018; Panke-Buisse et al. 2014), and altering plant phenology (Wagner et al. 2014). Conversely, plant hosts have been shown to selectively recruit microorganisms present in their rhizosphere (Philippot, Raaijmakers, et al. 2013), a process which has been demonstrated to be heritable across plant cultivars (Peiffer et al. 2013; Walters et al. 2018; Favela, Bohn, and Kent 2021). This apparent heritability suggests that underlying genetic factors in the host shape how a plant interacts with the soil microbial community. Broadly, plant genetics and evolutionary divergence across plant species have been demonstrated to shape the microbiota that colonizes the plant, yet what this means for rhizosphere microbial community functional groups (i.e. nitrogen fixers, nitrifiers,

denitrifiers) has been relatively unexplored (Yeoh et al. 2017; Fitzpatrick et al. 2018). Domesticated plant cultivars provide a model to examine the effects of genetic divergence across closely related species, while also providing insight into how anthropogenic influences have transformed the plant's relationship with microbial functional groups important to ecosystem nutrient cycling.

Soil microbial functional groups (i.e. diazotrophs, nitrifiers, and denitrifiers) play a central role in ecosystem nitrogen (N) cycling processes (Stein et al. 2016; Madsen 2011; Schimel et al. 2017). In the highly nitrogen fertilized agroecosystem, a significant amount of research has been dedicated to controlling the activities of these N-cycling functional groups to reduce environmental pollution, maintain soil health, and maximize plant N-use efficiency (Philippot, Hallin, and Schloter 2007; Drinkwater and Snapp 2007; Vitousek et al. 1997). Previously, we have demonstrated that the recruitment of these nitrogen cycling functional groups to the rhizosphere microbiome can be altered by plant genetic variation (Favela, Bohn, and Kent 2021). Additionally, we found that more recently developed germplasm recruited fewer microbial taxa with the genetic capability for sustainable nitrogen provisioning and larger populations of microorganisms that contribute to N losses (Favela, Bohn, and Kent 2021). Following from this study, we explored the extent to which maize's ability to recruit a rhizosphere microbiome that participates in sustainable N cycling processes has eroded since domestication of this crop by comparing rhizosphere microbial recruitment between wild teosinte, maize's ancestral progenitor and more modern germplasm.

Maize was domesticated from its wild ancestor teosinte approximately 9500 years ago in southwestern Mexico (Doebley 2004; Matsuoka et al. 2002). In that time, sweeping genome- and phenome-wide changes occurred, leading maize to be one of the most consequential

industrialized crops (Hufford, Bilinski, et al. 2012; Wright et al. 2005; Swanson-Wagner et al. 2012; Gaudin, McClymont, and Raizada 2011). Additionally, the domestication of maize was associated with a population bottleneck that drastically reduced genomic diversity (Wright et al. 2005; Hufford, Xu, et al. 2012), led to the increase of deleterious alleles (L. Wang et al. 2017), and the development of traits that would be unfit for a wild environment (Pérez-Jaramillo, Mendes, and Raaijmakers 2015; Diamond 2002a). Previous work has determined that teosinte and modern maize rhizosphere microbiomes differ under the same soil environment (Johnston-Monje et al. 2014; M. Bouffaud et al. 2014; Szoboszlay et al. 2015; M. L. Bouffaud et al. 2012, 2016), yet grounding these differences in *functional* significance has been challenging.

The goal of this study was to determine if wild teosinte and inbred maize differed in the recruitment of N-cycling functional groups in the rhizosphere. First, we set out to characterize how the domestication status of the *Zea* cultivar influenced the diversity and composition of bacterial, and fungal rhizosphere microbiome. Specifically, we wanted to determine if prokaryotic and fungal taxonomic domains are both affected by the domestication status of a cultivar. Second, we determined whether domesticated and wild *Zea mays* differ in their ability to recruit assemblages of microbial functional groups involved in nitrogen fixation, nitrification, and denitrification. This study sheds light on the potential impact of domestication on sustainable N cycling processes in the maize rhizosphere. Understanding whether there is a *functional* difference in wild plant microbiome traits compared to our modern microbiome traits could be potentially useful in identifying (and recovering) traits involved in sustainability that were lost during domestication and crop improvement.

Methods:

Plant Genotype Selection and Greenhouse Experiment

Maize seed stocks were obtained from USDA North Central Regional Plant Introduction Station (Ames, Iowa) and Maize Genetics Cooperation stock center (Urbana, Illinois). Twelve cultivar lines were selected for comparison: 6 modern inbred maize and 6 ancestral teosintes. Within teosinte 2 subspecies were selected, Z. m. *mexicana* and *Z. m. parviglumis.* These subspecies originated from distinct biogeographic regions in Mexico, and are the closest related subspecies to modern maize (Hufford, Xu, et al. 2012). Metadata information about the genotypes is presented in supplementary material Table B.1. Seeds were surface sterilized by soaking for 5 mins in 8.25% NaClO, followed by one rinse with sterilized distilled water, a single rinse of 70% ethanol, and three rinses with sterile distilled water. Surface-sterilized seeds were dried on sterile filter paper in a sterile petri dish, then stored at 4°C overnight before sowing.

Maize lines were grown in greenhouse conditions to isolate the effects of genotype on the microbiome. Planting medium was a combination of live and autoclaved soil mix. The live inoculum soil was collected from agricultural soil located on the Crop Sciences Research and Education Center - South Farms at the University of Illinois at Urbana-Champaign, Urbana, IL. (40°03'31.0"N 88°14'13.4"W). At the time, the soil was out of agricultural rotation (corn-soy) for at least 2 years. Inoculum soil was sieved (2mm) then added (10%) to a steam pasteurized mix of soil: calcined clay: torpedo sand (1:1:1). An inoculum sample was collected before plant growth to characterize the microbiome before plant treatment.

For each genotype, 10 replicate classic 600 pots (2 gallon) were sown with three seeds in each. Pots were thinned a week after germination leaving only a single plant per pot for the

remainder of the growth. In total 120 plants were included in study. They were placed in a completely randomized design in the greenhouse with 16 hours of light and 8 hours of darkness. All plants were connected to an irrigation system that fertilized plants twice a week. Plants were fertilized with a liquid nutrient solution, specifically Cal-Mag (15-5-15), at a rate of 150 ppm. Nitrogen was applied as 11.8% nitrate nitrogen, 1.1% ammoniacal nitrogen, and 2.1% urea nitrogen. All plant treatments were maintained under the same fertilizer regime.

The roots were harvested 36 days after emergence. Plants were approximately in V4-V5 growth stage with 4-6 fully collared leaves. Plant rhizospheres were harvested by extracting root systems from the soil and shaking them vigorously to separate soil that is not tightly bound to roots. Rhizosphere soil was extracted by placing the root system in a 1-liter bottle with 40 mL of sterile distilled water and shaking vigorously for 5 minutes. (Li, Voigt, and Kent 2016). The resulting soil slurry was placed into 50 mL centrifuge tubes and lyophilized before DNA extraction using the FastDNA for Soil DNA extraction kit (MPBio, Solon, OH). Rhizosphere samples of all 10 replicates for each genotype were harvested for molecular analysis.

Microbial community Amplicon Sequencing

For this experiment, we characterized diagnostic functional groups related to three major transformations that occur in the nitrogen cycle: nitrogen fixation, nitrification, and denitrification. Amplicon sequencing was performed on prokaryotic 16S rRNA genes, fungal ITS2, bacterial *amoA,* archaeal *amoA, nirS, nirK, nosZ,* and *nifH* genes. The Fluidigm Access Array IFC chip was used to prepare sequencing amplicons. This method allows for the simultaneous amplification of target functional genes using multiple primer sets (Fluidigm, San Francisco, CA). Primer information is provided in supplemental Table B.2. Fluidigm amplification and Illumina sequencing were conducted at the Roy J. Carver Biotechnology

Center, University of Illinois (Urbana, IL, USA). Fast Length Adjustment of Short reads (FLASH) (Mag and Salzberg 2011) software was used to merge paired-end sequences from 16S rRNA genes. For functional genes and fungal ITS, only forward read sequences were used. Once reads were merged, they were filtered by quality using the FASTX-Toolkit (Gordon, Hannon, and Gordon 2014). Reads that did not have a minimum quality score of 30 across 90% of the bases were removed. Using the FASTX-Toolkit, *nirK* reads were trimmed to its amplicon size of 165-bp.

Once quality preprocessing was performed, FASTQ reads were converted to FASTA format. Using USEARCH-UPARSE version 8.1 (Edgar 2010a), sequences were binned into discrete OTUs based on 97% similarity and singleton DNA sequences were removed. Quantitative Insights into Microbial Ecology (QIIME) was used to generate OTU tables for downstream statistical analysis and to assign taxonomic information, this is done with a combination of the UCLUST algorithm and Greengenes database (Edgar 2010b; DeSantis et al. 2006). Once taxonomy was assigned, chloroplast, mitochondrial and protist OTUs were removed from the dataset. Rarefaction was performed to correct for differential sequencing depth across samples. Functional gene sequences were also assigned using QIIME (Caporaso et al. 2010) with the BLAST (Altschul et al. 1997) algorithm and custom gene-specific databases generated from reference sequences obtained from the FunGene repository (http://fungene.cme.msu.edu/) (Fish et al. 2013). All OTU tables used in statistical analyses were generated in QIIME. Singleton OTUs were filtered prior to statistical analysis.

The number of raw reads generated from sequencing run, reads present after quality filter, and the rarefaction level of reads per sample for 16S rRNA, ITS, and N-cycling genes are reported in supplemental Table B.3. Amplicon sequence data for 16S rRNA genes, fungal ITS2

region, and N-cycling functional genes is available for download on the NCBI SRA database at accession number: PRJNA635735 (https://www.ncbi.nlm.nih.gov/sra/PRJNA635735).

Quantifying Nitrogen cycling functional groups

Quantitative PCR (qPCR) was used to determine the abundance of functional genes in each of the rhizosphere microbial communities. Specific target amplification (STA), explained in (Ishii et al. 2014), was carried out on samples and standards to increase template DNA for amplification. STA and qPCR master mix recipes from (Edwards et al. 2018) were used for all samples. STA product and qPCR master mix were loaded into the Dynamic Array™ Microfluidics Fluidigm Gene Expression chip where amplification and quantification of functional genes were carried out simultaneously (Fluidigm, San Francisco, CA). All samples and standards were analyzed in 12 technical replicates. Fluidigm Real-Time PCR Analysis software version 4.1.3 was used to calculate gene threshold cycles (C_T). C_T values were converted to gene copy number using gene length and standard curves. All Fluidigm qPCR was conducted at the Roy J. Carver Biotechnology Center (Urbana, IL, USA). The final copy number of each functional gene amplicon was standardized by the ng of template DNA in the qPCR amplification.

Statistical Analysis

The microbial communities were evaluated as separate datasets for each amplicon (16S rRNA, fungal ITS, *nifH, nosZ, nirK, nirS*, bacterial *amoA* and archaeal *amoA*). The relative effect of genotype and domestication on the rhizosphere microbiome composition was assessed using permutational analysis of variance (PERMANOVA) with the 'adonis' function, from the community ecology R package, 'vegan' (Oksanen et al. 2007). To visualize differences from these models, non-metric multidimensional scaling (NMDS) ordinations were created using R

package ‘phyloseq’ and plotted with R package ‘ggplot2’ (McMurdie and Holmes 2013; Wickham 2007). Significant differences in functional gene abundance were evaluated using an ANOVA model, and the Tukey’s HSD test from the ‘stats’ package in base R (R Core Team 2013). ‘DESeq2' was used to determine OTUs that were significantly different by using a pairwise comparison among domestication groups (Love, Huber, and Anders 2014).

Results:

Domestication status influences the taxonomic rhizosphere microbial community

Modern inbred maize, teosinte, and the starting bulk soil inoculum all exhibited differences in the composition and richness of their rhizosphere microbial communities (Fig. 3.1). For most, plant genotype explained a significant amount of variance in the rhizosphere microbiome (PERMANOVA prokaryotic: n=120, $R^2=0.18$, $p<0.001$; fungal: n=120, $R^2=0.15$, $p<0.003$, Tables B.4-B.5). To focus on domestication effects, we carried out our remaining analysis on the genotype-mean microbial community as described in the methods. Our analysis of the genotype mean microbiome, revealed that domestication status explained 27% of the variation of the prokaryotic 16S rRNA, and 21% of the variation in fungal ITS (Fig. 3.1A, 3.1C, prokaryotic, n=12, $p<0.01$, fungal, n=12, $p<0.004$, Tables B.6-B.7). Furthermore, domesticated maize exhibited higher levels of species richness in their prokaryotic and fungal microbial communities compared to wild teosinte (Fig. 3.1B, 3.1D, Tukey’s HSD n=120, $p<0.05$).

To understand which microbial taxa were most affected by domestication status, we ran a differential gene expression analysis (DESeq2). This analysis revealed that domestication status influenced microbial membership of 346 different prokaryotic taxa (*alpha*=0.01). Of these, 260 OTUs were present in greater relative abundance in the inbred maize rhizosphere, while 86 had

greater relative abundance in the teosinte rhizosphere microbiome. Domesticated maize enriched OTUs across most of the major bacterial phylum, but was especially pronounced in *Proteobacteria*, and *Bacteroidetes* (Fig. 3.2). While teosinte microbiomes had greater abundance of *Firmicutes*, *Verrucomicrobia*, and *Actinobacteria* (Fig. 3.2). For the fungal microbiome, we found that domestication status influenced membership of 48 different fungal taxa (*alpha*=0.01). Of these, 37 had greater representation in the rhizosphere of modern inbred maize, while 11 were in greater relative abundance in the teosinte microbiome. Differences in the fungal abundance were primarily driven by enrichment in *Ascomycota* in the inbred maize microbiome.

Domestication status influences the nitrogen cycling genes present in the rhizosphere

Diversity, composition, and abundance of N-cycling functional groups were altered by domestication status of host plants (Fig. 3.3-4. Table B.8). Specifically, we observed that functional genes *nifH,* bacterial *amoA, nirK, nirS, and nosZ* were all significantly altered in composition in response to domestication status (Fig. 3.4. Table B.9). Furthermore, *nifH,* bacterial *amoA*, *nirS,* and *nosZ,* were all significantly more diverse (Tukey HSD*: $p<0.05$*) in the domesticated rhizosphere compared to the teosinte rhizosphere (Fig. 3.3A). Archaeal *amoA* did not show significant differences in gene composition or richness across domestication classes. Additionally, qPCR results showed that wild teosinte cultivars had higher copy numbers of archaeal *amoA,* bacterial *amoA,* and *nirK* (Fig. 3.3B, Tables B.10, Tukey HSD *$p<0.05$)*. These alpha diversity and abundance results showed an inverse relationship at the genotype level between functional gene diversity and abundance. Regression analysis revealed a strong negative relationship between gene abundance and diversity (Fig. B.1, R^2= -0.731, p<0.0123). Overall, domestication status explained 62% of the variation in mean richness of N-cycling functional groups among genotypes (PERMANOVA: n= 12, *$p<0.003$,* Table B.11.1*)*, and 65%

of the variation in average abundance of N-cycling functional groups (PERMANOVA: n= 12, *p<0.005*, Table B.11.2*).*

Discussion:

In this study we show that modern inbred maize and teosinte differ in microbial recruitment and that these differences extend to N-cycling functional groups within the microbiome. These findings suggest that the domestication and inbreeding process has resulted in an altered microbiome interaction within *Zea* and that teosinte germplasm contain microbiome-associated traits that have a potentially more sustainable N-cycling microbiome.

Our data shows that domesticated inbred maize hosts different assemblages and diversity of prokaryotic and fungal communities in the rhizosphere (Fig. 3.1-2). This result aligns with previous studies comparing the microbiome assemblages of teosinte and modern maize (Schmidt et al. 2020; Brisson et al. 2019; Johnston-Monje et al. 2014). Surprisingly, this study demonstrated that inbred maize displayed greater microbial diversity in the rhizosphere microbiome compared to teosinte. These finding suggest either that domesticated maize has an enhanced ability to maintain higher levels of diversity in the rhizosphere or a weakened ability to filter taxa from the rhizosphere. Furthermore, coincident with this diversity increase, we see greater abundance of copiotrophic bacteria (*Proteobacteria*) and potential pathogenic fungi (*Ascomycota*) (Fierer et al. 2007; Berbee 2001; Favela, Bohn, and Kent 2021). The microbial composition data lead us to believe the latter "weakened selection" hypothesis is more likely, with some support for this hypothesis coming from research on effects of domestication on arbuscular mycorrhizal (AM) symbiosis across 27 crop species (Martín-Robles et al. 2018). Martin-Robles et al. found that domesticated cultivars maintained less efficient AM symbiosis

with a weakened ability to down-regulate colonization under high nutrient conditions shifting their symbiosis from mutualistic to parasitic. A parallel process with domestication could be occurring with whole microbiome regulation as we observed in our study, charactered by modern maize having “weakened selection” to curb the growth of copiotrophic prokaryotes and pathogenic fungi.

Across other domesticated vs wild plant species, alpha diversity comparisons have shown mixed and contradictory results, with some domestication events causing decreases (Fierer et al. 2013) and other showing increases (Shenton et al. 2016; Coleman-Derr et al. 2015) in microbiome diversity. These repeated changes in microbiome diversity across a number of species may be suggestive of the strength of selection during domestication or the type of phenotypic (i.e., flavor, nutritional, size) selection the species experienced over the domestication process. Understanding the drivers of selection may highlight a shared domestication syndrome present across different cultivated agricultural crops that can be characterized by changes in microbiome diversity. Understanding the trade-offs and potential disruptions of microbial symbiosis will be important in improving our modern agricultural lines (Porter and Sachs 2020).

To gain an idea of the functional groups associated with these taxonomic community changes we took a targeted functional gene approach through the sequencing and quantification of diagnostic N-cycling genes. Understanding how specific functional groups respond to the unique rhizosphere effect presented by each plant genotype could be informative of how these microorganisms are processing nitrogen in the environment in proximity to the roots (Stein et al. 2016; Kuypers, Marchant, and Kartal 2018). We focused on diversity and abundance of functional genes related to denitrification, nitrification, and nitrogen fixation and found that

domestication played a role in shaping the functional groups related to all of these processes (Fig. 3.3-4). N-cycling functional gene abundances are influenced at different rates. Maize genotypes appeared to have higher diversity of N-cycling functional groups in the rhizosphere compared to teosinte genotypes, while teosinte genotypes had higher abundance of functional groups. This negative relationship between abundance and diversity perhaps suggests a trade-off in microbial interaction similar to those seen in AM interactions (Porter and Sachs 2020). Additionally, this disjunct between the diversity and abundance suggests different mechanisms of microbiome interaction across teosinte and maize. While teosinte appears to be more selective of the nitrogen transformers it allows to persist in the rhizosphere (lower diversity), it is also more effective in its propagation of those microbes (higher abundance). This conflicting abundance-diversity relationship is interesting as there is no well-established understanding for which microbial community characteristic is most predictive of specific N-cycling function in soils (Ma, Zilles, and Kent 2019). Some research in this area suggests that diversity is a more significant predictor of ecosystem function (Philippot, Spor, et al. 2013) while others show abundance to be more important (Ouyang et al. 2018). In the rhizosphere, further work is needed across a wide range of plants and soil type to disentangle the diversity-abundance-function relationship.

Diazotrophs were not significantly different in abundance between the two treatments. This finding was not surprising because plants were fertilized with nitrogen during the growing period, and diazotrophs would have no competitive advantage under these conditions. As with other functional groups, the maize rhizosphere hosted a considerable amount of diversity in *nifH* – we attribute this higher diversity to a potential inability to filter diazotroph colonization in their rhizospheres as mentioned above. Recent research displaying that some maize landraces can host

N-fixing taxa in their aerial roots (Van Deynze et al. 2018) has highlighted that maize has a more complicated relation with diazotrophs then previously understood. In addition, we have previously seen that within elite inbred maize, the modern breeding process has resulted in reduced *nifH* abundance and diversity in the rhizosphere since the 1940s (Favela, Bohn, and Kent 2021) . Further work needs to be carried out under a variety of field N conditions to understand whether these findings were caused by differences in the domestication or effects of fertilization.

In regard to nitrification functional groups, we were surprised to find that both archaeal and bacterial *amoA* were in higher abundance but lower in diversity in the teosinte rhizosphere compared to the maize rhizosphere. This result was surprising as nitrification is commonly thought of as a process that competes with plants for available N and can lead to considerable losses of N from the agroecosystem (Subbarao et al. 2013; Moreau et al. 2019) . Furthermore in a other cereal grass species it has been shown that some plants varieties, typically *uncultivated,* can produce secondary toxic compounds that biologically inhibit nitrification (BNI) (Coskun et al. 2017a, 2017b). Therefore, our hypothesis going into the study was that if teosinte showed more traits related to sustainability, these ancestral genotypes would limit nitrification and would presumably recruit a lower abundance of nitrifier taxa. Perhaps, teosinte still contains BNI traits, they just manifest as changes in the diversity (lower) of functional groups- but not in abundance (higher). This would not be too surprising as most of the established BNI work has been done with a single nitrifier in isolation outside of the nitrifier community context (Subbarao et al. 2006). Unfortunately, we did not characterize nitrification rates, just markers of function, further research is needed to determine the best predictors of nitrifier function in the rhizosphere in a soil community context.

In addition, we observed effects of plant domestication on genes diagnostic for denitrification functional groups (Fig. 3.3). Denitrification genes responsible for the conversion of nitrite into nitric oxide showed differences in abundance, with *nirK* being more abundant in the teosinte rhizosphere and *nirS* being greater in the maize rhizosphere. Previous work has shown that *nirS*-type denitrifiers are more sensitive to rhizosphere effects compared to *nirK*-type and that *nirK* communities have a broader profile for carbon substrate utilization (Bardon et al. 2016; Hou et al. 2018). Perhaps, *nirS* increase in maize rhizospheres is caused by having a weaker rhizosphere effect, while increases in *nirK* could be attributed to teosinte's likely more complex metabolic profile. Furthermore, studies have shown that the response of *nirS* and *nirK* functional groups to environmental gradients are markedly different, which supports the possibility that the two communities occupy different ecological niches (Jones and Hallin 2010; Wei et al. 2015; Azziz et al. 2017). Perhaps to the dentification functional groups the maize and teosinte rhizosphere present different ecological niches generated by altered patterns in plant exudation. These differences in denitrification community recruitment may also be attributed to phenotypic differences in biological denitrification inhibition (BDI) (Bardon et al. 2016). BDI, originally described in *Fallopia* has been defined as the ability of the plant to release secondary metabolites (like procyanidins) that inhibit denitrifers and therefore conserve nitrates in the rhizosphere environment (Bardon et al. 2014). Furthermore, studies across a number of species have shown that exudates from a variety of plant species have the ability to alter denitrification abundance and activity (Achouak et al. 2019). A key challenge will be understanding the genes and subsequent related secondary metabolites driving these ecosystem function differences.

We hypothesize that our differences in nitrifier and denitrifier communities between maize and teosinte are caused by differences in the production of plant secondary compounds

originating from domestication and breeding. Many recent comprehensive studies examining transcriptome and metabolomic differences between maize and teosinte have shown that alkaloids, terpenoids, lipids, and benzoxazinoids and their regulation has been altered during maize evolution (G. Xu et al. 2019; X. Wang et al. 2018). We propose that these genetic and chemical changes in maize result in altered recruitment of N-cycling functional groups in the rhizosphere and may even alter how maize obtains nutrients from the soil matrix. Understanding that maize and teosinte differ in recruitment of microbiome groups throughout the nitrogen cycle (Fig 3.4) is important as these functional groups play a central role in the movement of nitrogen in the agroecosystem (Kuypers, Marchant, and Kartal 2018; Bowles et al. 2018).

Determining the function of these lost and transformed ancestral plant microbiome traits will inform us to their usage in the agricultural system. Currently, a substantial fraction of nitrogen fertilizer applied to arable lands is often lost, leading to the pollution of terrestrial and aquatic ecosystems (Bowles et al. 2018). This failure of modern agriculture has led to global disruption and acceleration of the reactive N cycle. As maize is one of the most farmed and fertilized crops in the world and a staple food for many populations, finding a solution in this species is vital (Ladha et al. 2016). Misdirection of N away from plants is commonly attributed to microorganisms in the soil and rhizosphere that transform and use N. The fact that domesticated and wild *Zea* develop different functional nitrogen cycling genes within their rhizospheres suggest that plants may be able to intervene in these microbial activities.

In conclusion, we have shown that the domestication of teosinte into modern maize has resulted in taxonomic and N-cycling functional group changes to the rhizosphere microbiome. Modern maize appears to have a “weakened selection” on the rhizosphere microbiome compared to teosinte. It still needs to be determined if and how these characteristics influence the N-cycling

function of the rhizosphere microbiome in agroecosystem, but this does suggest that ancestral functional microbiome characteristics are different than modern agriculture (Pérez-Jaramillo, Mendes, and Raaijmakers 2015). The more we understand about how domestication has altered the functional microbiome interactions the closer we are to selecting and ‘re-wilding’ our modern lines with beneficial traits that contribute to agricultural sustainability.

Figures:

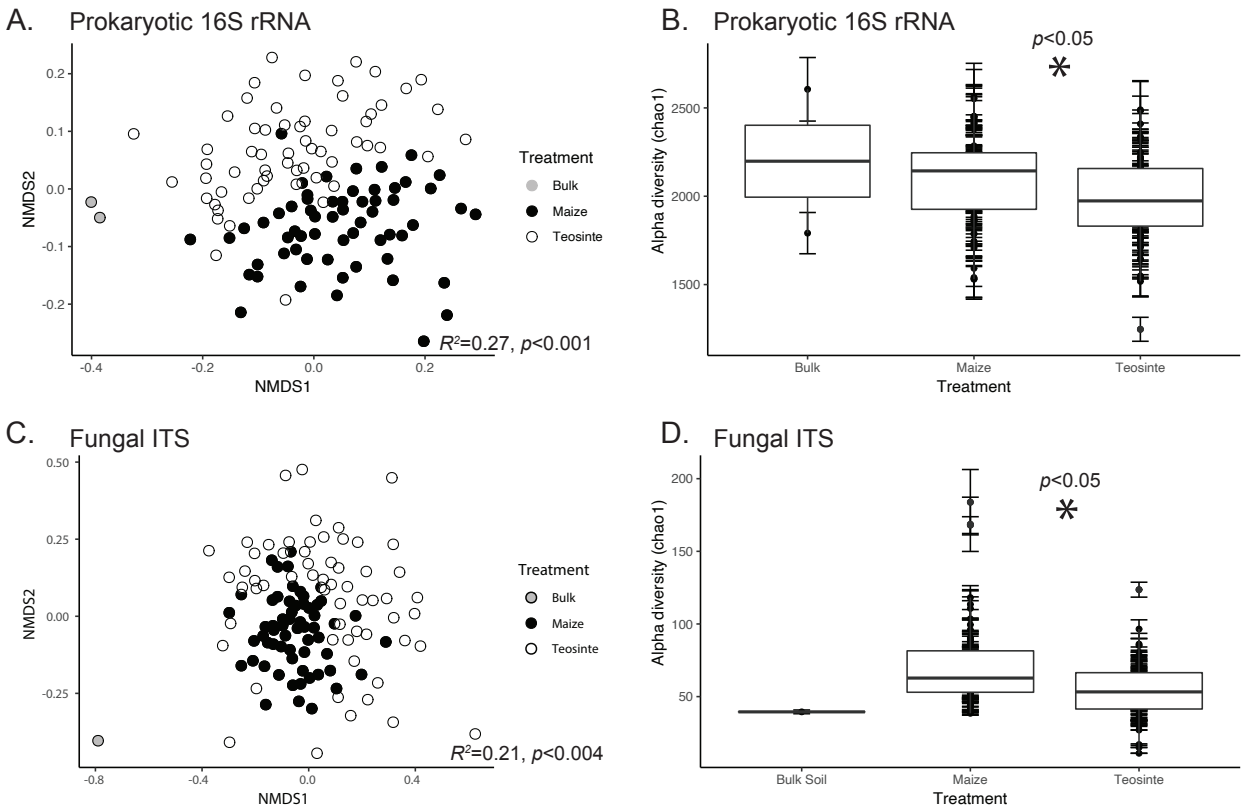

Figure 3.1 NMDS ordinations based on Bray-Curtis dissimilarity among prokaryotic 16S rRNA (**A**) and fungal ITS (**C**) rhizosphere microbiome samples compared among inbred maize, teosinte, and bulk soil. Statistics present in the figure show PERMANOVA model results (Table B.4-B.7). (**B, D**) Highlight differences in alpha diversity (chao1) across our inbred maize, teosinte, and bulk soil. Inbred maize and teosinte have significantly different diversity values according to the T-test.

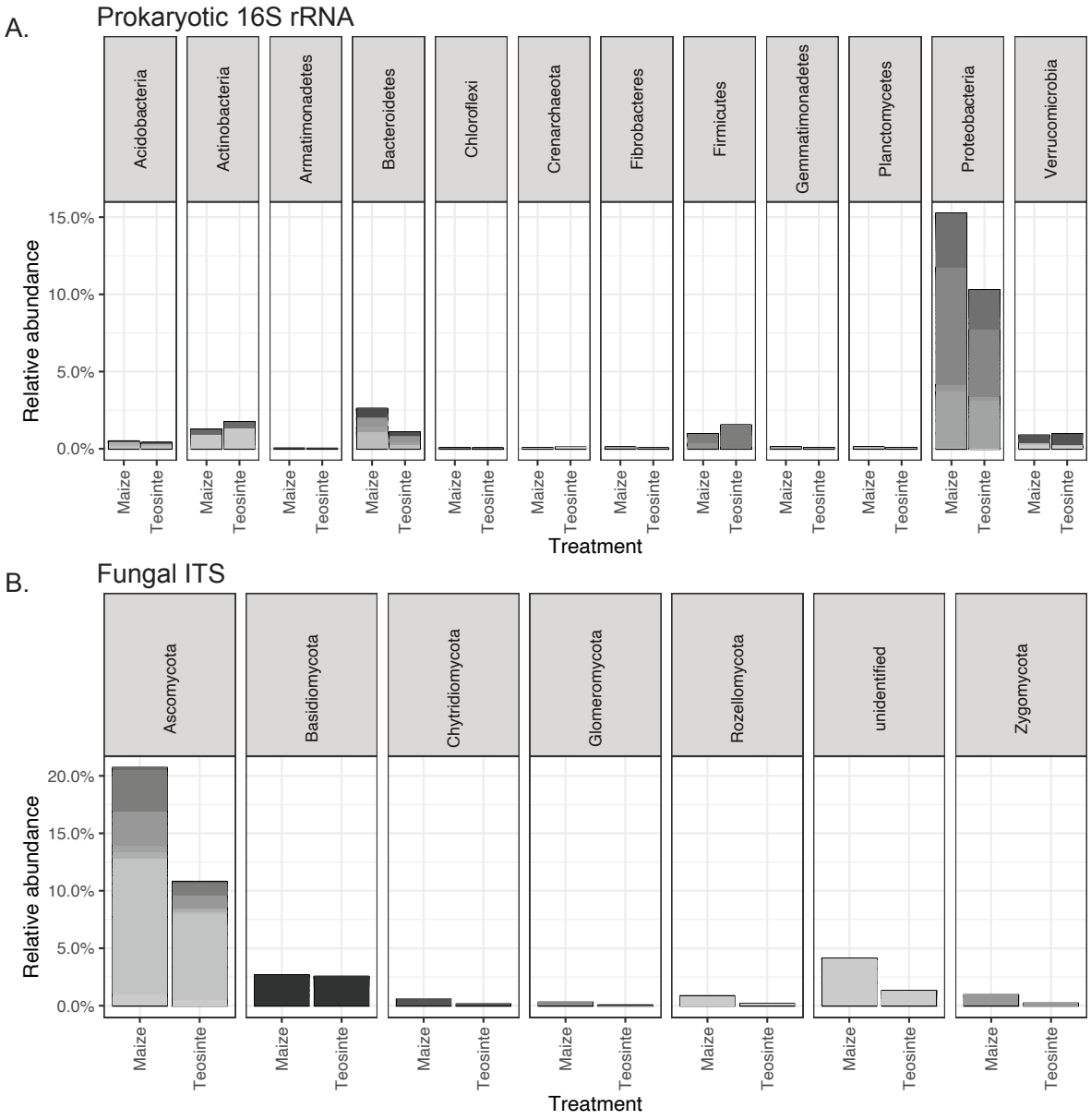

Figure 3.2 Denotes significantly different OTUs between inbred maize and teosinte rhizospheres as identified by DESEQ2. **A**) Stack plots show the relative abundance of differential abundant prokaryotic 16S rRNA OTUs facetted by phylum. **B**) Stack plots show the relative abundance of differential abundant fungal ITS OTUs facetted by phylum. Greyscale within stack plots are included to show taxonomic class identity. List of OTUs differential enriched and stack plots within highly abundant taxonomic groups included in supplemental.

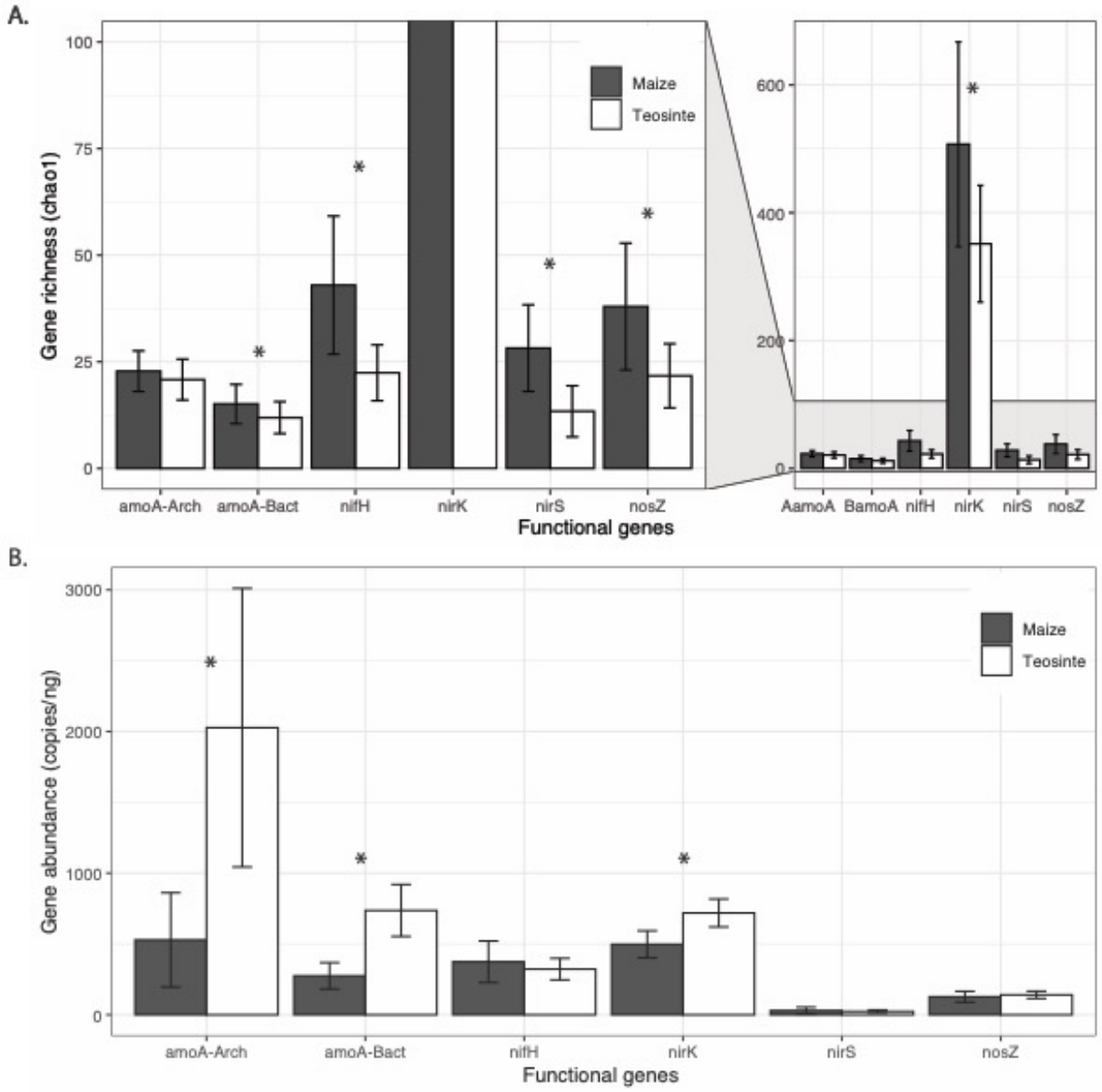

Figure 3.3 Here we display the comparison of functional gene richness and abundance across the maize and teosinte rhizosphere. **A**) Displays the gene richness (chao1) across the functional genes measured in this study. Note that the axis is replotted to correct for the high richness in the *nirK* gene. **B**) Displays the gene abundance (copies/ng) across the functional genes. Asterisk included in both figures to display significance among groups using t-test.

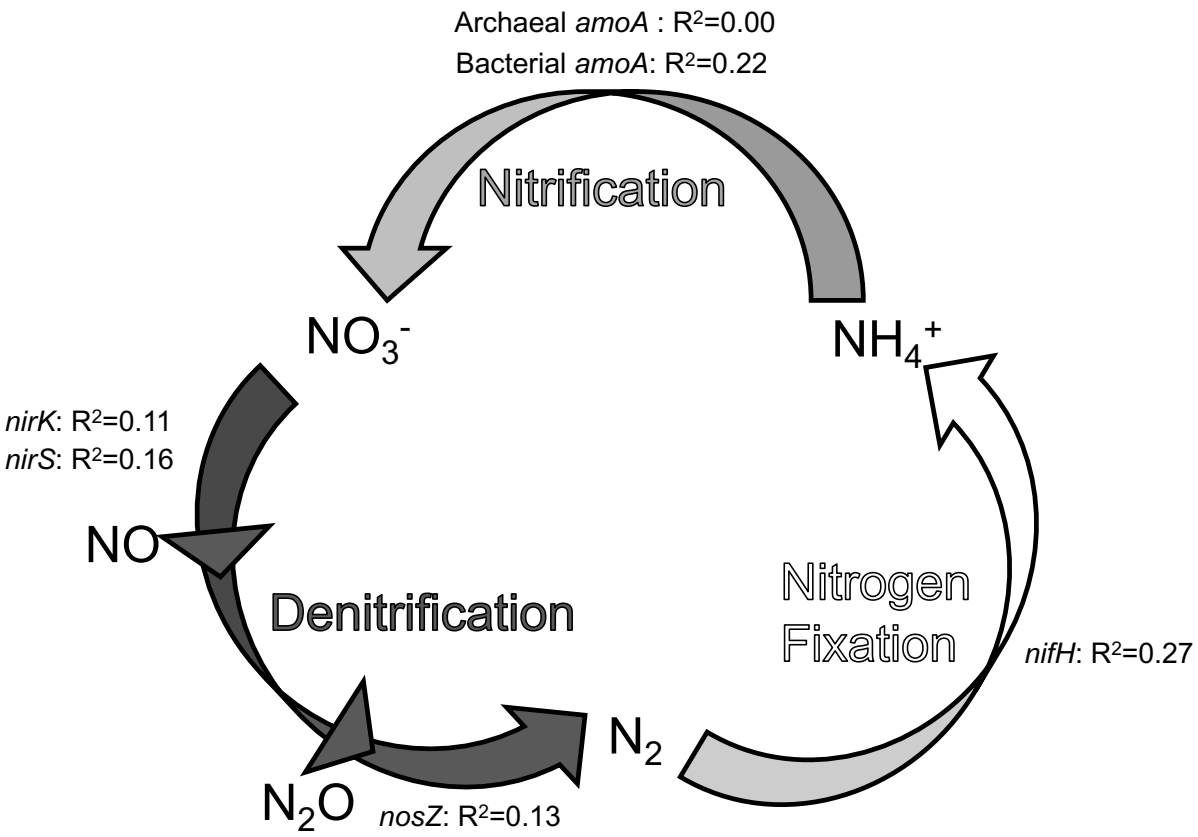

Figure 3.4 Minimal Nitrogen cycling is used as a graphical tool to display wherein the N-cycling domestication status influenced the composition of the groups. Percentages denote the amount of variance in the functional gene composition explained by the domestication factor in PERMANOVA.

References:

Achouak, Wafa, Danis Abrouk, Julien Guyonnet, Mohamed Barakat, Philippe Ortet, Laurent Simon, Catherine Lerondelle, Thierry Heulin, and Feth El Zahar Haichar. 2019. "Plant Hosts Control Microbial Denitrification Activity." *FEMS Microbiology Ecology* 95 (3): 21. https://doi.org/10.1093/femsec/fiz021.

Altschul, Stephen F, Thomas L Madden, Alejandro A Schäffer, Jinghui Zhang, Zheng Zhang, Webb Miller, and David J Lipman. 1997. "Gapped BLAST and PSI-BLAST: A New Generation of Protein Database Search Programs." *Nucleic Acids Research* 25 (17): 3389–3402.

Azziz, Gastón, Jorge Monza, Claudia Etchebehere, and Pilar Irisarri. 2017. "NirS- and NirK-Type Denitrifier Communities Are Differentially Affected by Soil Type, Rice Cultivar and Water Management." *European Journal of Soil Biology* 78 (January): 20–28. https://doi.org/10.1016/j.ejsobi.2016.11.003.

Bardon, Clément, Florence Piola, Floriant Bellvert, Feth el Zahar Haichar, Gilles Comte, Guillaume Meiffren, Thomas Pommier, Sara Puijalon, Noelline Tsafack, and Franck Poly. 2014. "Evidence for Biological Denitrification Inhibition (BDI) by Plant Secondary Metabolites." *New Phytologist* 204 (3): 620–30. https://doi.org/10.1111/nph.12944.

Bardon, Clément, Franck Poly, Florence Piola, Muriel Pancton, Gilles Comte, Guillaume Meiffren, and Feth el Zahar Haichar. 2016. "Mechanism of Biological Denitrification Inhibition: Procyanidins Induce an Allosteric Transition of the Membrane-Bound Nitrate Reductase through Membrane Alteration." *FEMS Microbiology Ecology* 92 (5): 1–11. https://doi.org/10.1093/femsec/fiw034.

Berbee, Mary L. 2001. "The Phylogeny of Plant and Animal Pathogens in the Ascomycota." *Physiological and Molecular Plant Pathology* 59 (4): 165–87. https://doi.org/10.1006/pmpp.2001.0355.

Bouffaud, Marie-lara, Marie-andrée Poirier, Daniel Muller, and Yvan Moënne-loccoz. 2014. "Root Microbiome Relates to Plant Host Evolution in Maize and Other Poaceae" 16: 2804–14. https://doi.org/10.1111/1462-2920.12442.

Bouffaud, Marie Lara, Martina Kyselkov, Brigitte Gouesnard, Genevieve Grundmann, Daniel Muller, and Yvan Mo??nne-Loccoz. 2012. "Is Diversification History of Maize Influencing Selection of Soil Bacteria by Roots?" *Molecular Ecology*. https://doi.org/10.1111/j.1365-294X.2011.05359.x.

Bouffaud, Marie Lara, Sebastien Renoud, Yvan Moenne-Loccoz, and Daniel Muller. 2016. "Is Plant Evolutionary History Impacting Recruitment of Diazotrophs and NifH Expression in the Rhizosphere?" *Scientific Reports* 6. https://doi.org/10.1038/srep21690.

Bowles, Timothy M, Shady S Atallah, Eleanor E Campbell, Amélie C.M. Gaudin, William R Wieder, and A Stuart Grandy. 2018. "Addressing Agricultural Nitrogen Losses in a Changing Climate." *Nature Sustainability* 1 (8): 399–408. https://doi.org/10.1038/s41893-018-0106-0.

Brisson, Vanessa L, Jennifer E Schmidt, Trent R Northen, John P Vogel, and Amélie C.M. Gaudin. 2019. "Impacts of Maize Domestication and Breeding on Rhizosphere Microbial Community Recruitment from a Nutrient Depleted Agricultural Soil." *Scientific Reports* 9 (1). https://doi.org/10.1038/s41598-019-52148-y.

Bulgarelli, Davide, Ruben Garrido-Oter, Philipp C. Münch, Aaron Weiman, Johannes Dröge, Yao Pan, Alice C McHardy, and Paul Schulze-Lefert. 2015. “Structure and Function of the Bacterial Root Microbiota in Wild and Domesticated Barley.” *Cell Host and Microbe* 17 (3): 392–403. https://doi.org/10.1016/j.chom.2015.01.011.

Caporaso, J Gregory, Justin Kuczynski, Jesse Stombaugh, Kyle Bittinger, Frederic D Bushman, Elizabeth K Costello, Noah Fierer, et al. 2010. “QIIME Allows Analysis of High-Throughput Community Sequencing Data.” *Nature Methods* 7 (5): 335–36. https://doi.org/10.1038/nmeth.f.303.

Coleman-Derr, Devin, Damaris Desgarennes, Citlali Fonseca-Garcia, Stephen Gross, Scott Clingenpeel, Tanja Woyke, Gretchen North, Axel Visel, Laila P. Partida-Martinez, and Susannah Tringe. 2015. “Biogeography and Cultivation Affect Microbiome Composition in the Drought-Adapted Plant Subgenus Agave.” *In Review*, 798–811. https://doi.org/10.1111/nph.13697.

Coskun, Devrim, Dev T Britto, Weiming Shi, and Herbert J Kronzucker. 2017a. “How Plant Root Exudates Shape the Nitrogen Cycle.” *Trends in Plant Science* 22 (8): 661–73. https://doi.org/10.1016/j.tplants.2017.05.004.

Coskun. 2017b. “Nitrogen Transformations in Modern Agriculture and the Role of Biological Nitrification Inhibition.” *Nature Plants*. https://doi.org/10.1038/nplants.2017.74.

DeSantis, T. Z., P Hugenholtz, N Larsen, M Rojas, E L Brodie, K Keller, T Huber, D Dalevi, P Hu, and G L Andersen. 2006. “Greengenes, a Chimera-Checked 16S RRNA Gene Database and Workbench Compatible with ARB.” *Applied and Environmental Microbiology* 72 (7): 5069–72. https://doi.org/10.1128/AEM.03006-05.

Deynze, Allen Van, Pablo Zamora, Pierre Marc Delaux, Cristobal Heitmann, Dhileepkumar Jayaraman, Shanmugam Rajasekar, Danielle Graham, et al. 2018. “Nitrogen Fixation in a Landrace of Maize Is Supported by a Mucilage-Associated Diazotrophic Microbiota.” *PLoS Biology* 16 (8): e2006352. https://doi.org/10.1371/journal.pbio.2006352.

Diamond, Jared. 2002a. “Evolution, Consequences and Future of Plant and Animal Domestication.” *Nature* 418 (6898): 700–707. https://doi.org/10.1038/nature01019.

Doebley, John. 2004. “THE GENETICS OFMAIZE EVOLUTION.” *Annu. Rev. Genet.*, 37–59. https://doi.org/10.1146/annurev.genet.38.072902.092425.

Drinkwater, L E, and S S Snapp. 2007. “Nutrients in Agroecosystems: Rethinking the Management Paradigm.” *Advances in Agronomy*. https://doi.org/10.1016/S0065-2113(04)92003-2.

Edgar, Robert C. 2010a. “Search and Clustering Orders of Magnitude Faster than BLAST.” *Bioinformatics* 26 (19): 2460–61. https://doi.org/10.1093/bioinformatics/btq461.

Edwards, Joseph D., Cameron M. Pittelkow, Angela D. Kent, and Wendy H. Yang. 2018. “Dynamic Biochar Effects on Soil Nitrous Oxide Emissions and Underlying Microbial Processes during the Maize Growing Season.” *Soil Biology and Biochemistry* 122 (December 2017): 81–90. https://doi.org/10.1016/j.soilbio.2018.04.008.

Favela, Alonso, Martin O. Bohn, and Angela D. Kent. 2021. “Maize Germplasm Chronosequence Shows Crop Breeding History Impacts Recruitment of the Rhizosphere Microbiome.” *ISME Journal*. https://doi.org/10.1038/s41396-021-00923-z.

Fierer, Noah, Mark A. Bradford, and Robert B. Jackson. 2007. “Toward an Ecological Classification of Soil Bacteria.” *Ecology* 88 (6): 1354–64. https://doi.org/10.1890/05-1839.

Fierer, Noah, Joshua Ladau, Jose C. Clemente, Jonathan W. Leff, Sarah M. Owens, Katherine S. Pollard, Rob Knight, Jack A. Gilbert, and Rebecca L. McCulley. 2013. "Reconstructing the Microbial Diversity and Function of Pre-Agricultural Tallgrass Prairie Soils in the United States." *Science* 342 (6158): 621–24. https://doi.org/10.1126/science.1243768.

Fish, Jordan A., Benli Chai, Qiong Wang, Yanni Sun, C. Titus Brown, James M. Tiedje, and James R. Cole. 2013. "FunGene: The Functional Gene Pipeline and Repository." *Frontiers in Microbiology* 4 (OCT): 1–14. https://doi.org/10.3389/fmicb.2013.00291.

Fitzpatrick, Connor R., Julia Copeland, Pauline W. Wang, David S. Guttman, Peter M. Kotanen, and Marc T.J. Johnson. 2018. "Assembly and Ecological Function of the Root Microbiome across Angiosperm Plant Species." *Proceedings of the National Academy of Sciences of the United States of America* 115 (6): E1157–65. https://doi.org/10.1073/pnas.1717617115.

Gaillard, Mickaël D.P., Gaétan Glauser, Christelle A.M. Robert, and Ted C.J. Turlings. 2018. "Fine-Tuning the 'Plant Domestication-Reduced Defense' Hypothesis: Specialist vs Generalist Herbivores." *New Phytologist* 217 (1): 355–66. https://doi.org/10.1111/nph.14757.

Gaudin, Amelie C M, Sarah A. McClymont, and Manish N Raizada. 2011. "The Nitrogen Adaptation Strategy of the Wild Teosinte Ancestor of Modern Maize, Zea Mays Subsp. Parviglumis." *Crop Science* 51 (6): 2780–95. https://doi.org/10.2135/cropsci2010.12.0686.

Gordon, A, G J Hannon, and Gordon. 2014. "FASTX-Toolkit." *[Online] Http://Hannonlab. Cshl. Edu/Fastx_ Toolkit Http://Hannonlab. Cshl. Edu/Fastx_ Toolkit*.

Hou, Shengpeng, Chao Ai, Wei Zhou, Guoqing Liang, and Ping He. 2018. "Structure and Assembly Cues for Rhizospheric NirK- and NirS-Type Denitrifier Communities in Long-Term Fertilized Soils." *Soil Biology and Biochemistry* 119 (April): 32–40. https://doi.org/10.1016/j.soilbio.2018.01.007.

Hufford, Matthew B, Paul Bilinski, Tanja Pyhäjärvi, and Jeffrey Ross-Ibarra. 2012. "Teosinte as a Model System for Population and Ecological Genomics." *Trends in Genetics*. https://doi.org/10.1016/j.tig.2012.08.004.

Hufford, Matthew B, Xun Xu, Joost Van Heerwaarden, Tanja Pyhäjärvi, Jer Ming Chia, Reed A Cartwright, Robert J Elshire, et al. 2012. "Comparative Population Genomics of Maize Domestication and Improvement." *Nature Genetics* 44 (7): 808–11. https://doi.org/10.1038/ng.2309.

Ishii, Satoshi, Gaku Kitamura, Takahiro Segawa, Ayano Kobayashi, Takayuki Miura, Daisuke Sano, and Satoshi Okabe. 2014. "Microfluidic Quantitative PCR for Simultaneous Quantification of Multiple Viruses in Environmental Water Samples." *Applied and Environmental Microbiology* 80 (24): 7505–11. https://doi.org/10.1128/AEM.02578-14.

Jensen, Helen, Rachel S Meyer, Ashley E Duval, and Helen R Jensen. 2012. "Tansley Review Patterns and Processes in Crop Domestication: An Historical Review and Quantitative Analysis of 203 Global Food Crops." *New Phytologist* 196: 29–48. https://doi.org/10.1111/j.1469-8137.2012.04253.x.

Johnston-Monje, David, Walaa Kamel Mousa, George Lazarovits, and Manish N Raizada. 2014. "Impact of Swapping Soils on the Endophytic Bacterial Communities of Pre-Domesticated, Ancient and Modern Maize." *BMC Plant Biology* 14. https://doi.org/10.1186/s12870-014-0233-3.

Jones, Christopher M., and Sara Hallin. 2010. "Ecological and Evolutionary Factors Underlying Global and Local Assembly of Denitrifier Communities." *ISME Journal* 4 (5): 633–41. https://doi.org/10.1038/ismej.2009.152.

Kuypers, Marcel M.M., Hannah K. Marchant, and Boran Kartal. 2018. "The Microbial Nitrogen-Cycling Network." *Nature Reviews Microbiology* 16 (5): 263–76. https://doi.org/10.1038/nrmicro.2018.9.

Lau, Jennifer A, Jay T Lennon, Jennifer A Laua, Jay T Lennon3-'-, and David M Karl. 2012. "Rapid Responses of Soil Microorganisms Improve Plant Fitness in Novel Environments." *Source: Proceedings of the National Academy of Sciences of the United States of America* 109 (35): 14058–62. http://www.jstor.org/stable/41701642.

Li, Dongfang, Thomas B. Voigt, and Angela D. Kent. 2016. "Plant and Soil Effects on Bacterial Communities Associated with Miscanthus × Giganteus Rhizosphere and Rhizomes." *GCB Bioenergy* 8 (1): 183–93. https://doi.org/10.1111/gcbb.12252.

Love, Michael I, Wolfgang Huber, and Simon Anders. 2014. "Moderated Estimation of Fold Change and Dispersion for RNA-Seq Data with DESeq2." *Genome Biology* 15 (12). https://doi.org/10.1186/s13059-014-0550-8.

Ma, Yanjun, Julie L. Zilles, and Angela D. Kent. 2019. "An Evaluation of Primers for Detecting Denitrifiers via Their Functional Genes." *Environmental Microbiology* 21 (4): 1196–1210. https://doi.org/10.1111/1462-2920.14555.

Madsen, Eugene L. 2011. "Microorganisms and Their Roles in Fundamental Biogeochemical Cycles." *Current Opinion in Biotechnology*. https://doi.org/10.1016/j.copbio.2011.01.008.

Mag, Tanja, and Steven L Salzberg. 2011. "FLASH: Fast Length Adjustment of Short Reads to Improve Genome Assemblies" 27 (21): 2957–63. https://doi.org/10.1093/bioinformatics/btr507.

Martín-Robles, Nieves, Anika Lehmann, Erica Seco, Ricardo Aroca, Matthias C Rillig, and Rubén Milla. 2018. "Impacts of Domestication on the Arbuscular Mycorrhizal Symbiosis of 27 Crop Species." *New Phytologist* 218 (1): 322–34. https://doi.org/10.1111/nph.14962.

Matsuoka, Yoshihiro, Yves Vigouroux, Major M Goodman, J. Sanchez G., Edward Buckler, and John Doebley. 2002. "A Single Domestication for Maize Shown by Multilocus Microsatellite Genotyping." *Proceedings of the National Academy of Sciences* 99 (9): 6080–84. https://doi.org/10.1073/pnas.052125199.

McMurdie, Paul J., and Susan Holmes. 2013. "Phyloseq: An R Package for Reproducible Interactive Analysis and Graphics of Microbiome Census Data." *PLoS ONE* 8 (4): e61217–e61217. https://doi.org/10.1371/journal.pone.0061217.

Moreau, Delphine, Richard D. Bardgett, Roger D. Finlay, David L. Jones, and Laurent Philippot. 2019. "A Plant Perspective on Nitrogen Cycling in the Rhizosphere." *Functional Ecology* 33 (4): 540–52. https://doi.org/10.1111/1365-2435.13303.

Oksanen, Jari, Roeland Kindt, Pierre Legendre, Bob O'hara, M Henry, and H Stevens Maintainer. 2007. "The Vegan Package Title Community Ecology Package." Http://Cran.r-Project.Org/, Http://R-Forge.r-Project.Org/Projects/Vegan/. 2007. http://ftp.uni-bayreuth.de/math/statlib/R/CRAN/doc/packages/vegan.pdf.

Ouyang, Yang, Sarah E Evans, Maren L Friesen, and Lisa K Tiemann. 2018. "Effect of Nitrogen Fertilization on the Abundance of Nitrogen Cycling Genes in Agricultural Soils: A Meta-Analysis of Field Studies." https://doi.org/10.1016/j.soilbio.2018.08.024.

Pandey, Girdhar Kumar, Raffaella Balestrini, Consiglio Nazionale Delle Ricerche, Stanislav Kopriva, Manuela Peukert, Richard Jacoby, Antonella Succurro, and Anna Koprivova. 2017. "The Role of Soil Microorganisms in Plant Mineral Nutrition—Current Knowledge and Future Directions." https://doi.org/10.3389/fpls.2017.01617.

Panke-Buisse, Kevin, Angela C Poole, Julia K Goodrich, Ruth E Ley, and Jenny Kao-Kniffin. 2014. “Selection on Soil Microbiomes Reveals Reproducible Impacts on Plant Function.” *The ISME Journal* 9 (10): 980–89. https://doi.org/10.1038/ismej.2014.196.

Peiffer, Jason A, Aymé Spor, Omry Koren, Zhao Jin, Susannah Green Tringe, Jeffery L Dangl, Edward S. Buckler, and Ruth E. Ley. 2013. “Diversity and Heritability of the Maize Rhizosphere Microbiome under Field Conditions.” *Proceedings of the National Academy of Sciences of the United States of America* 110 (16): 6548–53. https://doi.org/10.1073/pnas.1302837110.

Pérez-Jaramillo, Juan E, Víctor J Carrión, Mattias de Hollander, and Jos M Raaijmakers. 2018. “The Wild Side of Plant Microbiomes.” *Microbiome* 6 (1). https://doi.org/10.1186/s40168-018-0519-z.

Pérez-Jaramillo, Juan E, Rodrigo Mendes, and Jos M Raaijmakers. 2015. “Impact of Plant Domestication on Rhizosphere Microbiome Assembly and Functions.” *Plant Molecular Biology* 90 (6): 635–44. https://doi.org/10.1007/s11103-015-0337-7.

Philippot, Laurent, Sara Hallin, and Michael Schloter. 2007. “Ecology of Denitrifying Prokaryotes in Agricultural Soil.” *Advances in Agronomy*. https://doi.org/10.1016/S0065-2113(07)96003-4.

Philippot, Laurent, Jos M Raaijmakers, Philippe Lemanceau, and Wim H. Van Der Putten. 2013. “Going Back to the Roots: The Microbial Ecology of the Rhizosphere.” *Nature Reviews Microbiology* 11 (11): 789–99. https://doi.org/10.1038/nrmicro3109.

Philippot, Laurent, Aymé Spor, Catherine Hénault, David Bru, Florian Bizouard, Christopher M Jones, Amadou Sarr, and Pierre-Alain Maron. 2013. “Loss in Microbial Diversity Affects Nitrogen Cycling in Soil.” *The ISME Journal* 734: 1609–19. https://doi.org/10.1038/ismej.2013.34.

Porter, Stephanie S, and Joel L Sachs. 2020. “Agriculture and the Disruption of Plant–Microbial Symbiosis.” *Trends in Ecology and Evolution*. https://doi.org/10.1016/j.tree.2020.01.006.

R Core Team. 2013. “R: A Language and Environment for Statistical Computing.” *R Foundation for Statistical Computing*. Vienna, Austria. URL http://www.R-project.org/. https://doi.org/10.1007/978-3-540-74686-7.

Ryan, Clarence A, Christopher J Lamb, Andre T Jagendorf, Pappachan E Kolattukudy, R James Cook, Linda S Thomashow, David M Weller, et al. 1995. “Molecular Mechanisms of Defense by Rhizobacteria against Root Disease.” Vol. 92. https://www.pnas.org/content/pnas/92/10/4197.full.pdf.

Schimel, Joshua P, Jennifer Bennett, Noah Fierer, Richard D Bardgett, Michael B Usher, and David W Hopkins. 2017. “Microbial Community Composition and Soil Nitrogen Cycling: Is There Really a Connection?” *Biological Diversity and Function in Soils*. https://doi.org/10.1017/CBO9780511541926.011.

Schmidt, Jennifer E., Jorge L. Mazza Rodrigues, Vanessa L. Brisson, Angela Kent, and Amélie C.M. Gaudin. 2020. “Impacts of Directed Evolution and Soil Management Legacy on the Maize Rhizobiome.” *Soil Biology and Biochemistry* 145 (April). https://doi.org/10.1016/j.soilbio.2020.107794.

Shenton, Matthew, Chie Iwamoto, Nori Kurata, and Kazuho Ikeo. 2016. “Effect of Wild and Cultivated Rice Genotypes on Rhizosphere Bacterial Community Composition.” *Rice* 9 (42). https://doi.org/10.1186/s12284-016-0111-8.

Stein, Lisa Y, Gerald Moser, Silvia Pajares, and Brendan J M Bohannan. 2016. “Ecology of Nitrogen Fixing, Nitrifying, and Denitrifying Microorganisms in Tropical Forest Soils.” https://doi.org/10.3389/fmicb.2016.01045.

Subbarao, G V, Ae T Ishikawa, Ae O Ito, Ae K Nakahara, H Y Wang, W L Berry, Ae H Y Wang, and Ae W L Berry. 2006. “A Bioluminescence Assay to Detect Nitrification Inhibitors Released from Plant Roots: A Case Study with Brachiaria Humidicola” 288: 101–12. https://doi.org/10.1007/s11104-006-9094-3.

Subbarao, G V, K L Sahrawat, K Nakahara, I M Rao, M Ishitani, C T Hash, M Kishii, D G Bonnett, W L Berry, and J C Lata. 2013. “A Paradigm Shift towards Low-Nitrifying Production Systems: The Role of Biological Nitrification Inhibition (BNI).” *Annals of Botany*. https://doi.org/10.1093/aob/mcs230.

Swanson-Wagner, Ruth, Roman Briskine, Robert Schaefer, Matthew B Hufford, Jeffrey Ross-Ibarra, Chad L Myers, Peter Tiffin, and Nathan M Springer. 2012. “Reshaping of the Maize Transcriptome by Domestication.” *Proceedings of the National Academy of Sciences* 109 (29): 11878–83. https://doi.org/10.1073/pnas.1201961109.

Szoboszlay, Márton, Julie Lambers, Janet Chappell, Joseph V Kupper, Luke A Moe, and David H. McNear. 2015. “Comparison of Root System Architecture and Rhizosphere Microbial Communities of Balsas Teosinte and Domesticated Corn Cultivars.” *Soil Biology and Biochemistry* 80: 34–44. https://doi.org/10.1016/j.soilbio.2014.09.001.

Vitousek, Peter M, John D Aber, Robert H Howarth, Gene E Likens, Pamela A Matson, David W Schindler, William H Schlesinger, and David G Tilman. 1997. “Human Alteration Of the Global Nitrogen Cycle: Source and Consequences.” *Ecol Appl* 7 (3): 737–50. https://doi.org/10.1038/nn1891.

Wagner, Maggie R, Derek S Lundberg, Devin Coleman-Derr, Susannah G Tringe, Jeffery L Dangl, and Thomas Mitchell-Olds. 2014. “Natural Soil Microbes Alter Flowering Phenology and the Intensity of Selection on Flowering Time in a Wild Arabidopsis Relative.” *Ecology Letters* 17 (6): 717–26. https://doi.org/10.1111/ele.12276.

Walters, William A, Zhao Jin, Nicholas Youngblut, Jason G Wallace, Jessica Sutter, Wei Zhang, Antonio González-Peña, et al. 2018. “Large-Scale Replicated Field Study of Maize Rhizosphere Identifies Heritable Microbes.” *Proceedings of the National Academy of Sciences of the United States of America* 115 (28): 7368–73. https://doi.org/10.1073/pnas.1800918115.

Wang, Li, Timothy M Beissinger, Anne Lorant, Claudia Ross-Ibarra, Jeffrey Ross-Ibarra, and Matthew B Hufford. 2017. “The Interplay of Demography and Selection during Maize Domestication and Expansion.” *Genome Biology* 18 (1). https://doi.org/10.1186/s13059-017-1346-4.

Wang, Xufeng, Qiuyue Chen, Yaoyao Wu, Zachary H Lemmon, Guanghui Xu, Cheng Huang, Yameng Liang, et al. 2018. “Genome-Wide Analysis of Transcriptional Variability in a Large Maize-Teosinte Population.” *Molecular Plant* 11 (3): 443–59. https://doi.org/10.1016/j.molp.2017.12.011.

Wei, Wei, Kazuo Isobe, Tomoyasu Nishizawa, Lin Zhu, Yutaka Shiratori, Nobuhito Ohte, Keisuke Koba, Shigeto Otsuka, and Keishi Senoo. 2015. “Higher Diversity and Abundance of Denitrifying Microorganisms in Environments than Considered Previously.” *ISME Journal* 9 (9): 1954–65. https://doi.org/10.1038/ismej.2015.9.

Whitehead, Susan R, Martin M Turcotte, and K. Poveda. 2016. “Domestication Impacts on Plant-Herbivore Interactions: A Meta-Analysis.” *Phil. Trans. R. Soc.* 372 (1712): 1–9. http://dx.doi.org/10.1098/rstb.2016.0034.

Wickham, Hadley. 2007. “Ggplot2–Elegant Graphics for Data Analysis.” *Journal of Statistical Software* 99 (2): 260. https://doi.org/10.18637/jss.v077.b02.

Wright, Stephen I, Irie Vroh Bi, Steve G Schroeder, Masanori Yamasaki, John F Doebley, Michael D McMullen, and Brandon S Gaut. 2005. “The Effects of Artificial Selection on the Maize Genome.” *Science (New York, N.Y.)* 308 (5726): 1310–14. https://doi.org/10.1126/science.1107891.

Xu, Guanghui, Jingjing Cao, Xufeng Wang, Qiuyue Chen, Weiwei Jin, Zhen Li, and Feng Tian. 2019. “Evolutionary Metabolomics Identifies Substantial Metabolic Divergence between Maize and Its Wild Ancestor, Teosinte.” *Plant Cell* 31 (9): 1990–2009. https://doi.org/10.1105/TPC.19.00111.

Xu, Ling, Dan Naylor, Zhaobin Dong, Tuesday Simmons, Grady Pierroz, Kim K Hixson, Young-Mo Kim, et al. 2018. “Drought Delays Development of the Sorghum Root Microbiome and Enriches for Monoderm Bacteria.” *Proceedings of the National Academy of Sciences* 115 (21): 201717308. https://doi.org/10.1073/pnas.1717308115.

Yeoh, Yun Kit, Paul G Dennis, Chanyarat Paungfoo-Lonhienne, Lui Weber, Richard Brackin, Mark A Ragan, Susanne Schmidt, and Philip Hugenholtz. 2017. “Evolutionary Conservation of a Core Root Microbiome across Plant Phyla along a Tropical Soil Chronosequence.” *Nature Communications* 8 (1): 215. https://doi.org/10.1038/s41467-017-00262-8.

CHAPTER 4: GENETIC VARIATION WITHIN *ZEA MAYS* ALTERS MICROBIOME ASSEMBLY AND NITROGEN CYCLING FUNCTION IN THE AGROECOSYSTEM

Abstract:

Overuse of synthetic nitrogen fertilizers in agroecosystems causes global level environmental pollution and human harm. These nitrogenous fertilizers provide a short-lived benefit to crops in the agroecosystem because of microbially-mediated nitrification and denitrification the remove N. Recent advances in plant-microbiome science suggest that plants can modulate the composition and activity of rhizosphere microbial communities. These rhizosphere communities seem to act like extended phenotypes informed by genetic variation in the plant host. Genetic variation in traits (e.g., plant secondary metabolites, immune system, etc.) act as mechanistic selective agents on the composition of the microbiome. Here we attempted to determine whether genetic variation existed in *Zea mays* for the ability to influence the extended phenotype of rhizosphere soil microbiome composition and function. Specifically, we wanted to characterize whether plants' influence on soil nitrogen cycling activities was heritable and thereby able to be selected for the purposes of breeding. To capture an extensive amount of genetic diversity within maize we sampled ex-PVP inbred lines, hybrids, and wild teosinte (*Z. mays* ssp. *mexicana* and *Z. mays* ssp. *parviglumis*). Within among these *Zea* lines we found that plant genetics explained a significant amounts variation in the microbiome and across different nitrification and denitrification functional genes. The greatest differences in rhizosphere microbiome recruitment were seen between teosinte genotypes and modern inbred maize genotypes, with major shifts in *Actinobacteria, Acidobacteria,* and *Proteobacteria.* We found that potential nitrification, potential incomplete denitrification, and overall denitrification rates,

but not qPCR abundance of N-cycling genes of rhizosphere soils were influenced by time of sampling (season) and plant genetics (genotype and group). Additionally, we observed that potential N cycling processes were heritable. Teosinte genotypes suppressed N-cycling activity while more modern inbred genotypes stimulated N-cycling activity. Taken together these results suggest that selection led to the loss of sustainable N-cycling processes in modern lines and that reintroducing teosinte traits into our modern germplasm may be a way manipulate soil microbiomes at both a composition and functional level to improve sustainability.

Introduction:

More than half the world's people depend on crops grown with synthetic nitrogen (N) fertilizers (Bowles et al. 2018). Regrettably, most of these synthetic N fertilizers inputs escape the agroecosystem and unintendedly pollute and degrade natural systems and harm human health (Zhang et al. 2015; Vitousek et al. 2013). Unfettered soil nitrogen cycling microorganisms (i.e. nitrifiers and denitrifiers) are major contributors to the leaky N agricultural systems (Kuypers, Marchant, and Kartal 2018). To improve the sustainability of our agricultural system, we need to understand how ecological drivers, such as plant-microbe interactions, influence soil's nitrogen cycling microorganisms and the movement of nitrogen (Moreau et al. 2015, 2019).

Genetic variation within crop species has been shown to play a significant role in plant-microbiome assembly and recruitment (Peiffer et al. 2013; Walters et al. 2018). Across large-scale and multi-year field trials, researchers find consistent sets of heritable core microbial taxa associated with specific plant genotypes (Walters et al. 2018; Xu et al. 2018). These taxonomic assembly differences are functionally relevant as microorganisms contain a diverse biochemical repertoire that allows plants to escape nutrient, drought, and pathogen stress (Philippot et al. 2013; Compant et al. 2019; Trivedi et al. 2020). In the rhizosphere plants exude complex

cocktails of chemical compounds, the production of which is directed by the plant genome. These exudates traits in tandem with root phenology and physiology act as an ecological filter which has direct fitness consequences for the surrounding soil microbial communities (Huang et al. 2019; Canarini et al. 2019). Soil microorganisms that are phytochemically competent to the ecological filter of the rhizosphere survive and persist near the plant root (Philippot et al. 2013). It follows, then, that the ecological filtering for rhizosphere occupancy that arises from genotypic variation contributing to agents of selection will have direct consequences on biogeochemical cycling activities carried out by the rhizosphere microbiome.

Rhizosphere soil microorganisms are key contributors to essential ecosystem functions. Ecosystem processes, nitrification, and denitrification are primarily controlled by microorganisms in the soil and can result in a considerable loss of nitrogen from an ecosystem (Philippot, Hallin, and Schloter 2007; Davidson et al. 2012). Microorganisms are extremely diverse, and variation within species likely play a critical role in shaping how ecosystem processes occur in the ecological setting. In many ways, soil microorganism biodiversity is a foundational gatekeeper of the pathways by which nutrients can enter and exit an ecosystem. Furthermore, emerging research is beginning to show that genetic variation within plant species can have a considerable role in driving both soil community composition and biogeochemical relevant microorganisms (Subbarao et al. 2013; Pérez-Izquierdo et al. 2019). For example, we have shown that historic selection on plant genotype can drive the assemblage of the nitrogen cycling rhizosphere microbiome, both by changing the taxonomic composition and representation of nitrogen-cycling functional genes (Favela, Bohn, and Kent 2021). Yet we and many others have lacked evidence linking microbiome changes to altered nitrogen cycling processes within the ecosystem. Here, we attempted to address this in an agroecological field

setting. Specifically, we wanted to determine how predictive plant genotype is as a tool to understanding changes in the soil microbiome, particularly microbial functional groups, and to connect this extended phenotypic variation back to changes in important nitrogen cycling processes.

To evaluate the plant genetic effects on nitrogen cycling microbial functional groups, we grew a diverse panel of *Zea mays* (including elite inbred, hybrid, and wild lines) and measured their contribution to differences in microbial community assembly and nitrogen cycling processes. By doing this in a highly replicated manner within a single field, we were able to control for stochastic edaphic factors and parse the plant genetic contribution driving soil microbiome function in an agronomically relevant field setting. Previously, our research in elite inbred maize suggested that breeding of maize resulted in a narrowing and loss of sustainable N-cycling microbiome functions through the 20th century (Favela, Bohn, and Kent 2021). Informed by this prior research, we included maize hybrids to estimate if microbiome functions would be regained through heterosis. In addition to this, within *Zea mays*, we found microbiome recruitment and N-cycling functional groups differed the most between modern inbred maize and wild teosinte (Ch. 2: Favela *in prep*. 2021). Thereby, wild *Zea* was included as an outgroup to evaluate the influence of pre-domestication genetics and their ecological filtering traits influence on microbiome assembly and function. These treatments give us an understanding of how much plant genetic variation is necessary to induce changes in the microbiome of soils and provide insight into how domestication and breeding altered microbiome functions. With this information, we hoped to better understand how genetic alterations in maize can have cascading effects in plant microbiome recruitment and nitrogen cycling activity. Understanding these processes in an agroecological field setting is critical as to improving the sustainability of maize.

Methods:

Field Design

Field plots were located at the Crop Sciences Research and Education Center - South Farms at the University of Illinois, Urbana-Champaign, IL (40°03'30.4"N 88°13'50.4"W). We used a panel of *Zea* lines that encompass modern ex-PVP inbred lines, hybrids, and the wild progenitor of maize, teosinte (27 genotypes in total). Teosinte was represented by two subspecies *Zea mays. mexicana* and *Zea mays. parvaglumis* (3 genotypes of each). Across our field, each line had 4 replicate blocks that were arranged in Randomized-Block Design (Fig. C.1A-B). Each maize block contained 4 rows with 15 plants in each row. Maize lines were planted on 4/30/17 while teosinte lines were planted 5/19/17. These differences arose as maize was planted with an industrial planter while teosinte needed to be hand planted. Furthermore, due to seed limitations teosinte was planted in 2 row blocks as opposed to 4 row blocks like in maize.

Sample collection

Blocks were sampled 3 times across the growing season. Plants were sampled in approximately sampled in V4 (Both: 6/5/17), V6 (Maize:6/20/17, Teosinte:7/20/17), R2 (7/12/17, Teosinte: 8/11/17). Staggered sampling of teosinte and maize at later timepoints (T2, T3) was done to control for growth delays caused by delayed planting. Within each sampling event, four individual plants were sampled within a block, and samples were combined into a composite sample. Individual plants were never resampled, thereby maintaining independent sampling timepoints. Samples consisted of a soil core (10 cm depth) within the root zone of the plant. Rows were sampled by a replicated block to control for sampling effects. Sampled were placed on ice until they were transported to the lab. Once in the lab, soils were refrigerated at

4°C awaiting potential nitrification assays or potential denitrification assays (within 5 hours). Aliquots for DNA extraction were frozen immediately.

Potential nitrification assay

The potential nitrification assay was developed and modified from (Schinner et al. 1996). This assay was performed at substrate saturation and values presented should be interpreted as the maximum potential rate of transformation of ammonia to nitrite, the first-rate limiting step of nitrification. In principle, this assay uses ammonium sulfate as the substrate for the first step of nitrification during a 5-hour incubation. Nitrite products released during the incubation period were extracted with potassium chloride and concentration is determined colorimetrically at 520nm. Sodium chlorate was added to the assay to inhibit nitrate oxidation during the incubation period. Aliquots of homogenized field-moist root-zone soil (5 g) was placed in into two 50ml tubes (sample and control). Then we added 20ml of our substrate solution and 0.1 ml of sodium chlorate, mixed briefly, and closed the tubes. Sample tubes were incubated on a rotatory shaker for 5h and control tubes were stored at -20C for 5h. After incubation and thawing, KCl was used to filter both samples and controls. The amount of nitrite present in the samples was measured using a color reagent that binds to nitrite. Calibration standard curves were created by weighing out and diluting sodium nitrite and combining it with color reagent. Potential nitrification rates were arithmetically adjusted by initial soil moisture, soil weight, % dry matter, and initial nitrite in the sample.

Potential nitrification rate calculation below:

$$\frac{(S - C) * 25.1 * 1000 * 100}{2.5 * 5 * 5 * \%dm} = ngN * g^{-1}dm * h^{-1}$$

S value of sample (mg N)
C value of control (mg N)
25.1 volume of extract (ml)

1000 conversion factor (1 mg N = 1000ng N)
2.5 aliquot of filtrate (ml)
5 initial soil weight (g)
5 hour of assay duration
100*%$^{-1}$ *dm* factor for soil dry matter

Potential denitrification rates by acetylene-inhibition assay

Potential denitrification assays were carried out using a modified version of (Schinner et al. 1996; Peralta et al. 2016). Field-moist root-zone soil samples were incubated under anaerobic conditions in the presence of acetylene for 3h at 25C. The assay was done on 25g of root-zone soil in glass Wheaton jars. Incubations were done at substrate saturation of carbon (dextrose) and nitrogen (nitrate). Chloramphenicol was added to the incubation to act as a bacteriostatic agent to prevent further microbial growth and protein synthesis. Wheaton jars were purged of oxygen with either helium or acetylene. Helium samples were used to estimate the amount of incomplete denitrification (N_2O) occurring in the assay atmosphere. Acetylene purged samples are used to measure overall denitrification ($N_2O + N_2$). Acetylene is a commonly known inhibitor of nitrous oxide reduction. Initial and final gas samples were taken at the start and end of the incubation period. Initial and final nitrous oxide in gas samples was quantified using a GC-2014 Gas Chromatograph (Shimadzu, Kyoto, Japan) with an electron capture detector (GC-ECD). Potential denitrification rates were arithmetically adjusted by initial soil moisture, soil weight, % dry matter, sample volume, and headspace.

<u>Denitrification rate calculation is seen below:</u>

$$\frac{X * V * 0.6363 * 100}{IV * t * SW * \%dw} = \mu g N_2O - N * g^{-1} dm * h^{-1}$$

X $\mu g\ N_2O$ of the injected sample volume
V total volume of incubation flask minus soil volume (ml)
0.6363 factor to convert N_2O to N_2O-N
IV injected sample volume (ml)

t incubation time (h)
SW initial soil weight
$100*\%^{-1}$ *dm* factor for soil dry matter

Microbial Community Amplicon Sequencing

For this experiment, we characterized the microbiome and diagnostic functional genes related to transformations that occur in the nitrogen cycle: nitrogen fixation, nitrification, and denitrification. Amplicon sequencing was performed on bacterial and archaeal 16S rRNA genes, fungal ITS2, *amoA, nirS, nirK, nosZ,* and *nifH* genes. The Fluidigm Access Array IFC chip was used to prepare sequencing amplicons. This method allows for the simultaneous amplification of target functional genes using multiple primer sets (Fluidigm, San Francisco, CA). DNA sequencing was performed for bacterial, archaeal, and fungal amplicons using an Illumina HiSeq 2500 Sequencing System (Illumina, San Diego, CA). Primer information is provided in (Favela, Bohn, and Kent 2021) Fluidigm amplification and Illumina sequencing were conducted at the Roy J. Carver Biotechnology Center, University of Illinois (Urbana, IL, USA). Fast Length Adjustment of Short reads (FLASH) (Mag and Salzberg 2011) software was used to merge paired-end sequences from bacterial and archaeal 16S rRNA genes. For functional genes and fungal ITS, only forward read sequences were used. Once FLASH merging was performed, files were filtered by quality using the FASTX-Toolkit (Gordon, Hannon, and Gordon 2014). Reads that did not have a minimum quality score of 30 across 90% of the bases were removed. Using the FASTX-Toolkit, *nirK* sequences were trimmed to its amplicon size of 165-bp.
Once quality preprocessing was performed, FASTQ reads were converted to FASTA format. Using USEARCH-UPARSE version 8.1 (Edgar 2010), sequences were binned into discrete OTUs based on 97% similarity and singleton DNA sequences were removed. Quantitative Insights into Microbial Ecology (QIIME) was used to generate OTU tables for downstream

statistical analysis and to assign taxonomic information, this is done with a combination of the UCLUST algorithm and GreenGenes database (DeSantis et al. 2006; Edgar 2010; Caporaso et al. 2010). Once taxonomy was assigned, chloroplast and mitochondrial OTUs were removed from the dataset. Rarefaction was performed to correct for differential sequencing depth across samples. Functional gene sequences were also assigned using QIIME (Caporaso et al. 2010) with the BLAST (Altschul et al. 1997) algorithm and custom gene-specific databases generated from reference sequences obtained from the FunGene repository (http://fungene.cme.msu.edu/) (Fish et al. 2013). All OTU tables used in statistical analyses were generated in QIIME. Singleton OTUs were filtered prior to statistical analysis.

Statistical Analysis

Statistical analysis was performed in R, with the packages 'Vegan', 'ASReml', and 'WGCNA'. 'Vegan' was used to perform multivariate statistical comparisons across microbiome data (Oksanen et al. 2007; Butler et al. 2017; Langfelder and Horvath 2008). 'ASReml' was used to perform univariate comparisons of potential nitrification, denitrification and nitrogen cycling qPCR and potential assay results. WGCNA was carried out to compare our multivariate microbiome data to our univariate nitrogen cycling function data. Model factors used in statistical analysis were time of sampling, the location of the block, the row of block position, range of block position, the genotype within the block, and the interaction between genotype and sampling time. Typical model of analysis seen below:

$$Microbiome = Plant\ Genotype + Time\ of\ Sampling + Block + Range + Row + Range{:}Row\ Position + Genotype{:}Time\ Interaction + Residuals$$

In the ASReml mixed effect models, plant genotype and the genotype-time interaction were treated as fixed factors, while all other factors (block, range, row) were treated as random factors. In PERMANOVA models, block factor was constrained in permutations.

Quantifying nitrogen cycling functional groups

Quantitative PCR (qPCR) was carried out to determine the abundance of functional genes in each of the rhizosphere microbial communities. Specific target amplification (STA), explained in (Ishii et al. 2014), was carried out on samples and standards to increase template DNA for amplification. STA and qPCR master mix recipes from (Edwards et al. 2018) were used for all samples. STA product and qPCR master mix were loaded into the Dynamic Array™ Microfluidics Fluidigm Gene Expression chip where amplification and quantification of functional genes were carried out simultaneously (Fluidigm, San Francisco, CA). All samples and standards were analyzed in 12 technical replicates. Fluidigm Real-Time PCR Analysis software version 4.1.3 was used to calculate gene threshold cycles (C_T). C_T values were converted to gene copy number using gene length and standard curves. All Fluidigm qPCR was conducted at the Roy J. Carver Biotechnology Center (Urbana, IL, USA). The final copy number of each functional gene amplicon was standardized by the ng of template DNA in the qPCR reaction.

In situ N_2O flux measurements

Net soil-atmosphere N_2O fluxes were measured weekly from 6/20/17 to 8/23/17, samples were collected for a total of 6 weeks. As gas flux measurements are laborious and time consuming, sampling was targeted during plant peak primary plant growth and focused on the plant treatments that were hypothesized to have the largest effect on the microbiome function based on previous studies (Favela, Bohn, and Kent 2021). Specifically, the comparison focuses

on B73 inbred maize to PI566677 wild teosinte. Flux measurements were measured using static flux chambers as described in USDA-ARS GRACEnet Project protocol (Parkin and Venterea 2010). Chambers were installed in the field during the first sampling timepoint and remained in place throughout the maize growing season. Chambers consisted of two-pieces: PVC pipe with a 30 cm diameter (base installed 20 cm into soil), and sampling lids (10 cm in height). Gas sampling events occurred in the mornings between 10 am-noon; during this time 15 mL of gas were collected from chambers every 10 minutes for 30 mins. Samples were stored in evacuated aluminum crimp-top glass vials with a chlorobutyl stopper and sealed with clear silicone to prevent sample leakage. Gas samples were later quantified using a GC-2014 Gas Chromatograph with an electron capture detector (GC-ECD) (Shimadzu, Kyoto, Japan). Standard curves were used to quantify the amount of N_2O in gas sample. N_2O samples were corrected using ambient temperature and moisture conditions of day. 4 sampling timepoints were used to determine the rate of N_2O production (ppm of N_2O/min), while the total production was the sum of N20 measured over the time of collection (ppm).

Results:

In this field experiment, we identified 37,596 different 16S rRNA operational taxonomic units (OTUs, 97% similarity, rarefied to 100000 reads per sample), and 2236 fungal OTUs (rarefied to 10000) were identified from the ITS2 region.

Rhizosphere Microbiome Variation across the Field

Within the prokaryotic community (based on 16S rRNA gene sequences), we found that plant genotype, genotype × time interactions, the location of the block, and sampling time explained 74% of the variation within the microbiome; respectfully, 26% of the variation within the microbial community was unexplained (PERMANOVA, DF=26, $p<0.001$; Fig. 4.1; Table

C.1-C.3). In total, 34% of the variation in the prokaryotic microbiome was explained by plant genetics in some way; 18% of this 34% variation was independent of temporal effects while 16% were highly linked to the time of sampling. Interestingly, 20% of the variation in the soil microbial community was explained by block location alone. This would mean that across time, 20% of the microbiome was unchanged across the season. Sampling time (independent of genotype) explained 12% of the variation within the microbiome. These results suggest that plant driven microbiome assembly is to some degree dependent on date of sampling and growth. Roughly, these results suggest that plant genetics explained about a third of the variation in the agroecosystem microbiome. Spatial, and temporal effects seem to explain a third of the variation each within the microbiome. Finally, an additional third of variation within the soil microbiome goes unexplained. These results seem to highlight that plant genotype is a drivers of soil microbial community structure as much as random/uncontrollable factors such as time and space.

Cumulatively, plant genotype explained about 34% of the variation within the microbial community. Across plant group (inbred, hybrid, teosinte) showed the greatest differences in microbiome recruitment (Fig. 4.1-2; Table C1, C3). Specifically, teosinte and hybrid maize treatments have the strongest effect on the composition of the soil microbiome agroecosystem. Teosinte rhizosphere soils contained greater relative abundance of *Actinobacteria* and *Proteobacteria* (specifically, *Actinomycetales, Burkholderiales)* and less *Acidobacteria* (*iii1-15*, *Solibacteres)* compared to modern maize (Fig. C2-3). Additional analysis was carried out within plant category (i.e., within inbred, within hybrid, within teosinte), and inbred maize was the only category where genotype did not significantly contribute to differential microbiome recruitment.

Fungal communities showed similar results to the prokaryotic communities except for notably weaker effects of space. This may indicate that fungi are more limited spatially than

bacterial communities (Table C.1). When comparing the results of this model with bacterial and fungal results we can see that time and space interaction explain about half (47%) of the variation in fungi communities compared to 7% by bacterial communities. This result makes it clear to that fungal communities in the agroecosystem soil are far more context-dependent to the exact time and space of the environment compared to prokaryotes. They seem to exist more independently in this environment as compared to bacteria which seems to be more dependent on plants present.

Nitrogen Cycling Genes Community Across the Agroecosystem

From our analysis of nitrogen cycling functional genes, we observed 882 *nifH* OTUs, 210 archaeal *amoA* OTUs, 98 bacterial *amoA* OTUs, 21022 *nirK* OTUs, 2607 *nirS* OTUs, and 7294 *nosZ* OTUs. In response to genotype, 4 of 6 nitrogen cycling genes showed changes in community membership (Fig. 4.3; Table C.3), 1 of 6 nitrogen cycling genes changed in abundance (Table C.2.1). Conversely, plant group (inbred, hybrid, teosinte) affected 4 of 6 nitrogen cycling genes showed changes in community membership, and 2 of 6 nitrogen cycling genes changed in abundance among plant categories (Table C.2.2). Additionally, plant genotype and group interactions with time had a significant effect on N-cycling composition and functional gene abundance (Table C.2.1-2; Fig. C.5).

Nitrogen fixation genes

Plant genotype did not significantly influence the composition or abundance of *nifH* genes in the rhizosphere (Table C.2-3.1-3, Fig. C.5). Spatial and temporal factors within in the field were the only significant factors explaining variation in the diazotrophs communities. In total, spatial effects explained about 9% of the variation in the community and time explained 1% of the variation respectfully (Table C.3.1-3). Additionally, plant group (inbred, hybrid,

teosinte) did not have a significant influence on *nifH* community composition; however, it did have a significant effect on abundance (log of copies/ng) of *nifH* genes in the rhizosphere (Wald=6.14, p=0.04). Teosinte rhizosphere hosted fewer diazotrophs during the first and last sampling timepoints compared to hybrid and inbred maize (Fig. C.5).

Nitrification genes

The recruitment of nitrifiers (indicated by gene sequences for bacterial and archaeal ammonia monooxygenase – *amoA*) was not significantly impacted by plant genotype and plant group. While plant genotype explained a small but significant amount of variation for archaeal *amoA* (R^2=0.08, p<0.001, Fig. 4.3, Tables C.3.7-9), there was not a significant change in community composition of bacterial ammonia oxidizers in response to genotype (p=0.16, Fig. C.4B-C Table C.9.2). Regarding abundance, neither archaeal nor bacterial ammonia oxidizers were significantly influenced by plant genotype (archaeal *amoA* p=0.61, bacterial *amoA* p=0.99, Table C.4). Plant goups showed the same patterns as genotypes reported above (Fig. C.6, Table C.2, C.3.4, C.3.7, C.4).

Denitrification genes

All the denitrification genes surveyed were significantly different among genotypes and group (Fig. 4.3, C.6, Tables C.2, C.3.10-18). Communities of denitrifiers possessing both the cytochrome cd_1-type nitrite reductase (encoded by *nirS*) and the copper containing nitrite reductase (encoded by *nirK)* varied significantly among plant genotypes (*nirS:* R^2=0.09, Fig. 4.3, Table C.3.14; *nirK:* R^2=0.09, p=0.003, Fig. 4.3, Table C.3.11) In addition to this, *nosZ,* the gene that encodes typical nitrous oxide reductase, crucial in the consumption of N_2O, was found to be affected by plant genotype (R^2=0.09, p=0.011, Fig. 4.3, Table C.3.17). Quantitative PCR of denitrification genes showed no difference in the abundance of genes in the rhizosphere across

plant genotype and largely for plant group (Fig. C.5-6, Table C.2). One exception to this was *nosZ,* which was observed to be altered by plant group ($p<0.05$, Table C.4.11, Fig. C.5G). In addition to this, like *nifH* and *bacterial amoA*, the denitrification genes showed a strong and significant interaction between plant group and time (Fig. C.5). During the first sampling time point (V2-V4), the teosinte rhizosphere microbiome contained similar denitrification gene abundance, had greater levels of dentification genes during the final (R1-R3) sample point, and finally, had lower numbers of denitrification genes compared to inbred and hybrid maize by the end of season. Full analysis of plants groups effect and additional genotype models on denitrification genes present in Supplemental Tables C.3-4.

Potential Nitrification Assay

Potential nitrification rate (ngN/ghr) of rhizosphere soils was influenced by both time of sampling in season and plant genetics (Fig. 4.4, Table C.6.1-4). Specifically, M On average, teosinte genotypes suppressed potential nitrification rate by 9% compared to inbred maize which on average simulated potential nitrification rates by 4% (means difference of 13%, Fig. 4.5, C.8.1). It should also be noted that a considerable amount of variation in potential nitrification rates could be attributed to plant genotype ($p<0.05$, Table C.6). Furthermore, the log of potential nitrification rates appears to be heritable (i.e., explained by genetic variation), though this effect had disappeared by the final timepoint (T1: $p=0.012$, T2: $p<0.05$, T3: $p=0.73$; Table C.5). Heritability estimate at the first (V2-V4) time point was 0.14 ± 0.19 and 0.80 ± 0.28 at the second time point respectfully (Table C.5, C.6).

Potential Denitrification Enzyme Assay

We found that the variation in the potential incomplete denitrification (N_2O) and overall denitrification ($N_2O + N_2$) rate log(ngN/ghr) of rhizosphere soils to be influenced by time of

sampling in season and plant genetics (Fig. 4.4B, 4.6-7, incomplete: $p<0.001$, overall: $p<0.001$, Table C.7.1-6). On average teosinte genotypes suppressed the log of overall denitrification by 59% compared to inbred maize which stimulated it by 4% (mean difference 63%, Fig. 4.6B, Table C.8.2). For potential incomplete denitrification log(ngN/ghr) teosinte genotypes suppressed activity by 75% and inbred genotypes on average stimulated potential complete denitrification by 32% (mean difference 102%, Fig. 4.7B, Table C.8.3). Additionally, we found there to be a considerable amount of significant heritability in potential denitrification across the growing season (Table C.5, C.7). For the log of potential overall denitrification, we estimated heritability to be 0.34 ±0.17 at the first timepoint (V2-V4), 0.0±0.00 at the second timepoint (V10-V12), and 0.28±0.12 at the third (R1-R3) timepoint (Table C.5, C.7). For the log of potential incomplete denitrification, we found heritability to be to be 0.41 ±0.13 at the first timepoint (V2-V4), 0.03±0.02 at the second timepoint (V10-V12), and 0.06±0.08 at the third (R1-R3) timepoint (Table C.5, C.7).

N_2O Flux from static chambers

To estimate whether our potential denitrification and nitrification rates were reflected in ecosystem flux differences, we placed static flux chambers in blocks with two of our genotypes (B73 inbred maize and PI566677 wild teosinte). From these static chambers, we found that across the season the teosinte genotype soil produced significantly less N_2O (ppm/min) ($t=2.09$, $df=33$, $p=0.04$, Fig. 4.9A) and had lower total N_2O (ppm) compared to the inbred genotype ($t=2.01$, $df=29$, $p=0.05$, Fig. 4.9C). In addition to this, we saw a dynamic pattern in both N_2O production rates (ppm/min) and total N_2O (ppm) produced across the season – where early in the season *flux*es are similar early in the season but differentiate by the end (Fig. 4.9B, D).

Relationship between the microbial community and N-cycling function

To further understand the differential contribution of the rhizosphere microbiome to the potential function of a soil sample, we used weighted gene correlation network analysis (WGCNA) (Langfelder and Horvath 2008) to identify four unique co-correlated clusters of OTUs (modules) with a significant response to potential function (3 modules that were correlated to potential nitrification, and 1 module that was correlated to overall denitrification, Fig. 4.8). The "brown" taxa module was positively correlated to nitrification ($r=0.20$, $p<0.001$) and the "turquoise" and "green" modules were negatively correlated to nitrification (turquoise: $r=-0.25$, $p<0.001$; green: $r=-0.20$, $p<0.001$). The brown module contained 129 OTUs and was dominated by the presence of *Acidobacteria.* Interestingly, the second most dominate phylum in this module *Cholorflexi* was recently shown to have the ability to carry out nitrification(Spieck et al. 2020). The turquoise module contained 290 OTUs and the green module contained 38 OTUs, both modules were dominated by *Actinobacteria.* The "cyan" module was correlated to the rate of overall denitrification ($r=0.17$, $p<0.001$), contained 26 OTUs and was dominated by *Actinobacteria.*

Discussion:

Modulating plant genetic variation has been shown to alter the rhizosphere microbiome. Here, we show that the effect of plant –genotype extends to modulating microbially functions of the rhizosphere microbiome. Specifically, we observed that plant genotype influenced the recruitment of functional groups related to nitrification (*amoA)* and denitrification (*nirS, nirK, nosZ*) along with the potential rates of those ecosystem processes. Ultimately, these results

suggest that we can select for genetic variability within our agricultural lines that promotes sustainable ecosystem processes within the agricultural setting.

This study demonstrates that genetic variation within *Zea mays* plays a significant role in both the assembly of the microbiome and nitrogen cycling ability of the community, even in the stochastic setting of an agroecosystem. Our most genetically divergent treatments (wild and hybrid Z. *mays*) were seen to have the strongest effects on the composition and function of the microbiome. Both wild and hybrid *Z. mays* exerted strong effects on potential nitrification and denitrification, while inbred maize did not. We hypothesized that these weak genotypic effects of inbred maize were driven by genetic erosion during the inbreeding process that resulted in the loss of complex ecologically important traits, such as microbiome recruitment (Smýkal et al. 2018; Favela, Bohn, and Kent 2021) ; Ch. 2: Favela et al. *in prep 2021*). Furthermore, if ancestral genotypic variation exists in how plants modulate the activity of soil microbial taxa, then we can reintroduce this genetic variation in our modern lines and breed germplasm to have sustainable interactions with the nitrogen cycling microbes and their activities. Our previous results indicated that recruitment of nitrogen-cycling functional groups was altered through maize breeding (Favela, Bohn, and Kent 2021), which suggested that breeding for desirable microbiome functions is possible in maize. Here we provide a field study demonstrating alterations in the structure and nitrogen cycle functions of the rhizosphere microbiome corresponding to domestication and breeding.

In addition to genetic effects, we found that spatio-temporal gradients play a major role in shaping the composition and activity of the microbiome. Within these spatiotemporal effects, we see that about 20% of the microbiome is unchanging in both time and space and is unique to block. This portion of the community may represent and highlight the recalcitrant nature of soil

microbial communities. We are not the first research group to report on the recalcitrant nature of microorganisms in soils (Arnoldi et al. 2019); many other groups have shown that a large fraction of the soil microbiome represents either dormant or relic DNA (Locey 2010; Priscu et al. 2012; Carini et al. 2016). Here we hypothesize that the fraction of the microbiome that does not respond to plant or seasonal phenology represents either relic DNA or dormant microorganisms.

Furthermore, the effects of seasonal phenology and *Zea* genotype × time interaction over the growing season played a major role in predicting microbiome recruitment and function. We interpreted this to suggest that plant growth and development is playing a role in how maize lines interact with their soil microbial community. This makes intuitive sense as maize has different nutrient requirements across the growing season, and these nutrients are extracted from soil environment and its microbial community (Bender et al. 2013). In addition, previous studies have shown that the complexity of the microbiome is built through time (Shi et al. 2016). These temporal effects are important to consider, as they can dramatically influence the conclusions drawn about the interaction between plants and their microbiome.

We observed that potential nitrification (PN) and denitrification were highly dependent on the time of sampling (Fig. 4.4-5). Potential nitrification, for example, seemed to peak in the middle of the season, coincident with plant primary productivity (Fig. 4.4A, 4.5A-B). During peak growth, it appeared as if *Zea* was priming soils for release of plant-available nutrients, a process observed across plants shown to enhance the release of N (Phillips, Finzi, and Bernhardt 2011), perhaps explaining the increase in nitrification. Interestingly, inbred and hybrid maize showed the largest stimulation of PN over the growing season compared to teosinte (Fig. 4.4-5). These results suggest the teosinte may have a previously unrecognized mechanism to biologically suppress nitrification activity, an ability that has been lost in modern maize.

Biological nitrification inhibition (BNI) has been seen across a variety of different grass species (particularly in wild variants) but has not previously been reported within maize (Coskun et al. 2017b, 2017a). These BNI mechanisms may have been lost through domestication and plant breeding, as it confers no benefit and may even be costly in the high nitrogen conditions of modern agroecosystems, a parallel to what has been reported for nutritional symbioses with nitrogen-fixing microorganisms (Smercina et al. 2019). Investigating whether these wild teosinte characteristics that confer BNI can be reincorporated into modern maize maybe of interest to future breeders for improving sustainability of maize.

Interactions with denitrifying microorganisms followed a similar pattern to nitrifiers, except with considerably more variation. Over the growing season, genotype and group played a significant role in shaping potential denitrification activity (Figs. 4.4B, 4.6-7). These results were relatively surprising as maize is typically grown in aerobic soils and denitrification is an anaerobic process. Denitifryers are often facultative anaerobes and may not be active under field conditions but are in the potential assay. Interestingly, teosinte appears to strongly inhibit both potential incomplete denitrification (N_2O) and overall denitrification ($N_2O + N_2$) leading us to the conclusion that teosinte contains biological denitrification inhibition traits (BDI) not previously characterized. The mechanisms underlying BDI, like BNI, are typically the release of phytochemical that directly interferes with the proteins carrying out the said N-metabolism (Bardon et al. 2016). Work in rice, a crop grown in anaerobic soil, has also shown that genetic variation exists within the rice that can allow it to inhibit the activity of denitrifiers (Ishii et al. 2011; Ding et al. 2019). These traits are value to reintroduce to the agroecosystem as they would reduce N pollution and improve N conservation.

WGCNA identified four modules of microbial taxa that were significantly associated with both changes of potential nitrification and denitrification (Fig. 4.8). These results suggest that specific taxa and their interactions are play a role in driving the function of the microbiome and that, to some degree, plants can influence the activities of specific microbial groups. Interestingly, we observed that modules positively correlated with higher potential nitrification rates were dominated by gram-negative bacteria (*Acidobacteria)* while those that were negatively correlated with nitrification were dominated by gram-positive bacteria (*Actinobacteria)*. Contrastingly, overall denitrification was positively correlated to gram-positive bacteria (*Actinobacteria).* Perhaps, these cell wall differences are playing a role in how plants select for taxa to join the microbiome. Surprisingly these modules of correlated OTUs were not dominated by known nitrifying taxa, suggesting that nitrification processes may be in part dependent on the metabolism of other microbial members (Spieck et al. 2020), that nitrification is controlled by the level of transcriptional regulation rather than nitrifying population size or some other microbial interaction is controlling nitrification. This could be, in part, because the ammonia monooxygenase enzyme is readily inhibited by a variety of phytochemicals (Bedard and Knowles 1989). The gram-negative bacteria that are positively correlated with nitrification may be breaking down phytochemicals that would otherwise inhibit ammonia monooxygenase allowing nitrifiers to continue nitrification. While the negatively correlated gram-positive bacteria present in the module may not be breaking down plant phytochemical or producing some inhibitory compound. Generally, it has been observed that gram-positive bacteria are major producers of antibiotic compounds, while gram-negative bacteria are resistant to them. Determining how ecological interactions between microorganism within the microbiome is critical in understanding this and predicting the function of this complex system.

From a sustainability perspective, this study highlights a potential avenue to reduce agricultural GHG emissions generated by microbial actors. N_2O static chamber results (Fig. 4.9) provide support that these potential nitrification and denitrification assays may, in fact, reflect real ecosystem rates. This is an exciting finding as agriculture is the chief producer of N_2O emissions (Vitousek et al. 1997), and these results may give us a foot-hold on how to potentially curve this N pollution. While the results presented in this study are interesting, a major limitation of this study is that we only examined these lines in a single field. Further research on how heritable microbial function is across a wide range of biogeographic environments and the real impacts on ecosystem N conservation is needed to incorporate these into our agricultural practices.

Conclusion:

Plant –control of microbial functions likely evolved as a mechanism to control the available nutrients to the plant from the soil matrix (Philippot et al. 2013b; Delaux and Schornack 2021). It is becoming more and more clear that plant species can modulate the activities of their soil associated microbiome and that these alterations can impact how soil functions (Falkowski, Fenchel, and Delong 2008; Bohannan, Morris, and Meyer 2020). Identification of the genetic regions that direct microbiome recruitment of N-cycling microorganisms or modulation of their activities will enable progress on re-engineering the agroecosystem to be a minor contributor to N pollution (Johnson 2006). This paper adds to this growing body of work, by showing maize, an agronomically important crop, too has genetic variation that contributes to alterations in the microbiomes and function. Potentially, enough

variation to breed and incorporate these extended phenotype ecosystem traits into modern agricultural lines.

Figures:

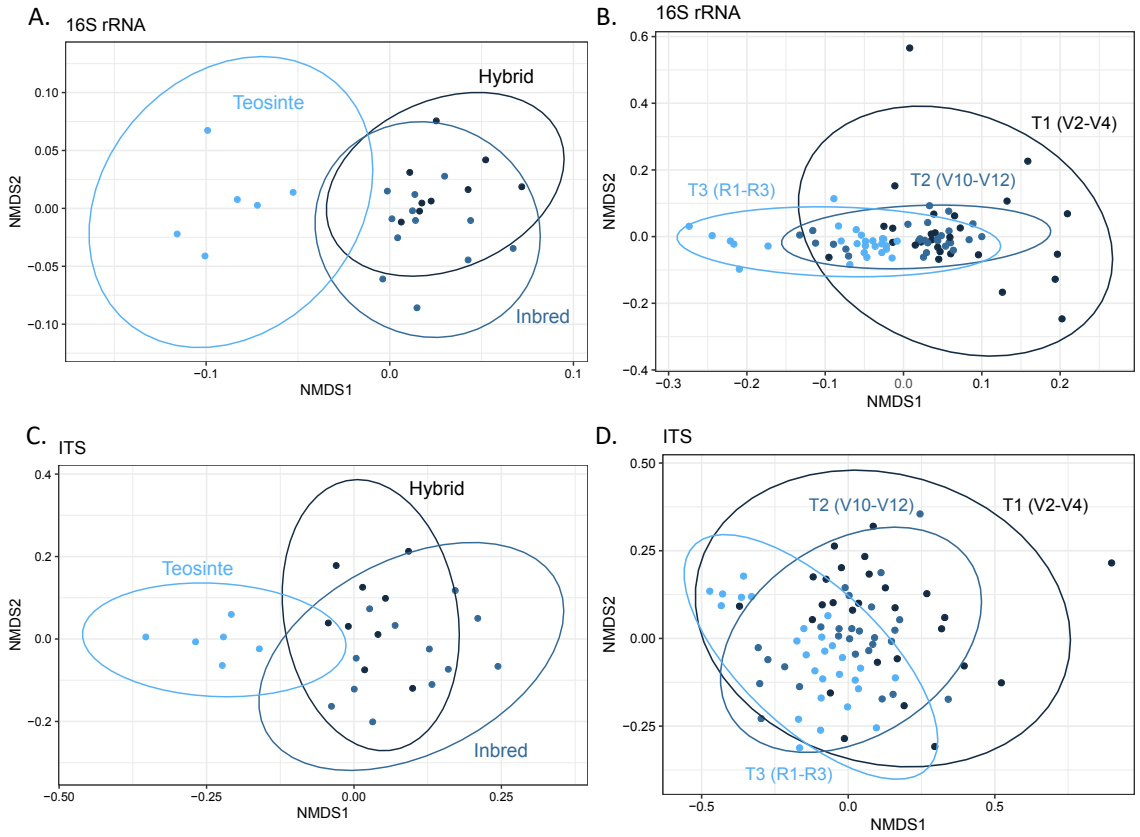

Figure 4.1 NMDS ordinations based on Bray-Curtis dissimilarity among prokaryotic 16S rRNA (**A-B**) and fungal ITS (**C-D**) displaying that genetic (**A, C**) and temporal (**B, D**) effects are driving changes in composition of the root zone microbiome. (**A, C**) shows that inbred, hybrid, and teosinte maize lines host different microbial taxa in the root zone under the same environmental conditions. Each point represents a genotypic mean (within mean n= 12) of the microbial community across the three different sampling time points. (**B, D**) highlights the temporal effects of the rhizosphere microbiome timepoint 1 (young plants V2-V4), 2 (Fast growing approaching flowering V10-V12), 3 (Reproductive R1-R3). (within mean n=4).

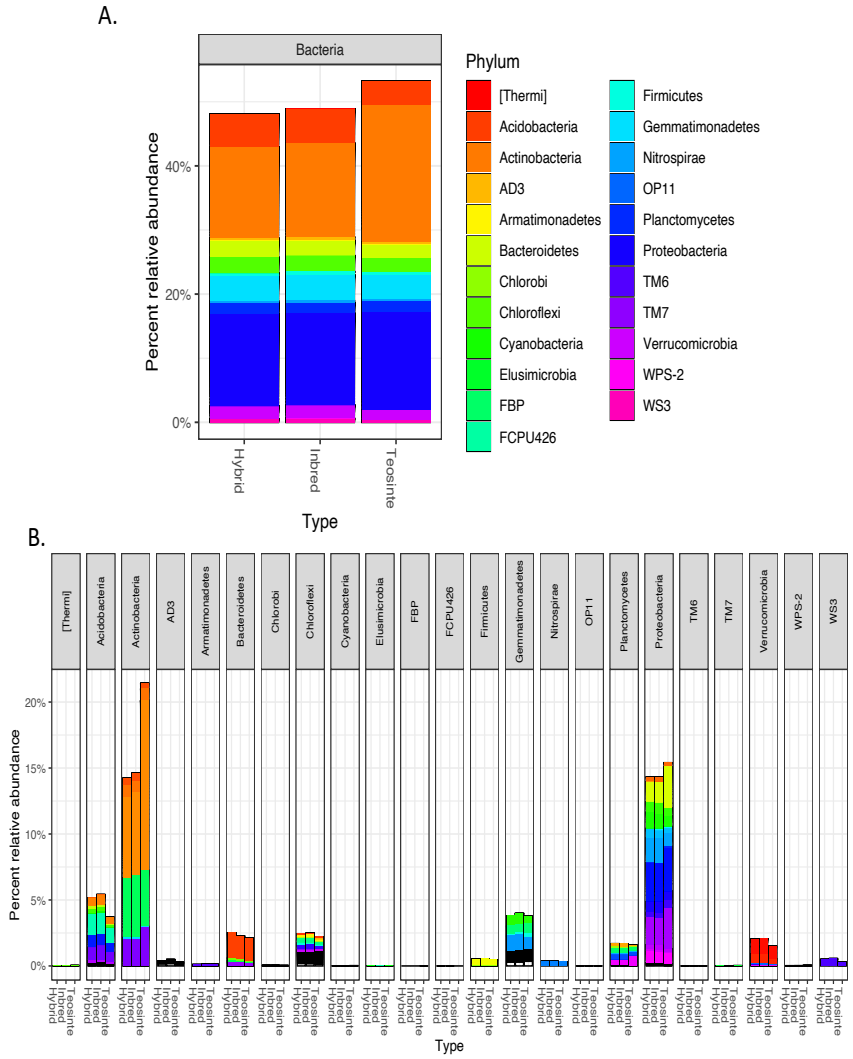

Figure 4.2 Stack plots showing the differentially abundant OTUs based on DESeq2 determined by teosinte and inbred maize comparison. **A.** Shows the relative abundance of bacterial OTUs colored by Phylum. Most contrasting difference seen in *Acidobacteria*, *Actinobacteria,* and *Proteobacteria*. **B.** Shows the same relative abundance data in A but faceted by Phylum and colored by taxonomic classification to improve clarity. Supplemental materials C.2-C.3 further highlights taxonomic differences in within *Acidobacteria*, *Actinobacteria,* and Proteobacteria.

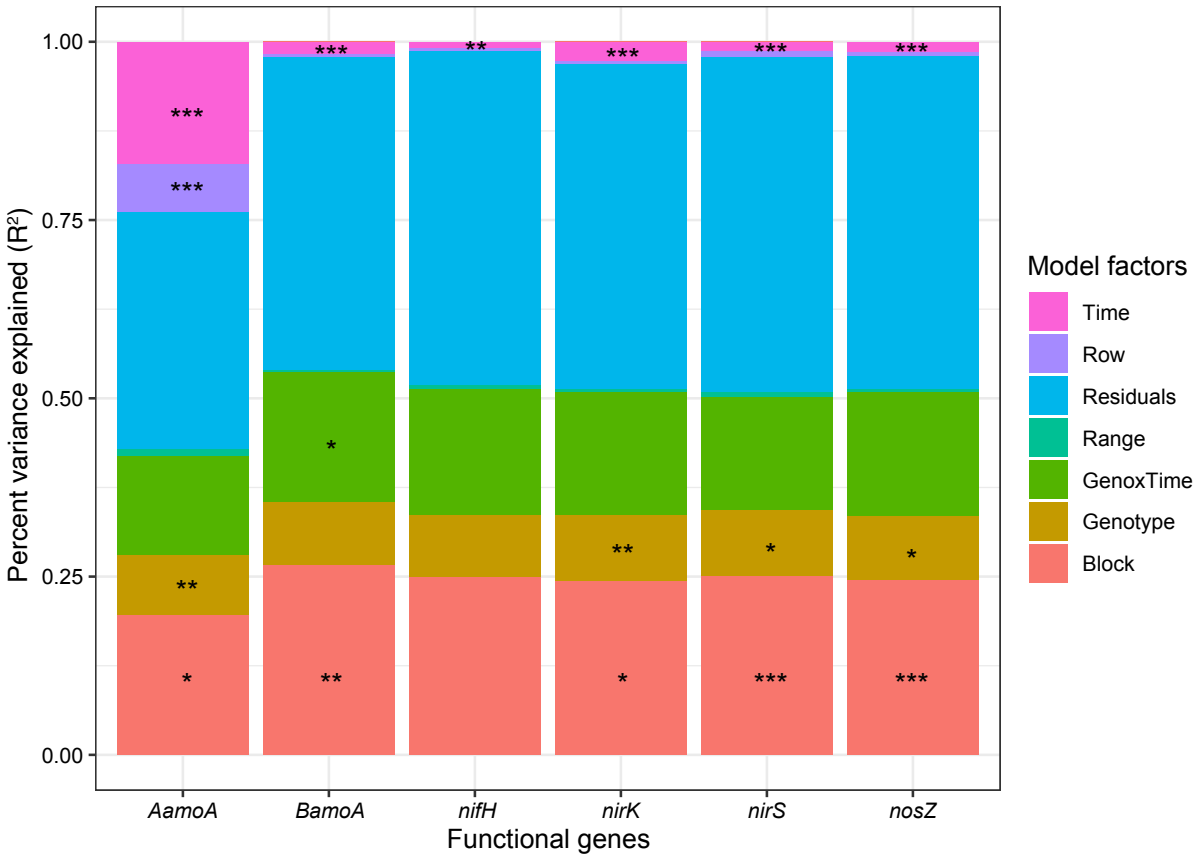

Figure 4.3 The figure above displaced the PERMANOVA results for the different nitrogen cycling functional genes included in this study. The y-axis shows R^2, percent variance explained by the treatment factor, and the x-axis shows the functional genes tested. * denote the level of p-value (*<0.05, **<0.001, ***<0.0001)

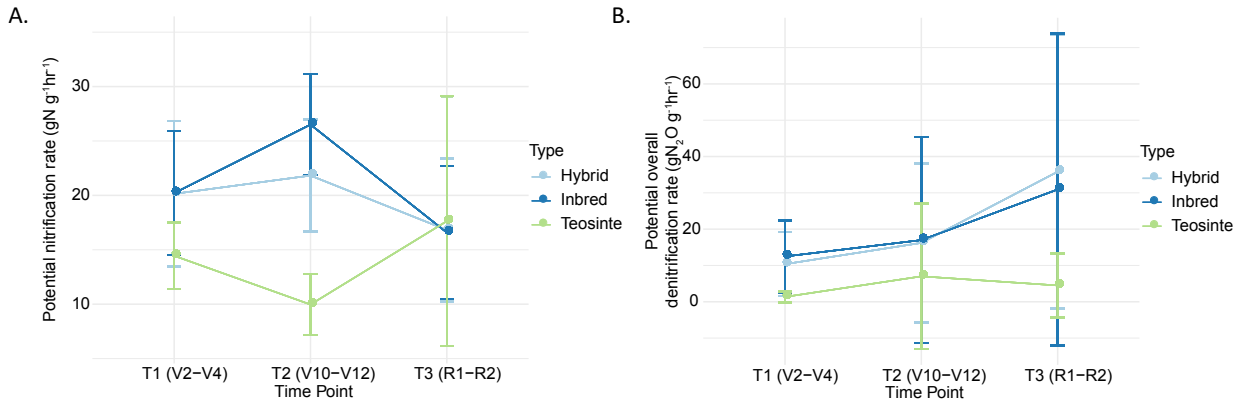

Figure 4.4 Seasonal variation in potential nitrification and denitrification rate compared among germplasm group across the season. LS Means and Standard Error were calculated using ASREML-r. **A.** Potential nitrification rate in (ngN/ghr) across the three sampling time points averaged over plant type. **B.** Overall dentification (ngN/ghr) across the growing season averaged over plant type, no differences in among plant classifications was observed, but potential denitrification rates increased slightly across the season. Statistical tests associated with figures are presented in supplemental materials C.6-C.7.

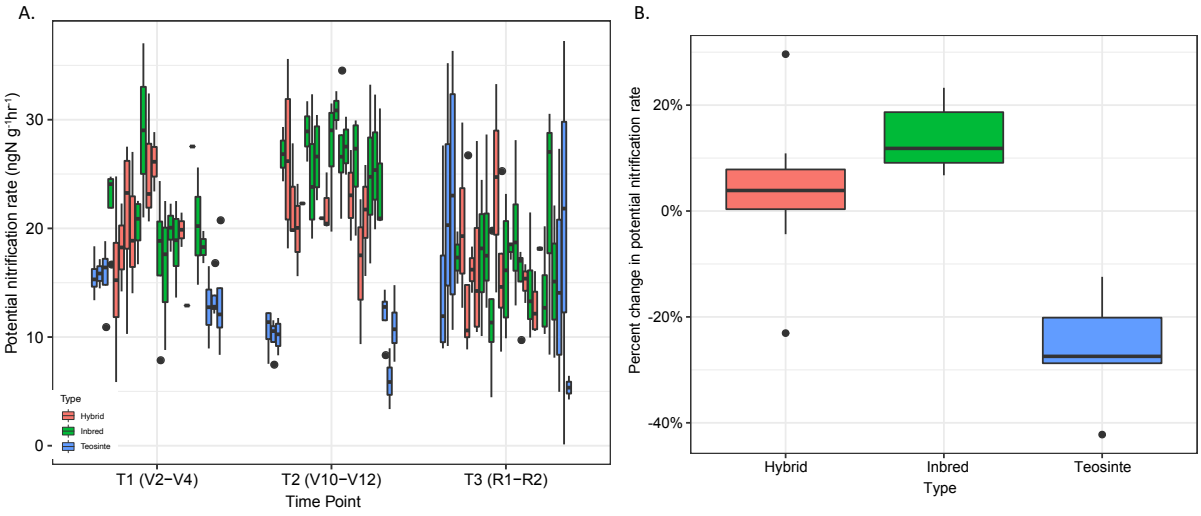

Figure 4.5 Displays the potential nitrification (ngN/ghr) results as influenced by plant genotype and type. **A.** Shows the potential nitrification rate (ngN/ghr) of all genotypes included in the study across our three sampling time points colored by plant type. Teosinte genotypes were observed as having the lowest nitrification rates in the T1 and T2. No differences were present at the T3 sampling time point. **B.** Shows the average genotypic effect of hybrid, inbred, and teosintes genotypes on the potential nitrification significant (ngN/ghr) determined across the population. Statistical analysis for both figures in supplemental table C.5-C.6, C.8.1.

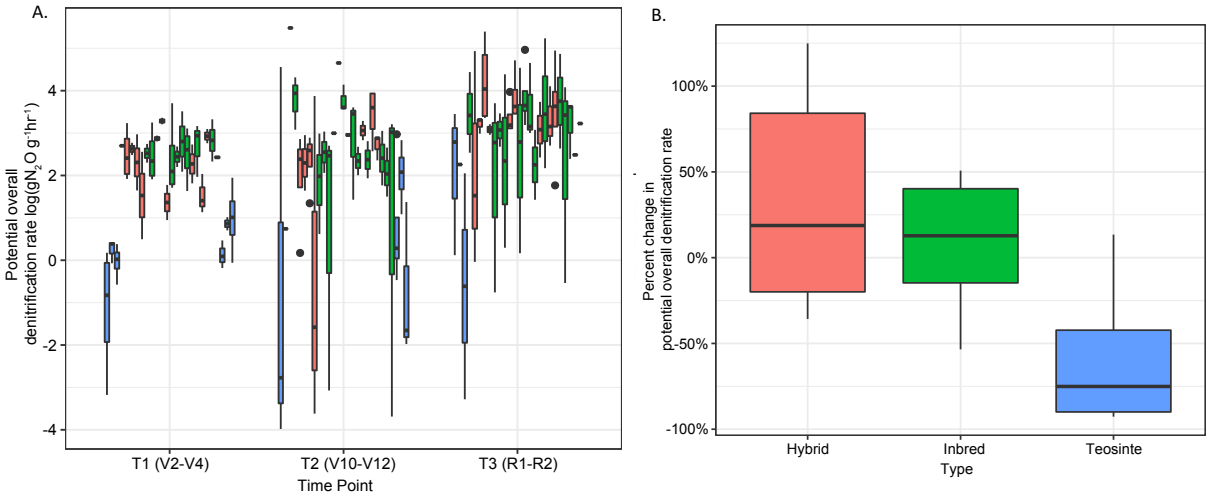

Figure 4.6 Displays the log of potential overall denitrification log(ngN/ghr) results as influenced by plant genotype and type. **A.** Shows the log of potential overall denitrification log(ngN/ghr) of all genotypes included in the study across our three sampling time points colored by plant type. **B.** average genotypic effect of hybrid, inbred, and teosintes genotypes on the log of potential overall denitrification log(ngN/ghr) determined across the population. Statistical analysis for both figures in supplemental table C.5-C.7, C.8.2.

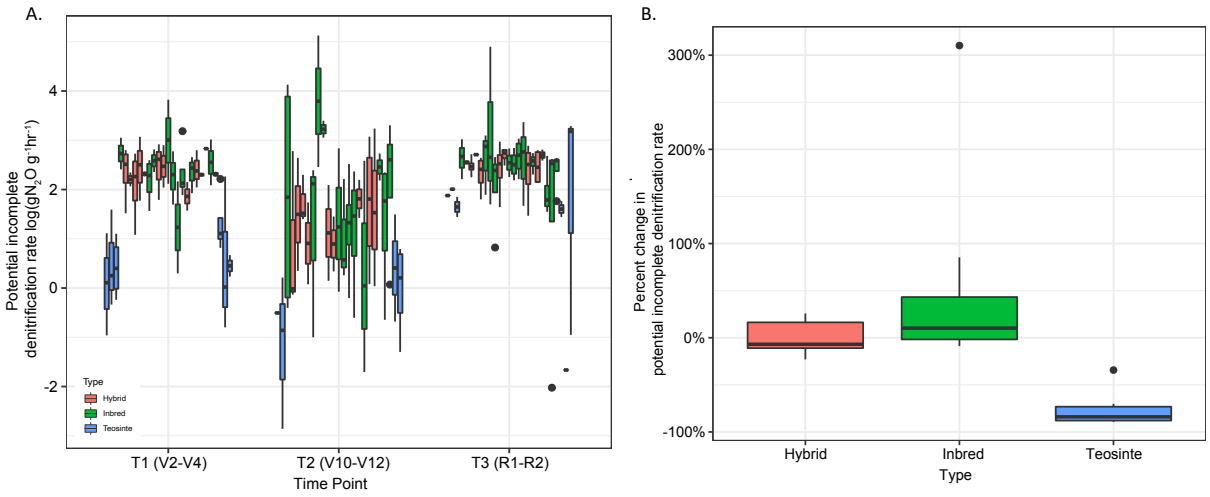

Figure 4.7 Displays the log of potential incomplete denitrification log(ngN/ghr) results as influenced by plant genotype and type. **A.** Shows the log of potential complete denitrification log(ngN/ghr) of all genotypes included in the study across our three sampling time points colored by plant type. **B.** Shows the average genotypic effect of hybrid, inbred, and teosintes genotypes on the log of potential incomplete denitrification log(ngN/ghr) determined across the population. Statistical analysis for both figures in supplemental table C.5-C.7, C.8.3.

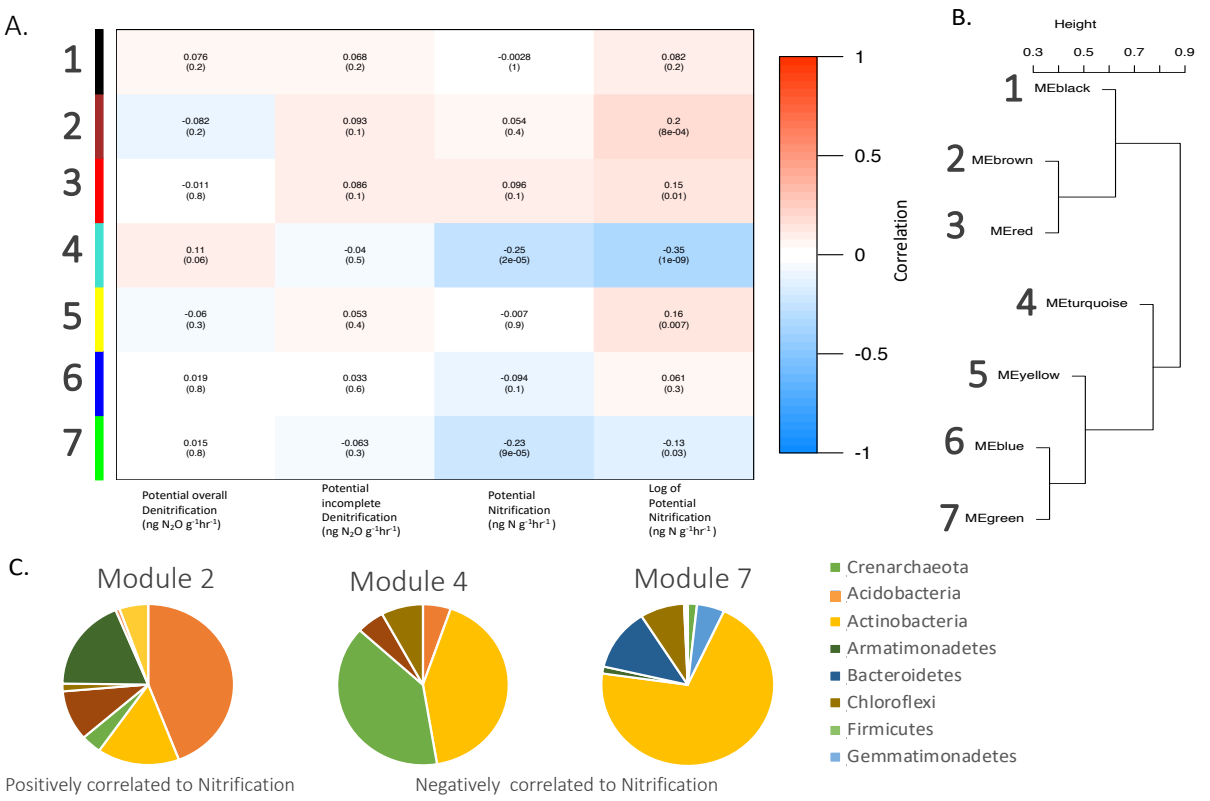

Figure 4.8 Shows the WGCNA results between potential denitrification and potential nitrification and microbial community composition. WGCNA starts by clustering microbial OTUs into modules of highly correlated taxa (based on abundance). These modules are then regressed against our explanatory factor (here that is denitrification and nitrification. **A.** Shows the strength and significance of correlation between microbial modules and nitrogen cycling function. **B.** Shows how correlated the microbial modules generated in the clustering process are to each other. **C.** Highlights the composition of significant modules that were correlated to changes in potential nitrification.

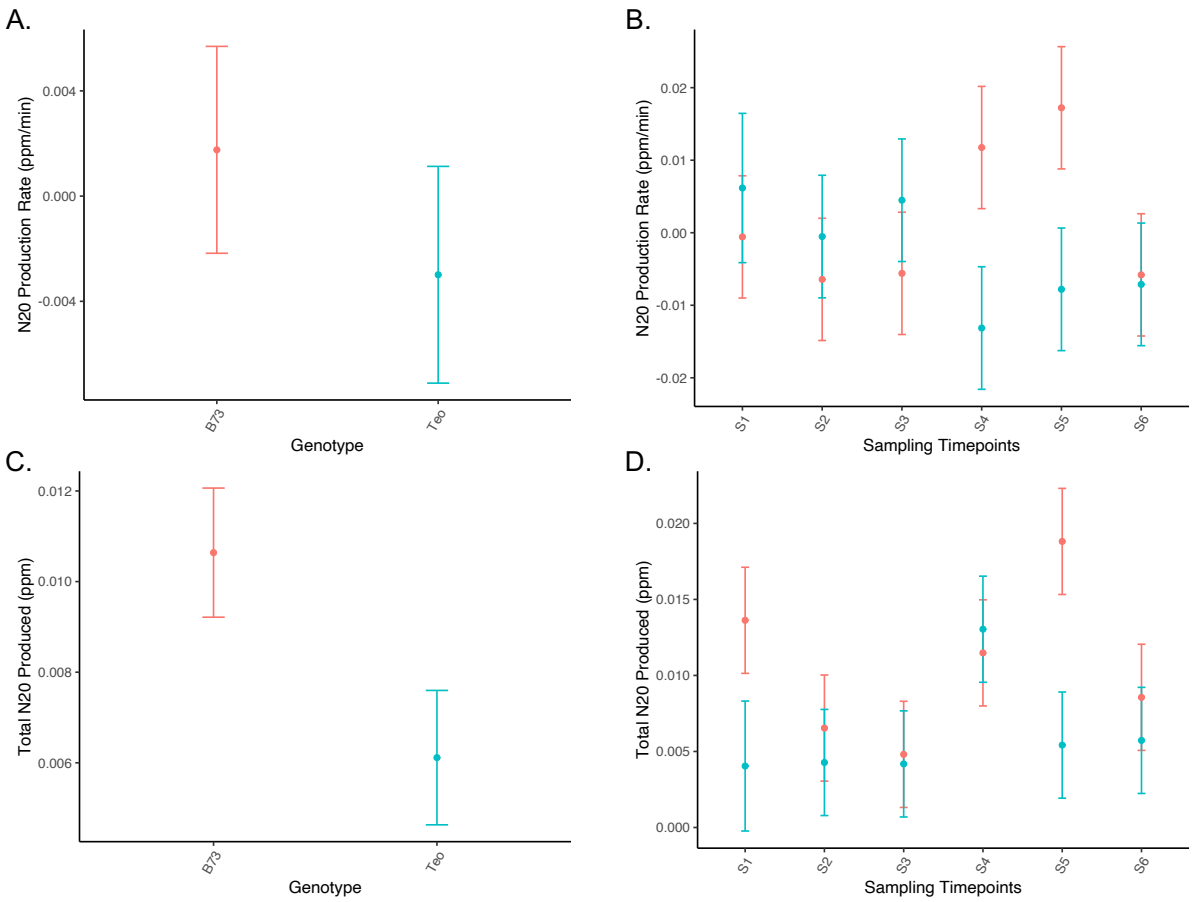

Figure 4.9 Displays the N_2O static flux chamber results over the growing season. **A.** Shows the N_2O production rate (ppm/min) comparing teosinte and B73 maize averaged over all the timepoints. **B.** Shows the N_2O production rate (ppm/min) comparing teosinte and B73 maize displaying all timepoints. **C.** Shows the total N_2O produced (ppm) averaged over the season comparing teosinte and B73 maize. **D.** Shows the total N_2O produced (ppm) for each sampling timepoint.

References:

Altschul, Stephen F, Thomas L Madden, Alejandro A Schäffer, Jinghui Zhang, Zheng Zhang, Webb Miller, and David J Lipman. 1997. "Gapped BLAST and PSI-BLAST: A New Generation of Protein Database Search Programs." *Nucleic Acids Research* 25 (17): 3389–3402.

Arnoldi, Jean-François, Sylvain Coq, Sonia Kéfi, and Sébastien Ibanez. 2019. "Positive Plant–Soil Feedback Trigger Tannin Evolution by Niche Construction: A Spatial Stoichiometric Model." *Journal of Ecology*, no. June: 1–14. https://doi.org/10.1111/1365-2745.13234.

Bardon, Clément, Franck Poly, Florence Piola, Muriel Pancton, Gilles Comte, Guillaume Meiffren, and Feth el Zahar Haichar. 2016. "Mechanism of Biological Denitrification Inhibition: Procyanidins Induce an Allosteric Transition of the Membrane-Bound Nitrate Reductase through Membrane Alteration." *FEMS Microbiology Ecology* 92 (5): 1–11. https://doi.org/10.1093/femsec/fiw034.

Bedard, Charles, and Roger Knowles. 1989. "Physiology, Biochemistry, and Specific Inhibitors of CH4, NH4+, and CO Oxidation by Methanotrophs and Nitrifiers." *Microbiology* 53 (1): 68–84. http://apps.isiknowledge.com/full_record.do?product=UA&search_mode=GeneralSearch&qid=11&SID=X16536DGgEAkOn8a882&page=1&doc=1&colname=WOS.

Bender, Ross R., Jason W. Haegele, Matias L. Ruffo, and Fred E. Below. 2013. "Nutrient Uptake, Partitioning, and Remobilization in Modern, Transgenic Insect-Protected Maize Hybrids." *Agronomy Journal* 105 (1): 161–70. https://doi.org/10.2134/agronj2012.0352.

Bohannan, Brendan, Andrew Morris, and Kyle Meyer. 2020. "Opinion Piece Linking Microbial Communities to Ecosystem Functions: What We Can Learn from Genotype-Phenotype Mapping in Organisms." https://doi.org/10.1098/rstb.2019.0244.

Bowles, Timothy M, Shady S Atallah, Eleanor E Campbell, Amélie C.M. Gaudin, William R Wieder, and A Stuart Grandy. 2018. "Addressing Agricultural Nitrogen Losses in a Changing Climate." *Nature Sustainability* 1 (8): 399–408. https://doi.org/10.1038/s41893-018-0106-0.

Butler, D G, B R Cullis, A R Gilmour, B J Gogel, and R Thompson. 2017. *ASReml-R Reference Manual Version 4*. *ASReml-R Reference Manual*.

Canarini, Alberto, Christina Kaiser, Andrew Merchant, Andreas Richter, and Wolfgang Wanek. 2019. "Root Exudation of Primary Metabolites: Mechanisms and Their Roles in Plant Responses to Environmental Stimuli." *Frontiers in Plant Science*. Frontiers Media S.A. https://doi.org/10.3389/fpls.2019.00157.

Caporaso, J Gregory, Justin Kuczynski, Jesse Stombaugh, Kyle Bittinger, Frederic D Bushman, Elizabeth K Costello, Noah Fierer, et al. 2010. "QIIME Allows Analysis of High-Throughput Community Sequencing Data." *Nature Methods* 7 (5): 335–36. https://doi.org/10.1038/nmeth.f.303.

Carini, Paul, Patrick J. Marsden, Jonathan W. Leff, Emily E. Morgan, Michael S. Strickland, and Noah Fierer. 2016. "Relic DNA Is Abundant in Soil and Obscures Estimates of Soil Microbial Diversity." *Nature Microbiology* 2 (December 2016). https://doi.org/10.1038/nmicrobiol.2016.242.

Compant, Stéphane, Abdul Samad, Hanna Faist, and Angela Sessitsch. 2019. "A Review on the Plant Microbiome: Ecology, Functions, and Emerging Trends in Microbial Application." *Journal of Advanced Research* 19: 29–37. https://doi.org/10.1016/j.jare.2019.03.004.

Coskun, Devrim, Dev T Britto, Weiming Shi, and Herbert J Kronzucker. 2017a. "How Plant Root Exudates Shape the Nitrogen Cycle." *Trends in Plant Science* 22 (8): 661–73. https://doi.org/10.1016/j.tplants.2017.05.004.

Coskun. 2017b. "Nitrogen Transformations in Modern Agriculture and the Role of Biological Nitrification Inhibition." *Nature Plants*. https://doi.org/10.1038/nplants.2017.74.

Davidson, Eric A, Mark B David, James N Galloway, Christine L Goodale, Richard Haeuber, John A Harrison, Robert W Howarth, et al. 2012. "Excess Nitrogen in the U.S. Environment: Trends, Risks, and Solutions." *Issues in Ecology* 15: 1–16. https://www.esa.org/esa/wp-content/uploads/2013/03/issuesinecology15.pdf.

Delaux, Pierre-Marc, and Sebastian Schornack. 2021. "Plant Evolution Driven by Interactions with Symbiotic and Pathogenic Microbes." *Science* 371 (6531): eaba6605-undefined. https://doi.org/10.1126/science.aba6605.

DeSantis, T. Z., P Hugenholtz, N Larsen, M Rojas, E L Brodie, K Keller, T Huber, D Dalevi, P Hu, and G L Andersen. 2006. "Greengenes, a Chimera-Checked 16S RRNA Gene Database and Workbench Compatible with ARB." *Applied and Environmental Microbiology* 72 (7): 5069–72. https://doi.org/10.1128/AEM.03006-05.

Ding, Long Jun, Hui Ling Cui, San An Nie, Xi En Long, Gui Lan Duan, and Yong Guan Zhu. 2019. "Microbiomes Inhabiting Rice Roots and Rhizosphere." *FEMS Microbiology Ecology* 95 (5): 1–13. https://doi.org/10.1093/femsec/fiz040.

Edgar, Robert C. 2010. "Search and Clustering Orders of Magnitude Faster than BLAST." *Bioinformatics* 26 (19): 2460–61. https://doi.org/10.1093/bioinformatics/btq461.

Edwards, Joseph D., Cameron M. Pittelkow, Angela D. Kent, and Wendy H. Yang. 2018. "Dynamic Biochar Effects on Soil Nitrous Oxide Emissions and Underlying Microbial Processes during the Maize Growing Season." *Soil Biology and Biochemistry* 122 (December 2017): 81–90. https://doi.org/10.1016/j.soilbio.2018.04.008.

Falkowski, Paul G, Tom Fenchel, and Edward F Delong. 2008. "The Microbial Engines That Drive Earth 's Biogeochemical Cycles." *Science* 320 (5879): 1034–39. https://doi.org/10.1126/science.1153213.

Favela, Alonso, Martin O. Bohn, and Angela D. Kent. 2021. "Maize Germplasm Chronosequence Shows Crop Breeding History Impacts Recruitment of the Rhizosphere Microbiome." *ISME Journal*. https://doi.org/10.1038/s41396-021-00923-z.

Fish, Jordan A., Benli Chai, Qiong Wang, Yanni Sun, C. Titus Brown, James M. Tiedje, and James R. Cole. 2013. "FunGene: The Functional Gene Pipeline and Repository." *Frontiers in Microbiology* 4 (OCT): 1–14. https://doi.org/10.3389/fmicb.2013.00291.

Gordon, A, G J Hannon, and Gordon. 2014. "FASTX-Toolkit." *[Online] Http://Hannonlab. Cshl. Edu/Fastx_ Toolkit Http://Hannonlab. Cshl. Edu/Fastx_ Toolkit*.

Huang, Ancheng C, Ting Jiang, Yong Xin Liu, Yue Chen Bai, James Reed, Baoyuan Qu, Alain Goossens, Hans Wilhelm Nützmann, Yang Bai, and Anne Osbourn. 2019. "A Specialized Metabolic Network Selectively Modulates Arabidopsis Root Microbiota." *Science* 364 (6440). https://doi.org/10.1126/science.aau6389.

Ishii, Satoshi, Seishi Ikeda, Kiwamu Minamisawa, and Keishi Senoo. 2011. "Minireview Nitrogen Cycling in Rice Paddy Environments: Past Achievements and Future Challenges." *Microbes Environ* 26 (4): 282–92. https://doi.org/10.1264/jsme2.ME11293.

Ishii, Satoshi, Gaku Kitamura, Takahiro Segawa, Ayano Kobayashi, Takayuki Miura, Daisuke Sano, and Satoshi Okabe. 2014. "Microfluidic Quantitative PCR for Simultaneous Quantification of Multiple Viruses in Environmental Water Samples." *Applied and*

Environmental Microbiology 80 (24): 7505–11. https://doi.org/10.1128/AEM.02578-14.
Johnson, Dale W. 2006. "PROGRESSIVE N LIMITATION IN FORESTS: REVIEW AND IMPLICATIONS FOR LONG-TERM RESPONSES TO ELEVATED CO $_2$." *Ecology* 87 (1): 64–75. https://doi.org/10.1890/04-1781.
Kuypers, Marcel M.M., Hannah K. Marchant, and Boran Kartal. 2018. "The Microbial Nitrogen-Cycling Network." *Nature Reviews Microbiology* 16 (5): 263–76. https://doi.org/10.1038/nrmicro.2018.9.
Langfelder, Peter, and Steve Horvath. 2008. "WGCNA: An R Package for Weighted Correlation Network Analysis." *BMC Bioinformatics* 9 (559): 1–13. https://doi.org/10.1186/1471-2105-9-559.
Locey, Kenneth J. 2010. "Synthesizing Traditional Biogeography with Microbial Ecology: The Importance of Dormancy." *Journal of Biogeography*, 2010. https://doi.org/10.1111/j.1365-2699.2010.02357.x.
Mag, Tanja, and Steven L Salzberg. 2011. "FLASH: Fast Length Adjustment of Short Reads to Improve Genome Assemblies" 27 (21): 2957–63. https://doi.org/10.1093/bioinformatics/btr507.
Moreau, Delphine, Richard D. Bardgett, Roger D. Finlay, David L. Jones, and Laurent Philippot. 2019. "A Plant Perspective on Nitrogen Cycling in the Rhizosphere." *Functional Ecology* 33 (4): 540–52. https://doi.org/10.1111/1365-2435.13303.
Moreau, Delphine, Barbara Pivato, David Bru, Hugues Busset, Florence Deau, Céline Faivre, Annick Matejicek, Florence Strbik, Laurent Philippot, and Christophe Mougel. 2015. "Plant Traits Related to Nitrogen Uptake Influence Plant- Microbe Competition." *Ecology* 96 (8): 2300–2310. https://doi.org/10.1890/14-1761.1.
Oksanen, Jari, Roeland Kindt, Pierre Legendre, Bob O'hara, M Henry, and H Stevens Maintainer. 2007. "The Vegan Package Title Community Ecology Package." Http://Cran.r-Project.Org/, Http://R-Forge.r-Project.Org/Projects/Vegan/. 2007. http://ftp.uni-bayreuth.de/math/statlib/R/CRAN/doc/packages/vegan.pdf.
Parkin, Timothy B., and Rodney T. Venterea. 2010. "USDA-ARS GRACEnet Project Protocols Chapter 3. Chamber-Based Trace Gas Flux Measurements." *Flux* 2010 (April 2003): 1–39.
Peiffer, Jason A, Aymé Spor, Omry Koren, Zhao Jin, Susannah Green Tringe, Jeffery L Dangl, Edward S. Buckler, and Ruth E. Ley. 2013. "Diversity and Heritability of the Maize Rhizosphere Microbiome under Field Conditions." *Proceedings of the National Academy of Sciences of the United States of America* 110 (16): 6548–53. https://doi.org/10.1073/pnas.1302837110.
Peralta, Ariane L., Eric R. Johnston, Jeffrey W. Matthews, and Angela D. Kent. 2016. "Abiotic Correlates of Microbial Community Structure and Nitrogen Cycling Functions Vary within Wetlands." *Freshwater Science* 35 (2): 573–88. https://doi.org/10.1086/685688.
Pérez-Izquierdo, Leticia, Mario Zabal-Aguirre, Santiago C. González-Martínez, Marc Buée, Miguel Verdú, Ana Rincón, and Marta Goberna. 2019. "Plant Intraspecific Variation Modulates Nutrient Cycling through Its below Ground Rhizospheric Microbiome." *Journal of Ecology* 107 (4): 1594–1605. https://doi.org/10.1111/1365-2745.13202.
Philippot, Laurent, Sara Hallin, and Michael Schloter. 2007. "Ecology of Denitrifying Prokaryotes in Agricultural Soil." *Advances in Agronomy*. https://doi.org/10.1016/S0065-2113(07)96003-4.
Philippot, Laurent, Jos M Raaijmakers, Philippe Lemanceau, and Wim H. Van Der Putten. 2013a. "Going Back to the Roots: The Microbial Ecology of the Rhizosphere." *Nature*

Reviews Microbiology 11 (11): 789–99. https://doi.org/10.1038/nrmicro3109.
———. 2013b. "Going Back to the Roots: The Microbial Ecology of the Rhizosphere." *Nature Reviews Microbiology* 11 (11): 789–99. https://doi.org/10.1038/nrmicro3109.
Phillips, Richard P., Adrien C. Finzi, and Emily S. Bernhardt. 2011. "Enhanced Root Exudation Induces Microbial Feedbacks to N Cycling in a Pine Forest under Long-Term CO2fumigation." *Ecology Letters* 14 (2): 187–94. https://doi.org/10.1111/j.1461-0248.2010.01570.x.
Priscu, John C, Brent C Christner, John E Dore, Marian B Westley, N Brian, Karen L Casciotti, W Berry Lyons, Brian N Popp, and W Berry. 2012. "Antarctic Lake : Molecular and Stable N2O in a Perennially Supersaturated Relict for a Biogeochemical Evidence Isotopic Activity" 53 (6): 2439–50.
Schinner, F., R. Ohlinger, E. Kandeler, and R. Margesin. 1996. *Methods in Soil Biology*. Springer. http://library1.nida.ac.th/termpaper6/sd/2554/19755.pdf.
Shi, Shengjing, Erin E. Nuccio, Zhili He, Jizhong Zhou, and Mary K. Firestone. 2016. "The Interconnected Rhizosphere: High Network Connectivity Dominates Rhizosphere Assemblages," 926–36. https://doi.org/10.1111/ele.12630.
Smercina, Darian N, Sarah E Evans, Maren L Friesen, and Lisa K Tiemann. 2019. "To Fix or Not To Fix: Controls on Free-Living Nitrogen-Fixation in the Rhizosphere." *Applied and Environmental Microbiology*. https://doi.org/10.1128/aem.02546-18.
Smýkal, Petr, Matthew N. Nelson, Jens D. Berger, and Eric J.B. Von Wettberg. 2018. "The Impact of Genetic Changes during Crop Domestication." *Agronomy* 8 (7): 1–22. https://doi.org/10.3390/agronomy8070119.
Spieck, Eva, Michael Spohn, Katja Wendt, Eberhard Bock, Jessup Shively, Jeroen Frank, Daniela Indenbirken, Malik Alawi, Sebastian Lücker, and Jennifer Hüpeden. 2020. "Extremophilic Nitrite-Oxidizing Chloroflexi from Yellowstone Hot Springs." *ISME Journal* 14 (2): 364–79. https://doi.org/10.1038/s41396-019-0530-9.
Subbarao, G V, K L Sahrawat, K Nakahara, I M Rao, M Ishitani, C T Hash, M Kishii, D G Bonnett, W L Berry, and J C Lata. 2013. "A Paradigm Shift towards Low-Nitrifying Production Systems: The Role of Biological Nitrification Inhibition (BNI)." *Annals of Botany*. https://doi.org/10.1093/aob/mcs230.
Trivedi, Pankaj, Jan E. Leach, Susannah G. Tringe, Tongmin Sa, and Brajesh K. Singh. 2020. "Plant–Microbiome Interactions: From Community Assembly to Plant Health." *Nature Reviews Microbiology* 18 (November). https://doi.org/10.1038/s41579-020-0412-1.
Vitousek, Peter M, John D Aber, Robert W Howarth, Gene E Likens, Pamela A Matson, David W Schindler, William H Schlesinger, David G Tilman, and David G Tilman9. 1997. "Human Alteration of the Global Nitrogen Cycle: Sources and HUMAN ALTERATION OF THE GLOBAL NITROGEN CYCLE: SOURCES AND CONSEQUENCES." *Source: Ecological Applications Ecological Applications Ecological Applications* 7 (3): 737–50. https://doi.org/10.1890/1051-0761(1997)007[0737:HAOTGN]2.0.CO;2.
Vitousek, Peter M, Duncan N.L. Menge, Sasha C Reed, and Cory C Cleveland. 2013. "Biological Nitrogen Fixation: Rates, Patterns and Ecological Controls in Terrestrial Ecosystems." *Philosophical Transactions of the Royal Society B: Biological Sciences* 368 (1621): 20130119. https://doi.org/10.1098/rstb.2013.0119.
Walters, William A, Zhao Jin, Nicholas Youngblut, Jason G Wallace, Jessica Sutter, Wei Zhang, Antonio González-Peña, et al. 2018. "Large-Scale Replicated Field Study of Maize Rhizosphere Identifies Heritable Microbes." *Proceedings of the National Academy of*

Sciences of the United States of America 115 (28): 7368–73. https://doi.org/10.1073/pnas.1800918115.
Xu, Jin, Yunzeng Zhang, Pengfan Zhang, Pankaj Trivedi, Nadia Riera, Yayu Wang, Xin Liu, et al. 2018. "The Structure and Function of the Global Citrus Rhizosphere Microbiome." *Nature Communications* 9 (1): 4894. https://doi.org/10.1038/s41467-018-07343-2.
Zhang, Xin, Eric A Davidson, Denise L Mauzerall, Timothy D Searchinger, Patrice Dumas, and Ye Shen. 2015. "Managing Nitrogen for Sustainable Development." https://doi.org/10.1038/nature15743.

CHAPTER 5: MAPPING THE GENETIC REGIONS UNDERLYING PLANT EXTENDED PHENOTYPE MICROBIOME RECRUITMENT AND FUNCTION

Significance:

There are genetic elements in organisms that directly shape the niche construction. The rhizosphere is an omnipresent example of niche construction carried out by plants. When plants alter their root niche, they are altering the capacity of microorganisms to colonize and grow in their surrounding soil. These alterations can influence how a soil processes and moves nutrients. These rhizosphere effects have the capacity to alter ecosystem-level processes. Using a panel of maize-teosinte near isogenic lines, we have identified genetic elements that alter the niche-forming capacity of the rhizosphere to exclude or enhance the colonization of microbes that work against sustainability. These genetic elements originated from maize's wild progenitor teosinte; thereby “rewilding” modern maize rhizosphere traits to recreate elements of the rhizosphere niche of the progenitor. This study suggests that we can determine plant alleles that modulate microbiome processes and interactions in the rhizosphere and potentially use this information to design a more sustainable agricultural system. These near-isogenic lines allow access to all the genetic variation within the evolutionary history of *Zea* to identify ancestral state plant niche-construction traits that may enable better management of the ecological inheritance caused by our agricultural system.

Abstract:

Plant genetics have been shown to play a significant role in shaping the microbiota, yet little work has been done to identify specific loci driving the structure and function of the

rhizosphere microbiome. Identifying host genetic elements influencing assembly or function of the host-associated microbiome could provide us with a novel method to manage and understand rhizosphere functions. To dissect the genetic basis of these ancestral microbiome traits, we used newly developed teosinte-maize near-isogenic lines (NILs). Using NIL populations allows for the fine mapping of extended phenotypes to specific genetic loci in the plant genome. A panel of 42 NILs, along with the parental lines (B73 and teosinte), were grown in the field and root zone microbiomes were characterized though amplicon sequencing and potential nitrogen cycling assays. From this maize-teosinte NIL experimental population, we identified 13 candidate genetic regions that drove major alterations to the root zone microbiome. Overall, teosinte near isogenic introgressions genetic variation explained a considerable amount of variation in the bacterial and fungal communities, along with nitrification and denitrification functional groups. From our potential activity assays, we identified eight unique NILs that altered the microbial communities N-cycling activity: two were shown to suppress potential nitrification rates, three were shown to suppress incomplete denitrification (N2O), and three were shown to suppress overall denitrification (N2O+N2). A number of unique metabolites were associated with the NILs involved in suppression of nitrification, suggesting potential mechanisms responsible for this trait, which has not previously been reported in maize. . Overall, these findings show how the plant genome can influence the recruitment, structure, and function of the microbiome. Furthermore, we show that wild cultivars possess ecologically important extended phenotypes that can be reincorporated into modern cultivars to improve sustainability. This type of understanding could provide us with a novel biological method by which to manage our agricultural ecosystems and global nitrogen cycle.

Introduction:

Feeding a growing world population amidst global change requires reducing the resource use and environmental impacts of agricultural production. A potential solution to this goal is to understand and harness the plant-associated microbiome and incorporate it into modern agriculture (Antwis et al. 2017). To accomplish this, we must comprehend the major ecological drivers of the microbial community, and determine if changes to these communities have functional consequences (Schimel and Gulledge 1998; Vigdis Torsvik 2002; Falkowski et al. 2008). Broadly, plant genetics have been shown to play a significant role in shaping the microbiota, yet what this means for microbial function has not entirely been resolved (Bulgarelli et al. 2013; Philippot et al. 2013). Research is needed to determine how, and which genes and genetic loci play a dominant role in interactions that influence microbial functional groups involved in nitrogen cycling in order to meaningfully manage the nitrogen cycle of our agroecosystem.

The degree to which plant genetics regulate microbial communities is of interest to crop breeders and evolutionary biologists. This is because the heritability of the microbiome determines whether the microbiome *and its functions* can evolve in response to selection on the host plant (Anderson et al. 2014; Wagner et al. 2016). Greenhouse and field studies have confirmed that genotypic variability in the host can alter the microbial community that establishes in the rhizosphere, the zone of soil tightly bound to the roots (Lundberg et al. 2012; Peiffer et al. 2013; Wagner et al. 2016). These intraspecific genetic differences extend past populations and have been seen across species (Berg and Smalla 2009; Yeoh et al. 2017). Further support across the phylogenetic tree of the angiosperm phylum demonstrates that evolutionary distance across plant species affects root microbial diversity and macro-ecologically relevant

traits (Fitzpatrick et al. 2018). Conversely, the rhizosphere microbiome is strongly influenced by the indigenous soil microbial communities which, in turn, is shaped by climate and edaphic factors (Ulrich and Becker 2006; Schreiter et al. 2014; Bakker et al. 2015). These environmental and plant genetic factors combine and ultimately shape the observed microbiome (Marques et al. 2014; Lambers et al. 2009; Qiao et al. 2017; Bulgarelli et al. 2013). However, microbial ecologists still lack an exact understanding of what shifts in these rhizosphere microbial communities mean functionally to both the plant and the ecosystem as a whole (Antwis et al. 2017; Graham et al. 2016; Mendes et al. 2013).

Nitrogen (N) cycling functions are of particular interest, as both plants and microorganisms require N for survival and growth (Zak et al. 1990; Kuzyakov and Xu 2013). Plant-microbe interactions are invoked when discussing plant strategies for nutrient acquisition (Moreau et al. 2015; Cantarel et al. 2015). In many cases, essential plant nutrients are converted to more usable forms by microbes before assimilation by plants (Edwards et al. 2014; H. Zhang et al. 2009; Long 1989; Bolan 1991). A mutualistic outcome of this interaction is not always the case (Bardgett et al. 2003; Kuzyakov and Xu 2013). Functionally, microbes in the soil ecosystem can either remove (denitrification or immobilization), increase (N-fixation or mineralization) or alter (nitrification or dissimilatory reduction of nitrate to ammonium) available reactive N (Sylvia et al. 2005; Kuypers, Marchant et al. 2018). While the effects of increased and decreased N on plant productivity are intuitive (Ingestad 1997), changing the chemical form of N is not, as plant species differ in their preferences for N form (nitrate, ammonium or organic nitrogen) (Boudsocq et al. 2012; Britto and Kronzucker 2013). The relative activity of these microbial processes can therefore either improve or hinder plant N acquisition. However, a systematic

understanding of how plant hosts and their genetic variability (and resulting phenotype) interact with these N-cycling microbial communities remains unknown (Coskun et al. 2017a).

Maize was domesticated from its wild ancestor teosinte approximately 9500 years ago in southwestern Mexico (Matsuoka et al. 2002; Piperno et al. 2009; van Heerwaarden et al. 2011). In that time sweeping genome- and phenome-wide changes occurred, leading maize to be one of the most consequential industrialized crops (Cassman et al. 2003; Lobell et al. 2011; Thenkabail et al. 2010; Jones and Thornton 2003). In addition, we have previously reported that modern breeding practices, characteristic of Green Revolution technologies, have altered recruitment of the maize rhizosphere microbiome in ways that are potentially less agriculturally sustainable (Favela, Bohn, and Kent 2021). Further, we have found that teosinte and modern elite maize varieties strongly differ in their interactions with the N-cycling microbiome and their ecosystem functions in both greenhouse and field settings (Chapter 2; Chapter 3). The expansive genetic variability within the *Zea* genus represents an ecologically diverse collection of plant species including domesticated maize and its closest wild relative, teosinte. Here, we use a panel of recently developed teosinte-maize near-isogenic lines (NIL) (Liu, Cook, et al. 2016) to dissect the genetic regions driving our previously established differences in recruitment of microbial functional groups between teosinte and maize, and to understand the relationship between host genetics and functions of the rhizosphere microbiome. Using NIL populations allows for the fine mapping of the previously reported microbial "extended phenotypes" to specific genetic loci in the plant genome as each NIL contains on average 4% of teosinte DNA in a random location (Fig. 5.1).

The overarching goal of this study was to determine if individual teosinte genetic introgressions into modern maize influence or predict changes in the rhizosphere microbiome

structure and nitrogen cycling function, and to identify potential mechanisms by which they are influencing this extended phenotype. Within these NILs, we assessed changes in microbial community composition and N-cycling function (potential nitrification and denitrification) in response to different genetic introgressions from teosinte. These results will allow us to determine if teosinte introgressions shape rhizosphere N-cycling functional groups and allow us to narrow down the genetic regions contributing to this phenotype. Furthermore, with the use of metabolomics we will gain further insight into the mechanisms driving differential microbial recruitment.

Methods and materials:

Germplasm and Field Experimental Design

We used a recently developed teosinte-maize near-isogenic lines (NILs) (Liu, Cook, et al. 2016). These lines were obtained partially through the authors of the paper and from the USDA/ARS Maize Genetics Cooperation Stock Center, located at the University of Illinois at Urbana-Champaign. The full table of NILs is presented in supplemental materials (Table D.1). NILs have previously been used to identify quantitative trait loci (QTL) and finely map specific genes in maize (Simić et al. 2012; G. I. Graham, Wolff, and Stuber 1997; Szalma et al. 2007; Liu, Garcia, et al. 2016), rice (Y. Zhang et al. 2006), and soybean (Jiang et al., 2009). The NILs used here(Liu, Cook, et al. 2016) contained an average of 2.4 chromosomal segments, encompassing about 4% of the teosinte genome, with the rest being homogenous B73 (Fig. 5.1). A set of 42 NILs was necessary to appropriately tile the teosinte genome within B73 and were included the experiment (Fig. 5.1). In addition to these NILs, the parental lines (B73 and PI384071) and their F1 hybrids were grown in the same field. By examining both of the parents

and their F1 hybrids, we should be able to capture the majority of the genetic variability driving differences in the microbiome between teosinte and maize (Langlade et al. 2005).

Field plots were located at the Crop Sciences Research and Education Center - South Farms at the University of Illinois, Urbana-Champaign, IL (40°03'46.7"N 88°13'44.8"W). We grew a total of 45 accessions (42 NILs, 2 parents, 1 hybrid). Plants were grown in 4-row blocks (24 plants per row) and were replicated and randomized four times across the field (180 total plots). To capture stochastic microbial community variability, present in the system, we sampled three technical replicates within each plot (45 accessions * 3 technical replicates * 4 replicate plots = 540 plants total). Plants were sampled twice, once during the vegetative growth stage V5-V6 (7/16/2018) and again during flowering (8/21/18). Samples consisted of a soil core (10 cm depth) within the root zone of the plant. As a control, field bulk soil was collected before planting and at each sampling time point. Sampled were placed on ice until they were transported to the lab. Once in the lab, soils were refrigerated at 4°C awaiting potential nitrification assays or potential denitrification assays (within 5 hours). Aliquots for DNA extraction were frozen immediately.

DNA Sequencing and Functional Gene qPCR

For this experiment, we characterized the microbiome and diagnostic functional genes related to transformations that occur in the nitrogen cycle: nitrogen fixation, nitrification, and denitrification. Amplicon sequencing was performed on bacterial and archaeal 16S rRNA genes, fungal ITS2, *amoA, nirS, nirK, nosZ,* and *nifH* genes. The Fluidigm Access Array IFC chip was used to prepare sequencing amplicons. This method allows for the simultaneous amplification of target functional genes using multiple primer sets (Fluidigm, San Francisco, CA). DNA sequencing was performed for bacterial, archaeal, and fungal amplicons using an Illumina HiSeq

2500 Sequencing System (Illumina, San Diego, CA). Primer information is provided in supplemental Table D.2. Fluidigm amplification and Illumina sequencing were conducted at the Roy J. Carver Biotechnology Center, University of Illinois (Urbana, IL, USA). Fast Length Adjustment of Short reads (FLASH) (Mag and Salzberg 2011) software was used to merge paired-end sequences from bacterial and archaeal 16S rRNA genes. For functional genes and fungal ITS, only forward read sequences were used. Once FLASH merging was performed, files were filtered by quality using the FASTX-Toolkit (Gordon, Hannon, and Gordon 2014). Reads that did not have a minimum quality score of 30 across 90% of the bases were removed. Using the FASTX-Toolkit, *nirK* sequences were trimmed to its amplicon size of 165-bp.

Once quality preprocessing was performed, FASTQ reads were converted to FASTA format. Using USEARCH-UPARSE version 8.1 (Edgar 2010), sequences were binned into discrete OTUs based on 97% similarity and singleton DNA sequences were removed. Quantitative Insights into Microbial Ecology (QIIME) was used to generate OTU tables for downstream statistical analysis and to assign taxonomic information, this is done with a combination of the UCLUST algorithm and GreenGenes database (DeSantis et al. 2006; Edgar 2010; Caporaso et al. 2010). Once taxonomy was assigned, chloroplast and mitochondrial OTUs were removed from the dataset. Rarefaction was performed to correct for differential sequencing depth across samples. Taxonomy was also assigned to functional gene sequences using QIIME (Caporaso et al. 2010) with the BLAST (Altschul et al. 1997) algorithm and custom gene-specific databases generated from reference sequences obtained from the FunGene repository (http://fungene.cme.msu.edu/) (Fish et al. 2013). All OTU tables used in statistical analyses were generated in QIIME. Singleton OTUs were filtered prior to statistical analysis.

Quantitative PCR (qPCR) was carried out to determine the abundance of functional genes in each of the rhizosphere microbial communities. Specific target amplification (STA), explained in (Ishii et al. 2014), was carried out on samples and standards to increase template DNA for amplification. STA and qPCR master mix recipes from (Favela, Bohn, and Kent 2021)were used for all samples. STA product and qPCR master mix were loaded into the Dynamic Array™ Microfluidics Fluidigm Gene Expression chip where amplification and quantification of functional genes were carried out simultaneously (Fluidigm, San Francisco, CA). All samples and standards were analyzed in 12 technical replicates. Fluidigm Real-Time PCR Analysis software version 4.1.3 was used to calculate gene threshold cycles (C_T). C_T values were converted to gene copy number using gene length and standard curves. All Fluidigm qPCR was conducted at the Roy J. Carver Biotechnology Center (Urbana, IL, USA). The final copy number of each functional gene amplicon was standardized by the ng of template DNA in the qPCR reaction.

Potential Assays

Potential denitrification assays were carried out using a modified version of the assay described in (Schinner et al. 1996; Peralta et al. 2016). Field-moist root-zone soil samples were incubated under anaerobic conditions in the presence of acetylene for 3h at 25°C. The assay was performed on 25g of root-zone soil in glass Wheaton jars. Incubations were carried out at substrate saturation of carbon (dextrose) and nitrogen (nitrate). Chloramphenicol 10 mg/Lwas added to the incubation to act as a bacteriostatic agent to prevent further microbial growth and protein synthesis. Wheaton jars were purged of oxygen with either helium or acetylene. Helium samples were used to estimate the amount of incomplete denitrification (N_2O) occurring in the assay atmosphere. Acetylene purged samples are used to measure overall denitrification (N_2O +

N_2). Acetylene is a commonly known inhibitor of nitrous oxide reduction. Initial and final gas samples were taken at the start and end of the incubation period. Initial and final nitrous oxide in gas samples was quantified using a GC-2014 Gas Chromatograph (Shimadzu, Kyoto, Japan) with an electron capture detector (GC-ECD).

The potential nitrification assay was developed and modified from (Schinner et al. 1996). This assay was performed at substrate saturation and values presented should be interpreted as the maximum potential rate of transformation of ammonia to nitrite, the first-rate limiting step of nitrification. In principle, this assay uses ammonium sulfate as the substrate for the first step of nitrification during a 5-hour incubation. Sodium chlorate is added to the assay to inhibit nitrate oxidation during the incubation period. Aliquots of homogenized field-moist root-zone soil (5 g) were placed in into two 50ml tubes (sample and control). Nitrite products released during the incubation period was extracted with potassium chloride and concentration was determined colorimetrically at 520nm.

Greenhouse Follow-up Experiment

To validate and elucidate a causal mechanism to explain differences in function, a greenhouse trial was carried out to 1) validate suppression of potential nitrification observed for NILs Z031E0021 and Z031E0047, 2) narrow down the introgression regions responsible for this phenotype using additional overlapping NILs not previously grown in the field, 3) determine a causal mechanism underlying microbiome function alterations. Greenhouse treatments included 15 NILs with overlapping introgressions to Z031E0021 and 11 NILs with overlapping introgressions to Z031E0047, along with B73 and bulk soils as controls (in total 30 treatments). Seeds were surface sterilized by soaking for 5 mins in 8.25% NaClO, followed by one rinse with sterilized distilled water, a single rinse of 70% ethanol, and three rinses with sterile distilled

water. Surface-sterilized seeds were dried on sterile filter paper in a sterile petri dish, then stored at 4°C overnight before sowing. Planting medium was a combination of live and autoclaved soil mix. The live inoculum soil was collected from agricultural soil located on the Crop Sciences Research and Education Center - South Farms at the University of Illinois at Urbana-Champaign, Urbana, IL. (40°04'58.7"N 88°12'43.6"W). Inoculum soil was sieved (2mm) then added (25%) to a steam pasteurized mix of soil: calcined clay: torpedo sand (1:1:1). For each line, 5 replicate 6'' classic 200 pots (1 liter) were sown with three seeds in each. Pots were thinned a week after germination, leaving only a single plant per pot for the remainder of growth. In total, 150 plants were grown. They were placed in a completely randomized design in the greenhouse with 16 hours of light and 8 hours of darkness. All plants were connected to an irrigation system that fertilized plants once a week. Plants were fertilized with a liquid nutrient solution, specifically Cal-Mag (N15-P5-K15), at a rate of 150 ppm. Nitrogen was applied as 11.8% nitrate nitrogen, 1.1% ammoniacal nitrogen, and 2.1% urea nitrogen. All plant treatments were maintained under the same fertilizer regime.

Seeds were planted 1/15/2020 and were grown for a total of a total of 5 weeks. Harvest occurred on 2/17/20. When collected, plants were cut into four samples: 1) the above ground portion used for plant biomass, 2) root zone soil which was collected for potential nitrification assay, 3) half of the root system with rhizosphere intact for microbiome, and 4) washed root system free of soil for metabolome. Rhizosphere samples were placed on ice until stored at -20 °C. Root tissue samples were immediately flash frozen and stored at -80°C.

Root Metabolite Extraction, GC-MS, and LC-MS Analysis

Root tissue were lyophilization and homogenized by grinding with a mortar and pestle in liquid nitrogen. Processed plant tissue (100 mg) was combined with 1 mL of LC-MS grade

acetonitrile:isoprpanol:H2O 3:3:2 (v:v:v) solvent was added to the vial. The resulting supernatant was divided into two aliquots for LC-MS and GC-MS metabolite analysis.

Samples were analyzed using a GC-MS and LC-MS system at the Metabolomics Laboratory of Roy J. Carver Biotechnology Center, University of Illinois at Urbana-Champaign, United States.

LC-MS conditions were used as previously described in (Elolimy et al. 2019). Briefly, Samples were analyzed with the Q-Exactive MS system (Thermo. Bremen, Germany). Xcalibur 4.1.31.9 was used for data acquisition. The Dionex Ultimate 3000 series HPLC system (Thermo, Germering, Germany) used had a degasser, an autosampler and a binary pump. The LC separation was performed on a Phenomenex Kinetex C18 column (4.6 × 100 mm, 2.6 μm) with mobile phase A (H_2O with 0.1% formic acid) and mobile phase B (acetonitrile with 0.1% formic acid). The flow rate was 0.25 mL/min. The linear gradient was as follows: 0–3 min, 100% A; 20–30 min, 0% A; 31–36 min, 100% A. The autosampler was set to 15°C and injection volume was 20 μL. Mass spectra were acquired under both positive (sheath gas flow rate: 45; aux gas flow rate: 11; sweep gas flow rate: 2; spray voltage: 3.5 kV; capillary temp: 250°C; Aux gas heater temp: 415°C) and negative electrospray ionization (sheath gas flow rate: 45; aux gas flow rate: 11; sweep gas flow rate: 2; spray voltage: −2.5 kV; capillary temp: 250°C; Aux gas heater temp: 415°C). The full scan mass spectrum resolution was set to 70,000 with scan range of m/z 67 ~ m/z 1,000, and AGC target was 1E6 with a maximum injection time of 200 ms. The 4-Chloro-DL-phenylalanine was spiked into the sample as the internal standard. LC-MS data were further analyzed with Thermo Compound Discoverer software (v. 2.1 SP1) for chromatographic alignment and compound/feature identification/quantitation. The workflow is Untargeted Metabolomics with Statistics Detect Unknowns with ID Using Online Databases. The following

settings were used in Select Spectra: minimum precursor mass (65 Da) and maximum precursor mass (5,000 Da); in Align Retention Time: Maximum shift (1 min) and Mass tolerance (5 ppm); in Detect unknown compounds: Mass tolerance (5 ppm), Intensity tolerance (30 %), S/N (3), and Minimum peak intensity (1000000).

GC-MS conditions were used as previously described in (Borgogna et al. 2020). Briefly, Metabolite profiles were acquired using a gas-chromatography mass-spectrometry (GC-MS) system (Agilent Inc, CA, USA) consisting of an Agilent 7890 gas chromatograph, an Agilent 5975 MSD and 7683B autosampler, as previously described. Briefly, gas chromatography was performed on a ZB-5MS (60 m × 0.32 mm I.D. and 0.25 mm film thickness) capillary column (Phenomenex, CA, USA). The inlet and MS interface temperatures were 250 °C, and the ion source temperature was adjusted to 230 °C. An aliquot of 1 ml was injected with the split ratio of 10:1. The helium carrier gas was kept at a constant flow rate of 2.4 ml/min. The temperature program was: 5-min isothermal heating at 70 °C, followed by an oven temperature increase of 5 °C/min to °C after which a final 10 min incubation at 310 °C was performed. The mass spectrometer was operated in positive electron impact mode (EI) at 69.9 eV ionization energy at m/z 30–800 scan range. The spectra of all chromatogram peaks were evaluated using the AMDIS 2.71 (NIST, MD, USA) using a custom-built database (460 unique metabolites) of the University of Illinois Carver Metabolomics Center. Throughout the sample preparation, data-acquisition and data-preprocessing, samples were compared to the QCs to evaluate potential variation that may have arisen in the dataset throughout the analytical study. All known artificial peaks were identified and removed prior to data mining. To allow comparison between samples, all data were normalized to the internal standard in each chromatogram and sample volume. The instrument variability was within the standard acceptance limit (5%).

Statistical Analysis

The microbial communities were evaluated as separate datasets for each amplicon (prokaryotic 16S rRNA, fungal ITS, *nifH, nosZ, nirK, nirS*, bacterial *amoA* and archaeal *amoA*). The relative effect of NIL, sampling time, range, row, and block on the root zone microbiome and root metabolome composition was assessed using permutational analysis of variance (PERMANOVA) with the 'adonis' function, from the community ecology R package, 'vegan' (Oksanen et al. 2007). To visualize differences from these models, non-metric multidimensional scaling (NMDS) ordinations were created using R package 'phyloseq' and plotted with R package 'ggplot2' (McMurdie and Holmes 2013; Wickham 2007). Genetic marker-microbiome comparisons were done using the 'matrixEQTL' package in R (Shabalin 2012). This method allowed for fast an efficient comparison of NIL genome and microbiome data. Using the 'asreml-r' package (Butler et al. 2017), additional restricted maximum-likelihood mixed effects models were used to examine the relationship between functional potential assay and introgression while controlling for edaphic environmental conditions. Modules of microbial taxa responding to the NIL germplasm were determined using a weighted correlation network analysis (WGCNA) in R (Langfelder and Horvath 2008). Prior to WGCNA, amplicon data was transformed using a central log ratio transformation (Gloor et al. 2017). Root metabolomic comparison was done in 'DESEQ2' in R (Love, Huber, and Anders 2014).

Results:

In this field experimental study, we identified 14,041 different 16S rRNA operational taxonomic units (OTUs, 97% similarity, rarefied to 30,152 reads per sample), and 2246 fungal OTUs (rarefied to 2302 reads per sample) were identified from the ITS2 region.

Introgressions influence on the rhizosphere microbiome

With the prokaryotic (16S rRNA) and fungal communities (ITS2), we found that genetic introgression (NIL genotype), time, location of block, and range and row explained 56% (prokaryotic) and 52% (fungal) of the variation in the microbiome. Genetic introgressions (NIL genotype) explained 13% of the variation in the prokaryotic 16S rRNA and 12% of the variation in the fungal ITS communities (PERMANOVA: 16SrRNA DF= 41, $p<0.001$; ITS2 DF=41, $p<0.001$; Table D.3-D.4). It should be noted that block location explained the greatest amount of variation in the both the prokaryotic and fungal communities around 30% and 28%, respectively. These models were all performed using the NIL genotype as a treatment factor. As shown in the genomic map (Fig. 5.1B), there is a considerable amount of complexity in the size, heterozygosity, and overlap of the genetic introgressions. To account for this variation, we also looked at the effects of each individual introgressions on the root zone microbiome. This analysis revealed that 23% of the loci in the *Zea* genome mapped to some change in the rhizosphere 16S rRNA microbiome, and most of the loci had a small effect on the relative abundance of OTUs. A total of 8 regions genomic regions had large effects (influencing more than 80 OTUs) on the 16S rRNA microbiome (Fig. 5.2).

Introgressions influence on the Nitrogen cycling functional group community

From our analysis of nitrogen cycling functional genes, we observed 1456 *nifH* OTUs, 74 archaeal *amoA* OTUs, 55 bacterial *amoA* OTUs, 4739 *nirK,* 1187 *nirS* OTUs, and 1655 *nosZ* OTUs. In response to teosinte introgressions (NIL genotype), 4 of 6 nitrogen cycling genes surveyed showed to changes in community membership (Table D.5), while none of the nitrogen cycling genes changed in abundance. The changes in N-cycling group membership were primarily in nitrification and denitrification. In regard to nitrification, variation in both archaeal

amoA, and bacterial *amoA* functional groups in the root zone were significantly explained by teosinte introgressions (NIL genotype), (PERMANOVA: archaeal R^2=0.15, DF= 41, p<0.001; bacterial R^2=0.13 n=313, DF=41, p<0.008; Table D.5.2-3). For denitrification, we observed that *nirK* and *nosZ* functional group community were also observed to be significantly influenced by teosinte introgressions (NIL genotype), (PERMANOVA: *nirK* R^2=0.13, DF= 41, p<0.022; *nosZ* R^2=0.12 n=329, DF=41, p<0.046; Table D.5.5-6). *nifH* and *nirS* were unresponsive to teosinte introgressions (Table D.5.1, D.5.4). Full statistical PERMANOVA model for all functional genes is present in supplemental information Tables D.5.

Introgressions influence potential nitrification and denitrification

We found that potential nitrification rate (ng N/g hr) of rhizosphere soils was influenced by teosinte genetic introgression (Fig. 5.3A, E, Table D.6). Furthermore, we only observed NIL genotypes effects at our second sampling timepoint, mid-season during peak growth (Wald test: p=0.005), but not during the first sampling timepoint (Wald test: p= 0.7509). From the second time point, we observed Z031E0047 and Z031E0021 NILs were shown to have similar teosinte-like nitrification phenotypes (Ch. 3). These NILs were shown to have a 50% (9% log-transformed) reduction in potential nitrification rate compared to the B73 control. Interestingly, a large number of NILs (T1:33/42, T2:34/42) were shown to stimulate potential nitrification rate compared to B73 (Fig. D.2).

Furthermore, potential incomplete denitrification (N_2O) and overall denitrification (N_2O+N_2) rate, log (ng N/g hr), of rhizosphere soils were influenced by teosinte introgressions (Fig. 5.3, Wald test incomplete: p<0.001, overall: p<0.001; Table D.6). Much like nitrification rates, it should be noted that the effects of introgressions in denitrification were variable across sampling timepoints. A significant effect of teosinte introgression on potential incomplete

denitrification (N_2O) was observed during the first sampling time point (Wald test: $p<0.001$), but not during the second sampling time point (Wald test: $p=0.10$). During the first timepoint, the NILs with the greatest effect on incomplete denitrification (Z31E0559, Z031E0047, and Z31E0059) suppressed potential incomplete denitrification (N_2O) 58% (20% log-transformed) more than control B73. Overall denitrification (N_2O+N_2) assays were not found to be significantly influenced by teosinte introgression during the first sampling time point (Wald test: $p=0.48$) but were during our secondary time point (Wald test: $p<0.01$). During the second timepoint, NILs Z031E0071, Z031E0012, and Z031E0591 displayed the greatest suppression of overall denitrification potential (N_2O+N_2) – 52% (37% log-transformed) more than control B73. During our first sampling timepoint we observed that most of the introgressions stimulated incomplete (T1:26/42, T2:7/42) and overall denitrification (T1:40/42, T2:8/42), while the opposite was observed during our later time points.

Linking Introgressions, microbiome function, and potential N-cycling rates

Weighted-gene correlation network analysis was used to identify co-correlated OTU modules in the microbiome that were related to introgression identity and rhizosphere N-cycling function. Analysis focused on our secondary sampling timepoint as this is where introgressions were seen to influence both potential nitrification and potential overall denitrification. From this analysis, we observed 18 OTU modules correlated with potential nitrification rates (11 modules: $p<0.05$, 7 modules: $p<0.10$). 12 of these 18 modules were negatively correlated (-0.18:-0.12), while 6 were positively correlated (0.12:0.16) with potential nitrification rates. Two separate OTU modules were correlated with the BNI NILs (Z031E0021, Z031E0047). The Z031E0021-associated module (cor =0.13, $p=0.07$) was negatively correlated to potential nitrification rates (cor=-0.15, $p=0.05$). The Z031E0047-associated module (cor=-0.15, $p=0.05$) was positively

correlated to potential nitrification rates (cor=0.15, p=0.05). So as these taxa increase or decrease in the root zone, we see the subsequent change in potential nitrification. For denitrification results, we observed 8 modules correlated to overall denitrification (N_2O+N_2) and 11 modules correlated to incomplete denitrification (N_2O) ($p<0.10$). Two modules shared a correlation with both incomplete (sharedM1: cor=0.14, p=0.06, sharedM2: cor=-0.15, p=0.048) and overall denitrification (sharedM1: cor=0.17, p=0.02, sharedM2: cor=-0.12, p=0.09). One module was correlated with overall DI NILs (Z031E0012) and another module was correlated with our incomplete DI NIL (Z031E0523). The Z031E0012-associated module (cor=0.15, p=0.04) was positively correlated with potential overall denitrification (cor=0.13, p=0.09), while the Z031E0523-associated module (cor=-0.14, p=0.06) was positively correlated with potential incomplete denitrification (cor=0.16, p=0.03). These modules potentially represent the taxa that are being selected and/or suppressed and are directly contributing to our potential functional differences.

Validating BNI introgressions and determining potential mechanism

Potential nitrification by Z031E0021 and Z031E0047 (Fig. 5.4A-B) was confirmed in a greenhouse trial focusing on BNI. Through analysis of NILs with overlapping introgressions, additional NILs with the ability to suppress nitrification activity in the soil were identified (Fig. 5.4A-B). This analysis narrowed down candidate introgression regions to Chr5: 190689917…192848761, Chr9: 18782106…25727342, and Chr9:88651842…110988044. Using MaizeGDB gene center (Portwood et al. 2019), we determined that the chromosome 5 introgression contained 61 previously mapped genes, while chromosome 9 introgressions contained 621 previously mapped genes (Table D.7). Genes related to phytochemical derivation and synthesis were present in both chromosome 5 introgressions (i.e, phenylalanine ammonia

lyase7, defense-like protein4) and chromosome 9 (i.e., acid phosphatase1, arginine decarboxylase1). These findings led to metabolomic characterization of NILs root tissue to potentially determine genes and mechanisms of BNI by NILs.

Using a combination of GC-MS and LC-MS, we characterized the metabolic profile of the root tissues of the B73 control, original BNI NILs, overlapping NILs with the BNI phenotype and negative control NILs without the BNI phenotype. Targeted GC-MS identified 152 metabolites, while untargeted LC-MS identified 2384 metabolites. Root metabolite analysis comparing contrasting BNI phenotypes, revealed significant differences in tissue levels of proline and raffinose ($p<0.05$, Fig. 5.4C-E) between lines with suppressed nitrifier activity in the root zone. Interestingly, increased galactose concentrations were reported in B73 compared to all NILs (Fig. 5.4E). Phenotype comparison of LC-MS data revealed that 12 metabolites were enriched in NILs with the ability to suppress nitrification. Paired comparisons of B73 metabolome to each individual NIL was performed and 13:17 (GC-MS:LC-MS) metabolites were found to be significantly enriched in the Chr5 BNI NIL root tissue compared to B73 ($p<0.05$, Table D.8). Only three metabolites related to Chr5 introgressions were classified: costunolide (Fig. 5.4F), icosadienoicacid, and stachydrine (Fig. 5.4G). One unclassified metabolite, C15H29NO, was found to be significantly enriched across both Chr 5 BNI NILs. While 8:46 (GC-MS:LC-MS) metabolites were found to be significantly enriched in the Chr9 BNI NIL root tissue compared to B73 ($p<0.05$, Table D.8). Chr9 introgressions showed 6 classified metabolites [6]-gingerol (Fig. 5.4H), quercetin-3β-D-glucoside, D-(-)-quinic acid, (1R,9S)-11-[(methylsulfanyl)acetyl]-3-(2-thienyl)-7,11-diazatricyclo[7.3.1.02,7]trideca-2,4-dien-6-one, 7,9-dimethyl-4-{[5-(4-pyridinyl)-1,3,4-oxadiazol-2-yl]sulfanyl}pyrido[3',2'

4,5]thieno[3,2-d]pyrimidine, and chlorogenic acid; 4 unclassified compounds were enriched across both of the BNI NILs.

Discussion:

Variation across genotypes has been shown to influence and contribute to the heritability of rhizosphere microbiome and N-cycling functions (Ch. 1-4) (Favela, Bohn, and Kent 2021). Using a panel of teosinte-maize near-isogenic lines, we show here that specific teosinte genetic loci are associated with altered root zone microbiome assembly and N-cycling function. Additionally, we identified specific teosinte introgressions that restore maize's ability to suppress nitrification (BNI) and denitrification (BDI) activities; traits which have not been previously reported in modern maize Furthermore, metabolomic analysis of root tissue collected from NILs capable of BNI revealed that altered root chemistry is likely a driving factor in altered nitrification suppression. Taken together, these findings suggest that we can genetically select and "rewild" how agricultural cultivars interact with their rhizosphere microbiome and effect desirable changes in microbiome functions. This potential breakthrough paves a novel way forward to breed agricultural cultivars with extended phenotypes that result in desired ecosystem services that improve sustainability of agroecosystems.

This field study demonstrates that NILs can be used to map genetic regions associated with changes in the microbiome (Fig. 5.2). Specifically, we observed teosinte introgressions to explain variation in the prokaryotic and fungal microbiome, along with N-cycling functional groups (bacterial *amoA,* archeal *amoA*, *nirK, nosZ).* Furthermore, using the NIL HapMap (Fig. 5.1), we identified loci correlated to changes in microbial taxa abundance and identified 8 major introgression regions causing large shifts in the rhizosphere prokaryotic microbiome. Work has been done across animals and plants to understand the underlying genetic loci that drive host

microbial communities, with many cases successfully identifying candidate genes related to the phenotype of interest (Horton et al. 2014; Belheouane et al. 2017; Lynch et al. 2017; Wallace et al. 2018; Goodrich et al. 2016). To date, the studies that have attempted to elucidate the relationship between plant genetic loci and the host microbiome have primarily focused on leaf-associated microbial communities (Horton et al. 2014; Wallace et al. 2018). Here we show that this work is viable in the complex soil rhizosphere environment and we take a step forward by characterizing the effects of specific loci on N-cycling functional groups and related potential function.

We have previously identified that maize breeding chronologically transformed the rhizosphere microbiome of elite inbred varieties to potentially be less agriculturally sustainable (Favela, Bohn, and Kent 2021). Additionally, we found that teosinte recruited differential microbial taxa and N-cycling functional groups in both greenhouse and field settings compared to modern maize (Chapter 2-3, Favela, Bohn, and Kent 2021). Further work on these teosinte lines have also shown that they can suppress potential nitrification and denitrification activity in the field setting, while modern elite varieties do not (Chapter 3, Favela, Bohn, and Kent 2021). An additional take away of our NIL study is that "rewilding" modern maize by the reincorporation of key teosinte loci may be a viable method to regain lost ecologically important traits such as microbial partnership or microbiome control.

Importantly, the effects of microbiome-associated loci manifest themselves as changes in microbial activity. Here, we determined that NILs with the ability to suppress potential nitrification and overall denitrification were also associated with changes in the prokaryotic microbiome (Fig 5.2). These results show a through line in microbiome recruitment to function, where teosinte genetic elements likely code for a metabolite that influences selection of taxa in

the rhizosphere and thereby limits or enhances the activity of these microbial functions. Work performed with synthetic microbial communities has shown that differences in exudation play a considerable role in altering microbial community recruitment in the rhizosphere (Sasse et al. 2018; Korenblum et al. 2020). Here we show that this additionally manifests as a change in the activity and function of the community.

Metabolomic analysis strengthened this microbial recruitment and function through line as it provided a potential mechanism by which to connect the two. From those results, we observed that root tissues of NILs capable of suppressing nitrification contained enriched levels of metabolites not present in the B73 parent or other negative controls. Other work in BNI and BDI have shown that certain plant species contain genes that code for secondary plant metabolites that are inhibitory to the activities of soil nitrifiers and denitrifers (Coskun et al. 2017b; Bardon et al. 2016). It is hypothesized that these secondary defensive metabolites were co-opted in plants as a way to limit potential N losses that can occur when microbial nitrification and denitrification are rampant (Coskun et al. 2017b; Bardon et al. 2016). Here, we hypothesize that our teosinte introgressions are returning some gene (or gene cluster) to modern maize that were lost during the domestication process. The restored gene then codes for a previously lost phytochemical used to alter microbiome composition and inhibit the growth of nitrifiers or denitrifers. Furthermore, the follow-up greenhouse experiment in this study was designed to determine whether we could identify a causal metabolite present in our candidate nitrification suppression lines. Those results showed a number of metabolites enriched in the NILs compared to the controls, some of which have strikingly similar structure to previously identified BNI compounds (Coskun et al. 2017b; Bardon et al. 2016; Bedard and Knowles 1989). One example of this is [6]-gingerol (Fig. 5.4H), a phenylpropanoid, synthesized from phenylalanine (a known

BNI compound) (Bedard and Knowles 1989). Interesting, [6]-gingerol has already been shown to have anti-microbial properties (Ficker et al. 2003) and may also inhibit nitrification. This is an important result as, to date, BNI and BDI compounds have yet to be reported in maize, and the discovery of which has the potential to improve the sustainability of the crop.

Unfettered microbial nitrification and denitrification processes within the soil ecosystem reduce agricultural sustainability. Nitrification results in the conversion of stable ammonium to readily leached nitrate, denitrification contributes to the loss of N and can result in the production of N_2O a potent greenhouse house gas. While historically these processes have been shown to be primarily controlled by soil edaphic conditions – a growing body of work is now highlighting that plant hosts can significantly alter the activity of N-cycling groups (Subbarao et al. 2013; Coskun et al. 2017b; Bardon et al. 2016). This study builds on our understanding of how genetic variation influences ecosystem processes mediated by microbial activity and finds novel candidate introgressions that drive the rhizosphere microbiome. These may be important findings to build our understand of ecosystem from a gene level.

Conclusion:

Our findings suggest that wild cultivars have genes and extended phenotypes that manipulate the rhizosphere microbiome. We identified a number of loci influencing the structure and N-cycling functions of the rhizosphere microbiome, and further used this genetic mapping to better understand mechanistically how these loci are achieving their extended phenotype. Our results suggest that we can tailor the maize genome to have predictable belowground rhizosphere microbiome interactions, and that "wild" genetic variation may present a reservoir of useful sustainability related traits. If these microbiome-related genes are incorporated into our modern

breeding practices, there is potential to manage agricultural microbiomes in a way that does not require major chemical inputs (pesticides, fertilizers, herbicides, novel bioinoculants, etc.) typical of our contemporary agricultural system. These plant microbiome interactions can further be selected to improve overall agricultural sustainability and management of the soil nitrogen cycle. Incorporating an understanding of microbiomes into our agroecosystems is essential in facing our future anthropogenic issues in feeding the world and dealing with the pressures of climate change.

Figures:

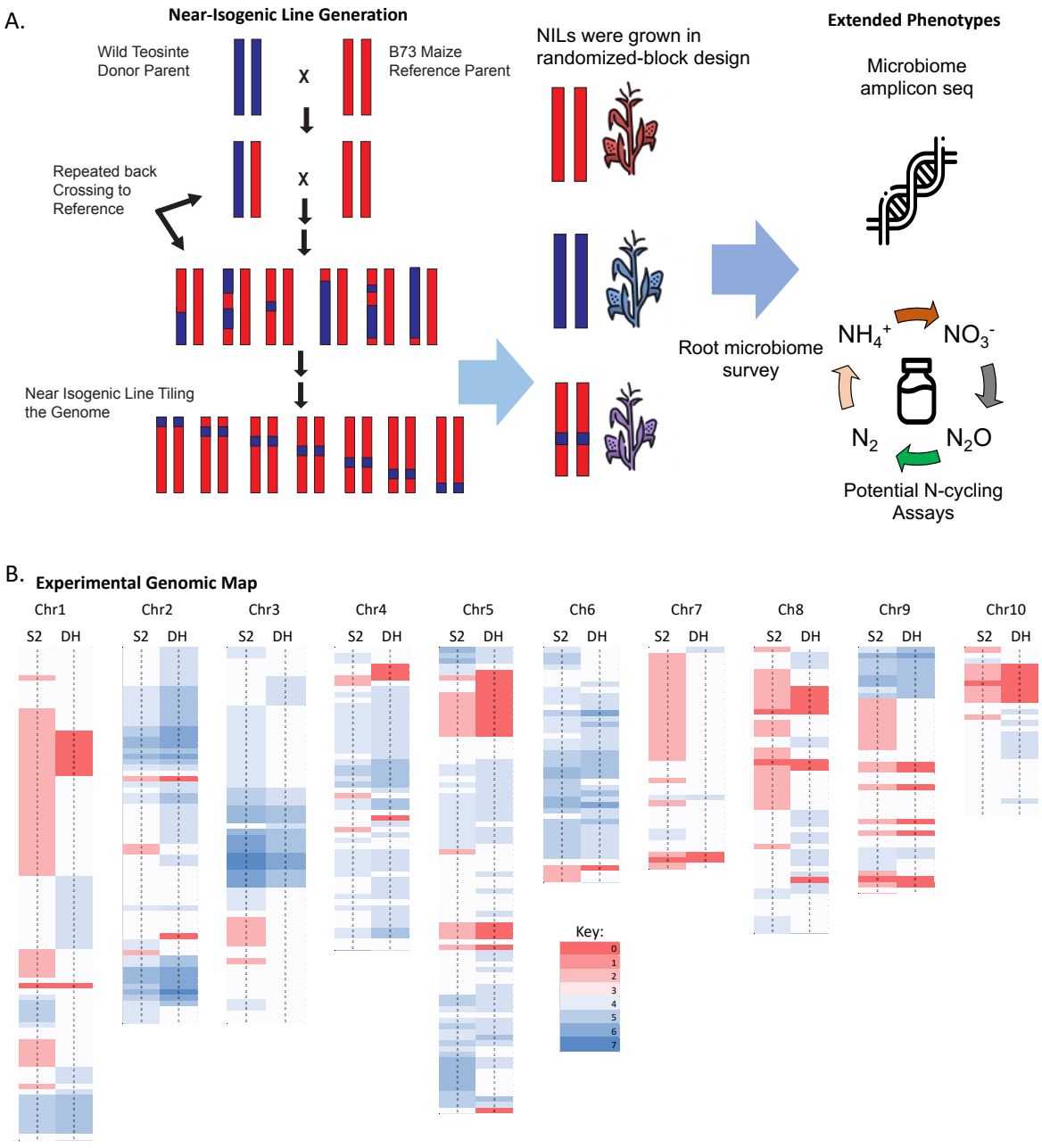

Figure 5.1 Near-isogenic line minimum tiling path used in study. A) NILs were generated by crossing B73 with Teosinte, then repeated backcrossing with B73 until the NILs contained an average of 4% teosinte loci. These lines were then grown and replicated in the field. Rhizosphere microbiome and potential N-cycling was characterized. B) Genetic map of NILs used in this study. Chr# indicates chromosome number. D.2 shows the number of teosinte introgressions present in a locus from the second backcrossing included in this study. DH represents the number of double haploids at that locus.

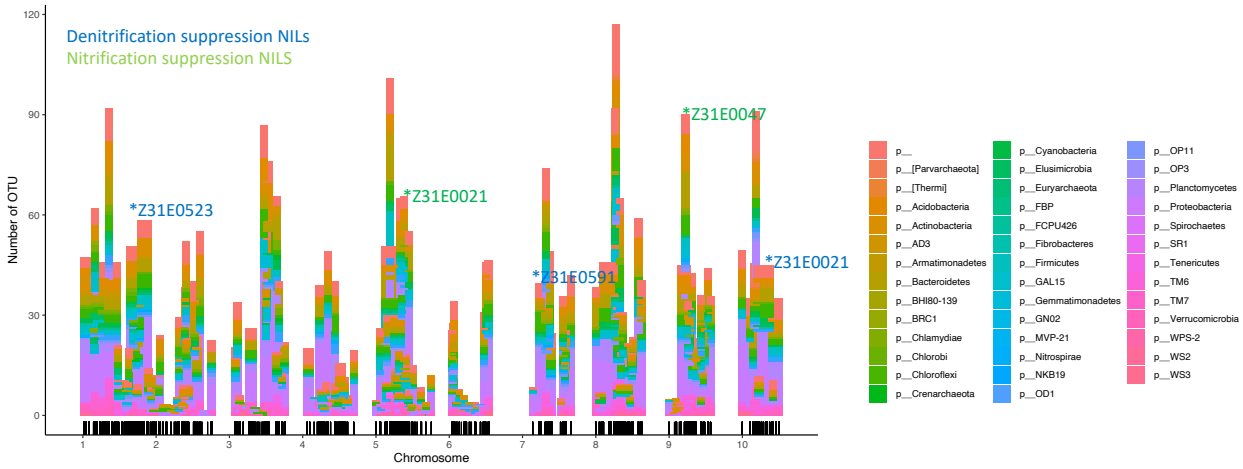

Figure 5.2 Prokaryotic OTUs were mapped to the maize genome. The x-axis displays the genetic map markers used in the study, while the Y axis includes number of OTUs significantly correlated to the introgression identified by Fast-exQTL. Significant OTUs are colored by phylum level identify to highlight the taxonomic differences in mapping. Significant NILs related to the suppression of potential nitrification and overall denitrification were overlayed on to map to highlight to show that these *functional* NILs influence the microbiome.

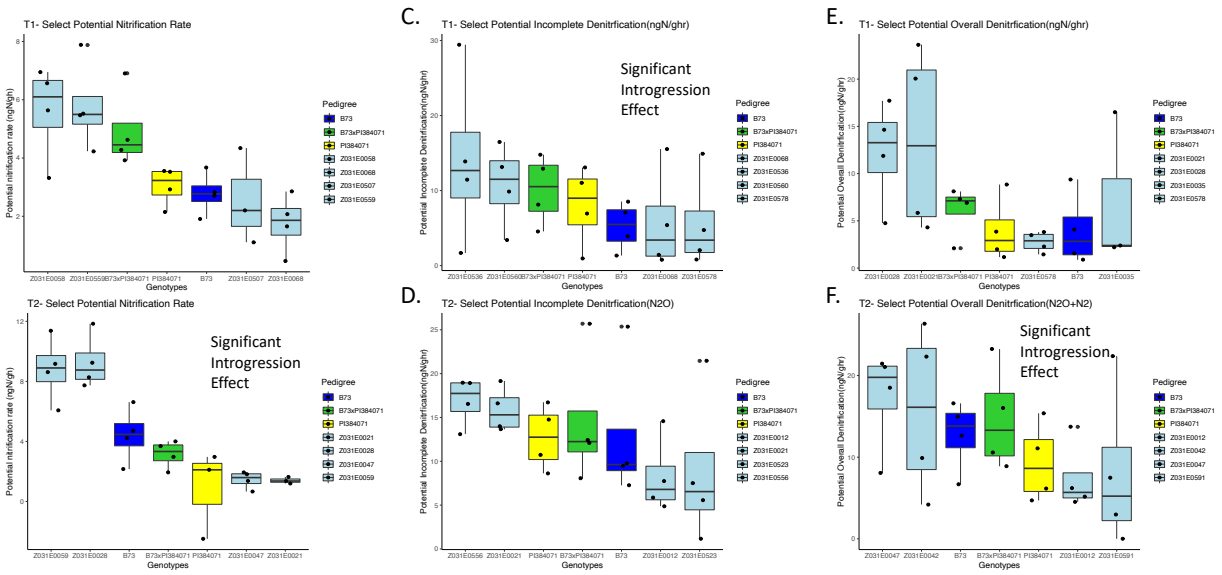

Figure 5.3 Potential nitrification, incomplete denitrification, and overall denitrification results across NILs. Potential N-cycling functions of the rhizosphere microbiome were compared among the B73 parent, teosinte parent, and F1 hybrid, along with 2 NILs each whose rhizosphere microbiome displayed the maximum and minimum N cycling rates across our different sampling timepoints. A) Potential nitrification rates in at timepoint 1. B) Potential nitrification rates at timepoint 2. C) Potential incomplete dentification rates at timepoint 1. D) Potential incomplete denitrification rates at timepoint 2. E) Potential overall dentification rates at timepoint 1. F) Potential overall denitrification rates at timepoint 2. Full set of potential N-cycling results is presented in supplemental material Figure D.2.

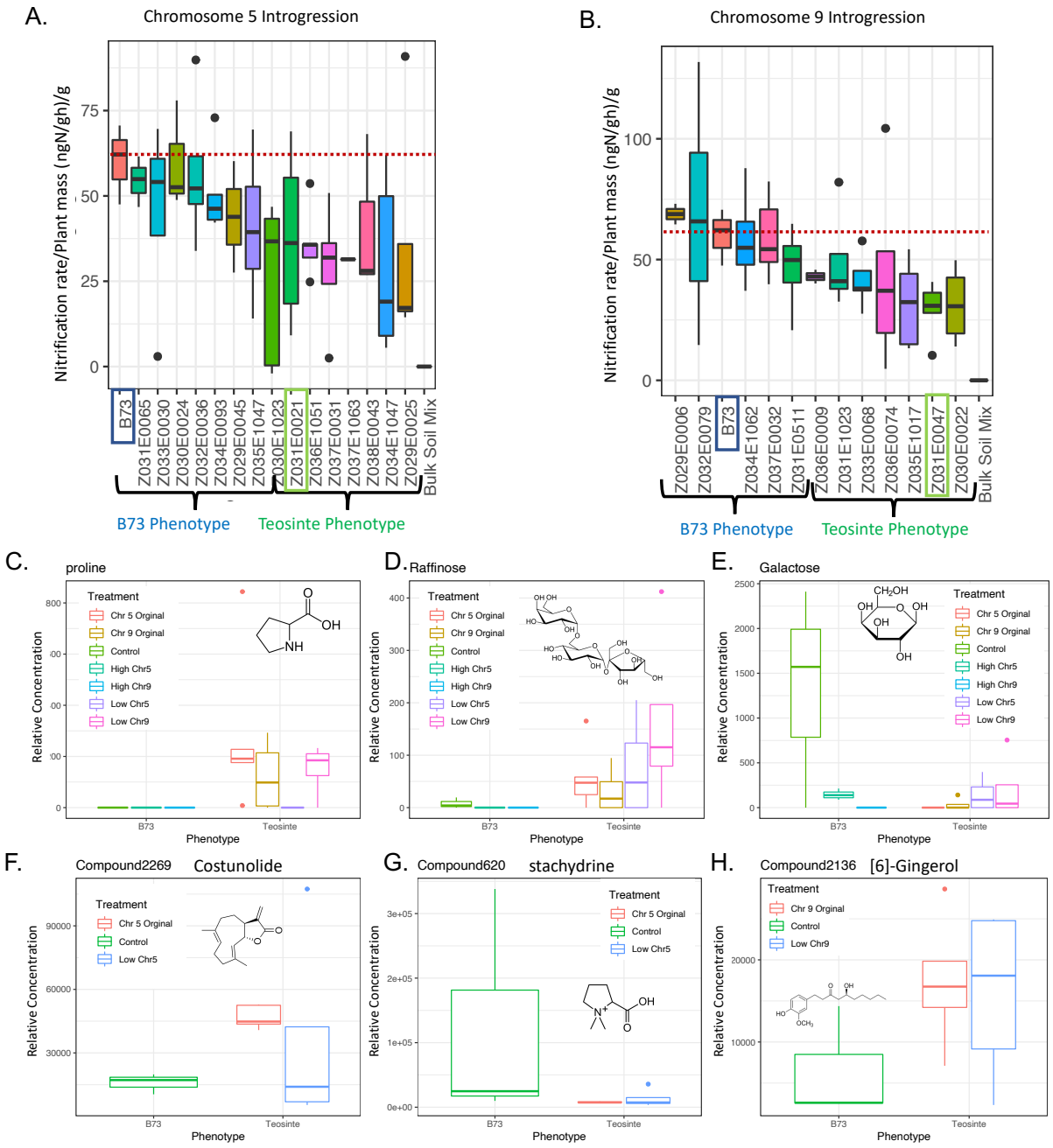

Figure 5.4 Potential mechanisms driving BNI suppression in NILs. A-B) BNI suppression in candidate NILs was confirmed in a greenhouse study and NILs with shared genetic regions also demonstrated suppression of nitrification activity. A) NILs with an introgression on chromosome 5. B) NILs with an introgression on chromosome 9. C-E) GC-MS metabolomic results collected from root tissue samples using the B73 (BNI -) and teosinte (BNI+) phenotypes highlighted in figure A-B. F-H) Classified LC-MS metabolome results present pair wise comparisons each individual chromosome introgression (BNI+) to B73 (BNI-). F-G) Show chromosome 5 differences compared to B73. H) Shows off these differences in chromosome 9. Full list of differentially enriched metabolites presents in Table D.8.

References:

Altschul, Stephen F, Thomas L Madden, Alejandro A Schäffer, Jinghui Zhang, Zheng Zhang, Webb Miller, and David J Lipman. 1997. "Gapped BLAST and PSI-BLAST: A New Generation of Protein Database Search Programs." *Nucleic Acids Research* 25 (17): 3389–3402.

Anderson, J. T., M. R. Wagner, C. A. Rushworth, K. V.S.K. Prasad, and T. Mitchell-Olds. 2014. "The Evolution of Quantitative Traits in Complex Environments." *Heredity* 112 (1): 4–12. https://doi.org/10.1038/hdy.2013.33.

Antwis, Rachael E., Sarah M. Griffiths, Xavier A. Harrison, Paz Aranega-Bou, Andres Arce, Aimee S. Bettridge, Francesca L. Brailsford, et al. 2017. "Fifty Important Research Questions in Microbial Ecology." *FEMS Microbiology Ecology* 93 (5): 1–10. https://doi.org/10.1093/femsec/fix044.

Bakker, Matthew G, Jacqueline M Chaparro, Daniel K Manter, and Jorge M Vivanco. 2015. "Impacts of Bulk Soil Microbial Community Structure on Rhizosphere Microbiomes of Zea Mays." *Plant and Soil* 392 (1–2): 115–26. https://doi.org/10.1007/s11104-015-2446-0.

Bardgett, Richard D., Tania C. Streeter, and Roland Bol. 2003. "Soil Microbes Compete Effectively with Plants for Organic-Nitrogen Inputs to Temperate Grasslands." *Ecology* 84 (5): 1277–87. https://doi.org/10.1890/0012-9658(2003)084[1277:SMCEWP]2.0.CO;2.

Bardon, Clément, Franck Poly, Florence Piola, Muriel Pancton, Gilles Comte, Guillaume Meiffren, and Feth el Zahar Haichar. 2016. "Mechanism of Biological Denitrification Inhibition: Procyanidins Induce an Allosteric Transition of the Membrane-Bound Nitrate Reductase through Membrane Alteration." *FEMS Microbiology Ecology* 92 (5): 1–11. https://doi.org/10.1093/femsec/fiw034.

Bedard, Charles, and Roger Knowles. 1989. "Physiology, Biochemistry, and Specific Inhibitors of CH4, NH4+, and CO Oxidation by Methanotrophs and Nitrifiers." *Microbiology* 53 (1): 68–84. http://apps.isiknowledge.com/full_record.do?product=UA&search_mode=GeneralSearch&qid=11&SID=X16536DGgEAkOn8a882&page=1&doc=1&colname=WOS.

Belheouane, Meriem, Yask Gupta, Sven Künzel, Saleh Ibrahim, and John F. Baines. 2017. "Improved Detection of Gene-Microbe Interactions in the Mouse Skin Microbiota Using High-Resolution QTL Mapping of 16S RRNA Transcripts." *Microbiome* 5 (1): 59. https://doi.org/10.1186/s40168-017-0275-5.

Berg, Gabriele, and Kornelia Smalla. 2009. "Plant Species and Soil Type Cooperatively Shape the Structure and Function of Microbial Communities in the Rhizosphere." https://doi.org/10.1111/j.1574-6941.2009.00654.x.

Bolan, N. S. 1991. "A Critical Review on the Role of Mycorrhizal Fungi in the Uptake of Phosphorus by Plants." *Plant and Soil*. https://doi.org/10.1007/BF00012037.

Borgogna, Joanna Lynn C., Michelle D. Shardell, Carl J. Yeoman, Khalil G. Ghanem, Herlin Kadriu, Alexander V. Ulanov, Charlotte A. Gaydos, et al. 2020. "The Association of Chlamydia Trachomatis and Mycoplasma Genitalium Infection with the Vaginal Metabolome." *Scientific Reports* 10 (1): 3420. https://doi.org/10.1038/s41598-020-60179-z.

Boudsocq, S., A. Niboyet, J. C. Lata, X. Raynaud, N. Loeuille, J. Mathieu, M. Blouin, L. Abbadie, and S. Barot. 2012. "Plant Preference for Ammonium versus Nitrate: A Neglected Determinant of Ecosystem Functioning?" *The American Naturalist* 180 (1): 60–69. https://doi.org/10.1086/665997.

Britto, Dev T., and Herbert J. Kronzucker. 2013. “Ecological Significance and Complexity of N-Source Preference in Plants.” *Annals of Botany* 112 (6): 957–63. https://doi.org/10.1093/aob/mct157.

Bulgarelli, Davide, Klaus Schlaeppi, Stijn Spaepen, Emiel Ver Loren Van Themaat, and Paul Schulze-Lefert. 2013. “Structure and Functions of the Bacterial Microbiota of Plants.” *Annual Review of Plant Biology*. https://doi.org/10.1146/annurev-arplant-050312-120106.

Butler, D G, B R Cullis, A R Gilmour, B J Gogel, and R Thompson. 2017. *ASReml-R Reference Manual Version 4*. *ASReml-R Reference Manual*.

Cantarel, Amlie A M, Thomas Pommier, Marie Desclos-Theveniau, Sylvain Diqu??lou, Maxime Dumont, Fabrice Grassein, Eva Maria Kastl, et al. 2015. “Using Plant Traits to Explain Plant-Microbe Relationships Involved in Nitrogen Acquisition.” *Ecology* 96 (3): 788–99. https://doi.org/10.1890/13-2107.1.sm.

Caporaso, J Gregory, Justin Kuczynski, Jesse Stombaugh, Kyle Bittinger, Frederic D Bushman, Elizabeth K Costello, Noah Fierer, et al. 2010. “QIIME Allows Analysis of High-Throughput Community Sequencing Data.” *Nature Methods* 7 (5): 335–36. https://doi.org/10.1038/nmeth.f.303.

Cassman, Kenneth G., Achim Dobermann, Daniel T. Walters, and Haishun Yang. 2003. “Meeting Cereal Demand While Protecting Natural Resources and Improving Environmental Quality.” *Annual Review of Environment and Resources* 28 (1): 315–58. https://doi.org/10.1146/annurev.energy.28.040202.122858.

Coskun, Devrim, Dev T Britto, Weiming Shi, and Herbert J Kronzucker. 2017a. “How Plant Root Exudates Shape the Nitrogen Cycle.” *Trends in Plant Science* 22 (8): 661–73. https://doi.org/10.1016/j.tplants.2017.05.004.

Coskun, Devrim, Dev T Britto, Weiming Shi, and Herbert J Kronzucker. 2017b. “Nitrogen Transformations in Modern Agriculture and the Role of Biological Nitrification Inhibition.” *Nature Plants*. https://doi.org/10.1038/nplants.2017.74.

DeSantis, T. Z., P Hugenholtz, N Larsen, M Rojas, E L Brodie, K Keller, T Huber, D Dalevi, P Hu, and G L Andersen. 2006. “Greengenes, a Chimera-Checked 16S RRNA Gene Database and Workbench Compatible with ARB.” *Applied and Environmental Microbiology* 72 (7): 5069–72. https://doi.org/10.1128/AEM.03006-05.

Edgar, Robert C. 2010. “Search and Clustering Orders of Magnitude Faster than BLAST.” *Bioinformatics* 26 (19): 2460–61. https://doi.org/10.1093/bioinformatics/btq461.

Edwards, Joseph, Cameron Johnson, Christian Santos-Medellín, Eugene Lurie, Natraj Kumar Podishetty, Srijak Bhatnagar, Jonathan A Eisen, and Venkatesan Sundaresan. 2014. “Structure, Variation, and Assembly of the Root-Associated Microbiomes of Rice.” *Proc Natl Acad Sci USA*. https://doi.org/10.1073/pnas.1414592112.

Elolimy, Ahmed, Abdulrahman Alharthi, Mohamed Zeineldin, Claudia Parys, Ariane Helmbrecht, and Juan J. Loor. 2019. “Supply of Methionine During Late-Pregnancy Alters Fecal Microbiota and Metabolome in Neonatal Dairy Calves Without Changes in Daily Feed Intake.” *Frontiers in Microbiology* 10 (September): 1–20. https://doi.org/10.3389/fmicb.2019.02159.

Falkowski, Paul G, Tom Fenchel, and Edward F Delong. 2008. “The Microbial Engines That Drive Earth ’s Biogeochemical Cycles.” *Science* 320 (5879): 1034–39. https://doi.org/10.1126/science.1153213.

Favela, Alonso, Martin O. Bohn, and Angela D. Kent. 2021. “Maize Germplasm Chronosequence Shows Crop Breeding History Impacts Recruitment of the Rhizosphere

Microbiome." *ISME Journal*. https://doi.org/10.1038/s41396-021-00923-z.
Ficker, C., M. L. Smith, K. Akpagana, M. Gbeassor, J. Zhang, T. Durst, R. Assabgui, and J. T. Arnason. 2003. "Bioassay-Guided Isolation and Identi?Cation of Antifungal Compounds from Ginger." *Phytotherapy Research* 17 (8): 897–902. https://doi.org/10.1002/ptr.1335.
Fish, Jordan A., Benli Chai, Qiong Wang, Yanni Sun, C. Titus Brown, James M. Tiedje, and James R. Cole. 2013. "FunGene: The Functional Gene Pipeline and Repository." *Frontiers in Microbiology* 4 (OCT): 1–14. https://doi.org/10.3389/fmicb.2013.00291.
Fitzpatrick, Connor R., Julia Copeland, Pauline W. Wang, David S. Guttman, Peter M. Kotanen, and Marc T.J. Johnson. 2018. "Assembly and Ecological Function of the Root Microbiome across Angiosperm Plant Species." *Proceedings of the National Academy of Sciences of the United States of America* 115 (6): E1157–65. https://doi.org/10.1073/pnas.1717617115.
Gallais, A. 1990. "Quantitative Genetics of Doubled Haploid Populations and Application to the Theory of Line Development." *Genetics* 124 (1): 199–206. https://www.ncbi.nlm.nih.gov/pmc/articles/PMC1203906/pdf/ge1241199.pdf.
Gloor, Gregory B., Jean M. Macklaim, Vera Pawlowsky-Glahn, and Juan J. Egozcue. 2017. "Microbiome Datasets Are Compositional: And This Is Not Optional." *Frontiers in Microbiology* 8 (NOV): 1–6. https://doi.org/10.3389/fmicb.2017.02224.
Goodrich, Julia K., Emily R. Davenport, Michelle Beaumont, Matthew A. Jackson, Rob Knight, Carole Ober, Tim D. Spector, Jordana T. Bell, Andrew G. Clark, and Ruth E. Ley. 2016. "Genetic Determinants of the Gut Microbiome in UK Twins." *Cell Host and Microbe* 19 (5): 731–43. https://doi.org/10.1016/j.chom.2016.04.017.
Gordon, A, G J Hannon, and Gordon. 2014. "FASTX-Toolkit." *[Online] Http://Hannonlab. Cshl. Edu/Fastx_ Toolkit Http://Hannonlab. Cshl. Edu/Fastx_ Toolkit*.
Graham, Emily B., Joseph E. Knelman, Andreas Schindlbacher, Steven Siciliano, Marc Breulmann, Anthony Yannarell, J. M. Beman, et al. 2016. "Microbes as Engines of Ecosystem Function: When Does Community Structure Enhance Predictions of Ecosystem Processes?" *Frontiers in Microbiology* 7 (February): 1–11. https://doi.org/10.3389/fmicb.2016.00214.
Graham, Geoffrey I., David W. Wolff, and Charles W. Stuber. 1997. "Characterization of a Yield Quantitative Trait Locus on Chromosome Five of Maize by Fine Mapping." *Crop Science* 37 (5): 1601–10. https://doi.org/10.2135/cropsci1997.0011183X003700050033x.
Heerwaarden, J. van, J. Doebley, W. H. Briggs, J. C. Glaubitz, M. M. Goodman, J. de Jesus Sanchez Gonzalez, and J. Ross-Ibarra. 2011. "Genetic Signals of Origin, Spread, and Introgression in a Large Sample of Maize Landraces." *Proceedings of the National Academy of Sciences* 108 (3): 1088–92. https://doi.org/10.1073/pnas.1013011108.
Horton, Matthew W, Natacha Bodenhausen, Kathleen Beilsmith, Dazhe Meng, Brian D Muegge, Sathish Subramanian, M Madlen Vetter, et al. 2014. "Genome-Wide Association Study of Arabidopsis Thaliana Leaf Microbial Community." *Nature Communications* 5 (May): 1–7. https://doi.org/10.1038/ncomms6320.
INGESTAD, TORSTEN. 1997. "Maximum Efficiency of Nitrogen Fertilizers." *Ambio*. http://www.jstor.org/stable/pdf/4312265.pdf.
Ishii, Satoshi, Gaku Kitamura, Takahiro Segawa, Ayano Kobayashi, Takayuki Miura, Daisuke Sano, and Satoshi Okabe. 2014. "Microfluidic Quantitative PCR for Simultaneous Quantification of Multiple Viruses in Environmental Water Samples." *Applied and Environmental Microbiology* 80 (24): 7505–11. https://doi.org/10.1128/AEM.02578-14.

Jones, Peter G., and Philip K. Thornton. 2003. “The Potential Impacts of Climate Change on Maize Production in Africa and Latin America in 2055.” *Global Environmental Change*. https://doi.org/10.1016/S0959-3780(02)00090-0.

Korenblum, Elisa, Yonghui Dong, Jedrzej Szymanski, Sayantan Panda, Adam Jozwiak, Hassan Massalha, Sagit Meir, Ilana Rogachev, and Asaph Aharoni. 2020. “Rhizosphere Microbiome Mediates Systemic Root Metabolite Exudation by Root - to - Root Signaling.” *PNAS*, 1–10. https://doi.org/10.1073/pnas.1912130117.

Kuypers, Marcel M.M., Hannah K. Marchant, and Boran Kartal. 2018. “The Microbial Nitrogen-Cycling Network.” *Nature Reviews Microbiology* 16 (5): 263–76. https://doi.org/10.1038/nrmicro.2018.9.

Kuzyakov, Yakov, and Xingliang Xu. 2013. “Competition between Roots and Microorganisms for Nitrogen: Mechanisms and Ecological Relevance.” *New Phytologist*. https://doi.org/10.1111/nph.12235.

Lambers, Hans, Christophe Mougel, Benoît Jaillard, and Philippe Hinsinger. 2009. “Plant-Microbe-Soil Interactions in the Rhizosphere: An Evolutionary Perspective.” *Plant and Soil*. https://doi.org/10.1007/s11104-009-0042-x.

Langfelder, Peter, and Steve Horvath. 2008. “WGCNA: An R Package for Weighted Correlation Network Analysis.” *BMC Bioinformatics* 9 (559): 1–13. https://doi.org/10.1186/1471-2105-9-559.

Langlade, Nicolas B, Xianzhong Feng, Tracy Dransfield, Lucy Copsey, Andrew I Hanna, C. Thebaud, Andrew Bangham, Andrew Hudson, and Enrico Coen. 2005. “Evolution through Genetically Controlled Allometry Space.” *Proceedings of the National Academy of Sciences* 102 (29): 10221–26. https://doi.org/10.1073/pnas.0504210102.

Liu, Zhengbin, Jason Cook, Susan Melia-Hancock, Katherine Guill, Christopher Bottoms, Arturo Garcia, Oliver Ott, et al. 2016. “Expanding Maize Genetic Resources with Predomestication Alleles: Maize–Teosinte Introgression Populations.” *The Plant Genome* 9 (1): 0. https://doi.org/10.3835/plantgenome2015.07.0053.

Liu, Zhengbin, Arturo Garcia, Michael D. McMullen, and Sherry A Flint-Garcia. 2016. “Genetic Analysis of Kernel Traits in Maize-Teosinte Introgression Populations.” *G3: Genes, Genomes, Genetics* 6 (8): 2523–30. https://doi.org/10.1534/g3.116.030155.

Lobell, David B, Wolfram Schlenker, and Justin Costa-Roberts. 2011. “Climate Trends and Global Crop Production since 1980.” *Science (New York, N.Y.)* 333 (6042): 616–20. https://doi.org/10.1126/science.1204531.

Long, Sharon R. 1989. “Rhizobium-Legume Nodulation: Life Together in the Underground.” *Cell*. https://doi.org/10.1016/0092-8674(89)90893-3.

Love, Michael I, Wolfgang Huber, and Simon Anders. 2014. “Moderated Estimation of Fold Change and Dispersion for RNA-Seq Data with DESeq2.” *Genome Biology* 15 (12). https://doi.org/10.1186/s13059-014-0550-8.

Lundberg, Derek S., Sarah L. Lebeis, Sur Herrera Paredes, Scott Yourstone, Jase Gehring, Stephanie Malfatti, Julien Tremblay, et al. 2012. “Defining the Core Arabidopsis Thaliana Root Microbiome.” *Nature* 488 (7409): 86–90. https://doi.org/10.1038/nature11237.

Lynch, Joshua, Karen Tang, Sambhawa Priya, Joanna Sands, Margaret Sands, Evan Tang, Sayan Mukherjee, Dan Knights, and Ran Blekhman. 2017. “HOMINID: A Framework for Identifying Associations between Host Genetic Variation and Microbiome Composition.” *GigaScience* 6 (12): 1–7. https://doi.org/10.1093/gigascience/gix107.

Mag, Tanja, and Steven L Salzberg. 2011. “FLASH: Fast Length Adjustment of Short Reads to Improve Genome Assemblies” 27 (21): 2957–63.

Marques, Joana M, Thais F. da Silva, Renata E Vollu, Arie F Blank, Guo Chun Ding, Lucy Seldin, and Kornelia Smalla. 2014. “Plant Age and Genotype Affect the Bacterial Community Composition in the Tuber Rhizosphere of Field-Grown Sweet Potato Plants.” *FEMS Microbiology Ecology* 88 (2): 424–35. https://doi.org/10.1111/1574-6941.12313.

Matsuoka, Yoshihiro, Yves Vigouroux, Major M Goodman, Jesus Sanchez G, Edward Buckler, and John Doebley. 2002. “A Single Domestication for Maize Shown by Multilocus Microsatellite Genotyping.” *Proceedings of the National Academy of Sciences of the United States of America* 99 (9): 6080–84. https://doi.org/10.1073/pnas.052125199.

McMurdie, Paul J., and Susan Holmes. 2013. “Phyloseq: An R Package for Reproducible Interactive Analysis and Graphics of Microbiome Census Data.” *PLoS ONE* 8 (4): e61217–e61217. https://doi.org/10.1371/journal.pone.0061217.

Mendes, Rodrigo, Paolina Garbeva, and Jos M Raaijmakers. 2013. “The Rhizosphere Microbiome: Significance of Plant Beneficial, Plant Pathogenic, and Human Pathogenic Microorganisms.” https://doi.org/10.1111/1574-6976.12028.

Moreau, Delphine, Barbara Pivato, David Bru, Hugues Busset, Florence Deau, Céline Faivre, Annick Matejicek, Florence Strbik, Laurent Philippot, and Christophe Mougel. 2015. “Plant Traits Related to Nitrogen Uptake Influence Plant- Microbe Competition.” *Ecology* 96 (8): 2300–2310. https://doi.org/10.1890/14-1761.1.

Oksanen, Jari, Roeland Kindt, Pierre Legendre, Bob O’hara, M Henry, and H Stevens Maintainer. 2007. “The Vegan Package Title Community Ecology Package.” Http://Cran.r-Project.Org/, Http://R-Forge.r-Project.Org/Projects/Vegan/. 2007. http://ftp.uni-bayreuth.de/math/statlib/R/CRAN/doc/packages/vegan.pdf.

Peiffer, J. A., A. Spor, O. Koren, Z. Jin, S. G. Tringe, J. L. Dangl, E. S. Buckler, and R. E. Ley. 2013. “Diversity and Heritability of the Maize Rhizosphere Microbiome under Field Conditions.” *Proceedings of the National Academy of Sciences* 110 (16): 6548–53. https://doi.org/10.1073/pnas.1302837110.

Peralta, Ariane L., Eric R. Johnston, Jeffrey W. Matthews, and Angela D. Kent. 2016. “Abiotic Correlates of Microbial Community Structure and Nitrogen Cycling Functions Vary within Wetlands.” *Freshwater Science* 35 (2): 573–88. https://doi.org/10.1086/685688.

Philippot, Laurent, Jos M Raaijmakers, Philippe Lemanceau, and Wim H. Van Der Putten. 2013. “Going Back to the Roots: The Microbial Ecology of the Rhizosphere.” *Nature Reviews Microbiology* 11 (11): 789–99. https://doi.org/10.1038/nrmicro3109.

Piperno, D. R., A. J. Ranere, I. Holst, J. Iriarte, and R. Dickau. 2009. “Starch Grain and Phytolith Evidence for Early Ninth Millennium B.P. Maize from the Central Balsas River Valley, Mexico.” *Proceedings of the National Academy of Sciences* 106 (13): 5019–24. https://doi.org/10.1073/pnas.0812525106.

Portwood, John L, Margaret R Woodhouse, Ethalinda K Cannon, Jack M Gardiner, Lisa C Harper, Mary L Schaeffer, Jesse R Walsh, et al. 2019. “Maizegdb 2018: The Maize Multi-Genome Genetics and Genomics Database.” *Nucleic Acids Research* 47 (D1): D1146–54. https://doi.org/10.1093/nar/gky1046.

Qiao, Qinghua, Furong Wang, Jingxia Zhang, Yu Chen, Chuanyun Zhang, Guodong Liu, Hui Zhang, Changle Ma, and Jun Zhang. 2017. “The Variation in the Rhizosphere Microbiome of Cotton with Soil Type, Genotype and Developmental Stage.” *Scientific Reports* 7 (1). https://doi.org/10.1038/s41598-017-04213-7.

Sasse, Joelle, Enrico Martinoia, and Trent Northen. 2018. “Feed Your Friends: Do Plant Exudates Shape the Root Microbiome?” *Trends in Plant Science* 23 (1): 25–41. https://doi.org/10.1016/j.tplants.2017.09.003.

Schimel, Joshua P., and Jay Gulledge. 1998. “Microbial Community Structure and Global Trace Gases.” *Global Change Biology* 4 (7): 745–58. https://doi.org/10.1046/j.1365-2486.1998.00195.x.

Schinner, F., R. Ohlinger, E. Kandeler, and R. Margesin. 1996. *Methods in Soil Biology*. Springer. http://library1.nida.ac.th/termpaper6/sd/2554/19755.pdf.

Schreiter, Susanne, Martin Sandmann, Kornelia Smalla, and Rita Grosch. 2014. “Soil Type Dependent Rhizosphere Competence and Biocontrol of Two Bacterial Inoculant Strains and Their Effects on the Rhizosphere Microbial Community of Field-Grown Lettuce.” *PLoS ONE* 9 (8). https://doi.org/10.1371/journal.pone.0103726.

Shabalin, Andrey A. 2012. “Matrix EQTL: Ultra Fast EQTL Analysis via Large Matrix Operations.” *Bioinformatics* 28 (10): 1353–58. https://doi.org/10.1093/bioinformatics/bts163.

Simić, Domagoj, Snezana Mladenović Drinić, Zvonimir Zdunić, Antun Jambrović, Tatjana Ledencan, Josip Brkić, Andrija Brkić, and Ivan Brkić. 2012. “Quantitative Trait Loci for Biofortification Traits in Maize Grain.” *The Journal of Heredity* 103 (1): 47–54. https://doi.org/10.1093/jhered/esr122.

Subbarao, G V, K L Sahrawat, K Nakahara, I M Rao, M Ishitani, C T Hash, M Kishii, D G Bonnett, W L Berry, and J C Lata. 2013. “A Paradigm Shift towards Low-Nitrifying Production Systems: The Role of Biological Nitrification Inhibition (BNI).” *Annals of Botany*. https://doi.org/10.1093/aob/mcs230.

Sylvia, David M., Jeffry J. Fuhrmann, Peter G. Hartel, David A. Zuberer, and Alison M. Cupples. 2005. *Principles and Applications of Soil Microbiology*. *Journal of Environment Quality*. Vol. 34. https://doi.org/10.2134/jeq2005.0731a.

Szalma, S. J., B. M. Hostert, J. R. LeDeaux, C. W. Stuber, and J. B. Holland. 2007. “QTL Mapping with Near-Isogenic Lines in Maize.” *Theoretical and Applied Genetics* 114 (7): 1211–28. https://doi.org/10.1007/s00122-007-0512-6.

Thenkabail, Prasad S., Munir A. Hanjra, Venkateswarlu Dheeravath, and Muralikrishna Gumma. 2010. “A Holistic View of Global Croplands and Their Water Use for Ensuring Global Food Security in the 21st Century through Advanced Remote Sensing and Non-Remote Sensing Approaches.” *Remote Sensing* 2 (1): 211–61. https://doi.org/10.3390/rs2010211.

Ulrich, Andreas, and Regina Becker. 2006. “Soil Parent Material Is a Key Determinant of the Bacterial Community Structure in Arable Soils.” *FEMS Microbiology Ecology* 56 (3): 430–43. https://doi.org/10.1111/j.1574-6941.2006.00085.x.

Vigdis Torsvik, Lise Øvreås. 2002. “Microbial Diversity and Function in Soil: From Genes to Ecosystems.” *Current Opinion in Microbiology* 5:240–245. https://ac.els-cdn.com/S1369527402003247/1-s2.0-S1369527402003247-main.pdf?_tid=cfe2f573-92db-4e97-a0c9-e1ec283ca71e&acdnat=1524029182_2920354489713a9dfdb6b9a15cfbccbf.

Wagner, Maggie R, Derek S Lundberg, Tijana G Del Rio, Susannah G Tringe, Jeffery L Dangl, and Thomas Mitchell-Olds. 2016. “Host Genotype and Age Shape the Leaf and Root Microbiomes of a Wild Perennial Plant.” *Nature Communications* 7. https://doi.org/10.1038/ncomms12151.

Wallace, Jason G., Karl A Kremling, and Edward S. Buckler. 2018. “Quantitative Genetic Analysis of the Maize Leaf Microbiome.” *BioRxiv*, 268532. https://doi.org/10.1101/268532.

Wickham, Hadley. 2007. “Ggplot2–Elegant Graphics for Data Analysis.” *Journal of Statistical Software* 99 (2): 260. https://doi.org/10.18637/jss.v077.b02.

Yeoh, Yun Kit, Paul G Dennis, Chanyarat Paungfoo-Lonhienne, Lui Weber, Richard Brackin, Mark A Ragan, Susanne Schmidt, and Philip Hugenholtz. 2017. “Evolutionary Conservation of a Core Root Microbiome across Plant Phyla along a Tropical Soil Chronosequence.” *Nature Communications* 8 (1): 215. https://doi.org/10.1038/s41467-017-00262-8.

Zak, D. R., P. M. Groffman, K. S. Pregitzer, S. Christensen, and J. M. Tiedje. 1990. “The Vernal Dam: Plant-Microbe Competition for Nitrogen in Northern Hardwood Forests.” *Ecology* 71 (2): 651–56. https://doi.org/10.2307/1940319.

Zhang, Huiming, Yan Sun, Xitao Xie, Mi Seong Kim, Scot E. Dowd, and Paul W. Paré. 2009. “A Soil Bacterium Regulates Plant Acquisition of Iron via Deficiency-Inducible Mechanisms.” *Plant Journal* 58 (4): 568–77. https://doi.org/10.1111/j.1365-313X.2009.03803.x.

Zhang, Yushan, Lijun Luo, Caiguo Xu, Qifa Zhang, and Yongzhong Xing. 2006. “Quantitative Trait Loci for Panicle Size, Heading Date and Plant Height Co-Segregating in Trait-Performance Derived near-Isogenic Lines of Rice (Oryza Sativa).” *Theoretical and Applied Genetics* 113 (2): 361–68. https://doi.org/10.1007/s00122-006-0305-3.

CHAPTER 6: CONCLUSIONS

The rhizosphere is the interface between plant roots and soil where interactions among a myriad of microorganisms affect biogeochemical cycling, plant growth, and tolerance to stress (Philippot et al. 2013). At this interface, we and many others have shown that plant genetics plays a role in predicting which microorganisms can grow and thrive (Lundberg et al. 2012; Walters et al. 2018; Xu et al. 2018; Favela, Bohn, and Kent 2021). These differences in rhizosphere microbial diversity are important as biodiversity within the microbiome will drive ecosystem functions of soil, as different microorganisms carryout different activities (Delgado-Baquerizo and Eldridge 2019) To date, we have not incorporated our understanding of genotype-driven microbiome recruitment into modern agriculture. This lack of incorporation is likely because we do not understand what having a different rhizosphere microbiome means *functionally*.

This dissertation focuses on characterizing some of the nitrogen cycling functions associated with plant genotype modification to rhizosphere microbiome recruitment. We pointily selected maize as our model system as it is a staple food crop, has undergone extensive genetic selection, and is one of the most fertilized crops in modern agriculture. By combining our understanding of plant genetics and microbial ecology we were able to show that: 1) historic breeding has altered the genetics related to how maize interacts with N-cycling taxa of the rhizosphere, 2) teosinte, maize's wild progenitor, recruits a different more sustainable N-cycling rhizosphere microbiome compared to modern maize, 3) these genotype recruitment effects replicate in the field and are heritable, 4) different specific genetic loci are related to rhizosphere microbiome recruitment and N-cycling function, 5) the modern maize microbiome can be improved by the reincorporation of "wild" teosinte loci, 6) genetics can be used as a tool to

develop a mechanistic understanding of how plants assemble their rhizospheres. These insights will hopefully allow us to improve the sustainability of our agricultural systems. Moreover, this dissertation critically highlights how we have consequently and inadvertently disturbed maize's rhizosphere microbiome, while also providing solutions to improve it.

While this dissertation has addressed several questions, it has resulted in the advent of many more. Under our simplified model, plant genotypes contain genes/phenes that selectively filter the microbiome by ether leading to the enhancement or suppression of specific taxa (Fig. 6.1A). These selected taxa can be associated with particular ecosystem functions (e.g., nitrifiers to nitrification). Yet further research needs to be done to determine how the rhizosphere effects scale up to the ecosystem level and if this would considerably reduce N loss from the agroecosystem. Additionally, research needs to be done to understand the legacy effects of this rhizosphere microbiome selection (Fig. 6.1B) – does this plant extended phenotype of filtering soil microbiome have consequences to the next crop (potentially harming or benefiting it)? Will these microbial communities under plant filtering eventually adapt/escape selection over time or will they disappear from the soil (i.e., microbial erosion)? On the plant genetics side, we are interested in understanding what the key gene/phenes that we should be targeting to have our preferred microbiome. Further, do these microbial association traits come at a cost to yield? Finally, can we use a combination of different plant species (and genotypes) to generationally select soil microbiomes with sustainable ecosystem functions (Fig. 6.1C)? Addressing these questions will enable us to improve and manage the microbiome using plant rhizosphere selection from the genotype to the ecosystem level.

Furthermore, while we have only shown maize to have genetic variation contributing to altered microbiome recruitment – this ability has been documented in phylogenetic distant taxa

from monocots (Bouffaud et al. 2016) and dicots (Xu et al. 2018; Lundberg et al. 2012). This leads me to conclude the rhizosphere microbiome recruitment is a fundamental function of the root and likely plays many important roles we have just begun to characterize (Bulgarelli et al. 2013). Moreover, we know that secondary plant metabolites play a large role in controlling the microbiome (Canarini et al. 2019) and we know that evolution of plants is intimately tied to the development of novel secondary plant metabolite (Anderberg et al. 2003). Is the evolution of these secondary plant metabolites in part driven by microbiome interaction and would we see rhizosphere microbiomes to be predicted by broader evolutionary relatedness? Understanding how rhizosphere microbiomes have evolutionarily shaped plants could allow us to connect concepts from ecology, evolution, and ecosystem sciences.

Final remarks:

For now, my work has shown that selection on the maize genetics can cause changes in the N-cycling rhizosphere microbiome, there are many regions of the maize genome that have large contributions to microbiome recruitment, and that this interaction is mediated by specific loci related to plant phytochemistry. In maize, it seems like teosinte provides a reservoir of ecologically important traits related to niche construction (Odling-smee et al. 2013) in a *wild* setting and can be used to identify candidate genes related to complex microbiome phenotypes. Also, this work shows how genetics can be leveraged to understand the basis of the microbiome-associated ecosystem processes, further supporting the genes to ecosystems framework (Whitham et al. 2006).

Applied, this dissertation has the potential to tame microbial activities such as nitrification and denitrification which contribute to the disruption of the global N-cycle (Coskun

et al. 2017; Galloway et al. 2008) and provides an example of how we can find genetic variation associated with microbial recruitment. In theory, agronomists could pair management practices (Huffman et al. 2018) with known plant microbiome selection (i.e., organic system, a genotype that enriches microbial mineralization) to have the germplasm work with the agricultural environment. This type of coordination between plant rhizosphere metabolic selection and agricultural fertilizer management practices could allow us to optimize the agroecosystems in a manner previously inaccessible. Yet, improving agroecosystem sustainability will require an understanding of trade-offs involved in the selection of the rhizosphere microbiome. It is possible that managing soil microbiomes through plant interactions will come at a cost to yield and will be challenging due to the complexity of microbiomes. Foundational research is needed to understand the limitations and mechanisms by which plants drive changes in soil microbiomes. Furthermore, ideas parallel to these are viable in animal agriculture (Wallace et al. 2019); suggesting that the future of agricultural sustainability will incorporate an understanding of the microbiome.

Figure:

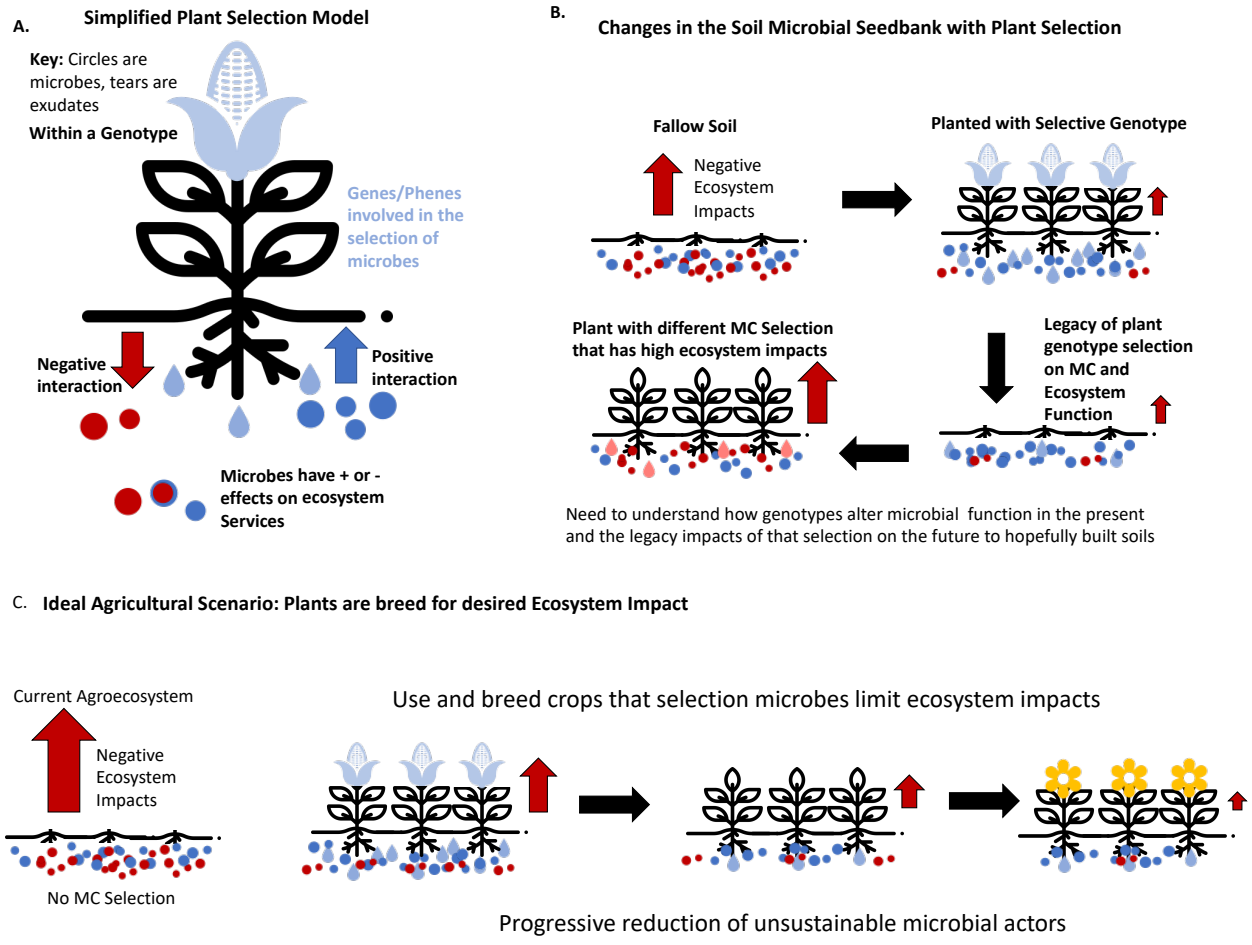

Figure 6.1 Conceptual diagram highlighting questions posed in the text. **A)** Shows the simplified model of plant selection. **B)** Shows the connection between plant microbiome selection and ecosystem processes **C)** Shows an idealized agricultural system where we know how genetic variation selects on soils and we intentionally grow lines to limit ecosystem actives.

References:

Anderberg, Arne A, Michael F Fay, Peter Goldblatt, Walter S Judd, Mari Källersjö, Jesper Kårehed, Kathleen A Kron, et al. 2003. "An Update of the Angiosperm Phylogeny Group Classification for the Orders and Families of Flowering Plants: APG II." *Botanical Journal of the Linnean Society*. Vol. 141. https://academic.oup.com/botlinnean/article-abstract/141/4/399/2433548.

Bouffaud, Marie Lara, Sebastien Renoud, Yvan Moenne-Loccoz, and Daniel Muller. 2016. "Is Plant Evolutionary History Impacting Recruitment of Diazotrophs and NifH Expression in the Rhizosphere?" *Scientific Reports* 6. https://doi.org/10.1038/srep21690.

Bulgarelli, Davide, Klaus Schlaeppi, Stijn Spaepen, Emiel Ver Loren Van Themaat, and Paul Schulze-Lefert. 2013. "Structure and Functions of the Bacterial Microbiota of Plants." *Annual Review of Plant Biology*. https://doi.org/10.1146/annurev-arplant-050312-120106.

Canarini, Alberto, Christina Kaiser, Andrew Merchant, Andreas Richter, and Wolfgang Wanek. 2019. "Root Exudation of Primary Metabolites: Mechanisms and Their Roles in Plant Responses to Environmental Stimuli." *Frontiers in Plant Science* 10 (February). https://doi.org/10.3389/fpls.2019.00157.

Coskun, Devrim, Dev T Britto, Weiming Shi, and Herbert J Kronzucker. 2017. "Nitrogen Transformations in Modern Agriculture and the Role of Biological Nitrification Inhibition." *Nature Plants*. https://doi.org/10.1038/nplants.2017.74.

Delgado-Baquerizo, Manuel, and David J Eldridge. 2019. "Cross-Biome Drivers of Soil Bacterial Alpha Diversity on a Worldwide Scale." *Ecosystems* 22 (6): 1220–31. https://doi.org/10.1007/s10021-018-0333-2.

Favela, Alonso, Martin O. Bohn, and Angela D. Kent. 2021. "Maize Germplasm Chronosequence Shows Crop Breeding History Impacts Recruitment of the Rhizosphere Microbiome." *ISME Journal*. https://doi.org/10.1038/s41396-021-00923-z.

Galloway, James N, Alan R Townsend, Jan Willem Erisman, Mateete Bekunda, Zucong Cai, John R Freney, Luiz A Martinelli, Sybil P Seitzinger, and Mark A Sutton. 2008. "Transformattion of the Nitrogen Cycle: Recent Trends, Questions, and Potential Solutions." *Science* 320: 889–92. http://science.sciencemag.org/content/sci/320/5878/889.full.pdf.

Huffman, Ryan D., Craig A. Abel, Linda M. Pollak, Walter Goldstein, Richard C. Pratt, Margaret E. Smith, Kevin Montgomery, Lois Grant, Jode W. Edwards, and M. Paul Scott. 2018. "Maize Cultivar Performance under Diverse Organic Production Systems." *Crop Science* 58 (1): 253–63. https://doi.org/10.2135/cropsci2017.06.0364.

John Wallace, R, Goor Sasson, Philip C Garnsworthy, Ilma Tapio, Emma Gregson, Paolo Bani, Pekka Huhtanen, et al. 2019. "A Heritable Subset of the Core Rumen Microbiome Dictates Dairy Cow Productivity and Emissions." *Science Advances* 5 (7): 8391–94. https://doi.org/10.1126/sciadv.aav8391.

Lundberg, Derek S, Sarah L Lebeis, Sur Herrera Paredes, Scott Yourstone, Jase Gehring, Stephanie Malfatti, Julien Tremblay, et al. 2012. "Defining the Core Arabidopsis Thaliana Root Microbiome." *Nature* 488 (7409): 86–90. https://doi.org/10.1038/nature11237.

Odling-smee, John, Douglas H Erwin, Eric P Palkovacs, and Marcus W Feldman. 2013. "Of Biology" 88 (1): 3–28.

Philippot, Laurent, Jos M Raaijmakers, Philippe Lemanceau, and Wim H. Van Der Putten. 2013. "Going Back to the Roots: The Microbial Ecology of the Rhizosphere." *Nature Reviews*

Microbiology 11 (11): 789–99. https://doi.org/10.1038/nrmicro3109.
Walters, William A, Zhao Jin, Nicholas Youngblut, Jason G Wallace, Jessica Sutter, Wei Zhang, Antonio González-Peña, et al. 2018. "Large-Scale Replicated Field Study of Maize Rhizosphere Identifies Heritable Microbes." *Proceedings of the National Academy of Sciences of the United States of America* 115 (28): 7368–73. https://doi.org/10.1073/pnas.1800918115.
Whitham, Thomas G., Joseph K. Bailey, Jennifer A. Schweitzer, Stephen M. Shuster, Randy K. Bangert, Carri J. Leroy, Eric V. Lonsdorf, et al. 2006. "A Framework for Community and Ecosystem Genetics: From Genes to Ecosystems." *Nature Reviews Genetics*. https://doi.org/10.1038/nrg1877.
Xu, Jin, Yunzeng Zhang, Pengfan Zhang, Pankaj Trivedi, Nadia Riera, Yayu Wang, Xin Liu, et al. 2018. "The Structure and Function of the Global Citrus Rhizosphere Microbiome." *Nature Communications* 9 (1): 4894. https://doi.org/10.1038/s41467-018-07343-2.

APPENDIX A: SUPPLEMENTAL INFORMATION CHAPTER 2

Maize germplasm chronosequence shows crop breeding history impacts recruitment of the rhizosphere microbiome

Figures:

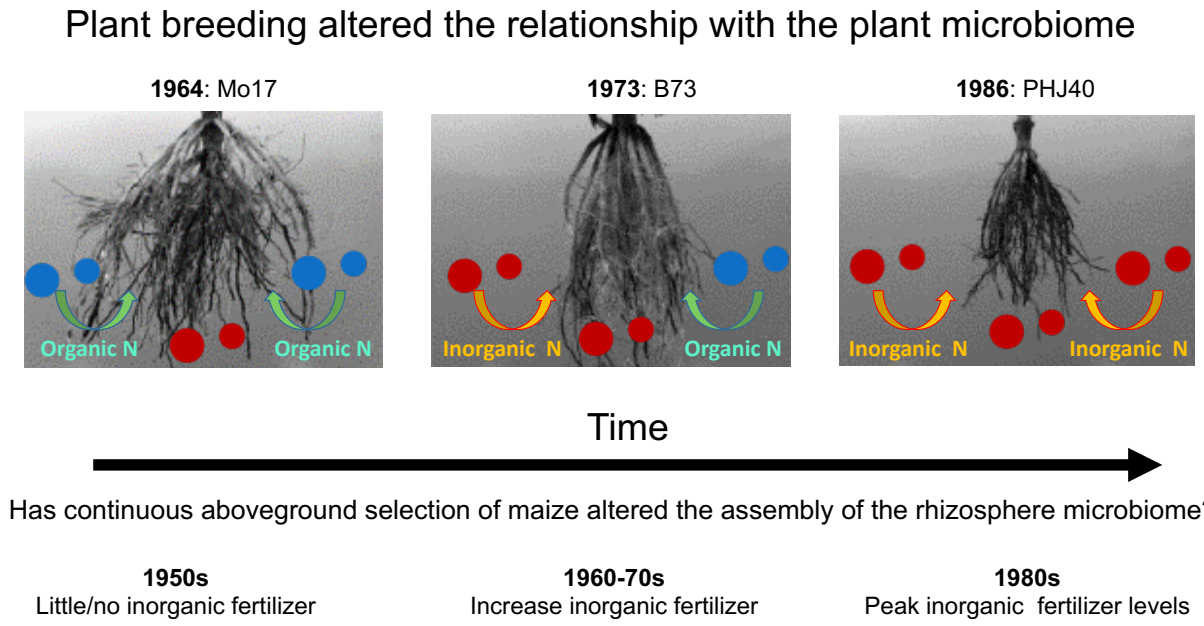

Figure A.1 Visual abstract highlighting the major conclusion of the research. Circles represent the microbial taxa present in the rhizosphere after microbial recruitment and arrows represent microbial-plant interaction with nutrient environment. The goal of the figure is to highlight the changing nutrient environment that maize has experienced across different agricultural breeding settings during the 21st century, and how this altered maize root systems and microbial interaction.

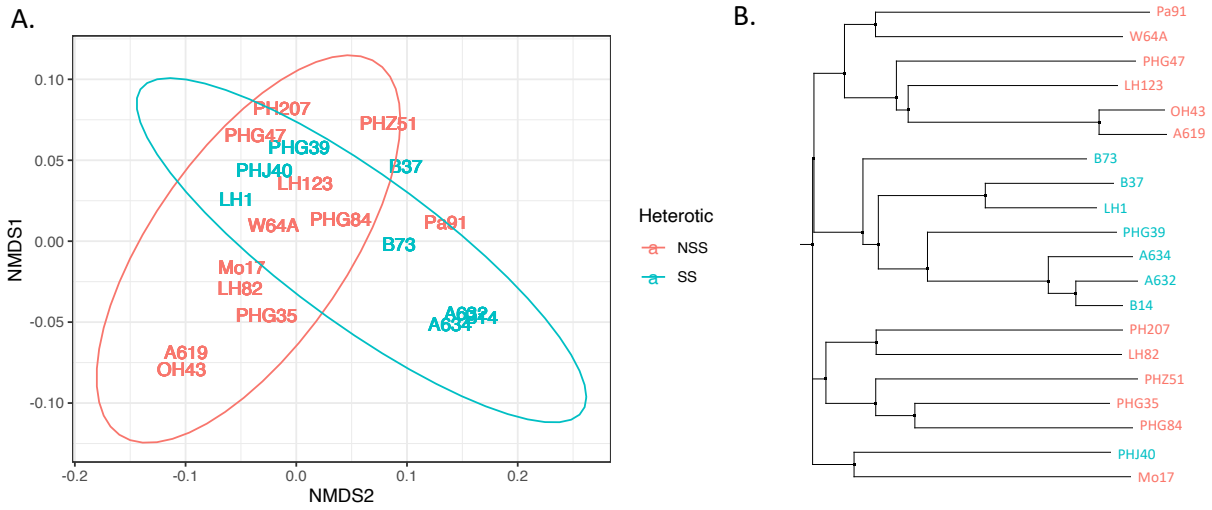

Figure A.2 Shows the relationship between the heterotic groups and genetic relatedness of the lines used in the study based on HapMap2 genetic information from Panzea (www.panzea.com). **A.** Non-metric multidimensional scaling (NMDS) ordination based on genetic distance data of the genotypes used in the study. NonStiffStalk lines are colored as red. StiffStalk lines are colored as blue. This figure validates the usage of heterotic group as a proxy for genetic relatedness. **B.** Dendrogram showing how maize lines mostly cluster by heterotic group. NonStiffStalk lines are colored as red. StiffStalk lines are colored as blue. PHJ40 and Mo17 are the only exception to the heterotic group clustering.

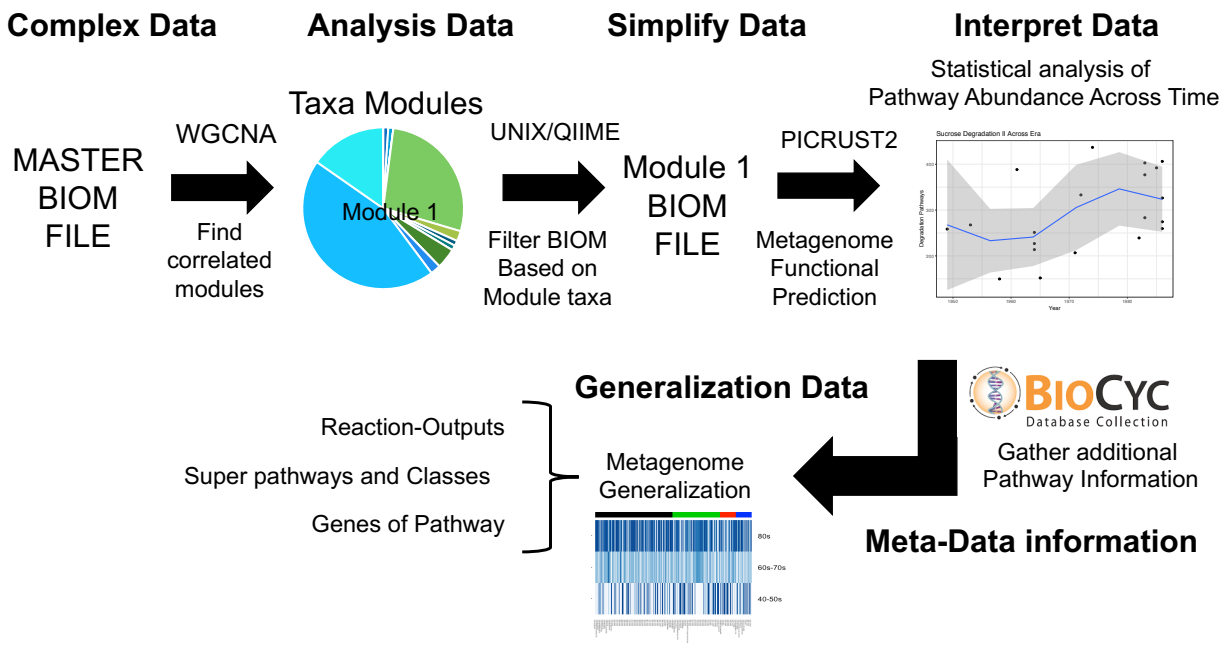

Figure A.3 Workflow for Module analysis using WGCNA and PICRUSt2. Microbial communities were first run through a weighted correlation network analysis (WGCNA) to determine taxa responding to our consequence. These OTUs were then subset into modules and run through PICRSt2 where we were able to determine the predicted genes for the responding OTUs. BioCyc database was used to obtain functional additional metadata on genes and pathways of interest. This additional BioCyc metadata allowed to classify pathways by nuance categories such as super pathways, pathway inputs/outputs, and genes involved in pathway.

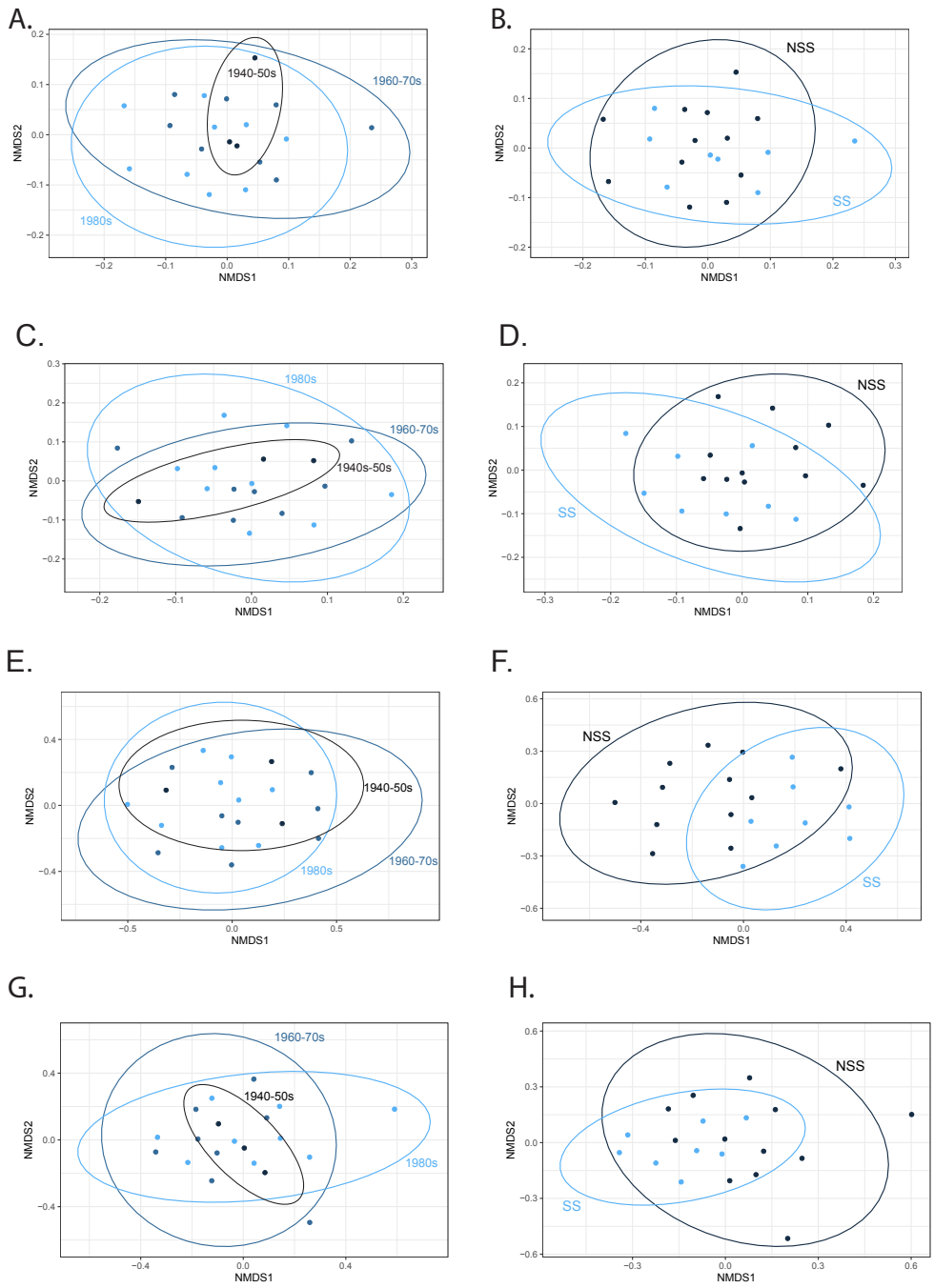

Figure A.4 Ordinations displaying sequence composition for genes related to nitrification. **A**. archaeal *amoA* gene composition across breeding decade. **B**. archaeal *amoA* gene composition by heterotic groups. **C**. Denitrification *nirK* gene composition by heterotic groups. **D**. Dentification *nirK* gene composition across heterotic groups. **E.** *nosZ* gene composition by breeding decade **F.** *nosZ* composition by heterotic group **G.** *norB* composition by breeding decade **H.** *norB* composition by heterotic group

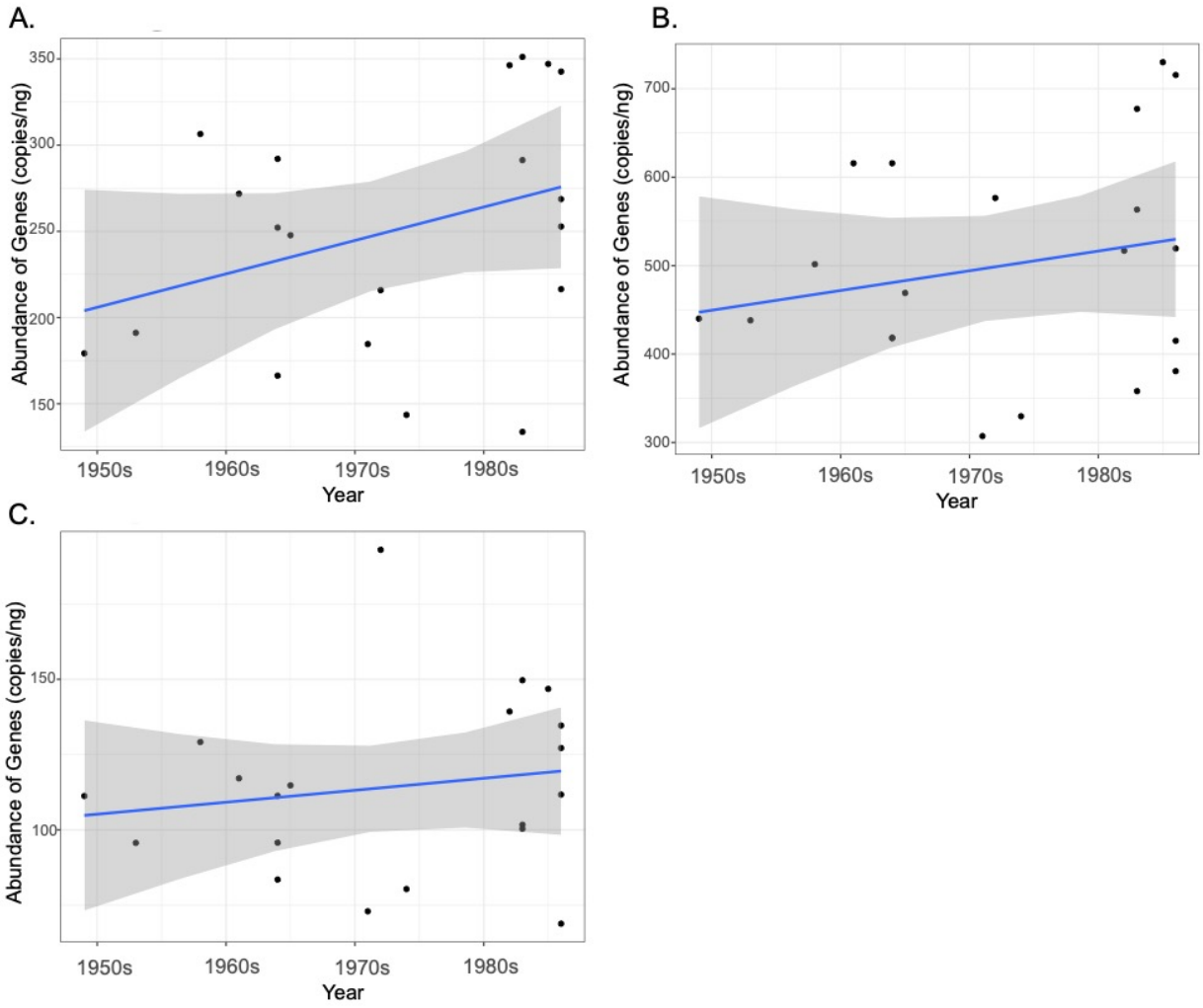

Figure A.5 Abundance of nitrogen cycling genes changes (determined by qPCR) across the germplasm chronosequence. **A**. Bacterial *amoA*. **B.** *nirK*. **C.** *nosZ*.

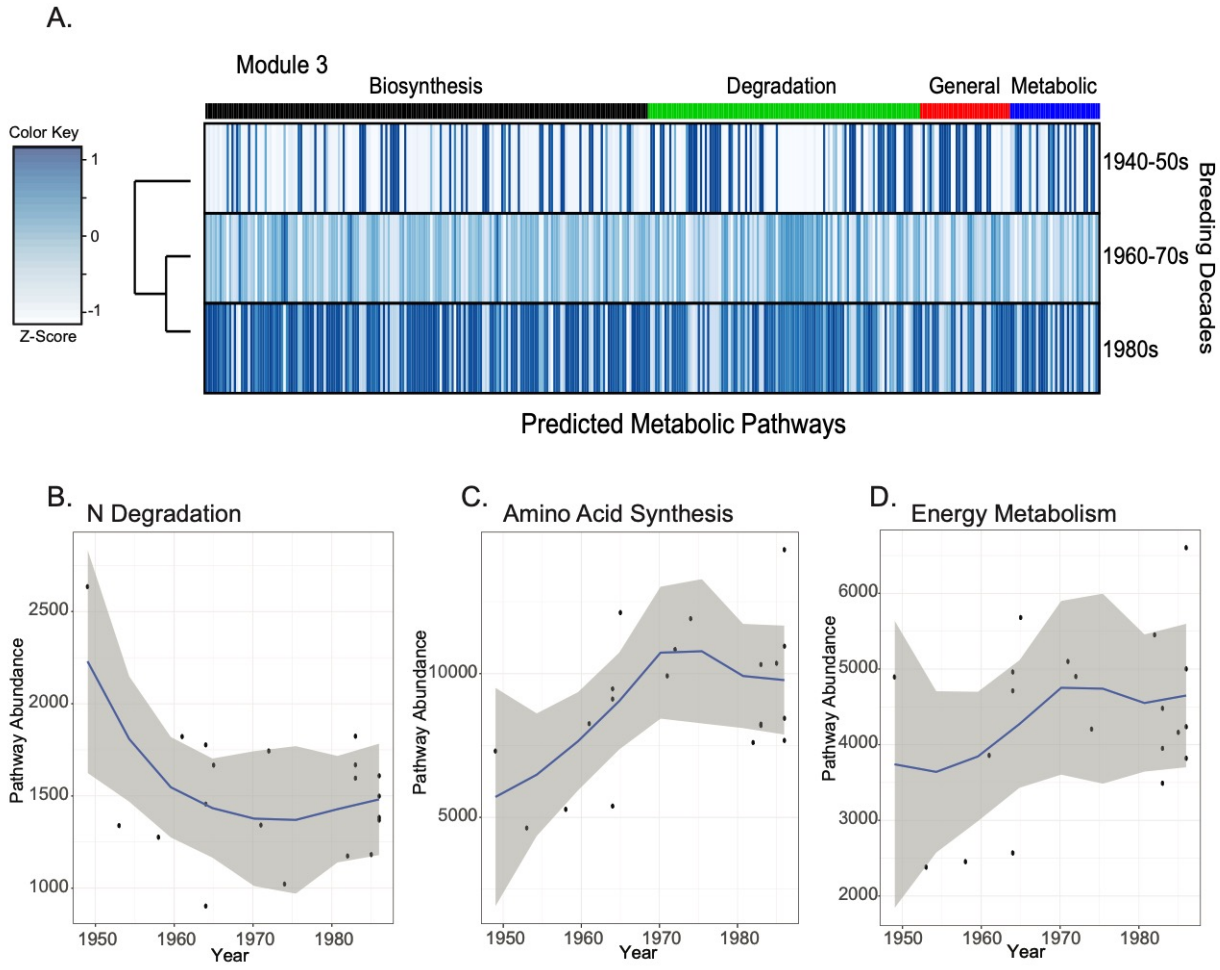

Figure A.6 Changes in predicted pathways across chronosequence. **A.** Heatmap displaying predicted pathway differences of Module 3 across the germplasm chronosequence. Decade of germplasm development is present on the right y-axis. Colors on the top x-axis indicate bins representing broad functional categories for each pathway. Dendrogram on the left y-axis represents the similarity of the treatment categories. Darker colors signify higher Z-score abundances of pathways. Z-scores are relative based on pathway abundance. Heatmaps for other modules present in supplemental information Fig A.6. **B**. Locally estimated scatter plot smoothing (LOESS) regression plot of the abundance for N degradation pathways over time. **C**. LOESS regression plot of the relative abundance of amino acid synthesis pathways over time. **D.** LOESS regression plot of the abundance of energy metabolism pathways across time.

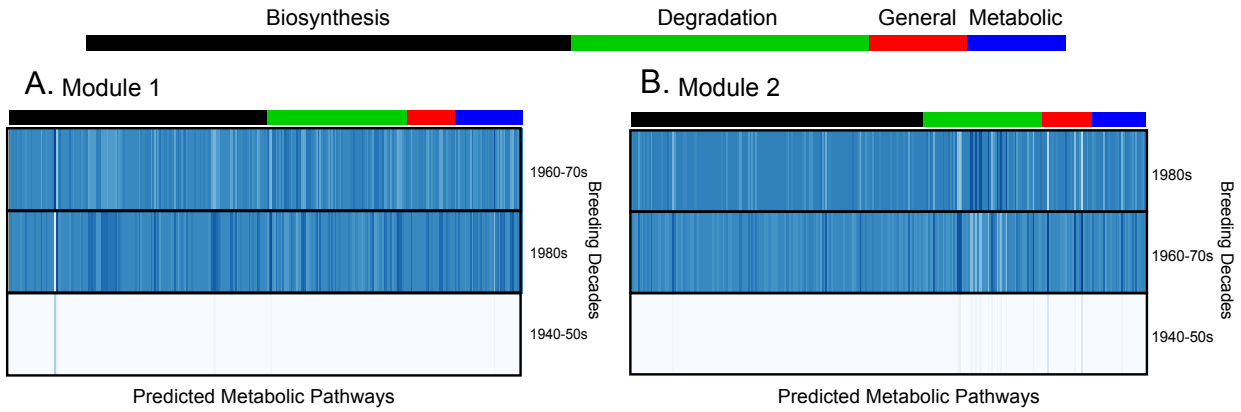

Figure A.7 Heatmap results displaying predicted pathway differences across the taxonomic modules: **A.** module 1, **B.** module 2. Decade of germplasm release is indicated on the right y-axis. Colors on the top x-axis represent the broader functional category that the pathway is part of. Dendrogram on the left y-axis represents the similarity of the treatment categories. Darker colors signify higher Z-score abundances of pathways. Z-scores are relative based on pathway abundance.

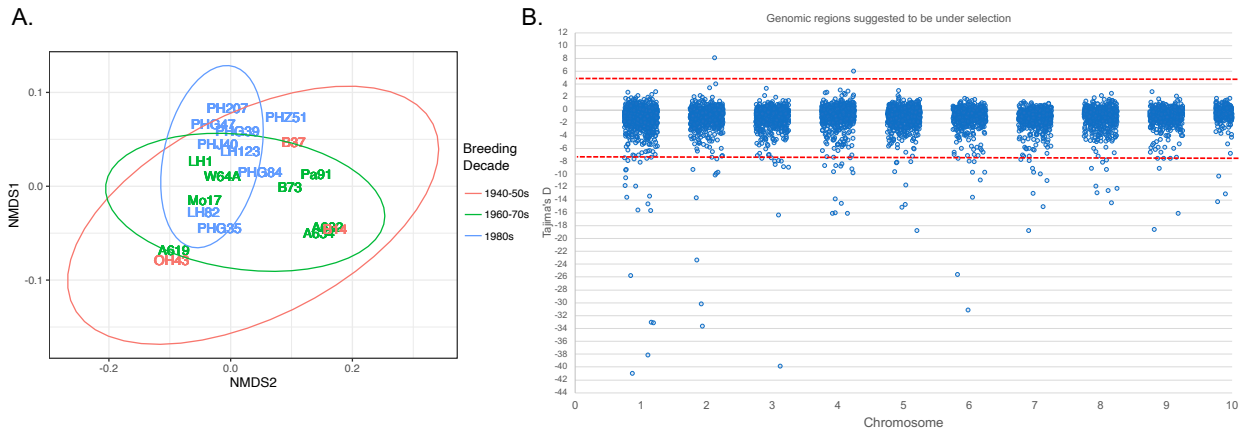

Figure A.8 Highlights the genomic changes that have occurred in these inbred lines over the chronosequence study. **A.** Non-metric multidimensional scaling (NMDS) ordination based on genetic distance data of the genotypes used in the study. Datapoint in this NMDS are the same as that in Fig A.7A. labeled with the breeding decade color. **B.** Shows the Tajima's D statistics across the HapMap of the lines included in this study. Tajima's D is a basic genetic test used to understand whether genetic regions are evolving under selection pressures or neutrally/randomly within a population. This analysis revealed that 85 genomic regions experienced selective sweeps within our population, 2 under balancing selection, and the majority evolving randomly. The dotted lines in this figure are threshold lines which are 3 standard deviations away from the mean. The dots outside of this threshold compromise the 87 regions under suggested selection.

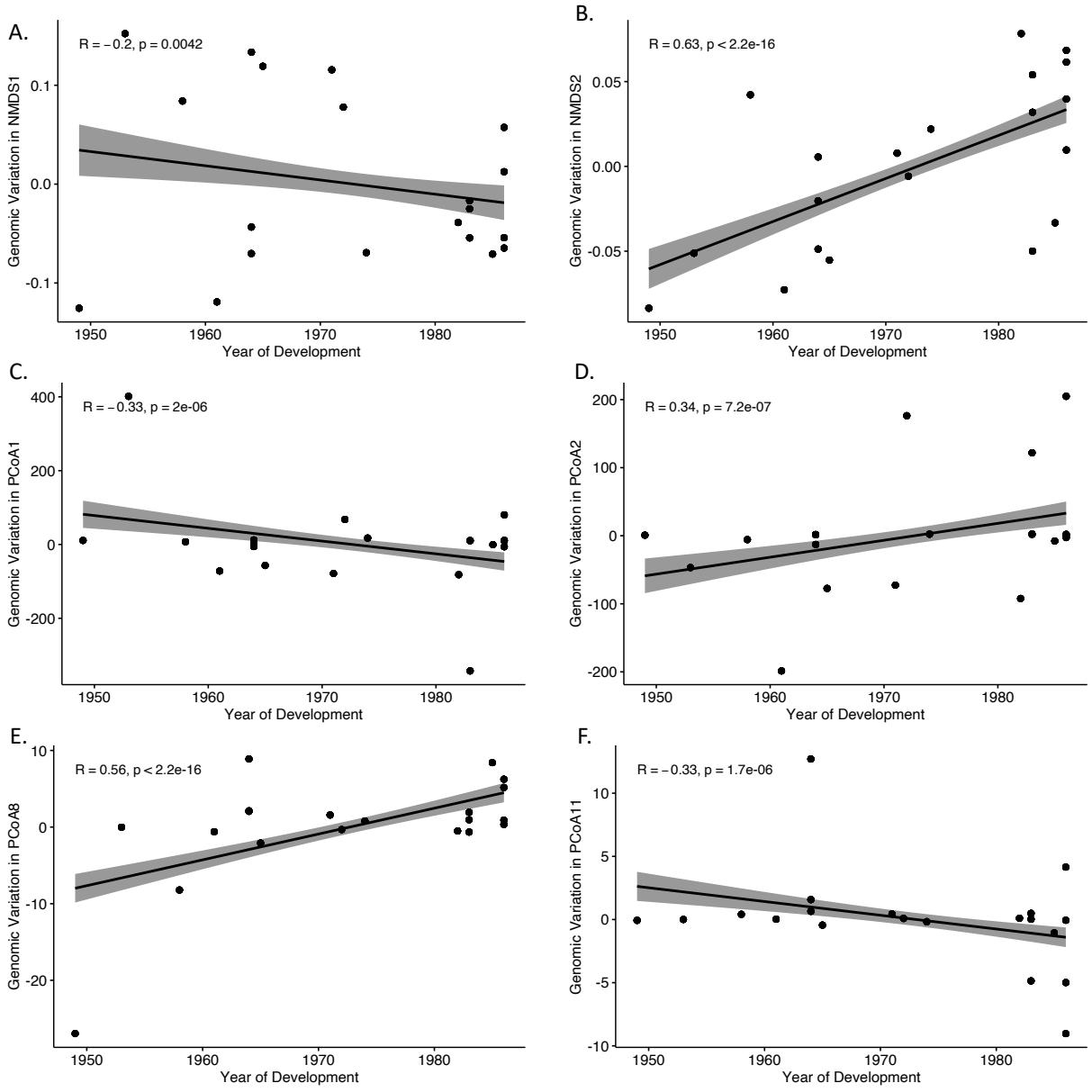

Figure A.9 These figures make it clear that a significant amount of genetic variation is associated with the germplasm chronosequence. **Panels A and B** show a regression between the NMDS axes in Fig B.8A and the year of germplasm development used in this study. Both figures show a significant amount of genomic variation is associated with the year of development. **A.** Highlights the regression between NMDS1 and year of development. **B.** Highlights the regression between NMDS2 and the year of development. These changes in genetic variation are likely what is driving microbiome patterns. **Panels C-F.** As NMDS dimensions are typically not used in regression analysis, we also ran a principal coordinates analysis (PCoA) to confirm our findings in A-B. The PCoA found 15 total axes in the HapMap genetic data. 10 of which were significantly correlated to with the year of development. Here we present the 4 significant correlations with the highest R values.

Tables:

Table A.1 Metadata of germplasm used in this study, sourced from the Mazie Genetic and Genomic Database (GDB).

Genotype	Heterotic group	Pedigree	Year	State	Decade
B14	StiffStalk	StiffStalkSyntheticC0	1953	Iowa	1940-50s
B37	StiffStalk	StiffStalkSyntheticC0	1958	Iowa	1940-50s
OH43	NonStiffStalk	Lancaster/Non-StiffStalk	1949	Iowa	1940-50s
A619	NonStiffStalk	Non-StiffStalk	1961	Minnesota	1960-70s
A632	StiffStalk	(Mt42 x B14)B14^3	1964	Minnesota	1960-70s
A634	StiffStalk	(Mt42 x B14)B14@B14^2	1965	Minnesota	1960-70s
B73	StiffStalk	StiffStalkSyntheticC5	1972	Iowa	1960-70s
LH1	StiffStalk	(B37 x 644) B37	1974	Iowa	1960-70s
Mo17	NonStiffStalk	Lancaster	1964	Missouri	1960-70s
Pa91	NonStiffStalk	Non-StiffStalk	1971	Pennsylvania	1960-70s
W64A	NonStiffStalk	Non-StiffStalk	1964	Wisconsin	1960-70s
LH123	NonStiffStalk	Broadbase	1983	Iowa	1980s
LH82	NonStiffStalk	Broadbase/Minnesota	1985	Iowa	1980s
PH207	NonStiffStalk	Iodent	1982	Iowa	1980s
PHG35	NonStiffStalk	Oh07-Midland/Iodent	1983	Iowa	1980s
PHG39	StiffStalk	Stiff Stalk C0/Maiz Amargo	1983	Iowa	1980s
PHG47	NonStiffStalk	Oh43/Broadbase	1986	Iowa	1980s
PHG84	NonStiffStalk	Oh07-Midland/Broadbase	1986	Iowa	1980s
PHJ40	StiffStalk	StiffStalkC0/Broadbase	1986	Iowa	1980s
PHZ51	NonStiffStalk	Lancaster/Broadbase	1986	Iowa	1980s

Table A.2 Primers used in amplicon sequencing and qPCR characterization of rhizosphere microbial community

Target	Encodes	Primer Name	Sequence	Reference
16S rRNA	Ribosomal RNA	515F	5'-GTGYCAGCMGCCGCGGTAA-3'	Fierer et al. 2011
16S rRNA	Ribosomal RNA	806R	5'-GGACTACVSGGGTATCTAAT-3'	Fierer et al. 2011
ITS	Internal Transcribed Spacer	ITS1F	5'-TTCGTAGGTGAACCTGCGG-3'	White et al. 1990
ITS	Internal Transcribed Spacer	ITS4R	5'-TCCTCCGCTTATTGATATGC-3'	White et al. 1990
nifH	Nitrogenase	PolF	5'-TGCGAYCCSAARGCBGACTC-3'	Poly et al. 2001
nifH	Nitrogenase	PolR	5'-ATSGCCATCATYTCRCCGGA-3'	Poly et al. 2001
bacterial *amoA*	Ammonia Monooxygenase	amoA-1F	5'-GGGGTTTCTACTGGTGGT-3'	Oakley et al. 2005
bacterial *amoA*	Ammonia Monooxygenase	amoA-2R	5'-CCCCTCKGSAAAGCCTTCTTC-3'	Oakley et al. 2005
archeal *amoA*	Ammonia Monooxygenase	CrenamoA23f	5'-ATGGTCTGGCTWAGACG-3'	Francis et al. 2005
archeal *amoA*	Ammonia Monooxygenase	CrenamoA616r	5'-GCCATCCATCTGTATGTCCA-3'	Francis et al. 2005
Typical *nosZ*	Nitrous oxide reductase	nosZ1F	5'-WCSYTGTTCMTCGACAGCCAG-3'	Henry et al. 2006
Typical *nosZ*	Nitrous oxide reductase	nosZ1R	5'-ATGTCGATCARCTGVKCRTTYTC-3'	Henry et al. 2006
nirK	Nitrite Reductase	nirK876	5'-ATYGGCGGVCAYGGCGA-3'	Henry et al. 2004
nirK	Nitrite Reductase	nirK1040	5'-GCCTCGATCAGRTTRTGGTT-3'	Henry et al. 2004
nirS	Nitrite Reductase	nirSCd3aF	5'-AACGYSAAGGARACSGG-3'	Kandeler et al. 2006
nirS	Nitrite Reductase	nirSR3cd	5'-GASTTCGGRTGSGTCTTSAYGAA-3'	Kandeler et al. 2006
norB	Nitric Oxide Reductase	cnorB2F	5'-GACAAGNNNTACTGGTGGT-3'	Braker et al. 2003
norB	Nitric Oxide Reductase	cnorB6R	5'-GAANCCCCANACNCCNGC-3'	Braker et al. 2003

Table A.3 Molecular sequencing raw reads generated from sequencing run, reads present after FASTX toolkit quality filter, and the rarefaction level of reads per sample for each gene used in this study.

Amplicon	Raw Reads	Quality Filtered Reads	Rarefaction Level
16S rRNA gene	45,616,533	39,079,559	34,000
fungal ITS	4,686,224	3,443,164	1,722
bacterial *amoA*	2,196,316	1,348,496	915
archaeal *amoA*	3,724,966	572,784	430
nifH	5,739,697	2,105,704	1353
nirK	13,544,866	4,972,273	999
nirS	3,375,608	1,102,622	165
nosZ	6,727,004	2,489,774	132
norB	2,317,818	560,953	100

Table A.4 Permutational multivariate ANOVA model results at the genotypic level for 16S rRNA genes, and Fungal ITS. Standard model was run on all amplicon sequence data. Bray-Curtis distance was used to calculate dissimilarity between microbiomes. 999 permutations were used in analysis. All factors in the model were run as fixed effect: ***Microbial Community Matrix = Decade of release + Heterotic Group + Residuals.*** This model was used to all other nitrogen cycling genes compositional changes.

Table A.4.1 16S rRNA: Genotypic means in PERMANOVA model

Terms	Df	SumsOfSqs	MeanSqs	F.Model	R^2	Pr(>F)	Sig
Decade	2	0.07246	0.036231	1.7886	0.16792	0.001	***
Heterotic	1	0.03496	0.034958	1.7257	0.08101	0.007	**
Residuals	16	0.3241	0.020257	0.75107			
Total	19	0.43152	1				

Signif. codes: 0 '***' 0.001 '**' 0.01 '*' 0.05 '.' 0.1 ' ' 1

Table A.4.2 Fungal ITS: Genotypic means in PERMANOVA model

Terms	Df	SumsOfSqs	MeanSqs	F.Model	R^2	Pr(>F)	Sig
Decade	2	0.20778	0.103889	1.047	0.1073	0.34	
Heterotic	1	0.14093	0.140935	1.4203	0.07278	0.028	*
Residuals	16	1.58763	0.099227	0.81991			
Total	19	1.93635	1				

Signif. codes: 0 '***' 0.001 '**' 0.01 '*' 0.05 '.' 0.1 ' ' 1

Table A.5 Functional genes that display significant patterns in composition and abundance across decades. Complete PERMANOVA and linear model outputs listed below. PERMANOVA Models: ***N-cycling Gene Matrix = Decade of release + Heterotic Group + Residuals.***

Process	Genes	Beta-Diversity Significance (p<0.05)	qPCR Abundance Significance in Relation to Time (p<0.05)
Nitrogen Fixation	*nifH*	Significant *	Significant *
Nitrification	Bacterial *amoA*	Significant *	Non-Significant
Nitrification	Archeal *amoA*	Non-Significant	Significant *
Denitrification	*nirK*	Non-Significant	Non-Significant
Denitrification	*nirS*	Near-Significant•	Non-Significant
Denitrification	*norB*	Non-Significant	Significant *
Denitrification	*nosZ*	Non-Significant	Non-Significant

Table A.6 Nitrogen cycling functional groups PERMANOVA result. Model: ***N-cycling Gene Matrix = Decade of release + Heterotic Group + Residuals.*** Includes *nifH,* Bacterial *amoA,* Archaeal *amoA, nirS, nirK, nosZ, norB.*

Table A.6.1 *nifH* gene: Genotypic Means PERMANOVA Model

Terms	Df	SumsOfSqs	MeanSqs	F.Model	R^2	Pr(>F)	Sig
Decade	2	0.07853	0.039263	1.7024	0.16123	0.001	***
Heterotic	1	0.03952	0.039515	1.7133	0.08113	0.003	**
Residuals	16	0.36902	0.023064	0.75764			
Total	19	0.48706	1				

Signif. codes: 0 '***' 0.001 '**' 0.01 '*' 0.05 '.' 0.1 ' ' 1

Table A.6.2 Bacterial *amoA* gene: Genotypic Means PERMANOVA Model

Terms	Df	SumsOfSqs	MeanSqs	F.Model	R^2	Pr(>F)	Sig
Decade	2	0.11113	0.055564	1.4361	0.1376	0.044	*
Heterotic	1	0.07745	0.077454	2.0019	0.0959	0.008	**
Residuals	16	0.61905	0.038691	0.7665			
Total	19	0.80763	1				

Signif. codes: 0 '***' 0.001 '**' 0.01 '*' 0.05 '.' 0.1 ' ' 1

Table A.6.3 Archaeal *amoA* gene: Genotypic Means PERMANOVA Model

Terms	Df	SumsOfSqs	MeanSqs	F.Model	R^2	Pr(>F)	Sig
Decade	2	0.020158	0.010079	0.77578	0.07965	0.755	
Heterotic	1	0.02505	0.02505	1.92813	0.09898	0.054	.
Residuals	16	0.207874	0.012992	0.82137			
Total	19	0.253082	1				

Signif. codes: 0 '***' 0.001 '**' 0.01 '*' 0.05 '.' 0.1 ' ' 1

Table A.6.4 *nirS* gene*:* Genotypic Means PERMANOVA Model

Terms	Df	SumsOfSqs	MeanSqs	F.Model	R^2	Pr(>F)	Sig
Decade	2	0.33868	0.16934	1.2166	0.12427	0.077	.
Heterotic	1	0.15965	0.15965	1.1469	0.05858	0.213	
Residuals	16	2.2271	0.13919	0.81716			
Total	19	2.72543	1				

Signif. codes: 0 '***' 0.001 '**' 0.01 '*' 0.05 '.' 0.1 ' ' 1

Table A.6.5 *nirK* gene: Genotypic Means PERMANOVA Model

Terms	Df	SumsOfSqs	MeanSqs	F.Model	R^2	Pr(>F)	Sig
Decade	2	0.4336	0.2168	1.0147	0.10599	0.365	
Heterotic	1	0.2387	0.23873	1.1173	0.05835	0.059	.
Residuals	16	3.4188	0.21367	0.83566			
Total	19	4.0911	1				

Signif. codes: 0 '***' 0.001 '**' 0.01 '*' 0.05 '.' 0.1 ' ' 1

Table A.6.6 *nosZ* gene: Genotypic Means PERMANOVA Model

Terms	Df	SumsOfSqs	MeanSqs	F.Model	R^2	Pr(>F)	Sig
Decade	2	0.5213	0.26066	0.93175	0.0975	0.841	
Heterotic	1	0.3497	0.34968	1.24996	0.0654	0.017	*
Residuals	16	4.4761	0.27975	0.83711			
Total	19	5.3471	1				

Signif. codes: 0 '***' 0.001 '**' 0.01 '*' 0.05 '.' 0.1 ' ' 1

Table A.6.7 *norB* gene: Genotypic Means PERMANOVA Model

Terms	Df	SumsOfSqs	MeanSqs	F.Model	R^2	Pr(>F)	Sig
Decade	2	0.6115	0.30577	1.0037	0.10355	0.445	
Heterotic	1	0.4202	0.42021	1.3794	0.07115	0.005	**
Residuals	16	4.8741	0.30463	0.8253			
Total	19	5.9059	1				

Signif. codes: 0 '***' 0.001 '**' 0.01 '*' 0.05 '.' 0.1 ' ' 1

Table A.7 Mixed effect models comparing qPCR of functional genes and year of germplasm release while corrected for the genetic relatedness between lines used in the study. Year of release was run as a fixed effect, genetic relatedness between lines was run as a random effect. Wald tests performed on statistical models to calculate significance. Statistical models were run in 'asreml-r'.

Table A.7.1 *nifH* gene:
asreml(fixed=*nifH qPCR*~1+Year, Random=vm(Genotype, inverseGmatrix)

Terms	Df	Sum of Sq	Wald Statistic	Pr(Chisq)	
(Intercept)	1	14097925	860.68	<2e-16	***
Year	1	66351	4.05	0.04415	*
residual (MS)		16380			

Signif. codes: 0 '***' 0.001 '**' 0.01 '*' 0.05 '.' 0.1 ' ' 1

Variance components of GMatrix

	component	std.error	z.ratio	bound	%ch
vm(Genotype, InvGMatrix)	22757.97	10339.839	2.200998	P	0.2
units!R	16380.04	5723.233	2.862025	P	0

Table A.7.2 Bacterial *amoA* gene:
asreml(fixed=*BamoAqPCR*~1+Year, Random=vm(Genotype, inverseGmatrix)

Terms	Df	Sum of Sq	Wald Statistic	Pr(Chisq)	
(Intercept)	1	1548270	332.22	<2e-16	***
Year	1	10159	2.18	0.1398	
residual (MS)		4660			

Signif. codes: 0 '***' 0.001 '**' 0.01 '*' 0.05 '.' 0.1 ' ' 1

Variance components of GMatrix

	component	std.error	z.ratio	bound	%ch
vm(Genotype, InvGMatrix)	22757.97	10339.839	2.200998	P	0.2
units!R	16380.04	5723.233	2.862025	P	0

Table A.7.3 Archaeal *amoA* gene:
asreml(fixed=*ArchamoA qPCR*~1+Year, Random=vm(Genotype, inverseGmatrix)

Terms	Df	Sum of Sq	Wald Statistic	Pr(Chisq)	
(Intercept)	1	15789973	97.925	<2e-16	***
Year	1	714521	4.431	0.03529	*
residual (MS)		161245			

Signif. codes: 0 '***' 0.001 '**' 0.01 '*' 0.05 '.' 0.1 ' ' 1

Variance components of GMatrix

	component	std.error	z.ratio	bound	%ch
vm(Genotype, InvGMatrix)	204081.8	109931.36	1.856448	P	0.2
units!R	161244.8	55997.15	2.879517	P	0

Table A.7.4 Sum of archaeal and bacterial *amoA* genes:
asreml(fixed=*AamoA qPCR*+*BamoA qPCR*~1+Year, Random=vm(Genotype, inverseGmatrix)

Terms	Df	Sum of Sq	Wald Statistic	Pr(Chisq)	
(Intercept)	1	27023187	138.268	2.00E-16	***
Year	1	895278	4.581	0.03233	*
residual (MS)		195441			

Signif. codes: 0 '***' 0.001 '**' 0.01 '*' 0.05 '.' 0.1 ' ' 1

Variance components of GMatrix

	component	std.error	z.ratio	bound	%ch
vm(Genotype, InvGMatrix)	225302.6	143531.36	1.56971	P	0.2
units!R	195440.6	67901.14	2.878311	P	0

Table A.7.5 *nirK* gene:
asreml(fixed=*nirK qPCR*~1+Year, Random=vm(Genotype, inverseGmatrix)

Terms	Df	Sum of Sq	Wald Statistic	Pr(Chisq)	
(Intercept)	1	5796044	357.98	<2e-16	***
Year	1	12693	0.78	0.3759	
residual (MS)		16191			

Signif. codes: 0 '***' 0.001 '**' 0.01 '*' 0.05 '.' 0.1 ' ' 1

Variance components of GMatrix

	component	std.error	z.ratio	bound	%ch
vm(Genotype, InvGMatrix)	4915.47	17857.128	0.2752666	P	23.5
units!R	16191.05	5676.988	2.8520498	P	0

Table A.7.6 *nirS* gene:
Here asreml-r model did not converge so we used a general genotypic means in linear Model

Terms	Estimate	Std.	Error	t	value	Pr(>|t|)
(Intercept)	-198.9049	528.6676	-0.376	0.711		
qPCR vs Year	0.1135	0.268	0.424	0.677		

Signif. codes: 0 '***' 0.001 '**' 0.01 '*' 0.05 '.' 0.1 ' ' 1

Table A.7.7 *norB* gene:
asreml(fixed=*norB qPCR*~1+Year, Random=vm(Genotype, inverseGmatrix)

Terms	Df	Sum of Sq	Wald Statistic	Pr(Chisq)	
(Intercept)	1	883.96	46.404	9.62E-12	***
Year	1	87.37	4.586	0.03223	*
residual (MS)		19.05			

Signif. codes: 0 '***' 0.001 '**' 0.01 '*' 0.05 '.' 0.1 ' ' 1

Variance components of GMatrix

	component	std.error	z.ratio	bound	%ch
vm(Genotype, InvGMatrix)	10.45639	17.18785	0.6083591	P	19.3
units!R	19.04921	6.68549	2.8493364	P	0

Table A.7.8 *nosZ* gene:
asreml(fixed=*nosZ qPCR*~1+Year, Random=vm(Genotype, inverseGmatrix)

Terms	Df	Sum of Sq	Wald Statistic	Pr(Chisq)	
(Intercept)	1	6530366	6340.7	<2e-16	***
Year	1	154	0.1	0.6988	
residual (MS)		1030			

Signif. codes: 0 '***' 0.001 '**' 0.01 '*' 0.05 '.' 0.1 ' ' 1

Variance components of GMatrix

	component	std.error	z.ratio	bound	%ch
vm(Genotype, InvGMatrix)	142.2504	6049.3431	0.02351502	?	93.7
units!R	1029.9048	737.2589	1.39693766	P	0

Table A.7.9 Average of denitrification genes:
asreml(fixed=*nosZ+norB+nirK+nirS)/4*~1+Year, Random=vm(Genotype, inverseGmatrix)

Terms	Df	Sum of Sq	Wald Statistic	Pr(Chisq)	
(Intercept)	1	706604	410.01	<2e-16	***
Year	1	1178	0.68	0.4084	
residual (MS)		1723			

Signif. codes: 0 '***' 0.001 '**' 0.01 '*' 0.05 '.' 0.1 ' ' 1

Variance components of GMatrix

	component	std.error	z.ratio	bound	%ch
vm(Genotype, InvGMatrix)	967.5626	1614.2786	0.5993777	P	19.8
units!R	1723.3808	607.6169	2.836295	P	0

Table A.8 Statistically significant modules and all WGCNA Results. Supplemental table with full correlations between microbial modules is available for downloaded.

Module	**Trait**	**Cor**	**pval**	**Sig**
Module 3	Year	-0.2816814	5.33E-05	TRUE
Module 2	Year	0.1454025	0.03994247	TRUE
Module 1	Year	0.34856317	4.24E-07	TRUE

Table A.9 Dominant taxonomic classes present in modules identified from the WGCNA.

Module 1		Module 2		Module 3	
Class	Count	Class	Count	Class	Count
Betaproteobacteria	16	Subgroup 6	23	Alphaproteobacteria	58
Alphaproteobacteria	16	Sphingobacteriia	17	Betaproteobacteria	29
Opitutae	11	Alphaproteobacteria	13	Gammaproteobacteria	19
Sphingobacteriia	10	Betaproteobacteria	13	Sphingobacteriia	16
Cytophagia	14	Gammaproteobacteria	11	Clostridia	10
Fibrobacteria	1	Blastocatellia	10	Gemmatimonadetes	7
Deltaproteobacteria	7	Gemmatimonadetes	9	Actinobacteria	5
Solibacteres	1	Holophagae	8	Deltaproteobacteria	4
Gammaproteobacteria	5	Nitrospira	6	Negativicutes	4
Melainabacteria	2	Deltaproteobacteria	5	Cytophagia	3
Flavobacteriia	3	S0134 terrestrial group	4	Verrucomicrobiae	3
Chlorobia	2	Cytophagia	3	Bacteroidia	2
Gemmatimonadetes	4	OPB35 soil group	2	Nitrospira	2
OPB35 soil group	3	Subgroup 5	2	Flavobacteriia	2
Verrucomicrobiae	1	Phycisphaerae	2	Holophagae	2
vadinHA49	2	Solibacteres	2	Subgroup 6	2
		Verrucomicrobiae	2	Fimbriimonadia	1
		Spartobacteria	1	Longimicrobia	1
		Subgroup 17	1	Planctomycetacia	1
		Anaerolineae	1	Opitutae	1
		Longimicrobia	1	Fibrobacteria	1
		OM190	1	WCHB1-32	1
		Subgroup 11	1	Proteobacteria	1
		Planctomycetacia	1	Acidimicrobiia	1
		uncultured bacterium	1	OPB35 soil group	1

Additional Date Tables: Appendix A Tables A.10-A.12.6.xlsx

Table A.10 Displays the list of pathways predicted for each of the taxonomic modules from PICRUSt2 analysis. Additional meta-information of the pathways is present in supplemental excel tables. Pathway names are in MetaCyc formatting. Supplemental excel table available for download.

Table A.11 Number of pathways significantly different pathways across decade of germplasm development from SIMPER comparison. Table A.14 contains full pathway names. Supplemental excel table available for download.

Table A.12 SIMPER results displaying pathways that are significantly different across the germplasm chronosequence. The mean differences values signify the differences in predicted gene abundance in pathway between the decades of comparisons. All pathways listed were shown to be statistically significant ($p<0.05$), pathways are organized by the degree of mean difference between the groups. Supplemental excel table available for download.

Table A.12.1 Results from Module 1 comparison between germplasm developed in the 1940-50s to the 1960-70s.

Table A.12.2 Results from Module 1 comparison between germplasm developed in the 1940-50s to the 1980s.

Table A.12.3 Results of Module 2 comparison between germplasm developed in the 1940-50s to the 1960-70s.

Table A.12.4 Results of Module 2 comparison between germplasm developed in the 40-50s to the 80s.

Table A.12.5 Results of Module 3 comparison between germplasm developed in the 1940-50s to the 1960-70s.

Table A.12.6 Results of Module 3 comparison between germplasm developed in the 1940-50s to the 1980s.

APPENDIX B: SUPPLEMENTAL INFORMATION CHAPTER 3

Differences in N-cycling microbiome recruitment between inbred and wild *Zea mays.*

Figure:

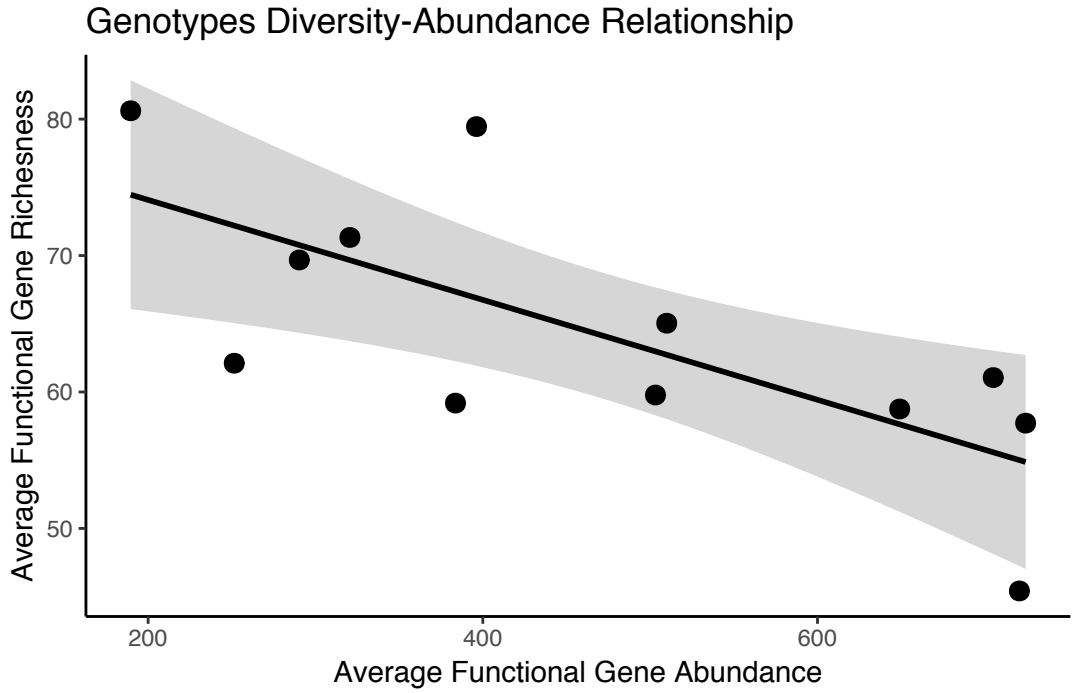

Figure B.1 Relationship between genotypic-mean of functional gene richness and functional gene abundance. Averaged across all functional genes included in this study.

Tables:

Table B.1 Germplasm used in this study.

Genotypes	Type	Group
A632	Modern	Inbred
B73	Modern	Inbred
LH82	Modern	Inbred
Mo17	Modern	Inbred
Pa91	Modern	Inbred
PH207	Modern	Inbred
PI566674	Teosinte	Teo.Mexicana
PI566677	Teosinte	Teo.Mexicana
PI566680	Teosinte	Teo.Mexicana
Ames21786	Teosinte	Teo.Parviglumis
Ames21789	Teosinte	Teo.Parviglumis
Ames21809	Teosinte	Teo.Parviglumis

Table B.2 Primers used in amplicon sequencing and qPCR characterization of rhizosphere microbial community

Target	Encodes	Primer Name	Sequence	Reference
16S rRNA	Ribosomal RNA	515F	5'-GTGYCAGCMGCCGCGGTAA-3'	Fierer et al. 2011
16S rRNA	Ribosomal RNA	806R	5'-GGACTACVSGGGTATCTAAT-3'	Fierer et al. 2011
ITS	Internal Transcribed Spacer	ITS1F	5'-TTCGTAGGTGAACCTGCGG-3'	White et al. 1990
ITS	Internal Transcribed Spacer	ITS4R	5'-TCCTCCGCTTATTGATATGC-3'	White et al. 1990
nifH	Nitrogenase	PolF	5'-TGCGAYCCSAARGCBGACTC-3'	Poly et al. 2001
nifH	Nitrogenase	PolR	5'-ATSGCCATCATYTCRCCGGA-3'	Poly et al. 2001
bacterial *amoA*	Ammonia Monooxygenase	amoA-1F	5'-GGGGTTTCTACTGGTGGT-3'	Oakley et al. 2005
bacterial *amoA*	Ammonia Monooxygenase	amoA-2R	5'-CCCCTCKGSAAAGCCTTCTTC-3'	Oakley et al. 2005
archeal *amoA*	Ammonia Monooxygenase	CrenamoA23f	5'-ATGGTCTGGCTWAGACG-3'	Francis et al. 2005
archeal *amoA*	Ammonia Monooxygenase	CrenamoA616r	5'-GCCATCCATCTGTATGTCCA-3'	Francis et al. 2005
Typical *nosZ*	Nitrous oxide reductase	nosZ1F	5'-WCSYTGTTCMTCGACAGCCAG-3'	Henry et al. 2006
Typical *nosZ*	Nitrous oxide reductase	nosZ1R	5'-ATGTCGATCARCTGVKCRTTYTC-3'	Henry et al. 2006
nirK	Nitrite Reductase	nirK876	5'-ATYGGCGGVCAYGGCGA-3'	Henry et al. 2004
nirK	Nitrite Reductase	nirK1040	5'-GCCTCGATCAGRTTRTGGTT-3'	Henry et al. 2004
nirS	Nitrite Reductase	nirSCd3aF	5'-AACGYSAAGGARACSGG-3'	Kandeler et al. 2006
nirS	Nitrite Reductase	nirSR3cd	5'-GASTTCGGRTGSGTCTTSAYGAA-3'	Kandeler et al. 2006
norB	Nitric Oxide Reductase	cnorB2F	5'-GACAAGNNNTACTGGTGGT-3'	Braker et al. 2003
norB	Nitric Oxide Reductase	cnorB6R	5'-GAANCCCCANACNCCNGC-3'	Braker et al. 2003

Table B.3 Molecular sequencing raw reads generated from sequencing run, reads present after FASTX toolkit quality filter, and the rarefaction level of reads per sample for each gene used in this study.

Amplicon	Raw Reads	Quality Filtered Reads	Rarefaction Level
16S rRNA gene	45,616,533	39,079,559	34,000
fungal ITS	4,686,224	3,443,164	1,722
bacterial *amoA*	2,196,316	1,348,496	915
archaeal *amoA*	3,724,966	572,784	430
nifH	5,739,697	2,105,704	1353
nirK	13,544,866	4,972,273	999
nirS	3,375,608	1,102,622	165
nosZ	6,727,004	2,489,774	132
norB	2,317,818	560,953	100

Table B.4 PERMANOVA results 16S Prokaryotic rRNA from rhizosphere. Models below consider all replicate samples.

Table B.4.1 Genotype model comparing the microbial community of lines presented in Table B.1.

Terms	Df	SumsOfSqs	MeanSqs	F.Model	R2	Pr(>F)	Sig
Genotype	11	2.3111	0.210104	2.3412	0.19254	0.001	***
Residuals	108	9.6921	0.089742	0.80746			
Total	119	12.0033	1				

Table B.4.2 Subspecies model comparing subsp. *mays,* subsp *parviglumis,* subsp *mexicana*

Terms	Df	SumsOfSqs	MeanSqs	F.Model	R2	Pr(>F)	Sig
Subspecies	2	1.0549	0.52744	5.6365	0.08788	0.001	***
Residuals	117	10.9484	0.09358	0.91212			
Total	119	12.0033	1				

Table B.4.3 Domestication model comparing the microbiome teosinte v. maize

Terms	Df	SumsOfSqs	MeanSqs	F.Model	R2	Pr(>F)	Sig
Domestication	1	0.7556	0.75561	7.9272	0.06295	0.001	***
Residuals	118	11.2477	0.09532	0.93705			
Total	119	12.0033	1				

Table B.5. PERMANOVA results ITS Fungal from rhizosphere. Models below consider all replicates samples.

Table B.5.1 Genotype model comparing the ITS community of lines presented in Table B.1.

Terms	Df	SumsOfSqs	MeanSqs	F.Model	R2	Pr(>F)	Sig
Genotype	11	5.616	0.51052	1.7448	0.15089	0.001	***
Residuals	108	31.601	0.2926	0.84911			
Total	119	37.217	1				

Table B.5.2 Subspecies model comparing subsp. *mays,* subsp *parviglumis,* subsp *mexicana*

Terms	Df	SumsOfSqs	MeanSqs	F.Model	R2	Pr(>F)	
Subspecies	2	1.975	0.98736	3.2779	0.05306	0.001	***
Residuals	117	35.242	0.30121	0.94694			
Total	119	37.217	1				

Table B.5.3 Domestication model comparing the microbiome teosinte v. maize

Terms	Df	SumsOfSqs	MeanSqs	F.Model	R2	Pr(>F)	Sig
Domestication	1	1.577	1.57732	5.2224	0.04238	0.001	***
Residuals	118	35.639	0.30203	0.95762			
Total	119	37.217	1				

Table B.6. PERMANOVA results 16S Prokaryotic rRNA from rhizosphere comparing the genotypic means. Note that this was achieved by calculating the mean abundance of each OTU within a genotype classification across replicates.

Table B.6.1 Subspecies model comparing subsp. *mays,* subsp *parviglumis,* subsp *mexicana*

Terms	Df	SumsOfSqs	MeanSqs	F.Model	R2	Pr(>F)	Sig
Subspecies	2	0.12574	0.06287	3.0721	0.40571	0.001	***
Residuals	9	0.18419	0.020465	0.59429			
Total	11	0.30993	1				

Table B.6.2 Domestication model comparing the microbiome teosinte v. maize

Terms	Df	SumsOfSqs	MeanSqs	F.Model	R2	Pr(>F)	Sig
Domestication	1	0.085129	0.085129	3.7869	0.27467	0.001	***
Residuals	10	0.224798	0.02248	0.72533			
Total	11	0.309927	1				

Table B.7. PERMANOVA results Fungal ITS from rhizosphere comparing the genotypic means. Note that this was achieved by calculating the mean abundance of each OTU within a genotype classification across replicates.

Table B.7.1 Subspecies model comparing subsp. *mays,* subsp *parviglumis,* subsp *mexicana*

Terms	Df	SumsOfSqs	MeanSqs	F.Model	R2	Pr(>F)	
Subspecies	2	0.44138	0.22069	2.0635	0.31439	0.002	**
Residuals	9	0.96254	0.10695	0.68561			
Total	11	1.40393	1				

Table B.7.2 Domestication model comparing the microbiome teosinte v. maize

Terms	Df	SumsOfSqs	MeanSqs	F.Model	R2	Pr(>F)	
Domestication	1	0.2981	0.2981	2.6957	0.21233	0.005	**
Residuals	10	1.1058	0.11058	0.78767			
Total	11	1.4039	1				

Table B.8 Overview of the statistical significance of the different functional genes characterized.

Ecosystem Process	Gene	Significant Composition Across Domestication ($p<0.05$)	qPCR Abundance Significance in Relation to Domestication ($p<0.05$)
Nitrogen Fixation	*nifH*	**Significant**	Non-Significant
Nitrification	Bacterial *amoA*	**Significant**	**Significant**
Nitrification	Archeal *amoA*	Non-Significant	**Significant**
Denitrification	*nirK*	**Significant**	**Significant**
Denitrification	*nirS*	**Significant**	Non-Significant
Denitrification	*nosZ*	**Significant**	Non-Significant

Table B.9 Compositional differences in functional genes.

Table B.9.1 *nifH*

Terms	Df	SumsOfSqs	MeanSqs	F.Model	R2	Pr(>F)	Sig
Domestication	1	0.09092	0.090918	3.6134	0.26543	0.003	**
Residuals	10	0.25161	0.025161	0.73457			
Total	11	0.34253	1				

Table B.9.2 Bacterial *amoA*

Terms	Df	SumsOfSqs	MeanSqs	F.Model	R2	Pr(>F)	Sig
Domestication	1	0.10311	0.103111	2.7683	0.21681	0.009	**
Residuals	10	0.37247	0.037247	0.78319			
Total	11	0.47558	1				

Table B.9.3 Archeal *amoA*

Terms	Df	SumsOfSqs	MeanSqs	F.Model	R2	Pr(>F)	Sig
Domestication	1	0.020754	0.020754	1.2809	0.11355	0.224	
Residuals	10	0.162023	0.016202	0.88645			
Total	11	0.182776	1				

Table B.9.4 *nirK*

Terms	Df	SumsOfSqs	MeanSqs	F.Model	R2	Pr(>F)	Sig
Domestication	1	0.30708	0.30708	1.2975	0.11485	0.001	***
Residuals	10	2.36668	0.23667	0.88515			
Total	11	2.67376	1				

Table B.9.5 *nirS*

Terms	Df	SumsOfSqs	MeanSqs	F.Model	R2	Pr(>F)	Sig
Domestication	1	0.33949	0.33949	1.8963	0.1594	0.004	**
Residuals	10	1.79029	0.17903	0.8406			
Total	11	2.12978	1				

Table B.9.6 *nosZ*

Terms	Df	SumsOfSqs	MeanSqs	F.Model	R2	Pr(>F)	Sig
Domestication	1	0.4995	0.49949	1.5048	0.1308	0.006	**
Residuals	10	3.3193	0.33193	0.8692			
Total	11	3.8188	1				

Tables B.10 Functional gene qPCR of these listed above

Table B.10.1 *nifH*

Terms	Df	SumOfSqs	Wald Statisitic	Pr (ChiSq)	Sig
(Intercept)	1	14554998	177.805	2.20E-16	***
Domestication	1	80715	0.986	0.3207	
Residuals (MS)		81859			

Table B.10.2 Bacterial *amoA*

Terms	Df	SumOfSqs	Wald Statisitic	Pr (ChiSq)	Sig
(Intercept)	1	30681256	241.934	2.20E-16	***
Domestication	1	6391292	50.398	1.26E-12	***
Residuals (MS)		126816			

Table B.10.3 Archeal *amoA*

Terms	Df	SumOfSqs	Wald Statisitic	Pr (ChiSq)	Sig
(Intercept)	1	193212039	59.846	1.02E-14	***
Domestication	1	68951105	21.357	3.81E-06	***
Residuals (MS)		3228508			

Table B.10.4 *nirK*

Terms	Df	SumOfSqs	Wald Statisitic	Pr (ChiSq)	Sig
(Intercept)	1	44381821	786.45	2.20E-16	***
Domestication	1	1467441	26	3.41E-07	***
Residuals (MS)		56433			

Table B.10.5 *nirS*

Terms	Df	SumOfSqs	Wald Statisitic	Pr (ChiSq)	Sig
(Intercept)	1	84279	41.256	1.34E-10	***
Domestication	1	1116	0.546	0.4598	
Residuals (MS)		2043			

Table B.10.6 *nosZ*

Terms	Df	SumOfSqs	Wald Statisitic	Pr (ChiSq)	Sig
(Intercept)	1	2148091	338.37	2.20E-16	***
Domestication	1	5374	0.85	0.3576	
Residuals (MS)		6348			

Table B.11 Here we treated the N-cycling functional genes as a multivariate dataset to access the overall effect of domestication status on the N-cycling functional groups we accessed. We compared the overall alpha diversity of these functional genes and the overall abundance of these functional genes as explained by domestication status.

Table B.11.1 Alpha diversity (chao1) of functional groups as explained by domestication status of cultivars

Terms	Df	SumsOfSqs	MeanSqs	F.Model	R2	Pr(>F)	Sig
Domestication	1	0.100267	0.100267	16.415	0.62143	0.002	**
Residuals	10	0.061081	0.006108	0.37857			
Total	11	0.161348	1				

Table B.11.2 Functional genes of functional groups as explained by domestication status of cultivars.

Terms	Df	SumsOfSqs	MeanSqs	F.Model	R2	Pr(>F)	Sig
Domestication	1	0.41099	0.41099	19.152	0.65697	0.007	**
Residuals	10	0.21459	0.02146	0.34303			
Total	11	0.62558	1				

APPENDIX C: SUPPLEMENTAL INFORMATION CHAPTER 4

Genetic variation within *Zea mays* alter microbiome assembly and nitrogen cycling function in the Agroecosystem

Figures:

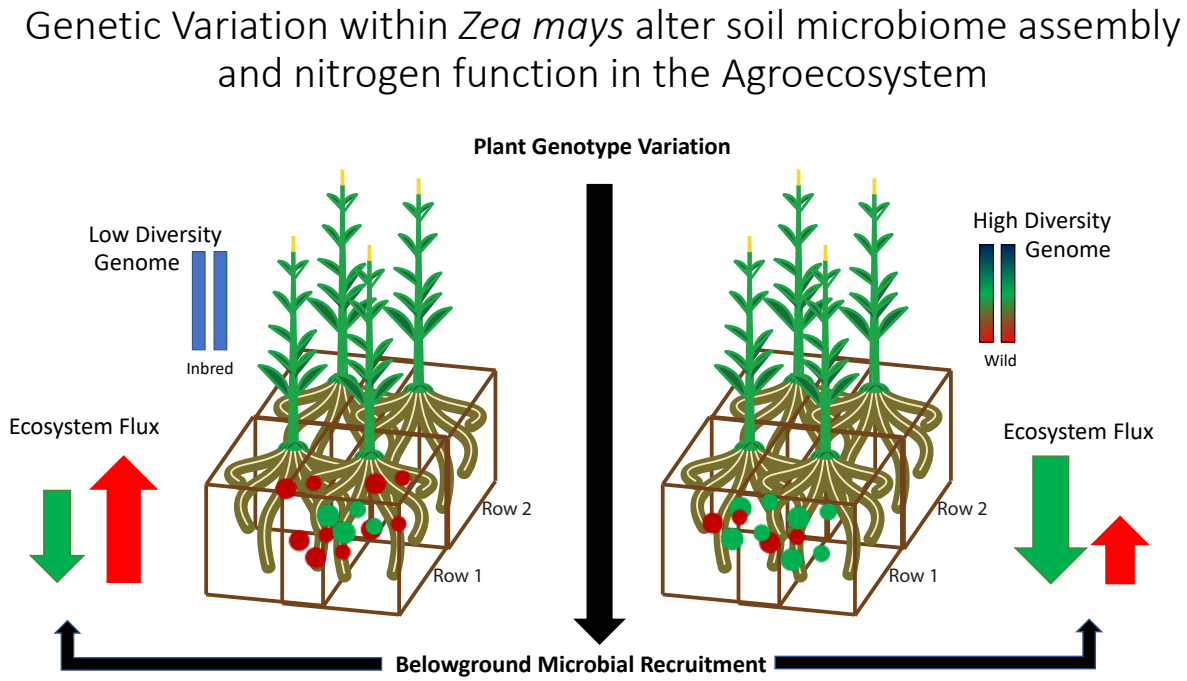

Figure C.1 A. Graphical abstract displaying the underlying concept of the study. It has been shown that plant genotype plays a role in microbial requitement- here we were interested in understanding if genotype driven differential requitement of the rhizosphere microbiome will result in alterations to microbial mediated ecosystem functions. To assess this question, we used extremely contrasting genetic models: modern agricultural inbred of maize and wild teosinte progenitors. This gives us a potential ceiling to how much of a role plant genetic can play.

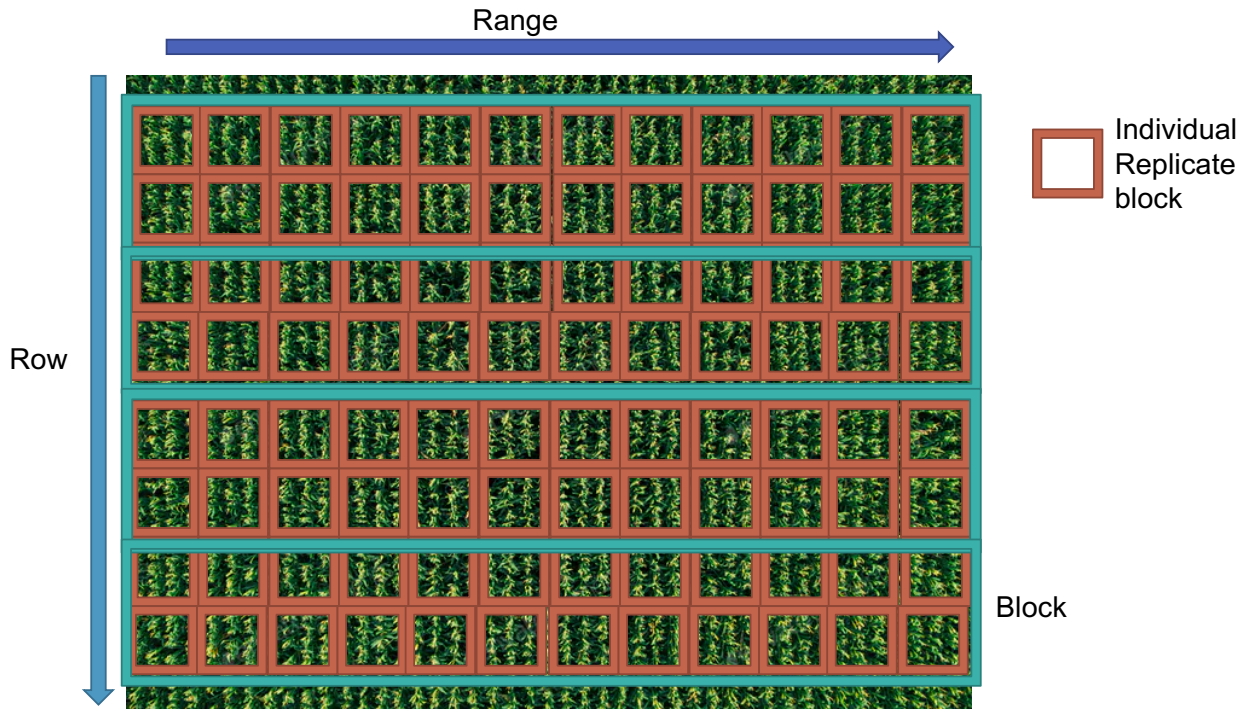

Figure C.1 B. Highlights the physical structure of the field setting. Replicate rectangular blocks are colored in teal and include all the genotypes included in the study. Individual genotype blocks are colored in brown and are randomized within the block. Range and row factors were included in model as continuous factors to represent space within the field. This scheme allowed us to control for stochastic spatial effects within our experiment.

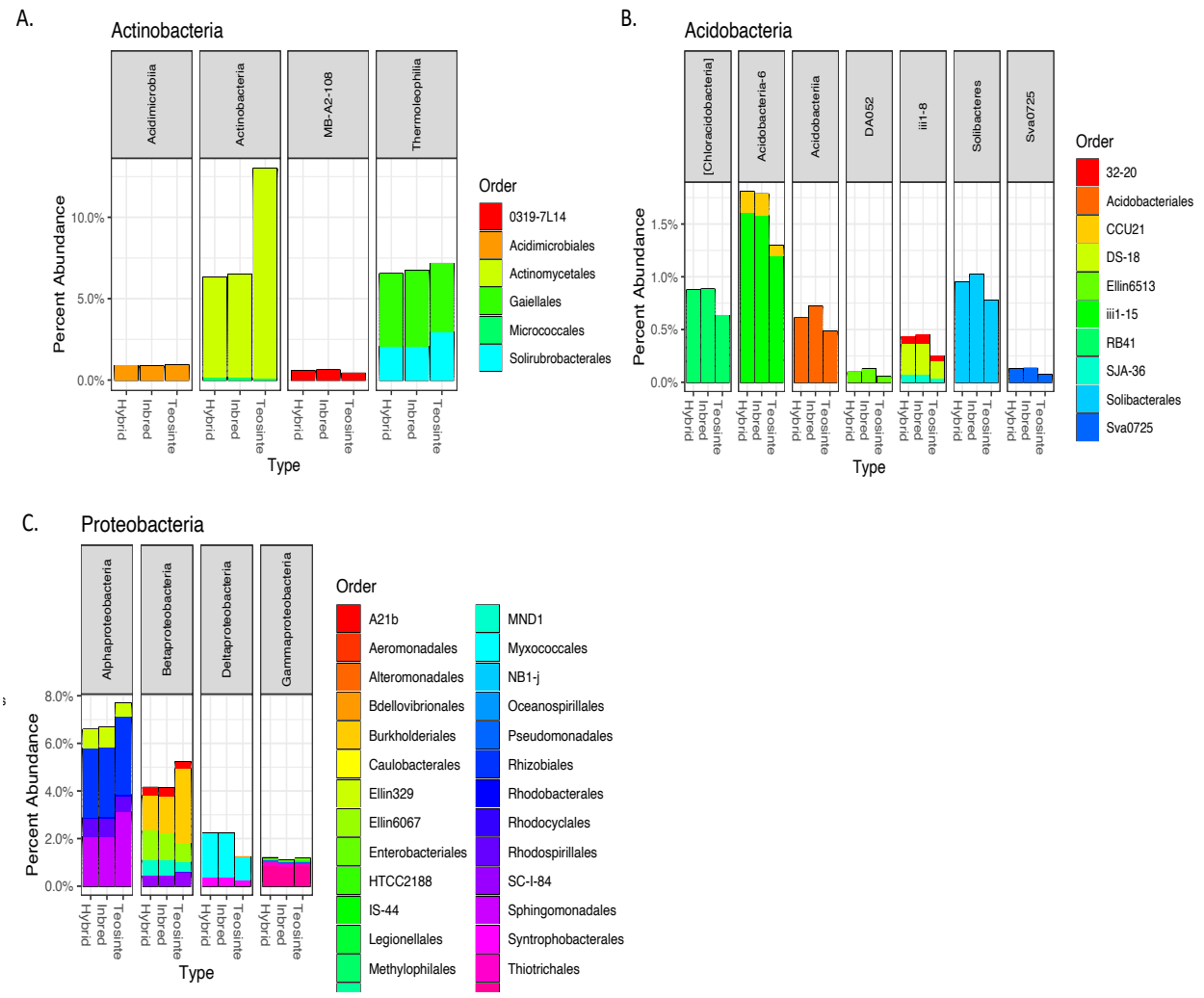

Figure C.2 Stack plots showing the differential abundant OTUs based on DESeq2 determined by teosinte and inbred maize comparison. **A.** Displays within order *Actinobacteria* differences among teosinte and inbred maize. **B.** Displays within order *Acidobacteria* differences among teosinte and inbred maize. **C.** Displays within order *Proteobacteria* differences among teosinte and inbred maize.

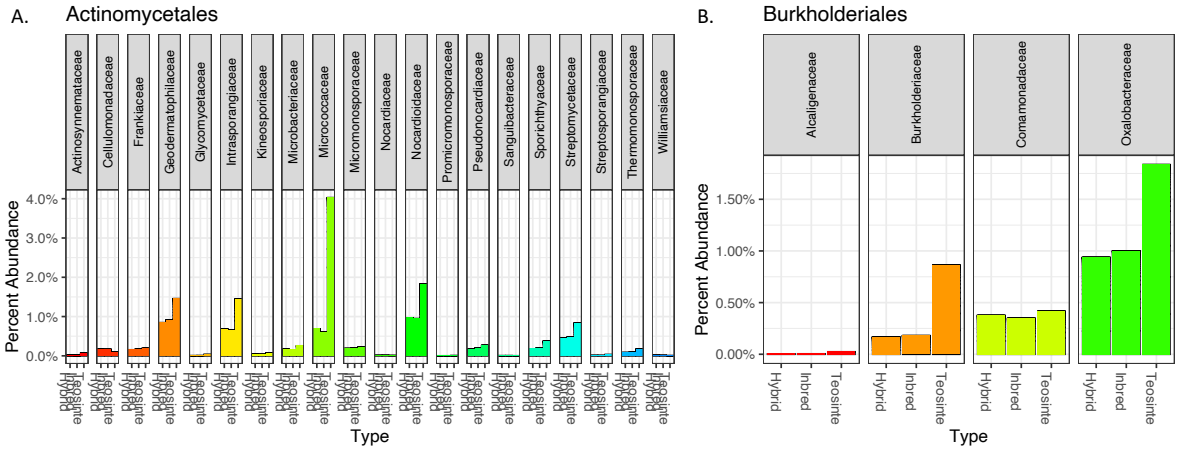

Figure C.3 Stack plots showing the differential abundant OTUs based on DESeq2 determined by teosinte and inbred maize comparison. These plots were made as these taxa were major contributors to the microbiome differences. **A.** Displays within order *Actinomycetales* differences among teosinte and inbred maize. **B.** Displays within order *Burkholderiales* differences among teosinte and inbred maize.

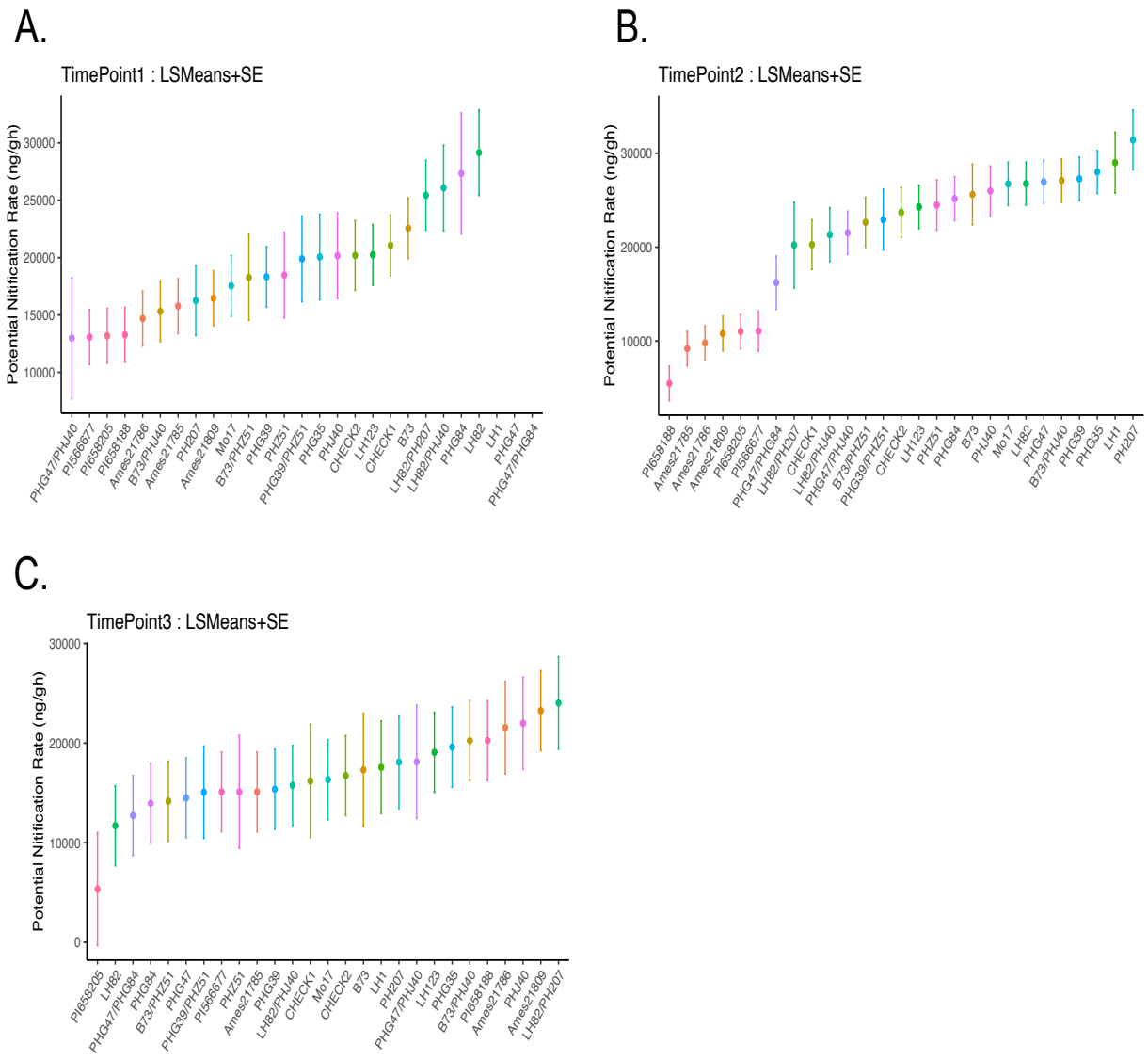

Figure C.4 Shows the potential nitrification of individual genotypes in study across different sampling timepoints. LS Means and Standard Error were calculated using ASREML-r. Supplemental Statistic are present in Table C.6. **A.** Shows the genotypic mean of potential nitrification at time point 1. **B.** Shows the genotypic mean of potential nitrification at time point 2. **C.** Shows the genotypic mean of potential nitrification at time point 3.

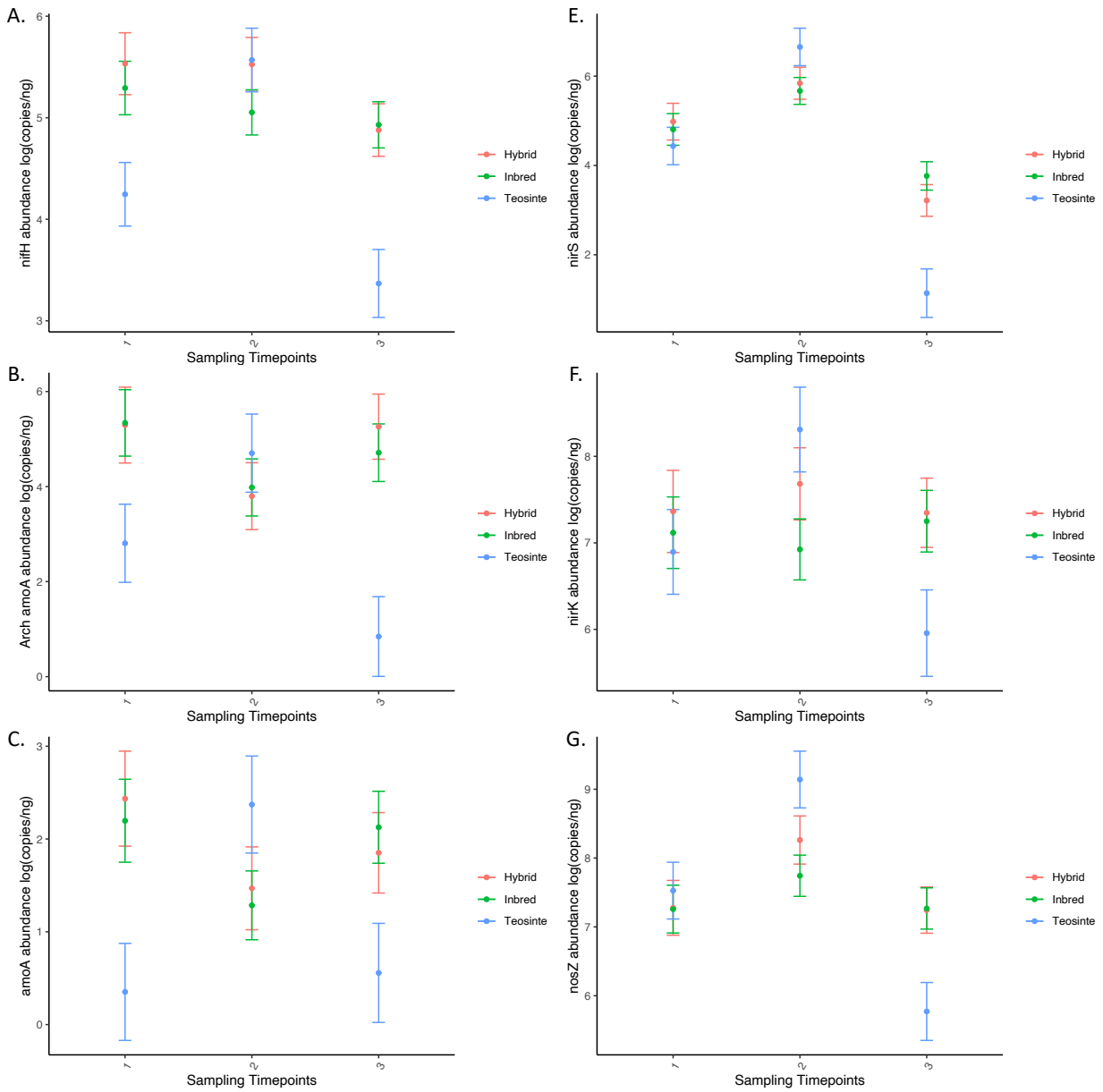

Figure C.5 Quantitative PCR Results for functional genes surveyed in the study across different timepoints over the season across plant type. LS Means and Standard Error were calculated using ASREML-r. Supplemental Statistic are present in Table C.2, C.4. **A.** Displays the log of *nifH* qPCR abundance across timepoints. **B.** Displays the log of archaeal *amoA* qPCR abundance across timepoints. **C.** Displays the log of bacterial *amoA* qPCR abundance across timepoints. **D.** Displays the log of *nirS* qPCR abundance across timepoints. **E.** Displays the log of *nirK* qPCR abundance across timepoints. **G.** Displays the log of *nosZ* qPCR abundance across timepoints.

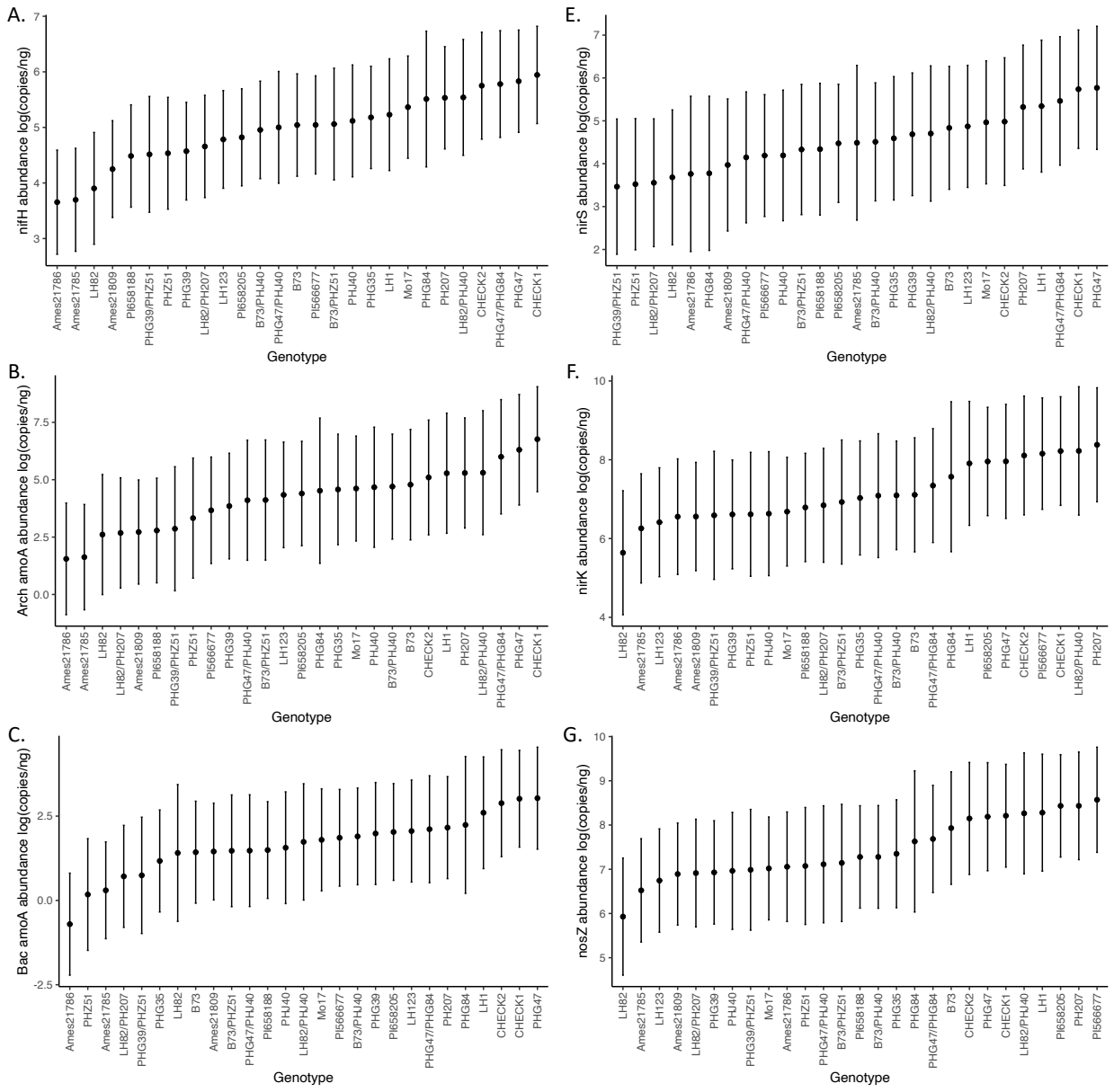

Figure C.6 Quantitative PCR Results for functional genes surveyed in the study averaged cross different timepoints displayed as genotypic means. LS Means and Standard Error were calculated using ASREML-r. Supplemental Statistic are present in Table C.2, C.4. **A.** Displays the log of *nifH* qPCR abundance across genotypes. **B.** Displays the log of archaeal *amoA* qPCR abundance across genotypes. **C.** Displays the log of bacterial *amoA* qPCR abundance across genotypes. **D.** Displays the log of *nirS* qPCR abundance across genotypes. **E.** Displays the log of *nirK* qPCR abundance across genotypes. **G.** Displays the log of *nosZ* qPCR abundance across timepoints.

Tables:

Tables C.1 Permutational multivariate ANOVA model results at the genotypic level for 16S rRNA genes, and Fungal ITS. Standard model was run on all amplicon sequence data. Bray-Curtis distance was used to calculate dissimilarity between microbiomes. 999 permutations were used in analysis. All factors in the model were run as fixed effect: ***Microbial Community Matrix = Type x Sampling Time + Row x Range + Residuals.*** This model was used to all other nitrogen cycling genes compositional changes. Interactions between plant type and time were incorporated to understand plant growth changes, while row and range interactions were used to understand spatial effects. Row and Range factors were stratified as they were random factors.

Table C.1.1 Type (inbred, hybrid, teosinte) x Time Prokaryotic 16S rRNA Model

Factor	Df	SumsOfSqs	MeanSqs	F.Model	R2	Pr(>F)	
Type	2	1.8712	0.93559	12.4209	0.06447	0.001	***
Time	2	2.0925	1.04623	13.8897	0.07209	0.001	***
Row	1	1.0681	1.06807	14.1797	0.0368	0.001	***
Range	1	0.3445	0.34454	4.5741	0.01187	0.001	***
Block	91	8.3838	0.09213	1.2231	0.28884	0.001	***
Type:Time	4	1.1803	0.29507	3.9174	0.04066	0.001	***
Residuals	187	14.0856	0.07532	0.48528			
Total	288	29.026	1				

‘

Table C.1.2 Here is the Genotype x Time Prokaryotic 16S rRNA Model (included all genotypes)

Factor	Df	SumsOfSqs	MeanSqs	F.Model	R2	Pr(>F)	
Genotype	26	4.2653	0.16405	2.2087	0.14695	0.001	***
Time	2	2.0737	1.03683	13.9596	0.07144	0.001	***
Row	1	0.8968	0.89683	12.0748	0.0309	0.001	***
Range	1	0.3204	0.32043	4.3142	0.01104	0.001	***
Block	72	6.6467	0.09231	1.2429	0.22899	0.001	***
Genotype:Time	52	4.8705	0.09366	1.2611	0.1678	0.001	***
Residuals	134	9.9526	0.07427	0.34289			
Total	288	29.026	1				

Table C.1.3 Nested Genotype-Type x Time Prokaryotic 16S rRNA Model

Factor	Df	SumsOfSqs	MeanSqs	F.Model	R2	Pr(>F)	
Type	2	1.8712	0.93559	12.5966	0.06447	0.001	***
Time	2	2.0925	1.04623	14.0862	0.07209	0.001	***
Row	1	1.0681	1.06807	14.3803	0.0368	0.001	***
Range	1	0.3445	0.34454	4.6388	0.01187	0.001	***
Block	91	8.3838	0.09213	1.2404	0.28884	0.001	***
Type:Genotype	5	0.4428	0.08855	1.1922	0.01525	0.069	.
Type:Time	4	1.1669	0.29174	3.9279	0.0402	0.001	***
Type:Genotype:Time	48	3.7036	0.07716	1.0388	0.1276	0.164	
Residuals	134	9.9526	0.07427	0.34289			
Total	288	29.026	1				

Table C.1.4 Type (inbred, hybrid, teosinte) x Time Fungal ITS Model

	Df	SumsOfSqs	MeanSqs	F.Model	R2	Pr(>F)	
Type	2	3.731	1.86552	6.0405	0.03629	0.001	***
Time	2	2.267	1.13329	3.6696	0.02205	0.001	***
Row	1	0.955	0.95467	3.0912	0.00929	0.001	***
Range	1	0.527	0.52721	1.7071	0.00513	0.003	**
Block	91	30.989	0.34054	1.1027	0.30143	0.001	***
Type:Time	4	4.423	1.10563	3.58	0.04302	0.001	***
Residuals	194	59.914	0.30883	0.58279			
Total	295	102.805	1				

Table C.1.5 Here is the Genotype x Time Fungal ITS Model (included all genotypes)

	Df	SumsOfSqs	MeanSqs	F.Model	R2	Pr(>F)	
Genotype	26	12.028	0.4626	1.5136	0.11699	0.001	***
Time	2	2.246	1.12316	3.675	0.02185	0.001	***
Row	1	0.995	0.99467	3.2546	0.00968	0.001	***
Range	1	0.536	0.53647	1.7553	0.00522	0.007	**
Block	72	24.303	0.33754	1.1044	0.2364	0.001	***
Genotype:Time	52	19.604	0.377	1.2336	0.19069	0.001	***
Residuals	141	43.093	0.30562	0.41917			
Total	295	102.805	1				

Table C.1.6 Nested Genotype-Type x Time Fungal ITS Model

	Df	SumsOfSqs	MeanSqs	F.Model	R2	Pr(>F)	
Type	2	3.731	1.86552	6.1041	0.03629	0.001	***
Time	2	2.267	1.13329	3.7082	0.02205	0.001	***
Row	1	0.955	0.95467	3.1237	0.00929	0.001	***
Range	1	0.527	0.52721	1.7251	0.00513	0.002	**
Block	91	30.989	0.34054	1.1142	0.30143	0.001	***
Type:Genotype	5	1.64	0.32795	1.0731	0.01595	0.191	
Type:Time	4	4.423	1.10563	3.6176	0.04302	0.001	***
Type:Genotype:Time	48	15.181	0.31628	1.0349	0.14767	0.155	
Residuals	141	43.093	0.30562	0.41917			
Total	295	102.805	1				

Table C.2 Functional gene summary of amplicon functional composition gene and qPCR abundance data from PerMANOVA and ASREML statistical analysis. C.2.1 displays the genotype summary. C.2.2 displays the plant type summary. Full statistical model presented in C.3-C.4.

Table C.2.1 Overview of statistical analysis for genotypes effects on different functional genes.

Ecosystem Process	**Gene**	**Significant Composition Across Genotype (p<0.05)**	**Significant Composition Genotype:Time Interaction (p<0.05)**	**qPCR Abundance Significance in Relation to Genotype (*p*<0.05)**	**qPCR Abundance Significance Genotype:Time Interaction (p<0.05)**
Nitrogen Fixation	*nifH*	Non-Significant	Non-Significant	Non-Significant	Non-Significant
Nitrification	Bacterial *amoA*	Non-Significant	**Significant**	Non-Significant	Non-Significant
Nitrification	Archeal *amoA*	**Significant**	**Near Significant**	Non-Significant	Non-Significant
Denitrification	*nirK*	**Significant**	Non-Significant	Non-Significant	**Near-Significant**
Denitrification	*nirS*	**Significant**	Non-Significant	Non-Significant	**Near-Significant**
Denitrification	*nosZ*	**Significant**	Non-Significant	**Near-Significant**	**Near-Significant**

Table C.2.2 Overview of statistical analysis for Type effects on different functional genes.

Ecosystem Process	Gene	Significant Composition Across Type (p<0.05)	Significant Composition Type:Time Interaction (p<0.05)	qPCR Abundance Significance in Relation to Type (*p*<0.05)	qPCR Abundance Significance Type:Time Interaction (p<0.05)
Nitrogen Fixation	*nifH*	Non-Significant	Non-Significant	**Significant**	**Significant**
Nitrification	Bacterial *amoA*	Non-Significant	**Significant**	Non-Significant	**Significant**
Nitrification	Archeal *amoA*	**Significant**	**Significant**	Non-Significant	Non-Significant
Denitrification	*nirK*	**Significant**	Non-Significant	Non-Significant	**Significant**
Denitrification	*nirS*	**Significant**	Non-Significant	Non-Significant	**Significant**
Denitrification	*nosZ*	**Significant**	**Significant**	**Significant**	**Significant**

Table C.3 Functional Gene Summary of amplicon functional from PerMANOVA models. 999 permutations were used in analysis. All factors in the model were run as fixed effect: ***Microbial Community Matrix = Genotype (or Type) x Sampling Time + Row x Range + Residuals.*** Interactions between plant type and time were incorporated to understand plant growth changes, while row and range interactions were used to understand spatial effects. Row and Range factors were stratified as they were random factors

Table C.3.1 *nifH* gene type (inbred, hybrid, teosinte) model

	Df	SumsOfSqs	MeanSqs	F.Model	R2	Pr(>F)	
Type	2	1.049	0.52467	1.07541	0.00731	0.13	
Time	2	1.176	0.58813	1.20546	0.00819	0.007	**
Row	1	0.617	0.61742	1.2655	0.0043	0.012	*
Range	1	0.635	0.63503	1.3016	0.00442	0.01	**
Block	91	44.958	0.49405	1.01263	0.31318	0.15	
Type:Time	4	1.932	0.48298	0.98995	0.01346	0.545	
Residuals	191	93.186	0.48788	0.64913			
Total	292	143.554	1				

Table C.3.2 *nifH* gene genotype Model

	Df	SumsOfSqs	MeanSqs	F.Model	R2	Pr(>F)	
Genotype	26	12.611	0.48502	0.99506	0.08785	0.566	
Time	2	1.185	0.59253	1.21561	0.00826	0.007	**
Row	1	0.655	0.65498	1.34373	0.00456	0.009	**
Range	1	0.628	0.62806	1.2885	0.00438	0.006	**
Block	72	35.756	0.49661	1.01883	0.24908	0.08	.
Genotype:Time	52	25.453	0.48948	1.0042	0.17731	0.361	
Residuals	138	67.266	0.48743	0.46858			
Total	292	143.554	1				

Table C.3.3 *nifH* gene nested genotype/type Model

	Df	SumsOfSqs	MeanSqs	F.Model	R2	Pr(>F)	
Type	2	1.049	0.52467	1.0764	0.00731	0.117	
Time	2	1.176	0.58813	1.20657	0.00819	0.007	**
Row	1	0.617	0.61742	1.26667	0.0043	0.016	*
Range	1	0.635	0.63503	1.3028	0.00442	0.009	**
Block	91	44.958	0.49405	1.01356	0.31318	0.133	
Type:Genotype	5	2.399	0.47972	0.98417	0.01671	0.668	
Type:Time	4	1.932	0.48298	0.99086	0.01346	0.535	
Type:Genotype:Time	48	23.521	0.49002	1.00531	0.16385	0.36	
Residuals	138	67.266	0.48743	0.46858			
Total	292	143.554	1				

Table C.3.4. Bacterial *amoA* Type (inbred, hybrid, teosinte) model

	Df	SumsOfSqs	MeanSqs	F.Model	R2	Pr(>F)	
Type	2	0.594	0.29722	0.86977	0.0056	0.661	
Time	2	1.691	0.84538	2.47386	0.01593	0.001	***
Row	1	0.533	0.53302	1.55979	0.00502	0.102	
Range	1	0.413	0.41304	1.20869	0.00389	0.256	
Block	91	35.427	0.38931	1.13926	0.3337	0.007	**
Type:Time	4	1.897	0.4742	1.38768	0.01787	0.028	*
Residuals	192	65.611	0.34172	0.618			
Total	293	106.166	1				

Table C.3.5 Bacterial *amoA* Genotype Model

	Df	SumsOfSqs	MeanSqs	F.Model	R2	Pr(>F)	
Genotype	26	9.403	0.36164	1.0811	0.08857	0.158	
Time	2	1.73	0.86514	2.5862	0.0163	0.001	***
Row	1	0.533	0.53267	1.5923	0.00502	0.087	.
Range	1	0.396	0.39591	1.1835	0.00373	0.274	
Block	72	28.34	0.39362	1.1767	0.26694	0.007	**
Genotype:Time	52	19.266	0.3705	1.1076	0.18147	0.042	*
Residuals	139	46.499	0.33452	ng			
Total	293	106.166	1				

Table C.3.6 Bacterial *amoA* Nested Genotype/Type Model

	Df	SumsOfSqs	MeanSqs	F.Model	R2	Pr(>F)	
Type	2	0.594	0.29722	0.88849	0.0056	0.623	
Time	2	1.691	0.84538	2.52712	0.01593	0.001	***
Row	1	0.533	0.53302	1.59338	0.00502	0.066	.
Range	1	0.413	0.41304	1.23471	0.00389	0.242	
Block	91	35.427	0.38931	1.16378	0.3337	0.001	***
Type:Genotype	5	1.743	0.34868	1.04231	0.01642	0.38	
Type:Time	4	1.897	0.4742	1.41756	0.01787	0.033	*
Type:Genotype:Time	48	17.369	0.36186	1.08171	0.1636	0.101	
Residuals	139	46.499	0.33452	0.43798			
Total	293	106.166	1				

Table C.3.7 Archeal *amoA* Type Model

	Df	SumsOfSqs	MeanSqs	F.Model	R2	Pr(>F)	
Type	2	0.464	0.232	2.452	0.01165	0.008	**
Time	2	6.806	3.403	35.955	0.17089	0.001	***
Row	1	3.224	3.2242	34.066	0.08096	0.001	***
Range	1	0.387	0.3867	4.086	0.00971	0.003	**
Block	91	9.43	0.1036	1.095	0.23678	0.123	
Type:Time	4	1.154	0.2886	3.049	0.02898	0.001	***
Residuals	194	18.361	0.0946	0.46103			
Total	295	39.827	1				

Table C.3.8 Archeal *amoA* Genotype Model

	Df	SumsOfSqs	MeanSqs	F.Model	R2	Pr(>F)	
Genotype	26	3.346	0.1287	1.374	0.08401	0.007	**
Time	2	6.798	3.3989	36.285	0.17068	0.001	***
Row	1	2.708	2.7076	28.905	0.06799	0.001	***
Range	1	0.406	0.4062	4.337	0.0102	0.002	**
Block	72	7.812	0.1085	1.158	0.19614	0.027	*
Genotype:Time	52	5.55	0.1067	1.139	0.13935	0.075	.
Residuals	141	13.208	0.0937	0.33163			
Total	295	39.827	1				

Table C.3.9 Archeal *amoA* nested Genotype/Type Model

	Df	SumsOfSqs	MeanSqs	F.Model	R2	Pr(>F)	
Type	2	0.464	0.232	2.477	0.01165	0.005	**
Time	2	6.806	3.403	36.329	0.17089	0.001	***
Row	1	3.224	3.2242	34.42	0.08096	0.001	***
Range	1	0.387	0.3867	4.129	0.00971	0.003	**
Block	91	9.43	0.1036	1.106	0.23678	0.101	
Type:Genotype	5	0.758	0.1516	1.618	0.01903	0.024	*
Type:Time	4	1.154	0.2886	3.081	0.02898	0.001	***
Type:Genotype:Time	48	4.396	0.0916	0.978	0.11037	0.591	
Residuals	141	13.208	0.0937	0.33163			
Total	295	39.827	1				

Table C.3.10 *nirK* Type Model

	Df	SumsOfSqs	MeanSqs	F.Model	R2	Pr(>F)	
Type	2	1.11	0.555	1.43	0.00933	0.004	**
Time	2	3.188	1.59391	4.1068	0.0268	0.001	***
Row	1	0.688	0.68803	1.7727	0.00578	0.002	**
Range	1	0.472	0.47213	1.2165	0.00397	0.09	.
Block	91	36.562	0.40178	1.0352	0.30733	0.042	*
Type:Time	4	1.654	0.41339	1.0651	0.0139	0.21	
Residuals	194	75.295	0.38812	0.6329			
Total	295	118.968	1				

Table C.3.11 *nirk* Genotype Model

	Df	SumsOfSqs	MeanSqs	F.Model	R2	Pr(>F)	
Genotype	26	10.984	0.42248	1.0986	0.09233	0.003	**
Time	2	3.142	1.57106	4.0854	0.02641	0.001	***
Row	1	0.556	0.55561	1.4448	0.00467	0.011	*
Range	1	0.483	0.48293	1.2558	0.00406	0.064	.
Block	72	29.081	0.4039	1.0503	0.24444	0.019	*
Genotype:Time	52	20.5	0.39424	1.0252	0.17232	0.162	
Residuals	141	54.222	0.38455	0.45577			
Total	295	118.968	1				

Table C.3.12 *nirK* Genotype/Type Model

	Df	SumsOfSqs	MeanSqs	F.Model	R2	Pr(>F)	
Type	2	1.11	0.555	1.4432	0.00933	0.001	***
Time	2	3.188	1.59391	4.1448	0.0268	0.001	***
Row	1	0.688	0.68803	1.7892	0.00578	0.001	***
Range	1	0.472	0.47213	1.2277	0.00397	0.089	.
Block	91	36.562	0.40178	1.0448	0.30733	0.024	*
Type:Genotype	5	2.226	0.44521	1.1577	0.01871	0.027	*
Type:Time	4	1.654	0.41339	1.075	0.0139	0.159	
Type:Genotype:Time	48	18.847	0.39264	1.021	0.15842	0.206	
Residuals	141	54.222	0.38455	0.45577			
Total	295	118.968	1				

Table C.3.13 *nirS* Type Model

	Df	SumsOfSqs	MeanSqs	F.Model	R2	Pr(>F)	
Type	2	1.303	0.65133	1.7675	0.01149	0.001	***
Time	2	1.415	0.70762	1.9202	0.01248	0.001	***
Row	1	1.224	1.22417	3.3219	0.0108	0.003	**
Range	1	0.799	0.79936	2.1691	0.00705	0.001	***
Block	91	35.535	0.3905	1.0597	0.31342	0.001	***
Type:Time	4	1.609	0.40222	1.0915	0.01419	0.185	
Residuals	194	71.492	0.36851	0.63056			
Total	295	113.377	1				

Table C.3.14 *nirS* Genotype Model

	Df	SumsOfSqs	MeanSqs	F.Model	R2	Pr(>F)	
Genotype	26	10.581	0.40697	1.08047	0.09333	0.031	*
Time	2	1.409	0.70462	1.8707	0.01243	0.001	***
Row	1	1.015	1.01503	2.69481	0.00895	0.001	***
Range	1	0.798	0.79755	2.11741	0.00703	0.001	***
Block	72	28.471	0.39543	1.04984	0.25112	0.054	.
Genotype:Time	52	17.994	0.34603	0.91868	0.15871	0.998	
Residuals	141	53.109	0.37666	0.46843			
Total	295	113.377	1				

Table C.3.15 *nirS* Nested Genotype/Type Model

	Df	SumsOfSqs	MeanSqs	F.Model	R2	Pr(>F)	
Type	1	0.34	0.3401	0.8887	0.00364	0.677	
Time	3	2.347	0.78227	2.04408	0.02512	0.001	***
Row	1	0.98	0.97993	2.56059	0.01049	0.001	***
Range	1	0.818	0.81839	2.13847	0.00876	0.002	**
Block	80	31.504	0.39379	1.029	0.33723	0.171	
Type:Time	2	0.748	0.37406	0.97742	0.00801	0.541	
Type:Genotype:Time	43	14.967	0.34808	0.90954	0.16022	0.999	
Residuals	109	41.714	0.3827	0.44653			
Total	240	93.418	1				

Table C.3.16 *nosZ* Type Model

	Df	SumsOfSqs	MeanSqs	F.Model	R2	Pr(>F)	
Type	2	1.288	0.64412	1.407	0.00935	0.001	***
Time	2	1.857	0.92856	2.0283	0.01347	0.001	***
Row	1	0.805	0.80456	1.7574	0.00584	0.001	***
Range	1	0.581	0.58138	1.2699	0.00422	0.001	***
Block	91	42.41	0.46604	1.018	0.30771	0.001	***
Type:Time	4	2.07	0.51758	1.1306	0.01502	0.013	*
Residuals	194	88.813	0.4578	0.64439			
Total	295	137.825	1				

Table C.3.17 *nosZ* Genotype Model

	Df	SumsOfSqs	MeanSqs	F.Model	R2	Pr(>F)	
Genotype	26	12.225	0.4702	1.0274	0.0887	0.011	*
Time	2	1.856	0.92801	2.0277	0.01347	0.001	***
Row	1	0.786	0.78573	1.7168	0.0057	0.151	
Range	1	0.546	0.54594	1.1929	0.00396	0.057	.
Block	72	33.931	0.47126	1.0297	0.24619	0.034	*
Genotype:Time	52	23.951	0.4606	1.0064	0.17378	0.271	
Residuals	141	64.53	0.45766	0.4682			
Total	295	137.825	1				

Table C.3.18 *nosZ* Genotype/Type Model

	Df	SumsOfSqs	MeanSqs	F.Model	R2	Pr(>F)	
Type	2	1.288	0.64412	1.40742	0.00935	0.006	**
Time	2	1.857	0.92856	2.02893	0.01347	0.001	***
Row	1	0.805	0.80456	1.75799	0.00584	0.003	**
Range	1	0.581	0.58138	1.27033	0.00422	0.008	**
Block	91	42.41	0.46604	1.01831	0.30771	0.008	**
Type:Genotype	5	2.403	0.4805	1.04992	0.01743	0.193	
Type:Time	4	2.07	0.51758	1.13093	0.01502	0.018	*
Type:Genotype:Time	48	21.881	0.45585	0.99605	0.15876	0.468	
Residuals	141	64.53	0.45766	0.4682			
Total	295	137.825	1				

Table C.4. Mixed effect models comparing qPCR of functional genes and genotype, type, space, and time. Genotype and time of sampling were run as a fixed effect, while sampling block, range, and row were run as random factors. Wald tests performed on statistical models to calculate significance. Statistical models were run in 'asreml-r'.

Table C.4.1 *nifH* qPCR Type Model

Factor	Df	Sum of Sq	Wald	Pr(Chisq)	
(Intercept)	1	16756611	89.194	2.00E-16	***
Type	2	1153454	6.14	0.04643	*
Time	2	3239876	17.246	0.00018	***
Type:Time	4	2423834	12.902	0.01177	*
residual		187867			

Table C.4.2 *nifH* qPCR Genotype Model

Factor	Df	Sum of Sq	Wald	Pr(Chisq)	
(Intercept)	1	13762521	69.647	2.20E-16	***
Genotype	26	4214024	21.325	0.724974	
Time	2	3245682	16.425	0.0002712	***
Genotype:Time	52	10876363	55.041	0.3602899	
residual		197605			

Table C.4.3 Bacterial *amoA* qPCR Type Model

Factor	Df	Sum of Sq	Wald	Pr(Chisq)	
(Intercept)	1	167727	135.24	2.20E-16	***
Type	2	157	0.127	0.93856	
Time	2	10205	8.229	0.01634	*
Type:Time	4	35000	28.221	1.13E-05	***
residual		1240			

Table C.4.4 Bacterial *amoA* qPCR Genotype Model

Factor	Df	Sum of Sq	Wald	Pr(Chisq)	
(Intercept)	1	159311	120.66	2.00E-16	***
Genotype	26	15361	11.634	0.99305	
Time	2	9378	7.103	0.02868	*
Genotype:Time	52	83863	63.517	0.13144	
residual		1320			

Table C.4.5 Arch *amoA* qPCR Type Model

Factor	Df	Sum of Sq	Wald	Pr(Chisq)	
(Intercept)	1	468689956	37.761	8.00E-10	***
Type	2	35436473	2.855	0.2399	
Time	2	43443468	3.5	0.1738	
Type:Time	4	76664810	6.177	0.1863	
residual		12412117			

Table C.4.6 Arch *amoA* qPCR Genotype Model

Factor	Df	Sum of Sq	Wald	Pr(Chisq)	
(Intercept)	1	772154049	59.269	1.38E-14	***
Genotype	26	305307733	23.435	0.6082	
Time	2	42938857	3.296	0.1924	
Type:Time	52	669965740	51.426	0.4964	
residual		13027864			

Table C.4.7 *nirK* qPCR Type Model

Factor	Df	Sum of Sq	Wald	Pr(Chisq)	
(Intercept)	1	3191339410	494.32	2.20E-16	***
Type	2	4872529	0.75	0.6856658	
Time	2	59666289	9.24	0.0098429	**
Type:Time	4	137359821	21.28	0.0002791	***
residual		6455991			

Table C.4.8 *nirK* qPCR Genotype Model

Factor	Df	Sum of Sq	Wald	Pr(Chisq)	
(Intercept)	1	3085673717	472.49	2.20E-16	***
Genotype	26	113556098	17.39	0.896892	
Time	2	61635999	9.44	0.008925	**
Genotype:Time	52	448758443	68.72	0.060059	.
residual		6530707			

Table C.4.9 *nirS* qPCR Type Model

Factor	Df	Sum of Sq	Wald	Pr(Chisq)	
(Intercept)	1	142927550	50.098	1.46E-12	***
Type	2	12327195	4.321	0.115275	
Time	2	91423589	32.045	1.10E-07	***
Type:Time	4	39142572	13.72	0.008244	**
residual	(MS)	2852939			

Table C.4.10 *nirS* qPCR Genotype Model

Factor	Df	Sum of Sq	Wald	Pr(Chisq)	
(Intercept)	1	3085673717	472.49	2.20E-16	***
Genotype	26	113556098	17.39	0.896892	
Time	2	61635999	9.44	0.008925	**
Genotype:Time	52	448758443	68.72	0.060059	.
residual		6530707			

Table C.4.11 *nosZ* qPCR Type Model

Factor	Df	Sum of Sq	Wald	Pr(Chisq)	
(Intercept)	1	294866123	20.09	7.39E-06	***
Type	2	295357031	20.124	4.27E-05	***
Time	2	1221569930	83.23	2.20E-16	***
Type:Time	4	719736962	49.038	5.73E-10	***
residual		14677047			

Table C.4.12 *nosZ* qPCR Genotype Model

Factor	Df	Sum of Sq	Wald	Pr(Chisq)	
(Intercept)	1	5127618121	308.503	2.00E-16	***
Genotype	26	607829600	36.57	0.08167	.
Time	2	1227441338	73.849	2.00E-16	***
Genotype:Time	52	1118209396	67.277	0.07547	.
residual		16620956			

Table C.5 Heritability estimates from mixed effect model in 'asreml-r' where all factors were running as random variable to calculate the variance attributed by each factor. Factors included genotype, block, range, and row. Model was run within each of the sampling timepoints. H2 was estimated by dividing the total variance attributed by genotype dived by the total variance in the model using the 'vpredict' function in 'asreml-r'.

Ecosystem Phenotype	Time Point	h2 Estimate	SE	P-Value
Log (nitrification rate)	1	0.144365	0.1933236	0.01218
Log (nitrification rate)	2	0.8034402	0.2779798	2.20E-16
Log (nitrification rate)	3	0	0.0497557	0.7337
Log (overall denitrification)	1	0.3469187	0.1770689	0.00997
Log (overall denitrification)	2	0	0	0.6158
Log (overall denitrification)	3	0.2840111	0.1233058	0.00689
Log (incomplete denitrification)	1	0.4143898	0.1300028	0.00022
Log (incomplete denitrification)	2	0.02828494	0.0265748	0.00598
Log (incomplete denitrification)	3	0.06985824	0.0840599	0.00676

Table C.6 Mixed effect models comparing potential nitrification and genotype, type, space, and time. Genotype and time of sampling were run as a fixed effect, while sampling block, range, and row were run as random factors. Wald tests performed on statistical models to calculate significance. Statistical models were run in 'asreml-r'.

Table C.6.1 Nitrification Rates per genotype

Terms	DF	Sum of Sq	Wald Statistic	Pr (Chisq)	Significant
(Intercept)	1	5.44E+10	801.02	< 2.2e-16	***
Genotype	26	2.65E+09	39.06	0.0480908	*
Time	2	4.06E+08	5.99	0.0501316	.
Genotype:Time	49	6.38E+09	94.04	0.0001154	***
residual		6.79E+07			

Table C.6.2 Log of Nitrification Rate Per Genotype

Terms	DF	Sum of Sq	Wald Statistic	Pr (Chisq)	Significant
(Intercept)	1	4598.5	86160	2.00E-16	***
Genotype	26	2.7	51	0.00214	**
Time	2	0.4	8	0.01644	*
Genotype:Time	49	2.3	43	0.70185	
residual		0.1			

Table C.6.3 Nitrification Rate Type

Terms	Terms	DF	Sum of Sq	Wald Statistic	Pr (Chisq)
(Intercept)	1	5.62E+10	871.66	2.20E-16	***
Type	2	1.33E+09	20.66	3.26E-05	***
Time	2	3.46E+08	5.36	0.06848	.
Type:Time	4	4.02E+09	62.35	9.31E-13	***
residual		6.45E+07			

Table C.6.4 log of Nitrification Rate per Type

Terms	Terms	DF	Sum of Sq	Wald Statistic	Pr (Chisq)
(Intercept)	1	4551.7	110078	2.20E-16	***
Type	2	2.3	57	4.75E-13	***
Time	2	0.7	16	0.0003174	***
Type:Time	4	1	24	8.10E-05	***
residual		0			

Table C.7. Mixed effect models comparing potential denitrification and genotype, type, space, and time. Genotype and time of sampling were run as a fixed effect, while sampling block, range, and row were run as random factors. Wald tests performed on statistical models to calculate significance. Statistical models were run in 'asreml-r'.

Table C.7.1 Overall Denitrification Enzyme Assay Genotype Model

Terms	DF	Sum of Sq	Wald Statistic	Pr (Chisq)	Significant
(Intercept)	1	22114	22.219	2.43E-06	***
Genotype	26	30475	30.621	0.2426957	
Time	2	16499	16.578	0.0002513	***
Genotype:Time	52	52263	52.513	0.454031	
residual		995			

Table C.7.2 log Overall Denitrification Enzyme Assay Genotype Model

Terms	DF	Sum of Sq	Wald Statistic	Pr (Chisq)	Significant
(Intercept)	1	4.039	2.227	0.13559	
Genotype	26	126.899	69.971	6.70E-06	***
Time	2	11.549	6.368	0.04142	*
Genotype:Time	52	127.85	70.495	0.04474	*
residual		1.814			

Table C.7.3 Overall Denitrification Enzyme Assay Type Model

Terms	DF	Sum of Sq	Wald Statistic	Pr (Chisq)	Significant
(Intercept)	1	36370	37.667	8.39E-10	***
Type	2	12806	13.263	0.0013183	**
Time	2	16442	17.028	0.0002006	***
Type:Time	4	10703	11.085	0.0256288	*
residual		966			

Table C.7.4 Incomplete Denitrification Enzyme Assay Genotype Model

Terms	DF	Sum of Sq	Wald Statistic	Pr (Chisq)	Significants
(Intercept)	1	772215	0.782	0.37639	
Genotype	26	29266385	29.654	0.28217	
Time	2	4429458	4.488	0.10602	
Genotype:Time	52	68615086	69.525	0.05261	
residual		986914			

Table C.7.5 Log of Incomplete Denitrification Enzyme Assay Genotype Model

Terms	DF	Sum of Sq	Wald Statistic	Pr (Chisq)	Significants
(Intercept)	1	200.446	148.726	2.20E-16	***
Genotype	26	122.241	90.7	4.29E-09	***
Time	2	22.864	16.965	0.0002071	***
Genotype:Time	52	58.044	43.067	0.806586	
residual		1.348			

Table C.7.6 Incomplete Denitrification Enzyme Assay Type Model

Terms	DF	Sum of Sq	Wald Statistic	Pr (Chisq)	Significants
(Intercept)	1	200.446	148.726	2.20E-16	***
Genotype	26	122.241	90.7	4.29E-09	***
Time	2	22.864	16.965	0.0002071	***
Genotype:Time	52	58.044	43.067	0.806586	
residual		1.348			

Table C.8. Genotype effect calculations for potential nitrification, incomplete denitrification, and complete denitrification rates. Table includes genotype mean, variance, genotype effects which was calculated as the difference between the genotypes mean – the population mean, and the percent change which is the genotypic effects divided by the population mean. These metrics were adapted from Bernardo et al. *Breeding for Quantitative Traits in Plants.*

Table C.8.1 Genotype effects on Potential Nitrification

Genotypes	Type	Mean	Variance	Genotype Effect	Percent Change
Ames21785	**Teosinte**	3223.202	1081182.57	-691.15308	-0.176568847
Ames21786	**Teosinte**	2774.953	88433.44	-1139.40144	-0.291082838
Ames21809	**Teosinte**	3133.105	746022.14	-781.24917	-0.199585692
B73	**Inbred**	3932.59	2127444.5	18.23587	0.004658717
B73/PHJ40	**Hybrid**	4063.868	2198144.3	149.51344	0.038196191
B73/PHZ51	**Hybrid**	3307.112	1437775.21	-607.24263	-0.155132249
CHECK1	**Hybrid**	3795.58	2885350.12	-118.77462	-0.030343348
CHECK2	**Hybrid**	3889.966	1355353.96	-24.38811	-0.006230428
LH1	**Inbred**	4412.906	1914200.4	498.55092	0.127364782
LH123	**Inbred**	4243.162	675978.9	328.80741	0.084000415
LH82	**Inbred**	4265.879	3109219.15	351.52435	0.089803911
LH82/PH207	**Hybrid**	5856.937	28458139.93	1942.58205	0.496271353
LH82/PHJ40	**Hybrid**	2983.589	3277029.92	-930.76514	-0.237782532
Mo17	**Inbred**	4000.014	1853836.7	85.6593	0.021883378
PH207	**Inbred**	4369.633	3803350.28	455.27798	0.116309845
PHG35	**Inbred**	3714.55	3813926.52	-199.8045	-0.051044047
PHG39	**Inbred**	3401.902	2167152.55	-512.45228	-0.130916162
PHG39/PHZ51	**Hybrid**	3243.783	4451418.24	-670.57131	-0.171310824
PHG47	**Inbred**	3825.386	3776140.43	-88.96846	-0.02272877
PHG47/PHG84	**Hybrid**	4195.987	5260178.39	281.63267	0.071948687
PHG47/PHJ40	**Hybrid**	3163.181	1001909.37	-751.17393	-0.191902373
PHG84	**Inbred**	4927.571	3589665.08	1013.2166	0.258846401
PHJ40	**Inbred**	4235.362	2139689.2	321.00759	0.082007795
PHZ51	**Inbred**	3673.76	1545063.7	-240.595	-0.061464796
PI566677	**Teosinte**	2987.754	1989648.34	-926.60081	-0.23671867
PI658188	**Teosinte**	4287.181	26627889.28	372.82631	0.095245921
PI658205	**Teosinte**	4870.039	26617163.44	955.68488	0.244148777

Table C.8.2 Genotype effects on Overall Denitrification

Genotypes	Type	Mean	Variance	Genotype Effect	Percent Change
Ames21785	**Teosinte**	12.225411	779.658009	-6.063614	-0.33154387
Ames21786	**Teosinte**	1.418217	7.923932	-16.870808	-0.92245529
Ames21809	**Teosinte**	20.975168	4754.027636	2.686142	0.14687182
B73	**Inbred**	26.411203	950.937289	8.122178	0.4441012
B73/PHJ40	**Hybrid**	20.062967	1457.794312	1.773942	0.09699487
B73/PHZ51	**Hybrid**	12.719734	120.740613	-5.569291	-0.30451545
CHECK1	**Hybrid**	38.901194	4490.550549	20.612169	1.12702391
CHECK2	**Hybrid**	11.884273	274.847049	-6.404752	-0.3501965
LH1	**Inbred**	11.165771	161.450221	-7.123254	-0.38948243
LH123	**Inbred**	12.949991	113.369208	-5.339034	-0.29192559
LH82	**Inbred**	15.97309	642.964529	-2.315935	-0.12662977
LH82/PH207	**Hybrid**	21.952365	250.834562	3.663339	0.20030261
LH82/PHJ40	**Hybrid**	41.578123	1951.876885	23.289098	1.27339201
Mo17	**Inbred**	25.755179	860.418624	7.466154	0.4082314
PH207	**Inbred**	27.86796	1651.695357	9.578935	0.52375319
PHG35	**Inbred**	23.894519	927.46544	5.605494	0.30649493
PHG39	**Inbred**	8.609285	73.497137	-9.67974	-0.52926496
PHG39/PHZ51	**Hybrid**	14.804714	201.503919	-3.484311	-0.19051378
PHG47	**Inbred**	27.369599	2933.639208	9.080574	0.49650398
PHG47/PHG84	**Hybrid**	25.585344	457.123644	7.296319	0.39894523
PHG47/PHJ40	**Hybrid**	34.053087	1716.381409	15.764062	0.86194108
PHG84	**Inbred**	24.404597	2230.25515	6.115572	0.3343848
PHJ40	**Inbred**	15.48927	355.858064	-2.799755	-0.15308389
PHZ51	**Inbred**	15.445163	208.991664	-2.843862	-0.15549553
PI566677	**Teosinte**	3.194778	37.371736	-15.094247	-0.82531722
PI658188	**Teosinte**	6.021103	68.286632	-12.267923	-0.67078056
PI658205	**Teosinte**	1.354084	5.715189	-16.934941	-0.92596192

Table C.8.3 Genotype effects on Incomplete Denitrification

Genotypes	Type	Mean	Variance	Genotype Effect	Percent Change
Ames21785	**Teosinte**	0.9733998	3.854093	-7.98603912	-0.891354826
Ames21786	**Teosinte**	1.3051623	6.296865	-7.6542766	-0.85432544
Ames21809	**Teosinte**	1.6059257	4.038354	-7.35351324	-0.820755999
B73	**Inbred**	16.8188358	405.154126	7.85939689	0.877219763
B73/PHJ40	**Hybrid**	7.4729687	48.611804	-1.48647024	-0.165911086
B73/PHZ51	**Hybrid**	8.1838818	32.706687	-0.7755571	-0.086563133
CHECK1	**Hybrid**	7.8783329	35.574311	-1.08110598	-0.120666705
CHECK2	**Hybrid**	8.4449126	45.474519	-0.51452636	-0.057428413
LH1	**Inbred**	8.6419164	55.18519	-0.31752254	-0.035440003
LH123	**Inbred**	37.2180497	3699.631325	28.25861081	3.154060322
LH82	**Inbred**	11.6609163	102.192998	2.70147736	0.301523051
LH82/PH207	**Hybrid**	10.7900266	38.394728	1.83058766	0.204319454
LH82/PHJ40	**Hybrid**	11.4109879	39.199536	2.45154898	0.273627512
Mo17	**Inbred**	12.0360989	190.165106	3.07665997	0.343398733
PH207	**Inbred**	8.5943683	34.988491	-0.36507061	-0.040747039
PHG35	**Inbred**	8.2722852	49.910295	-0.68715377	-0.076696072
PHG39	**Inbred**	9.8503228	80.708558	0.89088383	0.099435225
PHG39/PHZ51	**Hybrid**	6.9874882	20.942325	-1.97195076	-0.220097573
PHG47	**Inbred**	9.0023327	35.816546	0.04289375	0.004787548
PHG47/PHG84	**Hybrid**	10.5552713	38.582969	1.59583234	0.178117441
PHG47/PHJ40	**Hybrid**	9.0040367	74.346892	0.04459775	0.004977739
PHG84	**Inbred**	9.5751494	39.744606	0.61571051	0.068721995
PHJ40	**Inbred**	9.184837	40.428247	0.22539803	0.025157606
PHZ51	**Inbred**	12.2326943	46.872466	3.27325542	0.365341563
PI566677	**Teosinte**	2.7090858	8.303989	-6.25035314	-0.697627741
PI658188	**Teosinte**	1.0254465	8.225691	-7.93399238	-0.885545674
PI658205	**Teosinte**	5.9606611	106.052389	-2.99877777	-0.334705979

APPENDIX D: SUPPLEMENTAL INFORMATION CHAPTER 5

Mapping the genetic regions underlying plant extended phenotype microbiome recruitment and function

Tables:

Table D.1 List of NILs used in study. Highlighting the genetic composition of each lines.

Lines	%B73 homozygote	%heterozygote	%teo homozygote	%introgression
Z031E0009	89.64285714	5.357142857	4.642857143	10
Z031E0011	91.33064516	7.459677419	6.451612903	13.91129032
Z031E0012	93.39285714	2.678571429	3.035714286	5.714285714
Z031E0016	93.75	3.571428571	2.321428571	5.892857143
Z031E0021	94.46428571	2.321428571	3.214285714	5.535714286
Z031E0022	95.71428571	0.535714286	3.571428571	4.107142857
Z031E0028	92.5	2.678571429	4.642857143	7.321428571
Z031E0031	90.17857143	5.535714286	3.392857143	8.928571429
Z031E0035	96.22302158	1.618705036	1.798561151	3.417266187
Z031E0038	95.17857143	3.571428571	1.071428571	4.642857143
Z031E0040	92.67857143	3.75	3.571428571	7.321428571
Z031E0042	95.53571429	3.928571429	0	3.928571429
Z031E0047	96.41577061	0	3.584229391	3.584229391
Z031E0050	90.32258065	1.792114695	7.52688172	9.318996416
Z031E0052	93.75	3.571428571	2.321428571	5.892857143
Z031E0054	82.97491039	13.44086022	2.688172043	16.12903226
Z031E0057	97.12230216	3.057553957	0.179856115	3.237410072
Z031E0058	88.92857143	6.785714286	3.928571429	10.71428571
Z031E0059	94.28571429	0	5.714285714	5.714285714
Z031E0061	96.07142857	0.178571429	3.035714286	3.214285714
Z031E0067	95.35714286	2.321428571	1.964285714	4.285714286
Z031E0068	100.3649635	0.364963504	0	0.364963504
Z031E0070	95.34050179	3.584229391	0.896057348	4.480286738
Z031E0071	96.04316547	1.618705036	2.338129496	3.956834532
Z031E0074	94.10714286	3.392857143	2.321428571	5.714285714
Z031E0507	90.25270758	0.36101083	9.566787004	9.927797834
Z031E0523	92.83154122	0	7.168458781	7.168458781
Z031E0526	95.71428571	0	4.285714286	4.285714286
Z031E0536	89.28571429	0	10.71428571	10.71428571
Z031E0537	91.78571429	0	8.214285714	8.214285714
Z031E0545	98.01444043	0	2.346570397	2.346570397
Z031E0556	95.27272727	0.363636364	4.909090909	5.272727273
Z031E0559	98.21428571	0	1.607142857	1.607142857
Z031E0560	96.04316547	0	4.136690647	4.136690647

Table D.1 (cont.) List of NILs used in study. Highlighting the genetic composition of each lines.

Lines	%B73 homozygote	%heterozygote	%teo homozygote	%introgression
Z031E0577	97.14285714	0	2.678571429	2.678571429
Z031E0578	97.82608696	1.086956522	1.630434783	2.717391304
Z031E0580	98.55072464	0	1.992753623	1.992753623
Z031E0585	95.16129032	0.537634409	3.94265233	4.480286738
Z031E0591	97.29241877	0	2.346570397	2.346570397
Z031E0594	95.68345324	0.35971223	4.316546763	4.676258993
B73	100	0	0	0
B73xPI384071	50	50	50	0
PI384071	0	0	100	0

Table D.2 Primers

Target	Encodes	Primer Name	Sequence	Reference
16S rRNA	Ribosomal RNA	515F	5'-GTGYCAGCMGCCGCGGTAA-3'	Fierer et al. 2011
16S rRNA	Ribosomal RNA	806R	5'-GGACTACVSGGGTATCTAAT-3'	Fierer et al. 2011
ITS	Internal transcribed spacer	ITS1F	5'-TTCGTAGGTGAACCTGCGG-3'	White et al. 1990
ITS	Internal transcribed spacer	ITS4R	5'-TCCTCCGCTTATTGATATGC-3'	White et al. 1990
archaeal *16S*	Ribosomal RNA	Arch349F	5'-GYGCASCAGKCGMGAAW-3'	Park et al. 2009
archaeal *16S*	Ribosomal RNA	Arch806R	5'GGACTACVSGGGTATCTAAT-3'	Park et al. 2009
nifH	Nitrogenase	PolF	5'-TGCGAYCCSAARGCBGACTC-3'	Poly et al. 2001
nifH	Nitrogenase	PolR	5'-ATSGCCATCATYTCRCCGGA-3'	Poly et al. 2001
bacterial *amoA*	Ammonia Monooxygenase	amoA-1F	5'-GGGGTTTCTACTGGTGGT-3'	Oakley et al. 2005
bacterial *amoA*	Ammonia Monooxygenase	amoA-2R	5'-CCCCTCKGSAAAGCCTTCTTC-3'	Oakley et al. 2005
archeal *amoA*	Ammonia Monooxygenase	CrenamoA23f	5'-ATGGTCTGGCTWAGACG-3'	Francis et al. 2005
archeal *amoA*	Ammonia Monooxygenase	CrenamoA616r	5'-GCCATCCATCTGTATGTCCA-3'	Francis et al. 2005
Typical *nosZ*	Nitrous oxide reductase	nosZ1F	5'-WCSYTGTTCMTCGACAGCCAG-3'	Henry et al. 2006
Typical *nosZ*	Nitrous oxide reductase	nosZ1R	5'-ATGTCGATCARCTGVKCRTTYTC-3'	Henry et al. 2006

Table D.2 (cont.) Primers

Target	Encodes	Primer Name	Sequence	Reference
nrfA	Nitrite Reductase	nrfAR1	5'-TWNGGCATRTGRCARTC-3'	Cole et al. 2004
nirK	Nitrite Reductase	nirK876	5'-ATYGGCGGVCAYGGCGA-3'	Henry et al. 2004
nirK	Nitrite Reductase	nirK1040	5'-GCCTCGATCAGRTTRTGGTT-3'	Henry et al. 2004
nirS	Nitrite Reductase	nirSCd3aF	5'-AACGYSAAGGARACSGG-3'	Kandeler et al. 2006
nirS	Nitrite Reductase	nirSR3cd	5'-GASTTCGGRTGSGTCTTSAYGAA-3'	Kandeler et al. 2006

Table D.3 Introgressions (NIL genotypes) effects on amplicon diversity summary

Amplicon	Group	R2	Pr(>F)	
16S rRNA	Prokaryotic	0.12836	0.001	*
ITS	Fungal	0.12399	0.001	*
nifH	Nitrogen Fixation	0.12677	0.101	
arch *amoA*	Nitrification	0.15176	0.001	*
bac *amoA*	Nitrification	0.12605	0.008	*
nirS	Denitrification	0.12665	0.273	
nirK	Denitrification	0.12643	0.022	*
nosZ	Denitrification	0.12399	0.046	*

Table D.4 PERMANOVA 16S Genes. Here and in the text, we use NIL genotype and introgression interchangeably.

Table D.4.1 Prokaryotic 16SrRNA

Term	Df	SumsOfSqs	MeanSqs	F.Model	R2	Pr(>F)	Sig
NILGenotype	41	3.3834	0.08252	1.1609	0.12836	0.001	***
Time	1	0.3749	0.3749	5.274	0.01422	0.001	***
Row	21	1.9677	0.0937	1.3181	0.07465	0.001	***
Range	7	1.2873	0.18389	2.587	0.04883	0.001	***
Block	98	7.9018	0.08063	1.1343	0.29977	0.001	***
Residuals	161	11.4445	0.07108	0.43417	0.56583		
Total	329	26.3595	1				

Table D.4.2 Fungal ITS

Term	Df	SumsOfSqs	MeanSqs	F.Model	R2	Pr(>F)	Sig
NILGenotype	41	13.138	0.32043	1.0334	0.12399	0.001	***
Time	1	2.285	2.28518	7.3697	0.02157	0.001	***
Row	21	6.805	0.32405	1.0451	0.06422	0.001	***
Range	7	3.73	0.53279	1.7182	0.0352	0.001	***
Block	98	29.766	0.30374	0.9795	0.28093	0.001	***
Residuals	162	50.233	0.31008	0.47409	0.52591		
Total	330	105.956	1				

Table D.5 Functional Gene PERMANOVA Models. Here and in the text, we use NIL genotype and introgression interchangeably.

Table D.5.1 *nifH* nitrogen-fixation functional group

Term	Df	SumsOfSqs	MeanSqs	F.Model	R2	Pr(>F)	Sig
NILGenotype	41	17.954	0.4379	1.036	0.12677	0.101	
Time	1	0.545	0.54519	1.2898	0.00385	0.054	.
Row	21	9.795	0.46642	1.1034	0.06916	0.077	.
Range	7	3.707	0.52952	1.2527	0.02617	0.214	
Block	98	42.833	0.43707	1.034	0.30245	0.234	
Residuals	158	66.787	0.4227	0.47159			
Total	326	141.62	1				

Table D.5.2 Bacterial *amoA* nitrification functional group

Term	Df	SumsOfSqs	MeanSqs	F.Model	R2	Pr(>F)	Sig
NILGenotype	41	10.688	0.26068	0.97963	0.12605	0.008	**
Time	1	0.595	0.59455	2.23433	0.00701	0.015	*
Row	21	5.455	0.25978	0.97626	0.06434	0.083	.
Range	7	3.622	0.51742	1.94445	0.04272	0.026	*
Block	98	25.843	0.26371	0.99102	0.3048	0.005	**
Residuals	145	38.584	0.2661	0.45507			
Total	313	84.787	1				

Table D.5.3 Archaeal *amoA* nitrification functional group

Term	Df	SumsOfSqs	MeanSqs	F.Model	R2	Pr(>F)	Sig
NILGenotype	41	3.8991	0.095101	1.6246	0.15176	0.001	***
Time	1	0.2996	0.299628	5.1185	0.01166	0.001	***
Row	21	1.9779	0.094187	1.609	0.07698	0.001	***
Range	7	1.0956	0.156511	2.6737	0.04264	0.001	***
Block	98	8.996	0.091796	1.5681	0.35014	0.001	***
Residuals	161	9.4246	0.058538	0.36682			
Total	329	25.6929	1				

Table D.5.4 *nirS* denitrification functional group

Term	Df	SumsOfSqs	MeanSqs	F.Model	R2	Pr(>F)	Sig
NILGenotype	41	11.621	0.28345	1.0947	0.12665	0.273	
Time	1	0.31	0.31033	1.1985	0.00338	0.2	
Row	21	7.162	0.34103	1.3171	0.07805	0.209	
Range	7	2.829	0.4041	1.5607	0.03083	0.265	
Block	98	28.926	0.29517	1.14	0.31524	0.441	
Residuals	158	40.91	0.25892	0.44584			
Total	326	91.758	1				

Table D.5.5 *nirK* dentification functional group

Term	Df	SumsOfSqs	MeanSqs	F.Model	R2	Pr(>F)	Sig
NILGenotype	41	15.609	0.3807	1.0523	0.12643	0.022	*
Time	1	0.506	0.50563	1.3977	0.0041	0.02	*
Row	21	8.414	0.40067	1.1075	0.06815	0.018	*
Range	7	3.199	0.45702	1.2633	0.02591	0.14	
Block	98	37.489	0.38254	1.0574	0.30365	0.031	*
Residuals	161	58.245	0.36177	0.47177			
Total	329	123.461	1				

Table D.5.6 *nosZ* denitrification functional group

Term	Df	SumsOfSqs	MeanSqs	F.Model	R2	Pr(>F)	Sig
NILGenotype	41	18.163	0.443	1.0116	0.12399	0.046	*
Time	1	0.609	0.60897	1.3906	0.00416	0.021	*
Row	21	9.394	0.44736	1.0216	0.06413	0.087	.
Range	7	3.649	0.52129	1.1904	0.02491	0.229	
Block	98	44.17	0.45071	1.0292	0.30152	0.106	
Residuals	161	70.504	0.43791	0.48129			
Total	329	146.489	1				

Table D.6 ASREML-r linear model of Potential Function

Table D.6.1 Timepoint 1 – Potential Nitrification Rates

Terms	Df	SumsOfSqs	MeanSqs	Wald statistic	Pr(Chisq)
(Intercept)	1	4897	27807.7	2.00E-16	***
NILGenotype	43	6.4	36.4	0.7509	
Residual (MS)		0.2			

Table D.6.2 Timepoint 2 – Potential Nitrification Rates

Terms	Df	SumsOfSqs	MeanSqs	Wald statistic	Pr(Chisq)
(Intercept)	1	26826.1	79479	2.20E-16	***
NILGenotype	43	23.9	71	0.004753	**
Residual (MS)		0.3			

Table D.6.3 Timepoint 1 – Potential Incomplete Denitrification (N_2O) Rates

Terms	Df	SumsOfSqs	MeanSqs	Wald statistic	Pr(Chisq)
(Intercept)	1	1.67241	121.82	2.20E-16	***
NILGenotype	43	1.09625	79.85	0.0005432	***
Residual (MS)		0.01373			

Table D.6.4 Timepoint 2 – Potential Incomplete Denitrification (N_2O) Rates

Terms	Df	SumsOfSqs	MeanSqs	Wald statistic	Pr(Chisq)
(Intercept)	1	98.818	1028.85	2.00E-16	***
NILGenotype	43	5.28	54.98	0.1041	
Residual (MS)		0.096			

Table D.6.5 Timepoint 1 – Potential Overall Denitrification (N_2O+N_2) Rates

Terms	Df	SumsOfSqs	MeanSqs	Wald statistic	Pr(Chisq)
(Intercept)	1	13.3095	63.896	1.33E-15	***
NILGenotype	43	8.9015	42.735	0.4827	
Residual (MS)		0.2083			

Table D.6.6 Timepoint 2 – Potential Overall Denitrification (N_2O+N_2) Rates

Terms	Df	SumsOfSqs	MeanSqs	Wald statistic	Pr(Chisq)
(Intercept)	1	46.466	336.75	2.20E-16	***
NILGenotype	43	10.095	73.16	0.002786	**
Residual (MS)		0.138			

Table D.7 Genes in BNI introgressions as predicted by MaizeGDB from pervious mapping studies. Titles of subtables includes the genetic regions that were searched for previously established genetic regions.

Table D.7.1 Chr5: 190689917…192848761

Locus Name	Full Name	Gene Model	Line	Type	Chr	Version
cl18897_1		Zm00001d017317	B73	protein_coding	Chr5	Zm00001d.2
def4	defensin-like protein4	Zm00001d017292	B73	protein_coding	Chr5	Zm00001d.2
ein3	ethylene insensitive3	Zm00001d017280	B73	protein_coding	Chr5	Zm00001d.2
ga2ox4	gibberellin 2-oxidase4	Zm00001d017294	B73	protein_coding	Chr5	Zm00001d.2
GRMZM2G153368		Zm00001d017293	B73	protein_coding	Chr5	Zm00001d.2
myb41	MYB-transcription factor 41	Zm00001d017268	B73	protein_coding	Chr5	Zm00001d.2
pal1	phenylalanine ammonia lyase homolog1	Zm00001d017274	B73	protein_coding	Chr5	Zm00001d.2
pal7	phenylalanine ammonia lyase7	Zm00001d017279	B73	protein_coding	Chr5	Zm00001d.2
pal8	phenylalanine ammonia lyase8	Zm00001d017276	B73	protein_coding	Chr5	Zm00001d.2
pal9	phenylalanine ammonia lyase9	Zm00001d017275	B73	protein_coding	Chr5	Zm00001d.2
pip2d	plasma membrane intrinsic protein2	Zm00001d017288	B73	protein_coding	Chr5	Zm00001d.2
ppck3	phosphoenolpyruvate carboxylase kinase3	Zm00001d017270	B73	protein_coding	Chr5	Zm00001d.2
scoal1	succinyl-CoA ligase1	Zm00001d017258	B73	protein_coding	Chr5	Zm00001d.2
ysl14	yellow stripe-like transporter14	Zm00001d017323	B73	protein_coding	Chr5	Zm00001d.2
Zm00001d017285		Zm00001d017285	B73	protein_coding	Chr5	Zm00001d.2

Table D.7.2 Chr9:88651842…110988044

Locus Name	Full Name	Gene Model	Line	Type	Chr	Version
acs3	1-aminocyclopropane-1-carboxylate synthase3	Zm00001d045479	B73	protein_coding	Chr9	Zm00001d.2
adc1	arginine decarboxylase1	Zm00001d045470	B73	protein_coding	Chr9	Zm00001d.2
AY105451		Zm00001d045430	B73	protein_coding	Chr9	Zm00001d.2
AY109570		Zm00001d045478	B73	protein_coding	Chr9	Zm00001d.2
baf1	barren stalk fastigiate1	Zm00001d045427	B73	protein_coding	Chr9	Zm00001d.2
bbr4	BBR/BPC-transcription factor 4	Zm00001d045477	B73	protein_coding	Chr9	Zm00001d.2
bub3	budding inhibited by benzimidazoles homolog3	Zm00001d045389	B73	protein_coding	Chr9	Zm00001d.2
cl10045_1a		Zm00001d045488	B73	protein_coding	Chr9	Zm00001d.2
cl10614_1b		Zm00001d045421	B73	protein_coding	Chr9	Zm00001d.2
cl18247_1		Zm00001d045494	B73	protein_coding	Chr9	Zm00001d.2
cl34718_1		Zm00001d045351	B73	protein_coding	Chr9	Zm00001d.2
cl59603_1		Zm00001d045521	B73	protein_coding	Chr9	Zm00001d.2
cys3	cysteine synthase3	Zm00001d045344	B73	protein_coding	Chr9	Zm00001d.2
cys4	cysteine synthase4	Zm00001d045350	B73	protein_coding	Chr9	Zm00001d.2
cys5	cysteine synthase5	Zm00001d045327	B73	protein_coding	Chr9	Zm00001d.2
cys6	cysteine synthase6	Zm00001d045340	B73	protein_coding	Chr9	Zm00001d.2
cys7	cysteine synthase7	Zm00001d045341	B73	protein_coding	Chr9	Zm00001d.2
cys8	cysteine synthase8	Zm00001d045347	B73	protein_coding	Chr9	Zm00001d.2
dbb11	double B-box zinc finger protein11	Zm00001d045323	B73	protein_coding	Chr9	Zm00001d.2
dxs3	deoxy xylulose synthase3	Zm00001d045383	B73	protein_coding	Chr9	Zm00001d.2
e2f10	E2F-DP-transcription factor 210	Zm00001d045365	B73	protein_coding	Chr9	Zm00001d.2
eno1	enolase1	Zm00001d045431	B73	protein_coding	Chr9	Zm00001d.2
eps1	enolpyruvylshikimate phosphate synthase1	Zm00001d045450	B73	protein_coding	Chr9	Zm00001d.2
er3	erecta-like3	Zm00001d045481	B73	protein_coding	Chr9	Zm00001d.2
ereb33	AP2-EREBP-transcription factor 33	Zm00001d045378	B73	protein_coding	Chr9	Zm00001d.2
fat2	fatty acyl-ACP thioesterase2	Zm00001d045387	B73	protein_coding	Chr9	Zm00001d.2
ftr1	ferredoxin-thioredoxin1	Zm00001d045366	B73	protein_coding	Chr9	Zm00001d.2
gras42	GRAS-transcription factor 42	Zm00001d045507	B73	protein_coding	Chr9	Zm00001d.2
GRMZM2G114098		Zm00001d045417	B73	protein_coding	Chr9	Zm00001d.2
hb4	Homeobox-transcription factor 4	Zm00001d045400	B73	protein_coding	Chr9	Zm00001d.2

Table D.7.2 (cont.) Chr9:88651842…110988044

Locus Name	Full Name	Gene Model	Line	Type	Chr	Version
hb77	Homeobox-transcription factor 77	Zm00001d045398	B73	protein_coding	Chr9	Zm00001d.2
mkk2	mitogen-activated protein kinase kinase2	Zm00001d045359	B73	protein_coding	Chr9	Zm00001d.2
mpk2	MAP kinase2	Zm00001d045310	B73	protein_coding	Chr9	Zm00001d.2
msr3	methionine sulfoxide reductase3	Zm00001d045418	B73	protein_coding	Chr9	Zm00001d.2
nactf86	NAC-transcription factor 86	Zm00001d045463	B73	protein_coding	Chr9	Zm00001d.2
pco063808		Zm00001d045516	B73	protein_coding	Chr9	Zm00001d.2
pco083693		Zm00001d045529	B73	protein_coding	Chr9	Zm00001d.2
pco095664		Zm00001d045373	B73	protein_coding	Chr9	Zm00001d.2
pco103628		Zm00001d045509	B73	protein_coding	Chr9	Zm00001d.2
pco136657		Zm00001d045358	B73	protein_coding	Chr9	Zm00001d.2
prf5	Profilin homolog5	Zm00001d045323	B73	protein_coding	Chr9	Zm00001d.2
pza01272		Zm00001d045315	B73	protein_coding	Chr9	Zm00001d.2
rpp13lk3	recognition of Peronospora parasitica 13 like protein 3	Zm00001d045512	B73	protein_coding	Chr9	Zm00001d.2
rps22a	ribosomal protein S22 homolog	Zm00001d045448	B73	protein_coding	Chr9	Zm00001d.2
si687009g07		Zm00001d045381	B73	protein_coding	Chr9	Zm00001d.2
TIDP9202		Zm00001d045476	B73	protein_coding	Chr9	Zm00001d.2
tk1	transketolase 1	Zm00001d045451	B73	protein_coding	Chr9	Zm00001d.
umc1586		Zm00001d045517	B73	protein_coding	Chr9	Zm00001d.2
umc1634		Zm00001d045468	B73	protein_coding	Chr9	Zm00001d.2
umc1698		Zm00001d045392	B73	protein_coding	Chr9	Zm00001d.2
wrky39	WRKY-transcription factor 39	Zm00001d045375	B73	protein_coding	Chr9	Zm00001d.2
wx1	waxy1	Zm00001d045462	B73	protein_coding	Chr9	Zm00001d.2

Table D.7.3 Chr9: 18782106…25727342

Locus Name	Full Name	Gene Model	Line	Type	Chr	Version
acp1	acid phosphatase1	Zm00001d046593	B73	protein_coding	Chr9	Zm00001d.2
ago101	argonaute101	Zm00001d046438	B73	protein_coding	Chr9	Zm00001d.2
AI812156		Zm00001d046613	B73	protein_coding	Chr9	Zm00001d.2
arid10	ARID-transcription factor 10	Zm00001d046719	B73	protein_coding	Chr9	Zm00001d.2
arpg1	acid phosphatase-regulating gene1	Zm00001d046743	B73	protein_coding	Chr9	Zm00001d.2
arr4	ARR-B-transcription factor 4	Zm00001d046755	B73	protein_coding	Chr9	Zm00001d.2
asg63a		Zm00001d046501	B73	protein_coding	Chr9	Zm00001d.2
AW257883		Zm00001d046742	B73	protein_coding	Chr9	Zm00001d.2
AY103770		Zm00001d046697	B73	protein_coding	Chr9	Zm00001d.2
BE518809		Zm00001d046533	B73	protein_coding	Chr9	Zm00001d.2
bhlh69	bHLH-transcription factor 69	Zm00001d046759	B73	protein_coding	Chr9	Zm00001d.2
bnl5.04		Zm00001d046793	B73	protein_coding	Chr9	Zm00001d.2
brc2	brassinosteroid catabolism2	Zm00001d046422	B73	protein_coding	Chr9	Zm00001d.2
bzip35	bZIP-transcription factor 35	Zm00001d046664	B73	protein_coding	Chr9	Zm00001d.2
bzip60	bZIP transcription factor60	Zm00001d046718	B73	protein_coding	Chr9	Zm00001d.2
bzip70	bZIP-transcription factor 70	Zm00001d046751	B73	protein_coding	Chr9	Zm00001d.2
c3h18	C3H-transcription factor 318	Zm00001d046740	B73	protein_coding	Chr9	Zm00001d.2
cer2	eceriferum2	Zm00001d046865	B73	protein_coding	Chr9	Zm00001d.2
cl44093_1		Zm00001d046778	B73	protein_coding	Chr9	Zm00001d.2
cl54126_1		Zm00001d046790	B73	protein_coding	Chr9	Zm00001d.2
com1	completion of meiotic recombination1	Zm00001d046761	B73	protein_coding	Chr9	Zm00001d.2
csu147		Zm00001d046746	B73	protein_coding	Chr9	Zm00001d.2
csu193		Zm00001d046489	B73	protein_coding	Chr9	Zm00001d.2
dbptf4	DBP-transcription factor 4	Zm00001d046450	B73	protein_coding	Chr9	Zm00001d.2
dps1	dihydrodipicolinate synthase1	Zm00001d046898	B73	protein_coding	Chr9	Zm00001d.2
elfa9	elongation factor 1-alpha9	Zm00001d046449	B73	protein_coding	Chr9	Zm00001d.2
elm2	elongated mesocotyl2	Zm00001d046492	B73	protein_coding	Chr9	Zm00001d.2
emb18	embryo specific18	Zm00001d046555	B73	protein_coding	Chr9	Zm00001d.2

Table D.7.3 (cont.) Chr9: 18782106…25727342

Locus Name	Full Name	Gene Model	Line	Type	Chr	Version
ereb203	AP2-EREBP-transcription factor 203	Zm00001d046651	B73	protein_coding	Chr9	Zm00001d.2
fae2	fatty acid elongase2	Zm00001d046444	B73	protein_coding	Chr9	Zm00001d.2
farl14	FAR1-like-transcription factor 14	Zm00001d046441	B73	protein_coding	Chr9	Zm00001d.2
fat1	fatty acyl thioesterase1	Zm00001d046454	B73	protein_coding	Chr9	Zm00001d.2
gl15	glossy15	Zm00001d046621	B73	protein_coding	Chr9	Zm00001d.2
gpm68		Zm00001d046723	B73	protein_coding	Chr9	Zm00001d.2
gras70	GRAS-transcription factor 70	Zm00001d046783	B73	protein_coding	Chr9	Zm00001d.2
GRMZM2G031370		Zm00001d046882	B73	protein_coding	Chr9	Zm00001d.2
GRMZM2G085218		Zm00001d046888	B73	protein_coding	Chr9	Zm00001d.2
GRMZM2G145104		Zm00001d046624	B73	protein_coding	Chr9	Zm00001d.2
GRMZM2G398615		Zm00001d046828	B73	protein_coding	Chr9	Zm00001d.2
haf101b		Zm00001d046579	B73	protein_coding	Chr9	Zm00001d.2
hagtf35	GNAT-transcription factor 35	Zm00001d046823	B73	protein_coding	Chr9	Zm00001d.2
hak10	potassium high-affinity transporter10	Zm00001d046679	B73	protein_coding	Chr9	Zm00001d.2
hggt1	homogentisate geranylgeranyl transferase1	Zm00001d046558	B73	protein_coding	Chr9	Zm00001d.2
hlt1	high leaf temperature 1	Zm00001d046643	B73	protein_coding	Chr9	Zm00001d.2
hm2	Helminthosporium carbonum susceptibility2	Zm00001d046811	B73	protein_coding	Chr9	Zm00001d.2
ho3	heme oxygenase3	Zm00001d046493	B73	protein_coding	Chr9	Zm00001d.2
hpt1	homogentisate phytyltransferase1	Zm00001d046909	B73	protein_coding	Chr9	Zm00001d.2
hscf1	heat shock complementing factor1	Zm00001d046913	B73	protein_coding	Chr9	Zm00001d.2
IDP717		Zm00001d046513	B73	protein_coding	Chr9	Zm00001d.2
knox2	knotted related homeobox2	Zm00001d046568	B73	protein_coding	Chr9	Zm00001d.2
lim166		Zm00001d046916	B73	protein_coding	Chr9	Zm00001d.2
ltp2	lipid transfer protein2	Zm00001d046596	B73	protein_coding	Chr9	Zm00001d.2
mch1	maize CRY1 homolog1	Zm00001d046583	B73	protein_coding	Chr9	Zm00001d.2
mha10	membrane H( )-ATPase10	Zm00001d046560	B73	protein_coding	Chr9	Zm00001d.2

Table D.7.3 (cont.) Chr9: 18782106…25727342

Locus Name	Full Name	Gene Model	Line	Type	Chr	Version
mlo7	barley mlo defense gene homolog7	Zm00001d046781	B73	protein_coding	Chr9	Zm00001d.2
myb112	MYB-transcription factor 112	Zm00001d046632	B73	protein_coding	Chr9	Zm00001d.2
myb122	MYB-transcription factor 122	Zm00001d046517	B73	protein_coding	Chr9	Zm00001d.2
myb82	MYB-transcription factor 82	Zm00001d046518	B73	protein_coding	Chr9	Zm00001d.2
myb87	MYB-transcription factor 87	Zm00001d046519	B73	protein_coding	Chr9	Zm00001d.2
pco060490		Zm00001d046530	B73	protein_coding	Chr9	Zm00001d.2
pco069828		Zm00001d046569	B73	protein_coding	Chr9	Zm00001d.2
pco071634b		Zm00001d046472	B73	protein_coding	Chr9	Zm00001d.2
pco081548		Zm00001d046488	B73	protein_coding	Chr9	Zm00001d.2
pco082226		Zm00001d046682	B73	protein_coding	Chr9	Zm00001d.2
pco095310		Zm00001d046456	B73	protein_coding	Chr9	Zm00001d.2
pco099302		Zm00001d046749	B73	protein_coding	Chr9	Zm00001d.2
pco100106		Zm00001d046654	B73	protein_coding	Chr9	Zm00001d.2
pco103251		Zm00001d046552	B73	protein_coding	Chr9	Zm00001d.2
pco106241		Zm00001d046661	B73	protein_coding	Chr9	Zm00001d.2
pco119060		Zm00001d046890	B73	protein_coding	Chr9	Zm00001d.2
platz16	PLATZ-transcription factor 16	Zm00001d046688	B73	protein_coding	Chr9	Zm00001d.2
pld5	phospholipase D5	Zm00001d046508	B73	protein_coding	Chr9	Zm00001d.2
prh21	protein phosphatase homolog21	Zm00001d046506	B73	protein_coding	Chr9	Zm00001d.2
prh23	protein phosphatase homolog23	Zm00001d046831	B73	protein_coding	Chr9	Zm00001d.2
rdr3	RNA-dependent RNA polymerase3	Zm00001d046875	B73	protein_coding	Chr9	Zm00001d.2
rpo2	RNA polymerase2	Zm00001d046835	B73	protein_coding	Chr9	Zm00001d.2
rz682		Zm00001d046855	B73	protein_coding	Chr9	Zm00001d.2
sal1	supernumerary aleurone1	Zm00001d046599	B73	protein_coding	Chr9	Zm00001d.2
sbp4	SBP-domain protein4	Zm00001d046906	B73	protein_coding	Chr9	Zm00001d.2
si606045f03		Zm00001d046765	B73	protein_coding	Chr9	Zm00001d.2
si707015f08		Zm00001d046485	B73	protein_coding	Chr9	Zm00001d.2

Table D.7.3 (cont.) Chr9: 18782106…25727342

Locus Name	Full Name	Gene Model	Line	Type	Chr	Version
si707066f01		Zm00001d046923	B73	protein_coding	Chr9	Zm00001d.2
smr3	siamese-related3	Zm00001d046896	B73	protein_coding	Chr9	Zm00001d.2
TIDP2779		Zm00001d046813	B73	protein_coding	Chr9	Zm00001d.2
TIDP2910		Zm00001d046745	B73	protein_coding	Chr9	Zm00001d.2
TIDP3051		Zm00001d046729	B73	protein_coding	Chr9	Zm00001d.2
tipd1	tip growth defective1	Zm00001d046590	B73	protein_coding	Chr9	Zm00001d.2
umc114		Zm00001d046690	B73	protein_coding	Chr9	Zm00001d.2
umc1267		Zm00001d046786	B73	protein_coding	Chr9	Zm00001d.2
umc1743		Zm00001d046705	B73	protein_coding	Chr9	Zm00001d.2
umc2700		Zm00001d046460	B73	protein_coding	Chr9	Zm00001d.2
vpp5	vacuolar-type H - pyrophosphatase5	Zm00001d046591	B73	protein_coding	Chr9	Zm00001d.2
vq51	VQ motif-transcription factor51	Zm00001d046496	B73	protein_coding	Chr9	Zm00001d.2
vq52	VQ motif-transcription factor52	Zm00001d046728	B73	protein_coding	Chr9	Zm00001d.2
wrky124	WRKY-transcription factor 124	Zm00001d046805	B73	protein_coding	Chr9	Zm00001d.2
Zm00001d046658		Zm00001d046658	B73	protein_coding	Chr9	Zm00001d.2
Zm00001d046758		Zm00001d046758	B73	protein_coding	Chr9	Zm00001d.2
znf1	zinc finger protein1	Zm00001d046767	B73	protein_coding	Chr9	Zm00001d.2

Table D.8 Metabolomic results from Deseq2 comparison of enriched small molecules. D.8.1-2) show LC-MS results differently expressed between our candidate NILs and B73. Red compounds are shared across both suppression NILs. D.8.3-4) show GC-MS results and display the log-fold-change between suppression NIL and B73.

Table D.8.1 Chromosome 5

Compound ID	Possible Name	Possible Formula	Molecular Weight	Retention time [min]	ESI polarity
Compound1		C24 H30 O6	414.20413	1.003	positive
Compound2082*		C15 H29 N O	239.2246	17.395	positive
Compound2269	Costunolide	C15 H20 O2	232.14598	21.281	positive
Compound2366	Icosadienoicacid	C20 H36 O2	308.27086	29.138	positive
Compound2381		C25 H44 O	360.33885	30.6	positive
Compound620	Stachydrine	C7 H13 N O2	143.09453	4.087	positive

Table D.8.2 Chromosome 9

Compound ID	Possible Name	Possible Formula	Molecular Weight	Retention time [min]	ESI polarity
Compound620	Stachydrine	C7 H13 N O2	143.09453	4.087	positive
Compound649		C14 H28 N3 P S2	333.14766	4.122	positive
Compound796		C5 H18 Cl N8 O2 P	288.09747	4.213	negative
Compound836	Chlorogenic acid	C16 H18 O9	354.09492	4.242	positive
Compound840	Chlorogenic acid	C16 H18 O9	376.07675	4.245	positive
Compound852		C15 H21 N O3 S	295.12386	4.261	positive
Compound884	7,9-Dimethyl-4-{[5-(4-pyridinyl)-1,3,4-oxadiazol-2-yl]sulfanyl}pyrido[3',2' 4,5]thieno[3,2-d]pyrimidine	C18 H12 N6 O S2	392.05044	4.343	positive
Compound938*		C17 H12 N2 S	276.07204	4.962	Positive
Compound1009		C7 H11 Cl O10	290.00371	5.297	Positive
Compound1122		C22 H29 N5 O7	475.2053	10.181	positive
Compound1142		C7 H10 N5 O5 P	275.04204	10.293	positive
Compound1147	(1R,9S)-11-[(Methylsulfanyl)acetyl]-3-(2-thienyl)-7,11-diazatricyclo[7.3.1.02,7]trideca-2,4-dien-6-one	C18 H20 N2 O2 S2	360.10291	10.31	positive
Compound1158	(1R,9S)-11-[(Methylsulfanyl)acetyl]-3-(2-thienyl)-7,11-diazatricyclo[7.3.1.02,7]trideca-2,4-dien-6-one	C18 H20 N2 O2 S2	338.12089	10.333	positive

Table D.8.2 (cont.) Chromosome 9

Compound ID	Possible Name	Possible Formula	Molecular Weight	Retention time [min]	ESI polarity
Compound1160		C13 H18 O8	302.09975	10.342	positive
Compound1294			169.15218	11.277	positive
Compound1315		C15 H21 N O3 S	295.12392	11.601	positive
Compound1332	D-(-)-Quinic acid	C7 H12 O6	192.06228	11.732	negative
Compound1342		C45 H27 N10 O4 P	802.19545	11.77	negative
Compound1470		C35 H30 O2 S	514.19477	12.352	positive
Compound1498		C34 H37 O5 P3 S	650.1574	12.401	positive
Compound1687*			1100.25559	13.301	positive
Compound1704		C18 H12 N4 O6	380.07435	13.432	negative
Compound1709*	Quercetin-3β-D-glucoside	C21 H20 O12	464.09538	13.476	positive
Compound1870		C36 H43 N O8	617.29854	15.209	negative
Compound2090*		C22 H39 N O6	413.27745	17.508	positive
Compound2136	[6]-Gingerol	C17 H26 O4	294.1832	18.263	negative
Compound2156		C17 H33 N O	267.25557	18.869	positive
Compound2316		C34 H55 N O5	557.40758	26.227	positive
Compound2327		C15 H28 O2	240.2085	27.47	positive
Compound2381		C25 H44 O	360.33885	30.6	positive

Table D.8.3 GCMS chromosome 5. LFC between the two treatments being compared.

Sig Compound	LFC	Treatment
X11.Octadecenoic.acid	9.693099	E0065.B73
Uridine	-8.632235	E0065.B73
Levulinic.acid.enol	-2.428683	E0065.B73
Sedoheptulose	-2.241839	E0065.B73
Inosine	6.729508	E0065.B73
X2.Hexadecanoylglycerol	-6.588503	E0065.B73
X3.Methylthiopropylamine	6.410037	E0065.B73
XYLONIC.ACID.LACTONE	5.933746	E0065.B73
X2.Octadecanoylglycerol	8.521013	E0065.B73
Galactose	-12.947282	E0065.B73
X11.Octadecenoic.acid	9.077978	E0025.B73
Tetracosanol	8.310725	E0025.B73
Inosine	6.99775	E0025.B73
X9.12.15.Octadecatrienoic.acid	10.150196	E0025.B73
proline	9.606501	E0025.B73
adipic.acid	5.174632	E0025.B73
X11.Octadecenoic.acid	10.011003	E0021.B73
tyrosine	9.938063	E0021.B73
X2.Octadecanoylglycerol	9.109783	E0021.B73
X9.12.15.Octadecatrienoic.acid	8.823397	E0021.B73
UREA	6.702277	E0021.B73
Sedoheptulose	-1.831775	E0021.B73
X2.Hexadecanoylglycerol	-6.204784	E0021.B73

Table D.8.4 GCMS chromosome 6. LFC between the two treatments being compared.

Sig Compound	LFC	Treatment
X11.Octadecenoic.acid	9.81541	E0047.B73
proline	10.975642	E0047.B73
X9.12.15.Octadecatrienoic.acid	21.660819	E0047.B73
UREA	6.714503	E0047.B73
X3.Methylthiopropylamine	6.197698	E0047.B73
Galactose	-12.438638	E0047.B73
X11.Octadecenoic.acid	9.79392	E0022.B73
Sedoheptulose	-2.022724	E0022.B73
X11.Octadecenoic.acid	8.8732264	E0079.B73
tyrosine	10.0168686	E0079.B73
X2.Hexadecanoylglycerol	-6.0502467	E0079.B73
Inositol..myo	-0.7625842	E0079.B73
lactic.acid	-1.5023245	E0079.B73
p.coumaric.acid	1.1266603	E0079.B73
X9.12.15.Octadecatrienoic.acid	9.8493631	E0079.B73